The Structure and Functions of the Lysyl-tRNA Synthetase of *Bacillus stearothermophilus*

Teisuke Takita

1996

The Structure and Functions of the Lysyl-tRNA Synthetase of *Bacillus stearothermophilus*

Teisuke Takita

1996

CONTENTS

Abbreviations

Ant-ATP	anthraniloyl-ATP
ARS	aminoacyl-tRNA synthetase
B.s. ARS	ARS from *Bacillus stearothermophilus*
^{3}H-ATP	[2,8-^{3}H] adenosine 5'-triphosphate
^{3}H-L-lysine	[4,5-^{3}H] L-lysine
$K_{d,\,app}$	apparent K_d
$K_{eq\bullet A/0\bullet x}$	ratio of $tRNA_A$ against total tRNA
$K_{eq\bullet tRNA\bullet x}$	an equilibrium constant for the reaction $tRNA_A \rightleftharpoons tRNA_I$ at in the presence of x (M) sodium chloride
$K_{eq\bullet x}$	an equilibrium constant for the reaction, $Lys + ATP + tRNA_A \rightleftharpoons Lys\text{-}tRNA_A + AMP + PPi$ at in the presence of x (M) sodium chloride
L-Lysamd	L-lysine amide
L-Lyshxt	L-lysine hydroxamate
LysRS	lysyl-tRNA synthetase
^{32}P-ATP	adenosine 5'-[γ-^{32}P] triphosphate.
PMSF	phenylmethanesulfonyl fluoride
PTH	phenylthiohydantoin
SAEC	*S*-(2-aminoethyl)-L-cysteine

$tRNA_A$	active tRNA that can be charged with L-lysine by LysRS
$tRNA_I$	inactive tRNA that can not be charged with L-lysine by LysRS
V_0	initial velocity
V_s	the velocity estimated in a linear line following a curve observed in the continuous assay

The other aminoacyl-tRNA synthetases are also abbreviated as the three-letter code of their specific amino acid followed by RS.

General introduction

The accuracy of translation of genetic messages depends on the precision of two successive independent matchings: first, that of amino acids with tRNA and second, that of charged tRNA with ribosome-linked mRNAs. The latter is a relatively simple example of direct interaction between two short nucleotide sequences, the anticodon and the codon, by base pairing. The former, the matching between amino acid and tRNAs, on the other hand, is skillful. It is mediated by specific enzymes, aminoacyl-tRNA synthetase (ARS), which recognize the two heterogeneous partners and catalyze the first-step reaction in protein biosynthesis, the aminoacylation reaction. There, each amino acid is first activated by specific ARS accompanying the hydrolysis of ATP according to the reaction.

$$ARS + AA + ATP \rightleftharpoons ARS\bullet AA\sim AMP + PPi \quad (1)$$

where AA and PPi denotes amino acid and pyrophosphate, respectively. Then, the activated AA is transferred to its cognate tRNA and attached to 3' or 2' hydroxyl group of the terminal 3' adenosine according to the reaction.

$$ARS\bullet AA\sim AMP + tRNA \rightleftharpoons ARS + AA\text{-}tRNA + AMP \quad (2)$$

The aminoacylation reaction are crucial and critical stage for fidelity in the biosynthesis of proteins. Therefore, an extremely high degree of substrate specificity for its cognate amino acid and tRNAs must be required for each ARS. In fact, it gives a good example to this question how each of these ARSs select its cognate amino acid from among 20 protein-constituting ones and its cognate tRNAs from among, for example, approximately 80 tRNA species.

The development of molecular biology presented many nucleotide sequences of ARS, and the amino acid sequence-

alignment techniques revealed the presence of characteristic amino acid sequences, what is called, "signature sequences" or "motifs", indicating that ARSs is divided into two groups, Class I with "signature sequences" and Class II with "motifs" ***(1)***. This partition was supported by the studies on the initial aminoacylation site of tRNA. tRNAs specific for Class I ARS were aminoacylated at 2' hydroxyl group of 3' terminal adenosine, while those specific for Class II ARS were done at 3' hydroxyl group ***(2)***.

The development of molecular biology also broken down "the first problem" in the *in vitro* studies on ARS, the preparation of adequate amounts of high-purity ARS by use of protein expression systems, which further did "the second problem", the information of 3D-structure of ARS. At present, X-ray crystallo-graphic analysis has revealed high-resolution structures of 11 ARSs ***(3)***, supporting the partition, and indicating that Class I and Class II ARSs have Rossmann-fold like catalytic domain and anti-parallel fold one, respectively. The "signature sequences" involves HIGH and KMSKS and the "motifs" does motif 1, motif 2, and motif 3, respectively. The HIGH was shown to be involved in ATP binding and the KMSKS was shown to be essential for the amino acid activation ***(4)***. The motif 1 was shown to be associated with the dimeric interface and only observed in α_2 dimers of ARS and the motif 2 and 3 were shown to construct a cavity of active site ***(4)***. The 3 crystal structures of ARS•tRNA complex for GlnRS (Class I) ***(5)***, SerRS (Class II) ***(6)***, and AspRS (Class II) ***(7)*** suggested that the mode of recognition of the acceptor stem of tRNA is different in Class I and Class II ARS. GlnRS approaches the tRNA acceptor stem from the minor groove side, while SerRS and AspRS do it from

the major groove side, though the acceptor stems of these tRNAs are very similar.

Moreover, the development of molecular biology might clear "the third problem" in the *in vitro* studies on ARS, the preparation of adequate amounts of high-purity cognate tRNAs. *In vitro* transcription of tRNA genes by T7 RNA polymerase yielded a transcript that is identical in sequence to tRNA but that lacks the nucleoside modifications of the mature tRNA ***(8)***. These unmodified tRNAs are often , fortunately, near normal substrates for the cognate ARS. This technique revealed "tRNA identity" and "second genetic code" which describe the features of a tRNA molecule which make that tRNA recognizable to one ARS and prevent it from being recognized by all other ARS ***(9)***. The approach that proved most fruitful in the establishment of tRNA identity was one in which an attempt was made to alter, with the fewest possible changes, the specificity of tRNA. Those changes were by definition elements of the identity of the tRNA. Specificity was monitored by determination of the kinetic parameters of aminoacylation of the tRNA by cognate and non-cognate ARS. These results suggest that ARS recognizes its cognate tRNAs through a few characteristic contact-points. No overexpression systems of native / mature tRNA has been constructed partly because of the difficulty in overexpression of tRNA-modifing enzymes. But, commercial specific tRNA purified comes to be available recently.

As "the 3 problems" in the *in vitro* studies on ARS come to be cleared, precise static and kinetic analysis is more possible and more needed for the comprehensive understanding of high degree of substrate specificity of ARS. Nevertheless, detailed kinetics has not yet applied to these ARSs whose 3D-structure has been

revealed recently. Of them, yeast AspRS (Class II) ***(7)*** is investigated kinetically the most in detail, where kinetic parameters of many mutant AspRSs are estimated on the basis of steady-state kinetics and the agreement between kinetic results and the prospect of 3D-structure analysis is emphasized. However, apparent contradiction can be pointed out between the prospect of 3D-structural analysis and the static results; in other words, the former indicates that AspRS obeys the ordered sequential mechanism with L-Asp first-bound, while the latter indicates that AspRS is not bound with L-Asp in the absence of ATP ***(7)***. Such contradiction can be observed in the pioneering and prominent studies on TyrRS (Class I) of *Bacillus stearothermophilus*, where precise static, kinetic (steady-state and pre-steady state kinetics), and 3D-structure analysis (TyrRS•L-Tyr and TyrRS•Tyr~AMP complex) have been made ***(10, 11, 12, 13)***. Why such a contradiction exists? Though many reports on ARSs explain that ARS obeys the Equation (1) and (2) except for the cases of GlnRS, GluRS, and ArgRS, where the amino acid activation reaction does not occur in the absence of tRNA, the basis of two-step reaction mechanism (rate-limiting step is reaction (2)) depends mainly on Class I ARSs, *E. coli* IleRS and TyrRS systems ***(14)***. Can such a mechanism be applied to the cases of other ARSs, especially Class II ARSs? Further, since there is a diversity in the side-chains of protein-constituting amino acids, it is probable that each ARS has characteristic recognition and discrimination mechanism for amino acid. In fact, the amino acid binding is described as a "dark passage" and only two crystallographic systems for *B.s.* TyrRS and *E. coli* LysRS have described the amino acid binding site at atomic resolution ***(4, 10, 15)***, though the ATP binding site is well conserved in each Classe

and described in more detail ***(4, 16)***. The high degree of substrate specificity of ARS has been plausibly explained in part by a number of proposed "proof-reading" or "editing mechanism" that prevent incorrectly recognized amino acids from entering the aminoacyl-tRNA pool of the cell ***(17~23)***. To what extent such exclusion-mechanisms contribute to the accuracy of the aminoacylation reaction? It is considered not a fortuitous fact that the exclusion-mechanism exists for correcting mis-aminoacylation by hydrophobic amino acids. This may be explained tentatively as follows: ARSs specific for hydrophobic amino acid are the ones which need this correction mechanism more strictly, because their active sites are bound to be less specific than the enzymes for polar amino acids ***(4)***. Do the ARSs for polar amino acid have such mechanism? It was reported that though the hydroxy analogues of amino acid not only can form the aminoacyladenylate intermediate but also can be transferred to tRNA, and that the misactivated hydroxy analogues are hydrolytically removed in the cases of the Class I enzymes specific for hydrophobic amino acid ***(24, 25)***. Do the Class II ARSs for polar amino acid have such a mechanism? In order to get the clue to elucidate the "super specificity" of ARS, I think that it is worthwhile to evaluate totally the recognition and discrimination mechanism for amino acid and its analogues in each reaction step or, possibly each elementary step. As far as I know, no such study has been conducted.

For this purpose, I have chosen as the target LysRS (Class II) of *Bacillus stearothermophilus*. There are several analogues of lysine relatively easily available, and our preliminary test revealed that LysRS activity in the crude extracts of *B. stearothermophilus* was much more stable than that of *E. coli*. These should be

advantageous for the study of mechanism of substrate specificity. There has been only one report on *B.s.* LysRS in which they presented purification procedures, amino acid composition, crystallization, and the effect of temperature on the reaction rate and K_m values ***(26)***. Though the 3D-structure of *E. coli* LysRS (*lys U*-encoded) with L-Lys is available ***(15)***, the detailed reaction mechanism has not yet been cleared with LysRS of any origin ***(27)***.

In this thesis, I purified B.s. LysRS by a new process and postulated the reaction pathway. Then, on the basis of the pathway, I evaluated totally the recognition and discrimination mechanism for L-Lys and its analogues in each reaction steps. Further, for the speculation of 3D-structure of *B.s.* LysRS by comparing its primary structure with those of *E. coli* LysRS and yeast AspRS, I cloned the gene, sequenced the its sequence and presumed its amino acid sequence of *B.s.* LysRS.

REFERENCES

1) Eriani, G., Delarue, M., Poch, O., Gangloff, J., and Moras, D. (1990) Partition of tRNA synthetases into two classes based on mutually exclusive sets of sequence motifs. *Nature*, **347**, 203-206

2) Sprintzl, M. and Cramer, F. (1975) Site of aminoacylation of tRNAs from *Escherichia coli* with respect to the 2'- or 3'-hydroxyl group of the terminal adenosine. *Proc. Natl. Acad. Sci. USA*, **72**, 3049-3053

3) Cusack, S. (1995) Eleven down and nine to go. *Nature Structual Biology*, **2**, 824-831

4) Delarue, M. and Moras, D. (1992) Aminoacyl-tRNA synthetases: Partition into two classes. "*Nucleic Acid and Molecular Biology*", **6**, ed. by Eckstein, F. and Lilley, D. M. J., Springer-Verlag, Berlin, Heidelberg, pp.203-224

5) Rould, M. A., Perna, J. J., and Steitz, T. A. (1991) Structural basis of anticodon loop recognition by glutaminyl-tRNA synthetase. *Nature*, **352**, 213-218

6) Cusack, S., Berthet-Colominas, C., Hartlein, M., Nasser, N., and Leberman, R. (1990) A second class of synthetase structure revealed by X-ray analysis of *Escherichia coli* s eryl-tRNA synthetase at 2.5Å. *Nature*, **347**, 249-255

7) Cavarelli, J., Eriani, G., Rees, B., Ruff, M., Boeglin, M., Mitschler, A., Martin, F., Gangloff, J., Thierry, J. C., and Moras, D. (1994) The active site of yeast aspartyl-tRNA synthetase: structural and functional aspects of the aminoacylation reaction. *EMBO J.*, **13**, 327-337

8) Sampson, J., R. and Uhlenbeck, O., C. (1988) Biochemical and physical characterization of an unmodified yeast phenylalanine transfer RNA transcrived *in vitro*. *Proc. Natl. Acad. Sci. USA*, **85**, 1033-1037

9) Normanly, J. and Abelson J. (1989) tRNA identity. *Ann. Rev. Biochem.*, **58**, 1029-1049

10) Brick, P., Bhat, T. N., and Blow, D. M. (1988) Structure of tyrosyl-tRNA synthetase refined at 2.3Å resolution. *J. Mol. Biol.* **208**, 83-98

11) Carter, C. W., Jr. (1993) Cognition, mechanism, and evolutionary relationships in aminoacyl-tRNA synthetases. *Annu. Rev. Biochem.* **62**, 715-748

12) Wells, T. N. C. and Fersht, A. R. (1986) Use of binding energy in catalysis analyzed by mutagenesis of the tyrosyl-tRNA synthetase. *Biochemistry* **25**, 1881-1886

13) Fersht, A. R., Mulvey, R. S., and Koch, G. L. E. (1975) Ligand binding and enzymatic catalysis coupled through subunits in tyrosyl-tRNA synthetase. *Biochemistry* **14**, 13-18

14) Fersht, A. R., Kaethner, M., M. (1976) Mechanism of aminoacylation of tRNA. Proof of the aminoacyl adenylate pathway for the isoleucyl- and tyrosyl-tRNA synthetase from *Escherichia coli* K12. *Biochemistry* **15**, 818-823

15) Onesti, S., Miller, A. D., and Brick, P. (1995) The crystal structure of the lysyl-tRNA synthetase (LysU) from *Escherichia coli. Structure*, **3**, 163-176

16) Carter, C. W., Jr. (1993) Cognition, mechanism, and evolutionary relationships in aminoacyl-tRNA synthetases. *Annu. Rev. Biochem.* **62**, 715-748

17) Fersht, A. R., Kaethner, M., M. (1976) Enzyme hyperspecificity rejection of threonine by the valyl-tRNA synthetase by misacylation and hydrolytic editing. *Biochemistry* **15**, 3342-3346

18) Fersht, A. R. and Dingwall, C. (1979) Establishing the misacylation/deacylation of the tRNA pathway for the editing mechanism of prokaryotic and eukaryotic valyl-tRNA synthetase. *Biochemistry* **18**, 1238-1245

19) Fersht, A. R. and Dingwall, C. (1979) An editing mechanism for the methionyl-tRNA synthetase in the selection of amino acids in protein synthesis. *Biochemistry* **18**, 1250-1256

20) Eldred, E. W. and Schimmel, P. R. (1972) Rapid deacylation by isoleucyl transfer ribonucleic acid synthetase of

isoleucine-specific transfer ribonucleic acid aminoacylated with valine. *J. Bio. Chem.* **247**, 2961-2964

21) Yarus. M. (1972) Phenylalanyl-tRNA synthetase and isoleucyl-$tRNA^{Phe}$: A possible verification mechanism for aminoacyl-tRNA. *Proc. Natl. Acd. Sci. USA* **69**, 1915-1919

22) Jakubowski H. (1993) Proofreading and the evolution of a methyl donor function. *J. Biol. Chem.* **268**, 6549-6553

23) Jakubowski H. (1994) Editing function of *Escherichia coli* cysteinyl-tRNA synthetase: cyclization of cysteine to cysteine thiolactone. *Nucleic Acid Res.* **22**, 1155-1160

24) English, S., English, U., Haar, F. von der, and Cramer, F. (1986) The proofreading of hydroxy analogues of leucine and isoleucine by leucyl-tRNA synthetases from *E. coli* and yeast. *Nucleic. Acid. Res.* **14**, 7529-7539

25) English-Perters, S., Haar, von der F. , and Cramer, F. (1990) Fidelity in the aminoacylation of $tRNA^{Val}$ with hydroxy analogues of valine, leucine, and isoleucine by valyl-tRNA synthetases from Saccharomyces cerevisiae and *E. coli. Biochemistry* **29**, 7953-7958

26) Samuelsson, T. and Lundvik, L. (1978) Purification and some properties of asparagine, lysine, serine, and valine: tRNA ligases from *Bacillus stearothermophilus. J. Biol. Chem.* **253**, 7033-7039

27) Freist, W. and Gauss, D. H. (1995) Lysyl-tRNA synthetase. *Biol. Chem. Hoppe-Seyler*, **376**, 451-472

Classification, subunit composition,size, and status of structure determination of aminoacyl-tRNA synthetase

CLASS I				CLASS II			
	ARS	Subunit	Size (E.coli)		ARS	Subunit	Size (E.coli)
Ia				IIa			
	Cys	α	461 res.		Ser#	α_2	430 res.
	Val	α	951		Thr	α_2	642
	Ile	α	939		Pro	α_2	572
	Leu	α	860		His*	α_2	424
	Met*	α, α_2	677(α_2)		Gly*	α_2	506 (T.th)
	Arg	α	577				
Ib				IIb			
	Glu*	α	471		Asp#	α_2	590
	Gln#	α	550		Asn	α_2	465
					Lys*	α_2	505
Ic				IIc			
	Tyr*	α_2	424		Phe*	$(\alpha\beta)_2, \alpha$	327,795
	Trp*	α_2	334		Gly	$(\alpha\beta)_2$	303,689
					Ala	α_4, α	876 (α_4)
MOTIFS							
	Φ[1)]-h-Φ-G-h			(1)	gΦxxΦxxpΦ Φ		
	k-m-s-K-s			(2)	f-R-x-e-loop-h/rxxxfxxx(d/e)		
				(3)	gΦgΦgΦ(d/e)RΦ Φ Φ Φ Φ		
FOLD OF CATALYTIC DOMAIN							
	Rossmann-fold				Anti-parallel fold		
INITIAL SITE OF AMINOACYLATION							
	2'OH of term. rib.				3'OH of term. rib.		

*,# :The 3D structure of the enzyme(*) and the enzyme-tRNA complex(#) known

[1)]:hydrophobic

[After S.Cusack,*Nature St. Biol.* (1995)]

Schematic drawing of the catalytic domains of aminoacyl-tRNA synthetase

Class I ARS

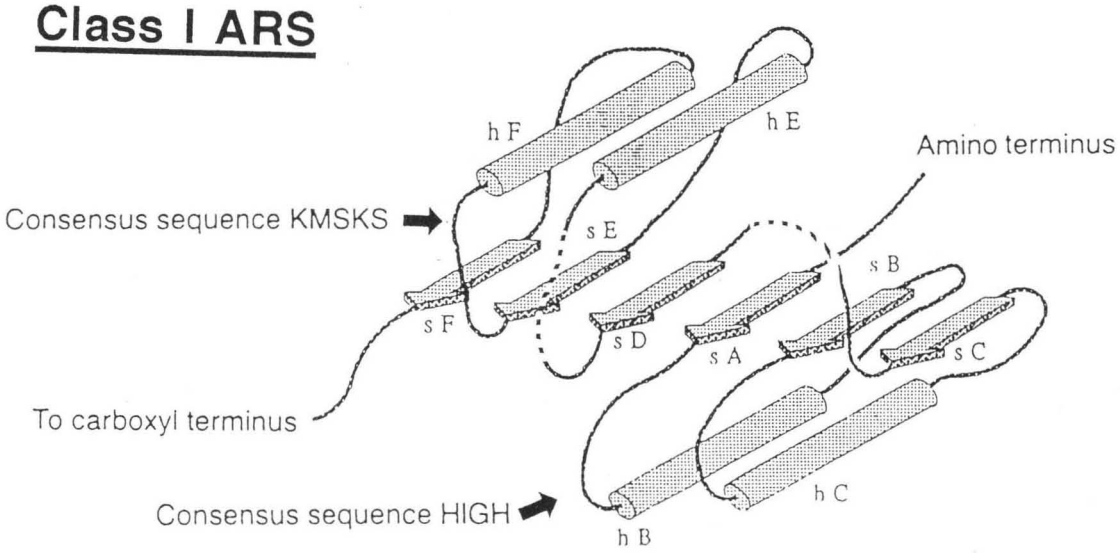

Class II ARS

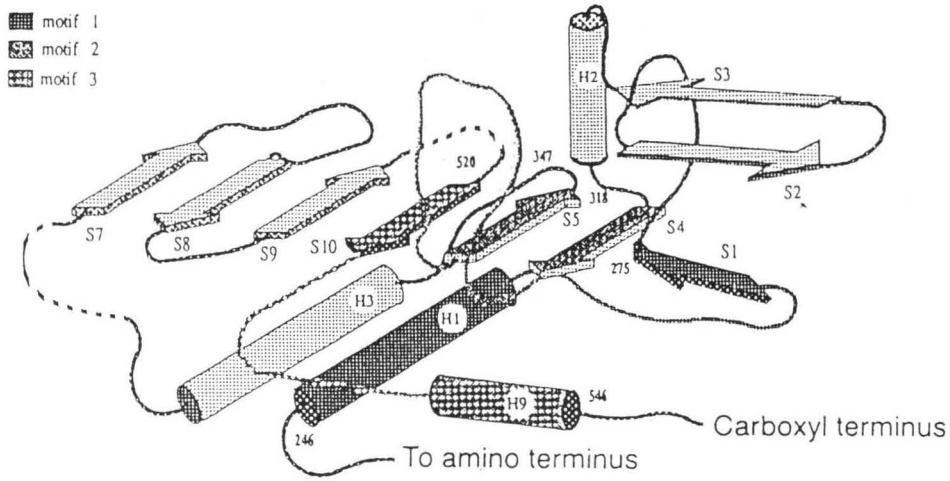

Aminoacylation reaction catalyzed by Class I ARS

$$E + AA + ATP \rightleftharpoons E{\cdot}AA{\sim}AMP + PPi \quad (1)$$

$$E{\cdot}AA{\sim}AMP + tRNA \rightleftharpoons E + AA\text{-}tRNA + AMP \quad (2)$$

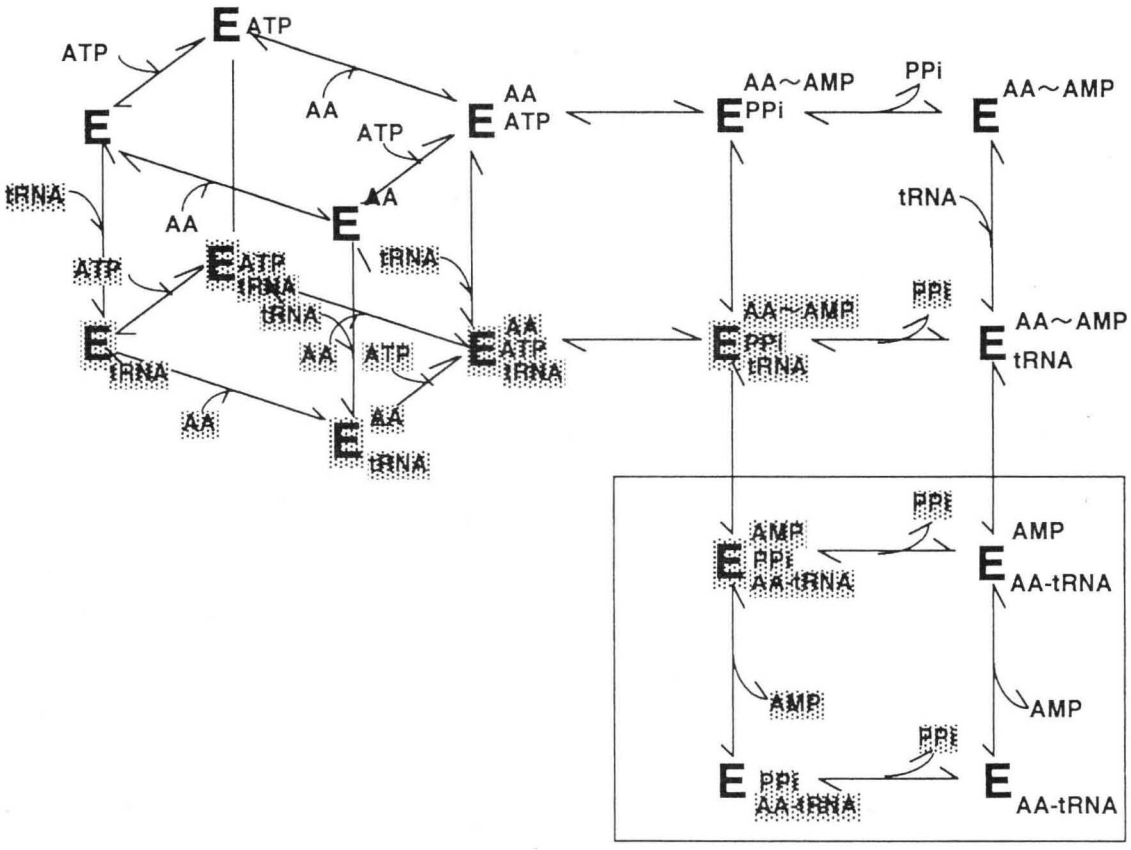

3D-Structure of *E. coli* LysRS complexed with L-lysine

Motif 1, white ribbon; Motif 2, pink ribbon; Motif 3, red ribbon. L-Lysine is shown by a sphere model, α-carboxyl (orange), α-amino (yellow), and ε-amino groups (blue).

3D-Structure of yeast AspRS complexed with ATP and $tRNA^{Asp}$

Motif 1, white ribbon; Motif 2, pink ribbon; Motif 3, red ribbon. ATP is shown green by a stick model. tRNA is shown orange by backbone except adenosine 76 of tRNA by a stick model (red point shows 3'-OH, the first aminoacylation site by Class II ARS).

Chapter 1
Purification, and Fluorometric and Kinetic Analysis of the Binding of Substrates, L-Lysine and ATP

An aminoacyl-tRNA synthetase (abbreviated to ARS) catalyzes the binding of an amino acid to the cognate tRNA, generally according to the following reaction scheme *(1)*.

$$E + AA + ATP \rightleftharpoons E{\bullet}AA{\sim}AMP + PPi \quad (1)$$

$$E{\bullet}AA{\sim}AMP + tRNA \rightleftharpoons E + AMP + AA\text{-}tRNA \quad (2)$$

where AA denotes the amino acid; E, ARS; PPi, inorganic pyrophosphate; and E•AA~AMP, an aminoacyl-adenylate-ARS complex. This tRNA aminoacylation reaction is crucial and critical for the fidelity of translation of the genetic information into the structure of a protein. A high degree of substrate specificity for each heterogeneous substrate: amino acids, nucleotides, and tRNAs, must be required for ARS. Elucidation of the mechanism for this strict discrimination of the substrate structure is of vital importance. ARSs for 20 kinds of amino acid that constitute proteins are not necessarily the same in their quaternary structures (monomers, dimers, and tetramers) *(2)*, and show considerable variations in the primary structure, although they catalyze the same type of chemical reactions. Detailed studies on the structure-function relationship is necessary for each ARS specific to each of 20 amino acids.

In recent years, determination of the primary structure of ARSs has rapidly progressed. Twenty kinds of ARSs can be classified into two classes according to their primary structure *(2, 3, 4)*. Class I enzymes include those specific for cysteine, methionine, valine, leucine, isoleucine, arginine, glutamic acid, glutamine, tyrosine, and tryptophan, whereas Class II enzymes include those for glycine,

alanine, serine, threonine, proline, histidine, lysine, aspartic acid, asparagine, and phenylalanine. Class I enzymes are characterized by the consensus signature sequence, HIGH and KMSKS, while Class II enzymes by three unique sequences, Motif 1, Motif 2, and Motif 3 ***(2, 3)***. Determination of the three dimensional structure of ARS by X-ray crystallography has been successful with TyrRS of *Bacillus stearothermophilus* ***(4, 5)***; MetRS ***(6)***, SerRS ***(7)***, GlnRS ***(8)***, and LysRS (*lys U*-encoded) ***(9)*** of *Escherichia coli*; SerRS ***(10)*** and GluRS ***(11)*** of *Thermus thermophilus*; TrpRS ***(12)***, PheRS ***(13)***, and AspRS of *Saccharomyces cerevisiae* ***(14)***. Analysis of structure-function relationship has progressed rapidly. However, as more structural information becomes available, more precise kinetic information obtained with the purified enzymes is wanted to analyze the molecular mechanism of the reaction. Apparent contradiction, for example, can be pointed out between the results of structural analysis and those of the kinetic analysis that have been regarded as superb achievement ***(2, 3, 5)***. Much effort is still required in enzyme chemistry.

I have strong interest in elucidating the molecular mechanism for the strict substrate specificity of ARSs and have chosen as the target LysRS of *Bacillus stearothermophilus*. There are several analogues of lysine relatively easily available, and my preliminary test revealed that LysRS activity in the crude extracts of *B. stearothermophilus* was much more stable than that of *E. coli*. These should be advantageous for the study of mechanism of substrate specificity.

There has been only a report on LysRS of *B. stearothermophilus* (abbreviated to *B.s.* LysRS) by Samuelsson and Lundvik ***(15)***, in which they presented purification procedures,

amino acid composition, crystallization, and the effect of temperature on the reaction rate and K_m values. However, most of the studies on LysRS have been done with *E. coli* ***(16~20)*** and yeast ***(21, 22)*** enzymes, and yet the detailed reaction mechanism has not been cleared with LysRS of any origin ***(23)***. As I wish to study *B.s.* LysRS more comprehensively, I need first to establish better purification procedure and to reveal other basic properties of the enzyme necessary for further development of the investigation.

In the present study, I have obtained a highly purified stable preparation of *B.s.* LysRS with a novel procedure giving a good yield, and have characterized some basic properties of the enzyme. I have also examined features of the binding of substrates, L-lysine and ATP, and of their analogues with ligand-induced quenching of protein fluorescence as probe as well as with equilibrium dialysis. In addition, the order of binding of these substrates to *B.s.* LysRS has been elucidated by steady state kinetic analysis.

MATERIALS AND METHODS

Amino acids and lysine analogues: All L-amino acids were purchased from either Wako Pure Chemical Industries, Nakarai Tesque, or Takara Kohsan Co. Cadaverine, 6-amino-*n*-hexanoic acid, L-norleucine, L-ornithine, and D-lysine were purchased from Nakarai Tesque. L-Lysine hydroxamate, L-lysine amide, *N*α-acetyl-L-lysine, *N*ε-methyl-L-lysine, *N*ε-acetyl-L-lysine, and 5-hydroxylysine (mixed DL and DL-allo) were obtained from Sigma Chemical Co. *S*-(2-aminoethyl)-L-cysteine was the product of Wako Pure Chemical Industries. *Threo*-4-hydroxy-L-lysine was purchased from Fluka Fine Chemicals.

Others: ATP (disodium salt), α,β-methyleneATP, $tRNA^{Lys}$ from *Escherichia coli* was the product of Sigma Chemical Co.; dialysis membrane Spectra/POR 7 (molecular weight cut off, 10,000), of Spectrum Medical Industries; charcoal (washed with hydrochloride), of Nakarai Tesque; adenosine, of Oriental Yeast Co.; isatoic anhydride, of Tokyo Kasei Kogyo Co.; ADP, AMP, GTP, CTP, and UTP, of P-L Biochemicals. Silica gel plate DC-Alufolien Kieselgel 60 F254 was purchased from E. Merck. [4,5-^{3}H] L-lysine was the product of NEN Research Products; ^{32}P-pyrophosphate, of Amersham International; [2,8-^{3}H] adenosine 5'-triphosphate tetraammonium salt, of Moravek Biochemicals; streptomycin sulfate, of Meiji Seika Kaisha. DEAE-Toyopearl 650M and AF Red Toyopearl 650 ML were the products of Tosoh Co.; Dyematrex Red A and Dyematrex Blue A, of Amicon Corporation; Lysine-sepharose 4B, Sephacryl S-200 Superfine, and a Mono Q HR5/5 prepacked column, of Pharmacia Fine Chemicals; glass microfiber filter (GF/C), of Whatman. Unfractionated tRNA from *E. coli* MRE 600 was purchased from Boehringer Mannheim. All other chemicals were of reagent grade.

Synthesis of anthraniloyl-ATP: Ant-ATP was synthesized according to the methods of Hiratsuka ***(24),*** lyophilized, and stored at -20°C until use.

Preparation of tRNA mixture: Unfractionated tRNA mixture was prepared from *E. coli* K12 cells by the method of Zubay ***(25)*** with some modifications ***(26)***. The tRNA mixture obtained was dissolved in sterile water and stored at -20°C until use.

Protein concentration: Protein concentration was measured either by the method of Lowry *et al.* ***(27)*** with crystalline bovine serum albumin as the standard, or spectrophotometrically with the

molar absorption coefficient, ε, at 280nm of 71,600 $M^{-1}cm^{-1}$ at pH 8.0 (see Results).

Aminoacylation reaction assay: The aminoacylation of tRNA with radioactive L-lysine was used to measure the activity of LysRS. The standard reaction mixture contained in 0.5ml: 100mM Tris-HCl buffer (pH 8.0), 10mM $MgCl_2$, 1mM ATP, 100μM ^{3}H-L-lysine (40mCi/mmol), and 20A_{260} units of tRNAmix obtained from *E. coli* K12. After preincubation at 37°C for 3min, the reaction was started by the addition of 50μl of the enzyme solution. The reaction was stopped, after incubation at 37°C for several different time intervals, by adding 3ml of cold 5% trichloroacetic acid. The mixture was kept at 0°C for 30min and filtered through Whatman GF/C glass fiber filter. The radioactivity remaining on the filter was measured in a Packard Liquid Scintillation Spectrometer Tri Carb 3255 as described previously ***(28)***. One unit of enzyme is defined as the amount that incorporates 1μmol of L-lysine into tRNA in 1min under these conditions. K_m and V_{max} were calculated by the nonlinear least-squares method ***(29)***.

ATP-PPi exchange reaction assay: LysRS activity was measured also by the ATP-PPi exchange reaction by the method of Seno *et al.* ***(30)*** with some modifications. The standard reaction mixture contained in 0.5ml: 100mM Tris-HCl buffer (pH 8.0), 10mM $MgCl_2$, 1mM ^{32}P-pyrophosphate (6.4mCi/mmol), 1mM L-lysine, and 1mM ATP. After preincubation at 37°C for 3min, the reaction was started by the addition of 50μl of the enzyme solution. The reaction was stopped, after incubation at 37°C for several different time intervals, by adding 7.5% perchloric acid containing 100mM sodium pyrophosphate. ATP was adsorbed to charcoal by adding 0.1ml of charcoal suspension (10% w/v). After 10min at 0°C

charcoal was collected on Whatman GF/C filter, and the radioactivity trapped on the filter was counted in the Packard Liquid Scintillation Spectrometer Tri Carb 3255 as described previously ***(28)***. K_m and V_{max} were calculated similarly as in the aminoacylation reaction.

Purification of LysRS: *B. stearothermophilus* NCA1503 cells were supplied by Unitika, Ltd, and stored at -20°C until use. All operations were done at 4°C unless otherwise mentioned. The standard buffer was 20mM Tris-HCl buffer (pH 8.0) containing 2mM EDTA, 10mM 2-mercaptoethanol, 0.1mM phenylmethanesulfonyl fluoride (abbreviated to PMSF), and 0.2% (v/v) isopropyl alcohol.

Step1. Cell extraction: *B. stearothermophilus* NCA1503 cells (300g) kept frozen at -20°C were suspended in 1l of the standard buffer. The suspension was sonicated for 30min in an ice bath. The sonicated suspension was centrifuged at 12,000×g for 60min at 4°C and the supernatant fraction was termed Crude extract (750ml).

Step 2. Streptomycin precipitation: Streptomycin sulfate was added to the Crude extract to the final concentration of 2.5% with stirring in an ice bath. After 30min of stirring, this solution was centrifuged at 8,000×g for 30min, and the supernatant fraction was collected (880ml).

Step 3. DEAE-Toyopearl 650 M chromatography: The supernatant solution obtained in Step 2 was loaded onto a DEAE-Toyopearl 650 M column (6.5×21cm) equilibrated with the standard buffer. The active fractions were obtained by stepwise elution with 100mM Tris-HCl buffer (pH 7.0) containing 0.17M NaCl, 2mM EDTA, 10mM 2-mercaptoethanol, 0.1mM PMSF, and 0.2% (v/v) isopropyl alcohol.

Step 4. Dyematrex Blue A column chromatography: The active fraction obtained in Step 3 was loaded onto a Dyematrex Blue A column (3.2×23cm) equilibrated with the standard buffer. The active fractions were obtained by stepwise elution at 0.35M NaCl.

Step 5. Dyematrex Red A column chromatography: The active fraction obtained in Step 4 was loaded onto a Dyematrex Red A column (2.8×20cm) equilibrated with the standard buffer. The active fractions were eluted stepwise at 0.45M NaCl and concentrated by ultrafiltration with Diaflo Membrane YM10 and then dialyzed against the standard buffer at 4°C.

Step 6. Lysine-Sepharose 4B chromatography: The dialyzed solution obtained in Step 5 was loaded onto a Lysine-Sepharose 4B column (2.4×13cm) equilibrated with the standard buffer. The enzyme was eluted with a linear concentration gradient of NaCl in the standard buffer. The fractions with enzyme activity that appeared at NaCl concentration from 40mM to 60mM were pooled.

Step 7. AF-Red Toyopearl 650 ML chromatography: The active fraction obtained in Step 6 was diluted twice with the standard buffer and loaded onto an AF-Red Toyopearl 650 ML column (2.8×17cm) equilibrated with the standard buffer. The enzyme was eluted with a linear concentration gradient of NaCl from 0.35M to 0.7M. The pooled fraction with enzyme activity was concentrated by ultrafiltration with Diaflo Membrane YM10 and then with a Centriprep-10 concentration tube.

Step 8. Column chromatography on Mono Q HR5/5:
In some batches of purification, the final LysRS preparation at Step 7 contained very minute amount of contamination on PAGE, and Step 8 was applied in such cases.

The concentrated sample in Step 7 was applied to a Mono Q HR5/5 column equilibrated with 100mM Tris-HCl buffer (pH 8.0) in a Pharmacia FPLC system at room temperature. The enzyme was eluted with a linear concentration gradient of NaCl from 0M to 1.0M. The active fractions were pooled and dialyzed against the standard buffer, and this was stored at 4°C as the final preparation.

Molecular weight determination: The molecular weight of LysRS was measured both by gel filtration with a Sephacryl S-200 column (2.5×79cm) and by SDS-PAGE with a Pharmacia Phast System with a PhastGel Gradient 8-25.

Amino acid composition analysis: The purified LysRS was hydrolyzed in vacuo at 110°C either in 6N HCl for 24, 48, and 72 h or in 4N methanesulfonic acid containing 0.2% 3-(2-aminoethyl) indole for 24 h. Amino acid analysis was conducted with ninhydrine reaction on a Hitachi 835 amino acid analyzer .

Effect of pH: In the aminoacylation reaction and the ATP-PPi exchange reaction, the enzyme activity was measured at 37°C in the pH range 5-10 as described above except that 10mM piperazine-glycylglycine buffer or 100mM glycine-NaOH buffer were used. All contained 0.1M NaCl and 10mM $MgCl_2$. The enzyme concentrations were 0.8nM and 4.0nM in the aminoacylation and the ATP-PPi exchange reaction, respectively. To examine the pH stability, the enzyme solutions (11nM) at different pH were incubated at 37°C for 1~6 h. In the pH range 4.3~9.3, 10mM piperazine-glycylglycine buffer was used. At pH 3.3 and 10.1, 100mM glycine-HCl buffer and glycine-NaOH buffer were used, respectively. All contained 0.1M NaCl and 10mM $MgCl_2$. The enzyme activity was measured in the aminoacylation

reaction under the conditions described above at pH 8.0, 37°C, $[E]_0$=1.0nM.

Effect of temperature: The effect of temperature on the enzyme activity was investigated in the range of 0 to 70°C in the aminoacylation reaction and the ATP-PPi exchange reaction both at pH 8.0. The enzyme concentration used was 1.7nM in the aminoacylation reaction and 4.0nM in the ATP-PPi exchange reaction. To examine heat stability, the enzyme solution (11nM in 10mM piperazine-glycylglycine buffer (pH8.0) containing 0.1M NaCl and 10mM $MgCl_2$) was incubated in the range of 20 to 60°C for 1~6 h. The remaining activity was measured in the aminoacylation reaction under the conditions described above at pH 8.0, 37°C, $[E]_0$=1.0nM.

Fluorescence spectroscopy: Fluorescence spectra were measured at 30°C with a Hitachi Fluorescence Spectrophotometer 850. The excitation spectra were obtained with the fixed emission wavelength of 340nm, and the emission spectra were recorded with the excitation at 280nm and 295nm. The purified LysRS was dialyzed, before the fluorescence measurement, against 100mM Tris-HCl buffer (pH 8.0) containing 10mM $MgCl_2$.

Fluorescence titration of *B.s.* LysRS with ligands was conducted at 30°C in the same buffer. The excitation wavelength and emission wavelength were 295nm and 340nm, respectively, when the quenching of LysRS fluorescence by the addition of L-lysine or ATP was measured. The excitation wavelength and emission wavelength were 375nm and 428nm, respectively, when quenching of Ant-ATP fluorescence was measured. The absorbance of the enzyme solution was less than 0.1cm^{-1} at the excitation wavelength, 295nm. The fluorescence intensity was corrected for

dilution of LysRS due to addition of the ligand solutions when the quenching of LysRS was measured. The enzyme solution was placed in a quartz cell thermostated at 30°C and then the ligand solutions were added to the enzyme solution with a micro syringe and stirred. After 2 min, the fluorescence intensity was measured.

The values of the dissociation constant (K_d) for the enzyme-ligand complex (E•L) and of the fluorescence intensity decrease (ΔF_{max}) at 340nm (as a percentage) that would be observed when the enzyme was saturated with the ligand were determined by assuming a simple bimolecular binding equilibrium between the enzyme, E, and ligand, L, (Equations 3, 4, and 5) using the nonlinear least squares method ***(29)***.

$$E + L \rightleftharpoons E\bullet L \qquad (3)$$

$$K_d = [E][L]/[E\bullet L] \qquad (4)$$

$$\Delta F\,(\%) = \Delta F_{max}[L]_0/(K_d + [L]_0) \qquad (5)$$

where $[L]_0$ is the total concentration of the ligand, $[L]_0=[L]+[E\bullet L]$, and ΔF is the fluorescence intensity change observed at 340nm when a certain amount of the ligand is added. This is expressed as a percentage of the fluorescence intensity of the enzyme; namely $\Delta F\,(\%) = 100\times(F_{E\bullet L}-F_E)/F_E$, where $F_{E\bullet L}$ and F_E are the fluorescence intensities at 340nm of the enzyme-ligand complex and the enzyme, respectively.

Equilibrium dialysis: All equilibrium dialysis experiments were done in a 4°C compartment. The buffer used for the experiments was 100mM Tris-HCl buffer (pH 8.0) containing 10mM $MgCl_2$. Each dialysis chamber was separated by membrane Spectra/POR 7. In the search for the binding between LysRS and L-lysine, one chamber (100μl) contained 13.9μM LysRS and the other (100μl) contained ^{3}H-L-lysine in the concentration range of

1μM to 1mM without ATP. In the search for the binding between LysRS and ATP, one chamber contained the same concentration of LysRS and the other contained ^{3}H-ATP in the same concentration range without L-lysine. After the apparatus was slowly rotated for 30 h at 4°C, samples were withdrawn from each chamber and the radioactivity of each sample was measured in a Packard Liquid Scintillation Spectrometer Tri Carb 3255. In the preliminary tests we found that 30 h were long enough to reach equilibrium under the conditions employed.

Kinetic determination of the order of substrate binding: Cole and Schimmel ***(31)*** and Santi *et al.* ***(32)*** have established procedures for the kinetic analysis of the ATP-PPi exchange reaction to determine the order of the binding of substrates among three possibilities: (a) AA binds first, (b) ATP binds first, and (c) AA and ATP bind in a random sequence. The effects of the substrate concentration on the initial velocity (v) of the ATP-PPi exchange reaction were examined at pH 8.0, 37°C according to their procedures. The concentration of one substrate (called the 'variable substrate' for convenience) was varied at each of several fixed concentrations of the other substrate (called the 'fixed substrate' for convenience). The effects of dead-end inhibitors (substrate analogues); cadaverine and adenosine, on the reaction rate were also examined. Graphic patterns of the double reciprocal plots, $1/v$ *versus* $1/$[variable substrate], at the several fixed concentrations of the fixed substrate or the dead-end inhibitors were examined. In each case, replots of the slopes and the vertical intercepts in the double reciprocal plots were tried.

RESULTS

Purification, molecular weight, and amino acid composition: Three mg of highly purified LysRS was obtained from 300g of frozen cells of *B. stearothermophilus*. The yield of activity in this novel purification procedure was about 30% with total purification of 1,100 fold (**Table I**). A single band was obtained both with PAGE and with SDS-PAGE. The molecular weight of LysRS was estimated to be 120,000 by gel filtration on a Sephacryl-S200 column and to be 60,000 by SDS-PAGE. The amino acid composition determined here is essentially consistent with the one previously reported by Samuelsson & Lundvik ***(15)*** only with some difference in the content of L-glutamic acid plus L-glutamine and that of L-alanine, and the minimum molecular weight calculated on this composition is about 57,700. Only one set of N-terminal amino acid sequence (Ser-His-Glu) has been obtained (Takita *et al.* to be published). From those results I conclude that *B.s.* LysRS is a homodimer.

UV absorption spectra and molar absorption coefficient: The UV absorption spectrum of LysRS was recorded at 25°C, pH 8.0 (λ_{max}=277nm, λ_{min}=250nm, A_{min}/A_{max}=0.44). The observed molar absorption coefficient, ε, at 280nm is 71,600$M^{-1}cm^{-1}$ ($A^{1\%}_{280}$=6.18) based on the molecular weight of the enzyme as dimer, 115,400. The value is consistent with 71,700$M^{-1}cm^{-1}$ ($A^{1\%}_{280}$=6.19) at pH 7.1 that is estimated from the content of the aromatic amino acids (3Trp, 16Tyr, and 24Phe / 57,700 protein).

pH-activity profile and pH-stability: The pH-activity profile of my highly purified *B.s.* LysRS (data not shown) in the ATP-PPi exchange reaction is broader in the alkaline pH region than that in the aminoacylation reaction, though the optimum pH is 8.3 in both

reactions. Examination of pH stability **(Fig. 1)** indicates that under my assay conditions for the pH-activity relationship (pH6~10, 37°C, 5min), denaturation of *B.s.* LysRS is negligible.

Optimum temperature and thermostability: The optimal temperature of *B.s.* LysRS is 50°C in both the aminoacylation reaction and the ATP-PPi exchange reaction at pH8, and both enzyme activities were completely lost at 70°C (data not shown). Since both activities similarly decreased at above 50°C, this heat inactivation is not due to the denaturation of tRNA. *B.s.* LysRS is stable below 50°C at pH 8.0 for 5 h. At 60°C, however, the aminoacylation activity is lost completely after 4 h. I compared the thermostability of the aminoacylation reaction in the crude extracts of *E. coli* K-12 and *B. stearothermophilus* NCA1503 at 50°C at pH 8.0. *E. coli* LysRS activity was completely lost within 5min, while *B.s.* LysRS activity was held full after 60min.

Kinetic parameters: K_m for L-lysine in the aminoacylation reaction and the ATP-PPi exchange reaction at pH 8.0, 37°C were 16.4±3.9μM and 23.6±2.1μM, respectively, over the range of L-lysine concentration of 5~200μM. K_m for ATP at pH 8.0, 37°C is 23.2±4.0μM in the aminoacylation reaction over the range of ATP concentration of 25~400μM, and 65.1±5.3μM in the ATP-PPi exchange reaction over the ATP concentration range of 10~1,000μM. The substrate inhibition by ATP was observed at the concentration more than 400μM in the aminoacylation reaction, but no such inhibition was detected in the ATP-PPi exchange reaction. The apparent k_{cat} was estimated as $3.2s^{-1}$ in the aminoacylation reaction and $40.9s^{-1}$ in the ATP-PPi exchange reaction.

Fluorescence spectrometry: **Figure 2** shows the excitation and emission spectra of fluorescence of *B.s.* LysRS at pH 8.0, 37°C. They are typical for a protein containing both tyrosine and tryptophan residues: λ_{max} of excitation is 282nm for the emission at 340nm. λ_{max} of emission is 328nm by excitation at 280nm and 335nm by excitation at 295nm. A small shoulder is detected around 320nm in the emission spectra by excitation at 295nm. At the excitation wavelength 295nm and emission wavelength 340nm, the relative fluorescence quantum yield of the enzyme was 0.27 when the relative quantum yield of *N*-acetyl-L-tryptophan ethyl ester was assumed 0.2 ***(33)***.

Addition of L-lysine to *B.s.* LysRS resulted in a decrease of the fluorescence intensity (**Fig. 2**), and the enzyme can be titrated by L-lysine with the fluorescence quenching as probe (**Fig. 3**). This titration curve was fitted to Equation 5, and K_d and ΔF_{max} were calculated to be 20.4±1.8μM and –16.2±0.3%, respectively (**Table II**). On the other hand, the addition of ATP, other nucleotides, or Ant-ATP caused no appreciable change in the fluorescence intensity (**Table II**). These results are consistent with the results of equilibrium dialysis study that will be presented below. Accordingly the lysine induced quenching of *B.s.* LysRS fluorescence can be regarded to represent the ligand-enzyme binding.

Fluorescence titration of LysRS with other amino acids: The ligand induced quenching of LysRS fluorescence was measured with several amino acids. The fluorescence change was observed with L-glycine , L-glutamine, and L-methionine among those amino acids tested (**Table II**). The K_ds for these amino acids were larger

than that of L-lysine more than 1000-fold, though ΔF_{max} was rather similar to that of L-lysine.

Fluorescence titration of LysRS with lysine analogues: Lysine analogues whose addition to *B.s.* LysRS caused the quenching of the enzyme fluorescence are classified into 2 groups **(Table III)**. The first group contains α-carboxyl group-modified compounds: L-lysine hydroxamate, L-lysine amide, and cadaverine. The second group contains D-lysine and the side-chain-modified compounds: *S*-(2-aminoethyl)-L-cysteine, *threo*-4-hydroxy-L-lysine, 5-hydroxylysine, and L-ornithine. **Figure 4** shows the titration curves with *S*-(2-aminoethyl)-L-cysteine, L-lysine-hydroxamate, and D-lysine for which K_d's were calculated by Equation 5 to be 197±24μM, 704±79μM, and 3,180±180μM, respectively.

Equilibrium dialysis: The binding of L-lysine and ATP to *B.s.* LysRS were examined separately by the equilibrium dialysis method at pH 8.0, 5°C, with ^{3}H-labeled substrates. **Figure 5** indicates that 1.79±0.28 moles of L-lysine are bound to a mole of dimer enzyme with apparent K_d of 5.44±0.41μM, and that ATP binding did not take place in the ATP concentration range of 1μM~1mM. These findings are consistent with the results of fluorometric studies shown above **(Table II)**.

ATP-PPi exchange reaction activity: All 20 L-amino acids constituting protein were tested for the amino acid dependent ATP-PPi exchange reaction catalyzed by *B.s.* LysRS. No activity was detected with 19 amino acids except L-lysine either at 1mM or 10mM of substrate concentration **(Table III)**. Lysine analogues were also examined for the activity of the ATP-PPi exchange reaction in the same manner. The activity was detected with *S*-(2-

aminoethyl)-L-cysteine, L-ornithine, 5-hydroxylysine, and threo-4-hydroxy-L-lysine. The estimated K_ms and k_{cat} are listed in **Table III**.

The enzymatic, L-lysine dependent synthesis of 5', 5' -diadenosine tetraphosphate (Ap_4A) was observed by HPLC with a Novapack C_{18} column (data not shown) by incubating 100nM *B.s.* LysRS with 2mM L-lysine and 5mM ATP in 20mM Tris-HCl buffer (pH 7.6) containing 150mM KCl and 130μM $ZnCl_2$, 37°C, for 2~6 hours.

Inhibition of the ATP-PPi exchange reaction by lysine-analogues: The inhibitory effects of lysine analogues on the L-lysine dependent ATP-PPi exchange reaction were examined **(Table III)**. Relative inhibition is represented by the percentage of the initial rate according to Equation 6.

$$\text{Inhibition } (\%) = (v\text{-}v_i)\times 100/v \qquad (6)$$

where v is the initial rate without inhibitors and v_i is the initial rate in the presence of the inhibitors at 4mM.

Those compounds in which α-carboxyl group was modified strongly inhibited the reaction. Among the compounds in which either ε- or α-amino group was modified, only 6-amino-*n*-hexanoic acid caused appreciable inhibition. D-Lysine inhibited effectively the reaction. The estimated inhibitor constants K_is are shown in **Table III**.

***Kinetic analysis of the order of binding of L-lysine and ATP* to *B.s.* LysRS:** When L-lysine was the variable substrate with different but fixed concentrations of ATP in the ATP-PPi exchange reaction, the point of intersection in the double reciprocal plots of the reaction rate and the variable substrate concentration was to the left of the vertical axis: the similar pattern to the non-competitive type inhibition. The replot of the slopes of each plot versus 1/[ATP]

showed a straight line passing through the origin. On the other hand, when ATP was the variable substrate with different but fixed concentrations of L-lysine, the point of intersection of the double reciprocal plots was on the vertical axis: the similar pattern to the competitive inhibition. The replot of the slopes versus 1/[L-Lysine] showed a straight line that does not pass through the origin. These patterns are consistent with those of the ordered bireactant mechanism where an amino acid is first bound to the enzyme ***(31, 32)*** **(Table IV)**.

Inhibition studies are useful to determine the order of the substrate binding. Cadaverine and adenosine were used as dead-end inhibitors against L-lysine and ATP, respectively. Cadaverine acts as a competitive inhibitor, regardless whether the variable substrate is L-lysine or ATP. Adenosine acts as an uncompetitive inhibitor of L-lysine and as a competitive inhibitor of ATP. These patterns also suggest that L-lysine is first bound to LysRS ***(31, 32)*** **(Table IV)**. The inhibitor constants (K_i) of cadaverine and adenosine are 77.1±8.1μM and 552±43μM, respectively. This is probably the first report that has proved by the kinetic analysis the sequential ordered substrate binding (amino acid first) in the reaction of Equation (1) (see Discussion).

DISCUSSION

Purification, molecular weight, amino acid composition, and basic properties: I have presented a novel purification procedure with a good yield of *B.s.* LysRS **(Table I)**. There was only a report describing the purification of *B.s.* LysRS ***(15)*** and several reports on the purification of *E. coli* LysRS ***(16~20)*** and yeast LysRS ***(21, 22)***.

The molecular weight and the amino acid composition of *B.s.* LysRS obtained here are essentially consistent with those previously reported ***(15)***. The values of K_m's in the ATP-PPi exchange reaction (23.6μM for L-lysine and 65.1μM for ATP, at pH 8.0, 37°C) are comparable to those previously reported (60μM for L-lysine and 20μM for ATP, at pH 7.0, 40°C) ***(15)***. Accordingly, I assume that I have isolated the same enzyme as that reported by Samuelsson and Lundvik ***(15)***, despite of considerably different purification procedures. The molecular weight, quaternary structure (a homodimer), and pH profile of the enzyme activity of *B.s.* LysRS are essentially similar to those of *E. coli* LysRS ***(16, 35)***. However, *B.s.* LysRS is more thermostable than the *E. coli* enzyme.

Binding of L-lysine and ATP to B.s. LysRS: The present results of fluorescence titration with the substrates of *B.s.* LysRS are different from those with *B.s.* ValRS (a monomer, Class I enzyme) reported previously, in which the addition of either L-valine or ATP lead to a quenching of protein fluorescence and the effects were additive ***(28, 36)***. I found with *B.s.* LysRS that the addition of L-lysine to the enzyme lead to a decrease of the protein fluorescence (**Figs. 2** and **3**) but that the addition of ATP did not cause appreciable fluorescence change. The fluorometrically estimated K_d for L-lysine (20.4±1.8μM) agrees with the K_m for L-lysine both in the aminoacylation reaction (16.4±3.9μM) and that in the ATP-PPi exchange reaction (23.6±2.1μM), and roughly with K_d obtained in the equilibrium dialysis (5.44±0.41μM) (**Fig. 5**). This indicates that the observed fluorescence quenching is a genuine reflection of L-lysine binding to *B.s.* LysRS, and that a tryptophan residue may be located in the vicinity of the L-lysine binding site of *B.s.* LysRS. A small bump is detected in the fluorescence titration curve (**Fig. 3**) at

around 100μM L-lysine. This is a reproducible observation, but at this moment I can not analyze what it indicates.

The results of equilibrium dialysis study **(Fig. 5)** suggest that two moles of L-lysine is bound to a mole of dimer *B.s.* LysRS in the range of 1μM to 1mM L-lysine with the same binding constants. The apparently identical two subunits of *B.s.* LysRS seems equivalent also in function at this stage of the reaction. This is similar to the observation with *E. coli* LysRS ***(37)***.

That the addition of ATP alone to the enzyme did not cause fluorescence change may suggest either that ATP is not bound to LysRS in the absence of L-lysine or that ATP alone is bound to the enzyme but no tryptophan residues are in the vicinity of the ATP binding site. The former possibility is favored because the addition of Ant-ATP, a fluorescent derivative, did not cause any change of its own fluorescence when added to *B.s.* LysRS. A considerable change of Ant-ATP fluorescence was observed when the ATP derivative was added to *B.s.* ValRS ***(38)***. The results of equilibrium dialysis study **(Fig. 5)** agree with this conclusion. To *E. coli* LysRS, however, 2 moles of ATP were reported to be bound without L-lysine ***(37)***. The primary structure of *B.s.* LysRS (Takita *et al.* to be published) shows a good homology (more than 50%) to *E. coli* LysRS, and yet the binding mechanism of ATP might be different in the two LysRSs. The recent report on the three dimensional structure of *E. coli* LysRS (u) complexed with L-lysine ***(9)*** represents no experimental data for ATP binding.

Discrimination of protein-constituting amino acids: It was reported with *E. coli* LysRS ***(17)*** that supplement of each of the other 19 L-amino acids than L-lysine that constitute protein caused no inhibition in the tRNA aminoacylation reaction, and that no

aminoacyl-tRNA could be detected by the substitution of ^{14}C-L-lysine with other ^{14}C-labeled amino acids. Then, a question is which step of the reaction, Equation 1 or 2, contributes more to this specificity of LysRS for the amino acid substrate.

In the present study, the results of fluorometric titration suggest that *B.s.* LysRS may discriminate L-lysine from the other 19 protein-constituting amino acids mainly at the binding step only with very weak interaction of a few amino acids **(Table II)**. The fluorometric titration experiments with amino acids were performed also in the presence of ATP where aminoacyladenylate could be formed; however, no significant sign of binding could be obtained except for L-lysine (data not shown). It was reported that *B.s.* ValRS bound L-threonine, L-isoleucine, L-glutamic acid, L-leucine, and D-valine, and misactivated L-threonine ***(36, 39)***. However, *B.s.* LysRS recognized only L-lysine as substrate in the ATP-PPi exchange reaction **(Table III)**, completely discriminating L-lysine from the other 19 amino acids at the step of lysyladenylate formation (Equation 1). Freist *et al.* investigated discrimination between L-lysine and the other 19 amino acids in the aminoacylation reaction with the native and the phosphorylated yeast LysRS and reported that L-cysteine was transferred to $tRNA^{Lys}$ effectively by both preparations of LysRS ***(40)***.

Discrimination of lysine analogues: The significance of three functional groups of the lysine molecule: ε-amino group, α-amino group, and α-carboxyl group, in the substrate binding were examined by the fluorometric titration. All α-carboxyl group modified analogues: L-lysine amide, L-lysine hydroxamate, and cadaverine, caused a decrease of the fluorescence of *B.s.* LysRS upon being added **(Table III)**. The difference in K_d between L-

lysine and cadaverine shows that the α-carboxyl group is important but not indispensable for the binding to *B.s.* LysRS. The comparison of K_d of L-lysine amide with that of L-lysine hydroxamate suggests the importance of the hydroxyl group introduced in L-lysine hydroxamate.

In the cases of the α-amino group modified compounds, the fluorescence of *B.s.* LysRS was not decreased by the addition of 6-amino-*n*-hexanoic acid and *N*α-acetyl-L-lysine below 20mM. These results suggest that the positive charge of α-amino group is important for the binding to the enzyme. The fluorescence intensity of *B.s.* LysRS did not change at all by the addition of any of the ε-amino group modified analogues, suggesting that ε-amino group is indispensable for the recognition of L-lysine at the binding step.

The recent X-ray crystallographic analysis of *E. coli* LysRS (u) complexed with L-lysine ***(9)*** shows that these 3 functional groups of L-lysine construct hydrogen-bond networks with enzyme indicating the importance of these groups for the substrate recognition. Some lysine analogues that have these three functional groups were also examined in the fluorometric titration (**Table III**). They were L-ornithine, in which the length of the side chain is shorter than in L-lysine; D-lysine; and those compounds that have modification on the side-chains: *S*-(2-aminoethyl)-L-cysteine, *threo*-4-hydroxy-L-lysine, and 5-hydroxylysine (mixed DL and DL-allo). Comparison of K_d of L-ornithine with that of D-lysine indicates that the position of the amino group of side-chain is more important than the enantiomeric configuration. The results with the analogues having side-chain modification show that the hydrophobicity of the methylene groups of the side-chain seems important in the binding process.

Among those compounds that were suggested by the fluorescence titration to be bound to *B.s.* LysRS, *S*-(2-aminoethyl)-L-cysteine, threo-4-hydroxy-L-lysine, 5-hydroxylysine, and L-ornithine were substrate of the ATP-PPi exchange reaction (**Table III**). K_m for *S*-(2-aminoethyl)-L-cysteine is much smaller than those for the other three analogues, and this agrees with the results of fluorometric titration experiments. I could not detect appreciable activity of the D-lysine dependent ATP-PPi exchange reaction by *B.s.* LysRS. It was reported with *E. coli* LysRS ***(16)*** that *S*-(2-aminoethyl)-L-cysteine and 5-hydroxylysine could replace L-lysine in the L-lysine dependent ATP-PPi exchange reaction with K_ms of 1.4μM and 300μM, respectively, and that DL-ornithine was not the substrate but an inhibitor. It was also reported with *E. coli* LysRS ***(17)*** that 4-oxalysine, 2,6-diamino-4-hexynoic acid, and *trans*-4-dehydrolysine were substrate in the ATP-PPi exchange reaction, and that *cis*-4-hydroxylysine was not the substrate but the competitive inhibitor for the reaction.

Each of the α-carboxyl group modified analogues strongly inhibited the L-lysine dependent ATP-PPi exchange reaction (**Table III**). It was reported with *E coli* LysRS ***(41)*** that L-lysine amide, L-lysine hydrazide, L-lysine methyl ester, and L-lysine ethyl ester inhibited competitively the aminoacylation reaction and that K_is for these derivatives were 7.7μM, 400μM, 100μM, and 66μM, respectively, while K_m for L-lysine was 2.5μM. It was also reported with TyrRSs of *E. coli* and *Bacillus subtilis* ***(42)*** that the L-tyrosine analogues in which the carboxyl group was modified inhibited competitively the ATP-PPi exchange reaction and that K_i values were quite small and in some cases even smaller than K_m for L-tyrosine. These results suggest that the α-carboxyl group modified

analogues are good competitive inhibitors for all ARSs. For the ε-amino group and α-amino group modified analogues, however, no appreciable inhibition was observed except for 6-amino-*n*-hexanoic acid (**Table III**). The comparison of either K_m or K_i estimated in the ATP-PPi exchange reaction with K_d observed in the fluorescence titration (**Table III**) indicates that the binding of those analogues to the enzyme is enhanced by the presence of ATP.

Order of substrate binding: ARSs were divided into two groups based on the kinetically determined order of substrate binding in the ATP-PPi exchange reaction ***(43)***. One group included ARSs that followed the sequential ordered mechanism (ATP binds first): LeuRS and SerRS of *E.coli* B, TrpRS of bovine pancreas, and ValRS of yeast. The other group included ARSs that followed the random sequence mechanism: PheRS of *E. coli* B, *E. coli* K12, and yeast; TyrRS of *E. coli*, MetRS of *E. coli*, and ValRS of *B. stearothermophilus*. Freist *et al.* investigated the order of substrate addition to ARSs in the aminoacylation reaction and reported that the addition of inorganic pyrophosphatase changed the aminoacylation mechanisms of ARSs ***(44, 45)***. In either case, however, the addition of the amino acid and ATP followed either a random or an ordered (ATP first) mechanism.

In my search, no ARS that follows the sequential ordered binding mechanism (amino acid first) has been reported by kinetic analysis except for my present study on *B.s.* LysRS (**Table IV**). My kinetic conclusion is entirely consistent with the results of fluorescence titration (**Table II**) and equilibrium dialysis (**Fig. 5**) and with the recent report on X-ray crystallographic analysis of *E. coli* LysRS (u) complexed with L-lysine ***(9)***.

From the conclusion thus obtained, the activation of L-lysine by *B.s.* LysRS (Equation 1) should be expanded at least to the following three steps:

$$E + \text{L-lysine} \rightleftharpoons E\bullet\text{L-lysine} \quad (7)$$

$$E\bullet\text{L-lysine} + ATP \rightleftharpoons E\bullet\text{L-lysine}\bullet ATP \quad (8)$$

$$E\bullet\text{L-lysine}\bullet ATP \rightleftharpoons E\bullet\text{L-lysine}\sim AMP + PPi \quad (9)$$

Structural features that make *B.s.* LysRS follow this unique sequential order should be interesting.

The three-dimensional structure of TyrRS, a Class I enzyme, from *B. stearothermophilus* complexed with tyrosyladenylate suggests that L-tyrosine has to bind before ATP, and otherwise its binding is blocked ***(5)***. The three dimensional structure of yeast AspRS complexed with aspartyladenylate, which is a Class II enzyme and considered to belong to the same subclass as LysRS, indicates that the access of L-aspartic acid to the enzyme is blocked when ATP is in place and that L-aspartic acid has to enter the active site first ***(14)***.

On the other hand, the kinetic analyses of *B.s.* TyrRS reaction were made with the random order mechanism ***(46, 47)***, and this has caused apparent contradiction with the structural information described above ***(2, 5)***. I can regard that the random order mechanism is the most general to represent the binding of two substrates and that the sequential ordered mechanisms are the extreme cases in which the equilibrium of a step shifts extremely to one direction. I have shown here clearly that *B.s.* LysRS follows the sequential ordered mechanism (L-lysine first), and wish that structural analysis of the enzyme will support this. In this respect, however, it should be pointed out that there are a few hints to suggest that *E. coli* LysRS may follow the random order

mechanism: One of the two active fractions of *E. coli* LysRS bound L-lysine and ATP independently ***(37)***, and the affinity labeling of *E. coli* LysRS with adenosine di or triphosphopyridoxals was made in the absence of L-lysine ***(48)***.

REFERENCES

1) Berg, P. (1961) Specificity in protein synthesis. *Annu. Rev. Biochem.* **30**, 293-324

2) Carter, C. W., Jr. (1993) Cognition, mechanism, and evolutionary relationships in aminoacyl-tRNA synthetases. *Annu. Rev. Biochem.* **62**, 715-748

3) Delarue, M. and Moras, D. (1992) "*Nucleic Acid and Molecular Biology*", **6**, ed. by Eckstein, F. and Lilley, D. M. J., Springer-Verlag, Berlin, Heidelberg, pp.203-224

4) Eriani, G., Delarue, M., Poch, O., Gangloff, J., and Moras, D. (1990) Partition of tRNA synthetases into two classes based on mutually exclusive sets of sequence motifs. *Nature*, **347**, 203-206

5) Brick, P., Bhat, T. N., and Blow, D. M. (1988) Structure of tyrosyl-tRNA synthetase refined at 2.3Å resolution. *J. Mol. Biol.* **208**, 83-98

6) Brunie, S., Zelwer, C., and Risler, J. L. (1990) Crystallographic study at 2.5Å resolution of the interaction of methionyl-tRNA synthetase from *Escherichia coli* with ATP. *J. Mol. Biol.* **216**, 411-424

7) Cusack, S., Berthet-Colominas, C., Hartlein, M., Nasser, N., and Leberman, R. (1990) A second class of synthetase structure revealed by X-ray analysis of *Escherichia coli*

seryl-tRNA synthetase at 2.5Å. *Nature*, **347**, 249-255

8) Rould, M. A., Perna, J. J., and Steitz, T. A. (1991) Structural basis of anticodon loop recognition by glutaminyl-tRNA synthetase. *Nature*, **352**, 213-218

9) Onesti, S., Miller, A. D., and Brick, P. (1995) The crystal structure of the lysyl-tRNA synthetase (LysU) from *Escherichia coli. Structure*, **3**, 163-176

10) Belrhali, H., Yaremchuk, A., Tukalo, M., Larsen, K., Berthet-Colominas, C., Leberman, R., Beijer, B., Sproat, B. , Als-Nielsen, J., Grübel, G., Legrand, J-F., Lehmann, M., and Cusack, S. (1994) Crystal structure at 2.5 angstrom resolution of seryl-tRNA synthetase complexed with two analogues of seryl adenylate. *Science*, **263**, 1432-1436

11) Nureki, O., Vassylyev, D. G., Katayanagi, K., Shimizu, T., Sekine, S., Kigawa, T., Miyazawa, T., Yokoyama, S., and Morikawa, K. (1995) Architectures of class-defining and specific domains of glutamyl-tRNA synthetase. *Science*, **267**, 1958-1965

12) Doublie, S, Bricogne, G., Gilmore, C., and Carter, C. W., Jr. (1995) Tryptophanyl-tRNA synthetase crystal structure reveals an unexpected homology to tyrosyl-tRNA synthetase. *Structure*, **3**, 17-31

13) Mosyak, L., Reshetnikova, L., Goldgur, Y., Delarue, M., and Safro, M., G. (1995) Structure of phenylalanyl-tRNA syntheatse from *Thermus thermophilus. Nature Structural Biology*, **2**, 537-547

14) Cavarelli, J., Eriani, G., Rees, B., Ruff, M., Boeglin, M., Mitschler, A., Martin, F., Gangloff, J., Thierry, J. C., and

Moras, D. (1994) The active site of yeast aspartyl-tRNA synthetase: structural and functional aspects of the aminoacylation reaction. *EMBO J.*, **13**, 327-337

15) Samuelsson, T. and Lundvik, L. (1978) Purification and some properties of asparagine, lysine, serine, and valine: tRNA ligases from *Bacillus stearothermophilus. J. Biol. Chem.* **253**, 7033-7039

16) Stern, R. and Mehler, A. H. (1965) Lysyl-sRNA synthetase from *Escherichia coli. Biochem. Z.* **342**,400-409

17) Lansford, E. M., Jr., Lee, N. M., and Shive, W. (1967) A study of lysyl-ribonucleic acid synthetase in relation to substrate conformation. *Arch. Biochem. Biophys.* **119**, 272-276

18) Waldenström, J. (1968) Purification and some properties of lysyl ribonucleic acid synthetase from *Escherichia coli. Eur. J. Biochem.* **3**, 483-487

19) Kisselev, L. L. and Baturina, I. D. (1972) Two enzymatically active forms of lysyl-tRNA synthetase from *E. coli* B. *FEBS Lett.* **22**, 231-233

20) Charlier, J. and Sanchez, R. (1987) Lysyl-tRNA synthetase from *Escherichia coli* K12. *Biochem. J.* **248**, 43-51

21) Chlumecká, V., von Tigerstrom, M., D'Obrenan, P.,and Smith, C. J. (1969) Purification and properties of lysyl transfer ribonucleic acid synthetase from baker's yeast. *J. Biol. Chem.* **244**, 5481-5488

22) Rymo, L. and Lagerkvist, U. (1970) Crystallization of lysyl transfer ribonucleic acid synthetase from yeast. *J. Biol. Chem.* **245**, 4308-4316

23) Freist, W. and Gauss, D. H. (1995) Lysyl-tRNA synthetase. *Biol. Chem. Hoppe-Seyler*, **376**, 451-472

24) Hiratsuka, T. (1983) New ribose-modified fluorescent analogues of adenine and guanine nucleotides available as substrates for various enzymes. *Biochim. Biophys. Acta* **742**, 496-508

25) Zubay, G. (1966) *"Procedures on Nucleic Acid Research"* ed by Cantoni, G. L. and Davies, D. R., Harper and Row Publishers, New York, pp. 455-460

26) Söll, D., Cherayil, J. D., and Bock, R. M. (1967) Studies on polynucleotides. *J. Mol. Biol.* **29**, 97-112

27) Lowry, O. H., Rosebrough, N. J., Farr, A. L., and Randall, R. J. (1951) Protein measurement with the Folin phenol reagent. *J. Biol. Chem.* **193**, 265- 275

28) Kakitani, M., Tonomura, B., and Hiromi, K. (1986) Valyl-tRNA synthetase from *Bacillus stearothermophilus*. Purification and binding with the substrate L-valine and ATP. *Agric. Biol. Chem.* **50**, 2437-2444

29) Sakoda, M. and Hiromi, K. (1976) Determination of the best-fit values of kinetic parameters of the Michaelis-Menten equation by the method of least squares with Taylor expansion. *J. Biochem.* **80**, 547-555

30) Seno, T., Agris, P. F. and Söll, D. (1974) Involvement of the anticodon region of *Escherichia coli* $tRNA^{Gln}$ and $tRNA^{Glu}$ in the specific interaction with cognate aminoacyl-tRNA synthetase. *Biochim. Biophys. Acta* **349**, 328-338

31) Cole, F. X. and Schimmel, P. R. (1970) On the rate law and mechanism of the adenosine triphosphate-pyrophosphate isotope exchange reaction of amino acyl transfer ribonucleic acid synthetases. *Biochemistry* **9**, 480-489

32) Santi, D. V., Webster, R. W., Jr., and Cleland, W. W. (1974) Kinetics of aminoacyl-tRNA synthetase catalyzed ATP-PPi exchange in *Methods in Enzymology* (Grossman, L. and Moldave, K., eds.) Vol. **29**, pp. 620-627, Academic Press, New York

33) Teale, F. W. J. and Weber, G. (1957) Ultraviolet fluorescence of the aromatic amino acids. *Biochem. J.* **65**, 476-482

34) Tonomura, B., Kakitani, M., Ohkubo, Y., Shima, H., and Hiromi, K. (1990) ATP binding plays a role in the selection of amino acid substrate by aminoacyl-tRNA synthetases. *N. Y. Acad. Sci.* **613**, 489-493

35) Stern, R. and Peterkofsky, A. (1969) Studies on lysyl transfer ribonucleic acid synthetase from *Escherichia coli.* *Biochemistry* **8**, 4346-4354

36) Kakitani, M., Tonomura, B., and Hiromi, K. (1987) Fluorometric study on the interaction of amino acids and ATP with valyl-tRNA synthetase from *Bacillus stearothermophilus. J. Biochem.* **101**,477-484

37) Rymo, L., Lundvik, L., and Lagerkvist, U. (1972) Subunit structure and binding properties of three amino acid transfer ribonucleic acid ligases. *J. Biol. Chem.* **247**, 3888-3899

38) Kakitani, M., Tonomura, B., and Hiromi, K. (1989) Static and kinetic studies on binding of a fluorescent analogue of ATP and valyl-tRNA synthetase from *Bacillus stearothermophilus. Biochim. Biophys. Acta* **996**, 76-81

39) Fersht, A. R. and Kaethner, M. (1976) Enzyme hyperspecificity. Rejection of threonine by the valyl-tRNA synthetase by misacylation and hydrolytic editing. *Biochemistry* **15**, 3342-3346

40) Freist, W., Sternbach, H., and Cramer, F. (1992) Lysyl-tRNA synthetase from yeast. Discrimination of amino acids by native and phosphorylated species. *Eur. J. Biochem.* **204**, 1015-1023

41) Baturina, I. D., Gnutchev, N. V., Khomutov, R. M., and Kisselev, L. L. (1972) Substrate specificity of lysyl-tRNA synthetase from *E. coli* B. *FEBS lett.* **22**, 235-237

42) Calendar, R. and Berg, P. (1966) The catalytic properties of tyrosyl ribonucleic acid synthetases from *Escherichia coli* and *Bacillus subtilis*. *Biochemistry* **5**, 1690-1695

43) Kakitani, M., Tonomura, B., and Hiromi, K. (1987) Order of binding of substrate to valyl-tRNA synthetase from *Bacillus stearothermophilus* in amino acid activation reaction. *Biochemistry International* **14**, 597-603

44) Freist, W., Sternbach, H., and Cramer, F. (1982) Isoleucyl-tRNA synthetase from *Escherichia coli* MRE 600. Different pathways of the aminoacylation reaction depending on the presence of pyrophosphatase, order of substrate addition in the pyrophosphate exchange, and substrate specificity with regard to ATP analogues. *Eur. J. Biochem.* **128**, 315-329

45) Freist, W., Sternbach, H., and Cramer, F. (1981) Arginyl-tRNA synthetase from baker's yeast. Order of substrate addition and action of ATP analogues in the aminoacylation reaction; Influence of pyrophosphate on the catalytic mechanism. *Eur. J. Biochem.* **119**, 477-482

46) Wells, T. N. C. and Fersht, A. R. (1986) Use of binding energy in catalysis analyzed by mutagenesis of the tyrosyl-tRNA synthetase. *Biochemistry* **25**, 1881-1886

47) Fersht, A. R., Mulvey, R. S., and Koch, G. L. E. (1975) Ligand binding and enzymatic catalysis coupled through subunits in tyrosyl-tRNA synthetase. *Biochemistry* **14**, 13-18

48) Hountondji, C., Gillet, S., Schmitter, J. -M., Fukui, T., and Blanquet, S. (1994) Affinity labeling of the two species of *Escherichia coli* lysyl-tRNA synthetase with adenosine di- and triphosphopyridoxals. *J. Biochem.* **116**, 493-501

Table I
Purification of LysRS from *B. stearothermophilus*

Purification step	Total protein (mg)	Total activity (units)	Specific activity (units/g)	Yield (%)	Purification fold
Crude extract	11,900	19.43	1.63	100	1
Streptomycin sulfate precipitation	5,350	11.85	2.22	61	1.4
DEAE-Toyopearl 650 M	2,000	10.88	5.44	56	3.3
Dyematrex Blue A	67.8	8.74	129	45	79
Dyematrex Red A	9.95	7.76	780	40	478
Lysine-Sepharose 4B	4.56	6.98	1,530	36	938
AF-Red Toyopearl 650 ML	3.15	5.64	1,790	29	1,098

1 unit is defined as the amount of the enzyme that forms 1μmol of [^{3}H]lys-tRNA in 1min at 37°C.

Table II
Fluorescence titration of LysRS with L-lysine, ATP, and some other ligands

Ligands	K_d (μM)	- ΔFmax (%)
L-lysine	20.4±1.8	16.2
L-glycine	21,000 ± 5,100	8.7
L-arginine	—*	0
L-glutamine	30,000 ±16,000	23.4
L-methionine	24,400 ±11,000	14.1
L-histidine	—	0
L-proline	—	0
L-serine	—	0
ATP	—	0
ADP	—	0
AMP	—	0
GTP	—	0
CTP	—	0
UTP	—	0
a,b-methyleneATP	—	0
Ant-ATP**	—	0

$[E]_0$=0.88μM, λ_{ex}=295nm, λ_{em}=340nm, pH 8.0, 30°C.

*, – indicates that the fluorescence change could not be detected.

**, $[E]_0$=4.2μM λ_{ex}=375nm, λ_{em}=428nm, pH 8.0, 30°C.

Table III
Fluorescence titration and ATP-PPi exchange reaction of LysRS with lysine analogues

	Fluorescence titration		ATP-PPi exchange reaction					
			Kinetic parameters[a]		Relative inhibition	Inhibitor constant		
	K_d (μM)	$-\Delta F_{max}$ (%)	K_m (μM)	k_{cat} (s^{-1})	(%)[c]	K_i (μM)	K_i/K_d (%)	K_m/K_d (%)
L-lysine	20.4± 1.8*	16.2*	23.6 ± 2.1	40.9[e] ± 0.6	/	/	/	115
other 19 amino acids	(see Table III)		—[b]	—	N.D.[d]	N.D.	/	
α-carboxyl group modified								
cadaverine	19,900 ± 900	15.6	—	—	85	77 ± 8	0.4	/
L-lysine hydroxamate	704 ± 79	11.0	—	—	100	0.6[e] ± 0.2	0.08	/
L-lysine amide	4,260 ± 210	16.6	—	—	95	30[e] ± 4	0.7	/
α-amino group modified								
6-amino-*n*-hexanoic acid	—**	0	—	—	44	480 ± 40		
Nα-acetyl-L-lysine	—	0	—	—	0	/	/	/
ε-amino group modified								
L-norleucine	—	0	—	—	0	/	/	/
Nε-methyl-L-lysine	—	0	—	—	0	/	/	/
Nε-acetyl-L-lysine	—	0	—	—	13	N.D.	/	
others								
D-lysine	3,180 ± 180	10.2	—	—	68	120[e] ± 20	3.7	/
S-(2-aminoethyl)-L-cysteine	197 ± 24	14.1	69.3[e] ± 8.7	10.2[e] ± 0.5	N.D.	N.D.	/	35.2
threo-4-hydroxy-L-lysine	3,230 ± 170	8.9	898 ± 68	36.6 ± 1.1	N.D.	N.D.	/	27.8
5-hydroxylysine (mixed DL and DL-allo)	18,600 ± 600	19.0	5,450 ± 260	57.1 ± 0.9	N.D.	N.D.	/	29.3
L-ornithine	14,700 ± 900	8.2	11,900[e] ± 2,040	29.8[e] ± 2.1	N.D.	N.D.	/	80.9

Fluorescence titration. $[E]_0$=4.2μM, λex=295nm, λem=340nm, pH 8.0, 30°C.

*, $[E]_0$=0.88μM.

**, — indicates that the fluorescence change could not be detected.

ATP-PPi exchange reaction.

a), $[E]_0$=15.9nM, 1mM ATP, 1mM PPi, pH 8.0, 37°C.

b), — indicates that the ATP-PPi exchange activity could not be detected.

c), Individual inhibitions were represented as follows;
(V-Vi) × 100/*V*, where *V* is the initial velocity in the absence of lysine analogues and *Vi* is that in the presence of 4mM analogues.
$[E]_0$=15.9nM, 50μM L-lysine, 1mM ATP, 1mM PPi, pH 8.0, 37°C.

d), N.D. indicates that this assay was not conducted.

e), These values appeared in a conference proceedings ***(34)***., and are cited here by permission of the New York Academy of Sciences.

Table IV
Effects of substrates and inhibitors on the ATP-PPi exchange reaction

Fixed substrate or inhibitor	L-Lys		ATP		Cadaverine		Adenosine	
Variable substrate	ATP	L-Lys	ATP	L-Lys	ATP	L-Lys		
Obtained pattern	B	A	B	B	C	B		
Ordered: AA first	B	A	B	B	C	B		
Ordered:ATP first	A	A	A	C	B	A		
Ordered:ATP first*	A	B	B	C	B	B		
Random	A	A	B	A	B	A		

A: Intersection is to the left of the vertical axis.

B: Intersection is on the vertical axis.

C: Parallel. * Rapid equilibrium. *(31, 32)*.

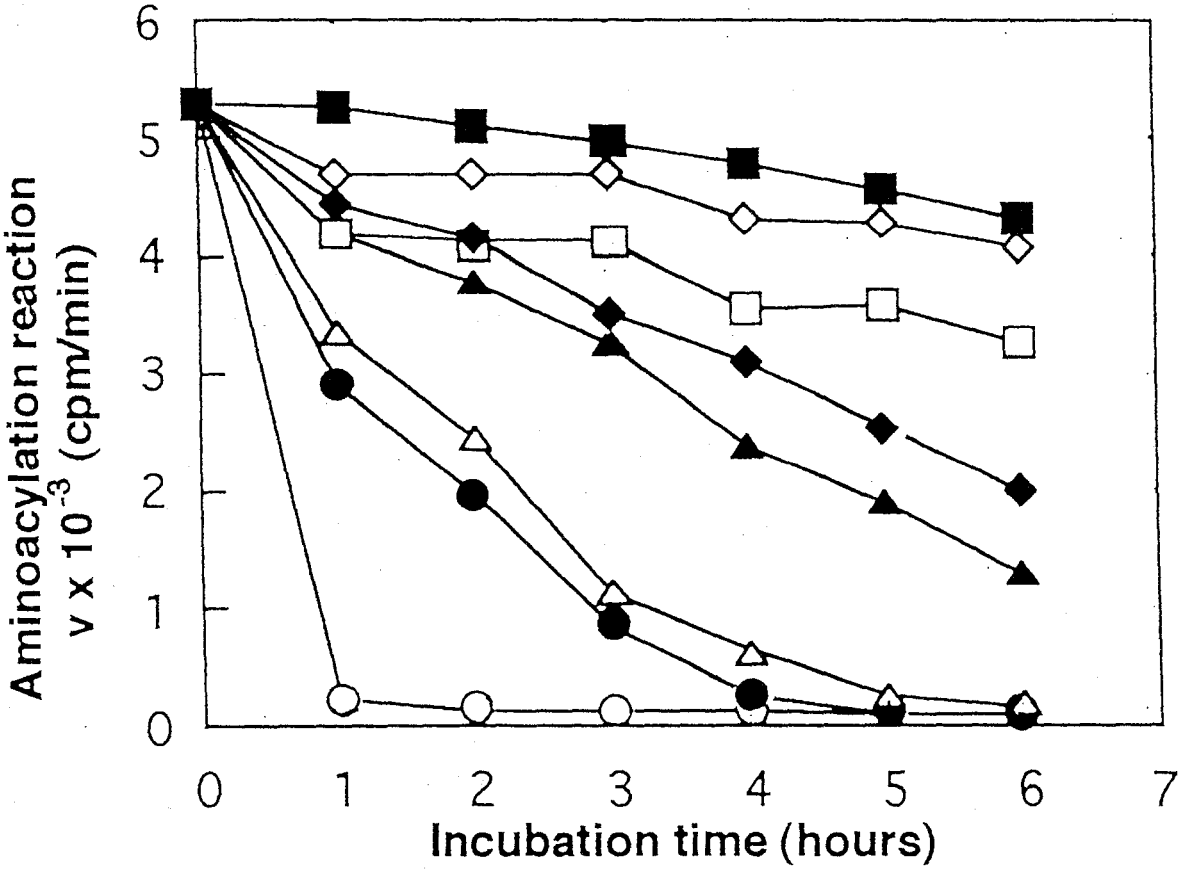

Figure 1

pH-Stability of *B.s.* LysRS

The remaining enzyme activity was measured in the aminoacylation reaction at pH 8.0, 37°C, $[E]_0$=1.0nM: (○), pH 3.3; (●), pH 4.4; (△), pH 5.4; (▲), pH 6.6; (□), pH7.3; (■), pH 8.3; (◇), pH 9.3; (◆), pH 10.1.

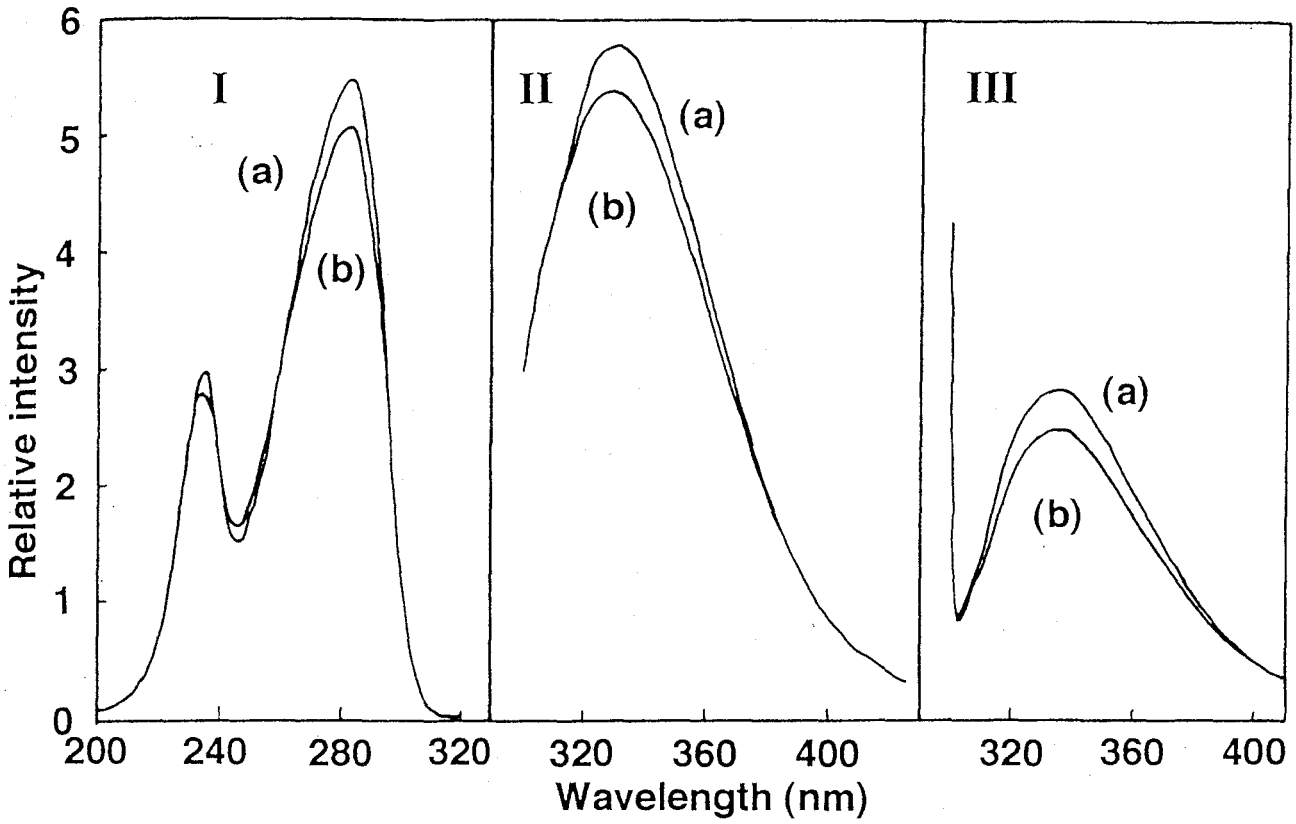

Figure 2

Fluorescence spectra of *B.s.* LysRS and effects of adding L-lysine

I, excitation spectra for the emission at 340nm.

II, emission spectra with excitation at 280nm.

III, emission spectra with excitation at 295nm.

$[E]_0$=4.9μM; pH 8.0, 30°C;

(a), [L-lysine]=0μM; (b), [L-lysine]=227μM.

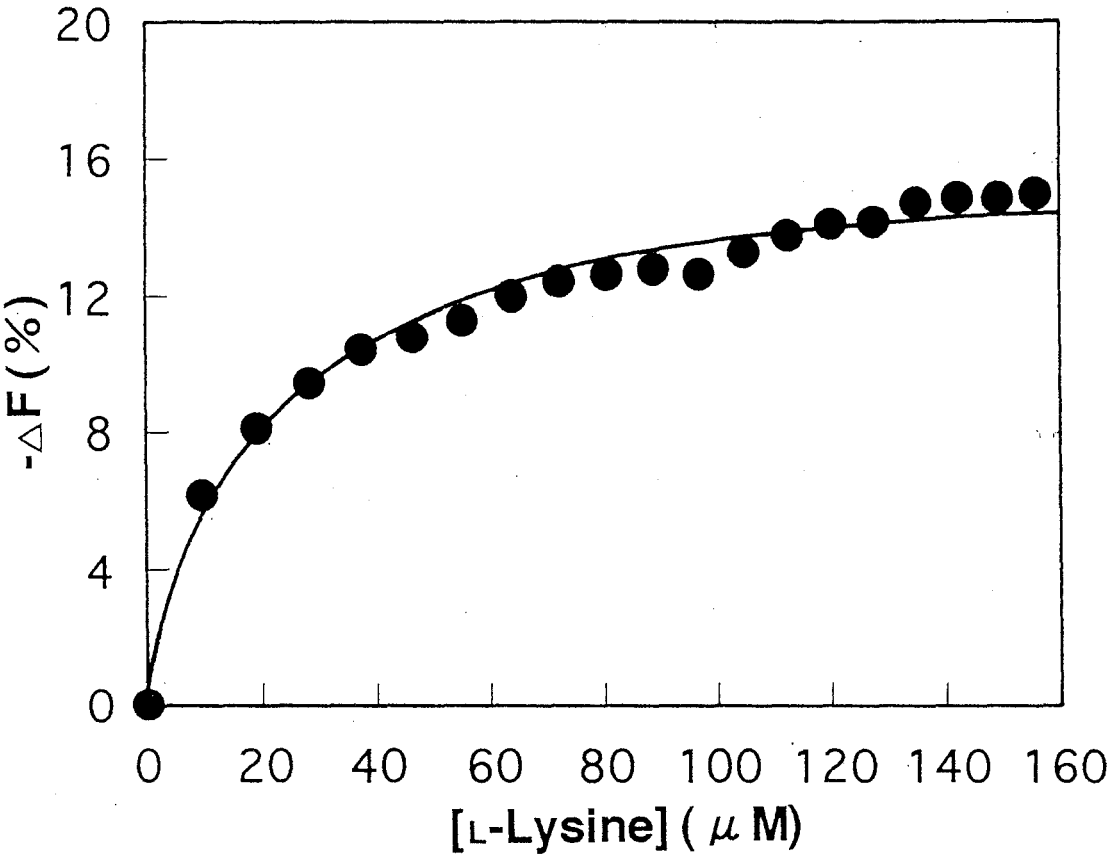

Figure 3

Fluorescence titration of *B.s.* LysRS with L-lysine

$[E]_0$=0.88μM, 10mM $MgCl_2$, λ_{ex}=295nm, λ_{em}=340nm, pH 8.0, 30°C. The solid line is the theoretical curve drawn according to Equation 5 with K_d=20.1μM and ΔF_{max}=-16.2%.

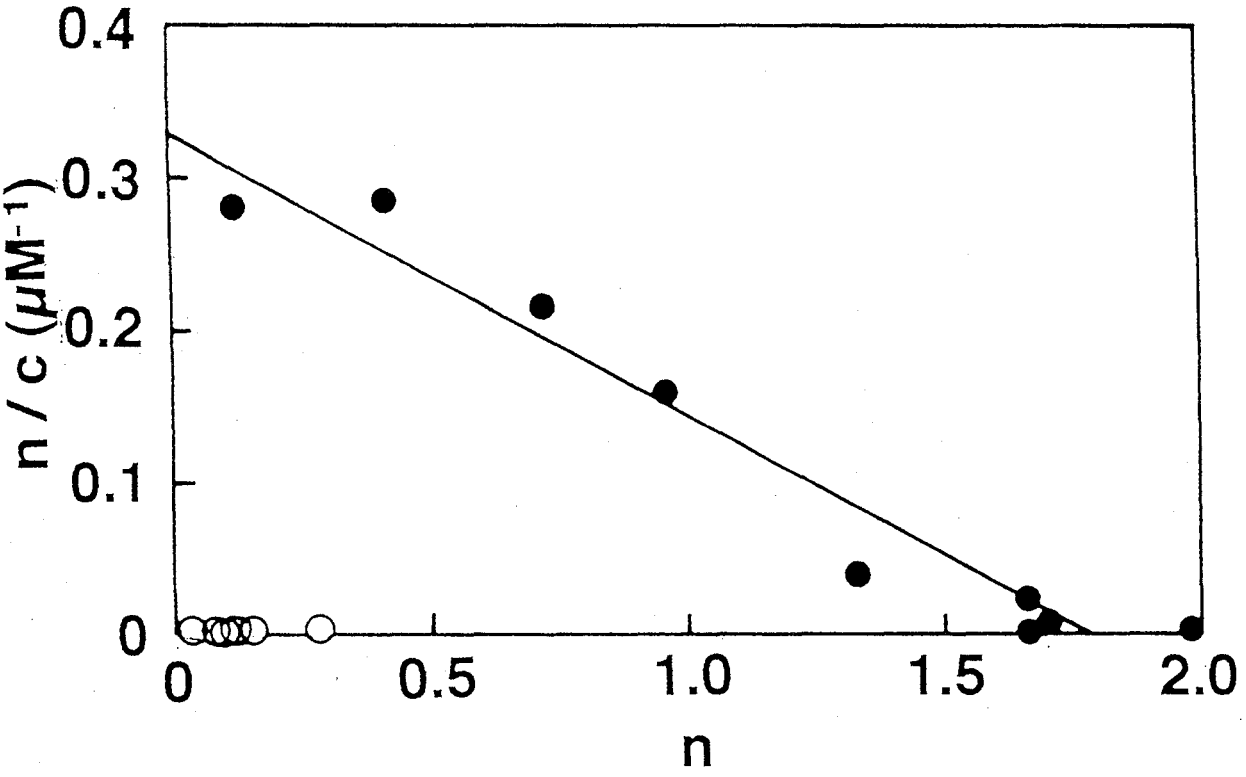

Figure 5

Scatchard plots for the binding of either L-lysine or ATP to *B.s.* LysRS as measured by equilibrium dialysis

$[E]_0$=13.9μM, 10mM $MgCl_2$, pH 8.0, 4°C, L-lysine binding (●), ATP binding (○). The solid line for L-lysine binding (●) are drawn by the least squres method. K_d=5.44μM and n=1.79.

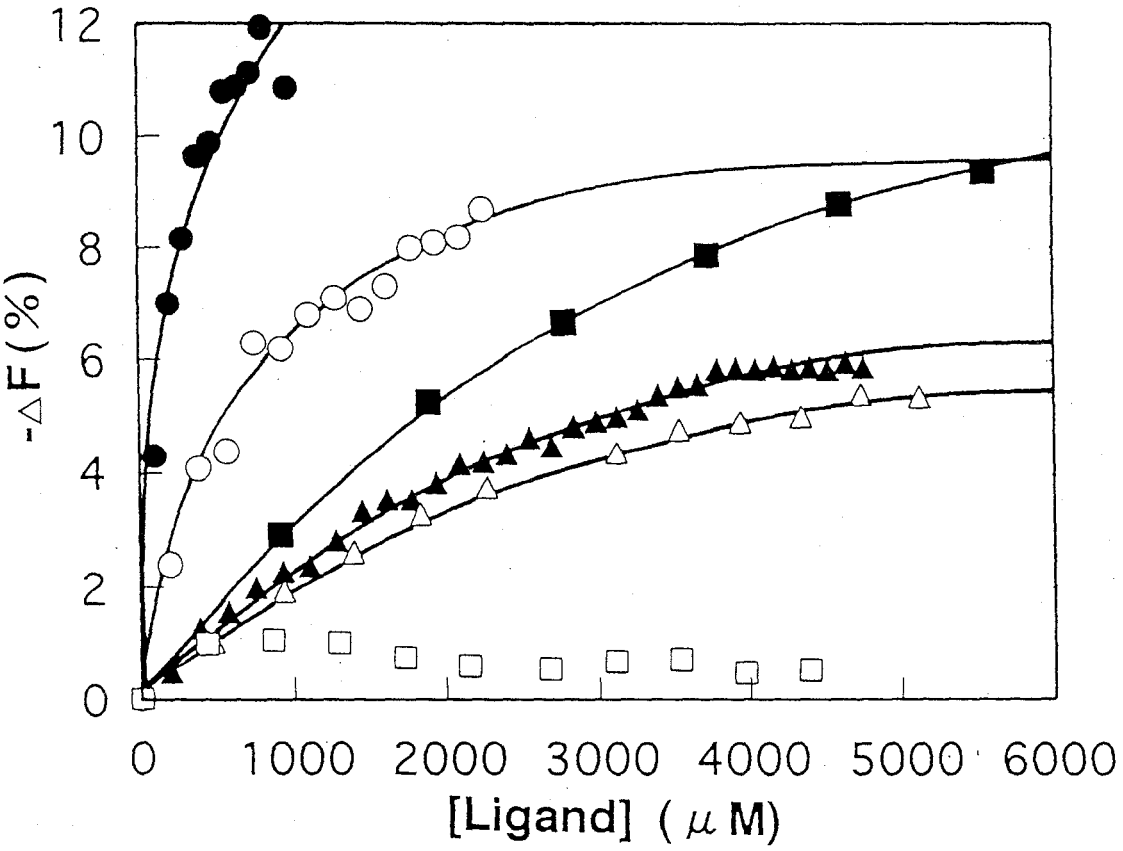

Figure 4

Fluorescence titration of *B.s.* LysRS with L-lysine analogues

$[E]_0$=4.2μM, 10mM $MgCl_2$, λ_{ex}=295nm, λ_{em}=340nm, pH 8.0, 30°C. SAEC (●), L-Lyshxt (○), L-Lysamd (■), *threo*-4-hydroxy-L-lysine(△), D-lysine (▲), and 6-amino-*n*-hexanoic acid (□). The solid lines are the theoretical curve drawn according to Equation 5 with K_d of 197μM (●), 704μM (○), 4,260μM (■), 3,230μM (△), and 3,180μM (▲).

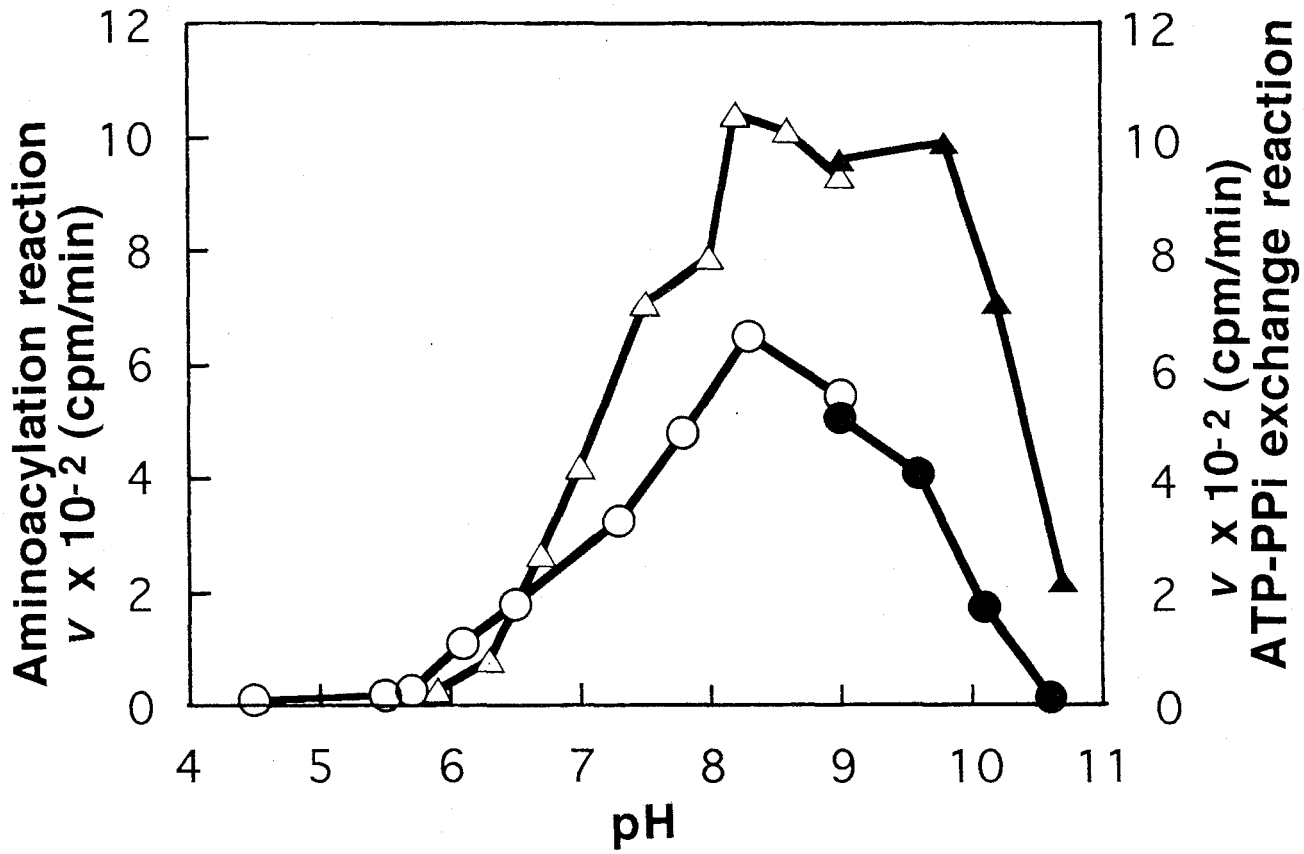

pH-Activity profile of *B.s.* LysRS

Aminoacylation reaction, $[E]_0$=0.8nM, 37°C; (○), piperazine-glycylglycine buffer; (●), glycine-NaOH buffer. ATP-PPi exchange reaction, $[E]_0$=4.0nM, 37°C; (△), piperazine-glycylglycine buffer; (▲), glycine-NaOH buffer.

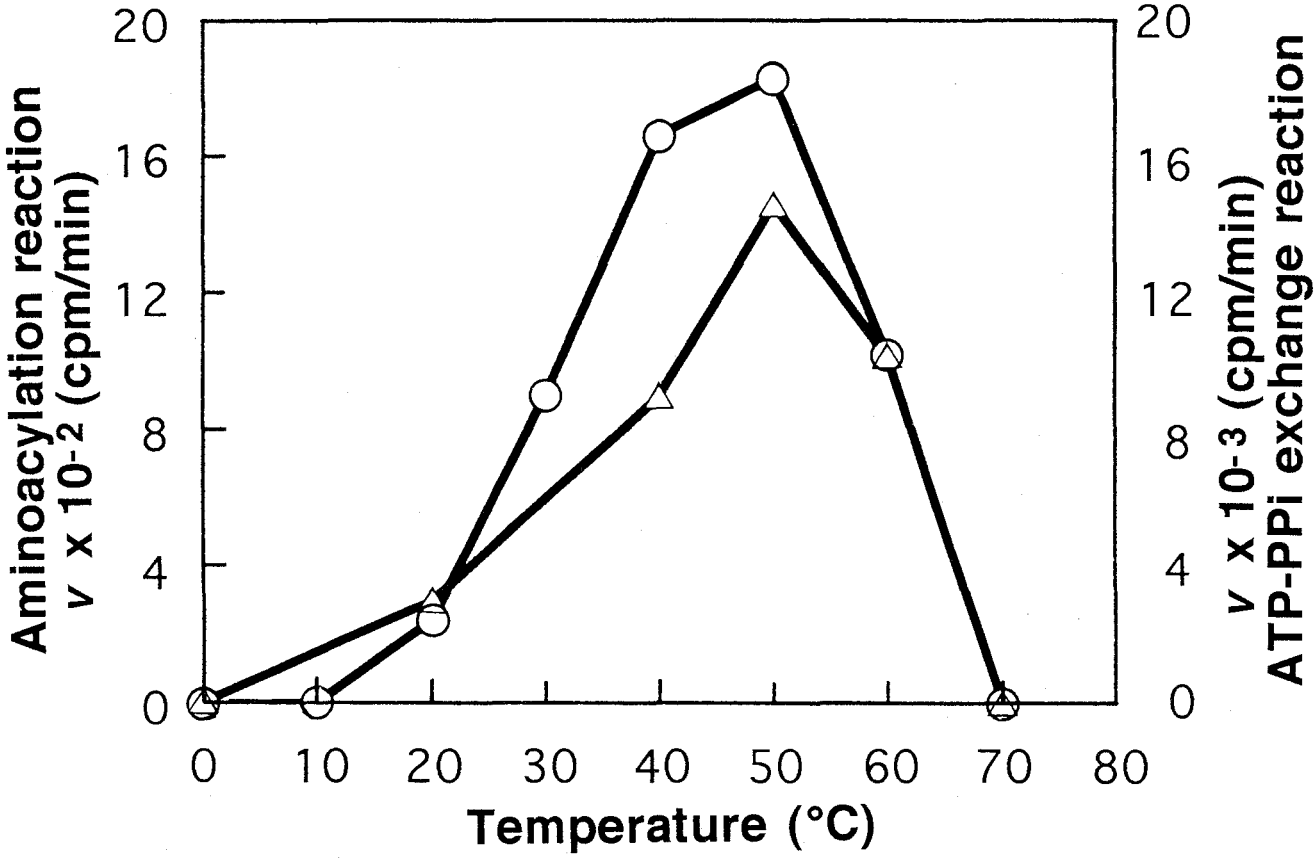

Temperature-activity profile of *B.s.* LysRS
Aminoacylation reaction, $[E]_0$=1.7nM, pH 8.0, (○);
ATP-PPi exchange reaction, $[E]_0$=4.0nM, pH 8.0, (△).

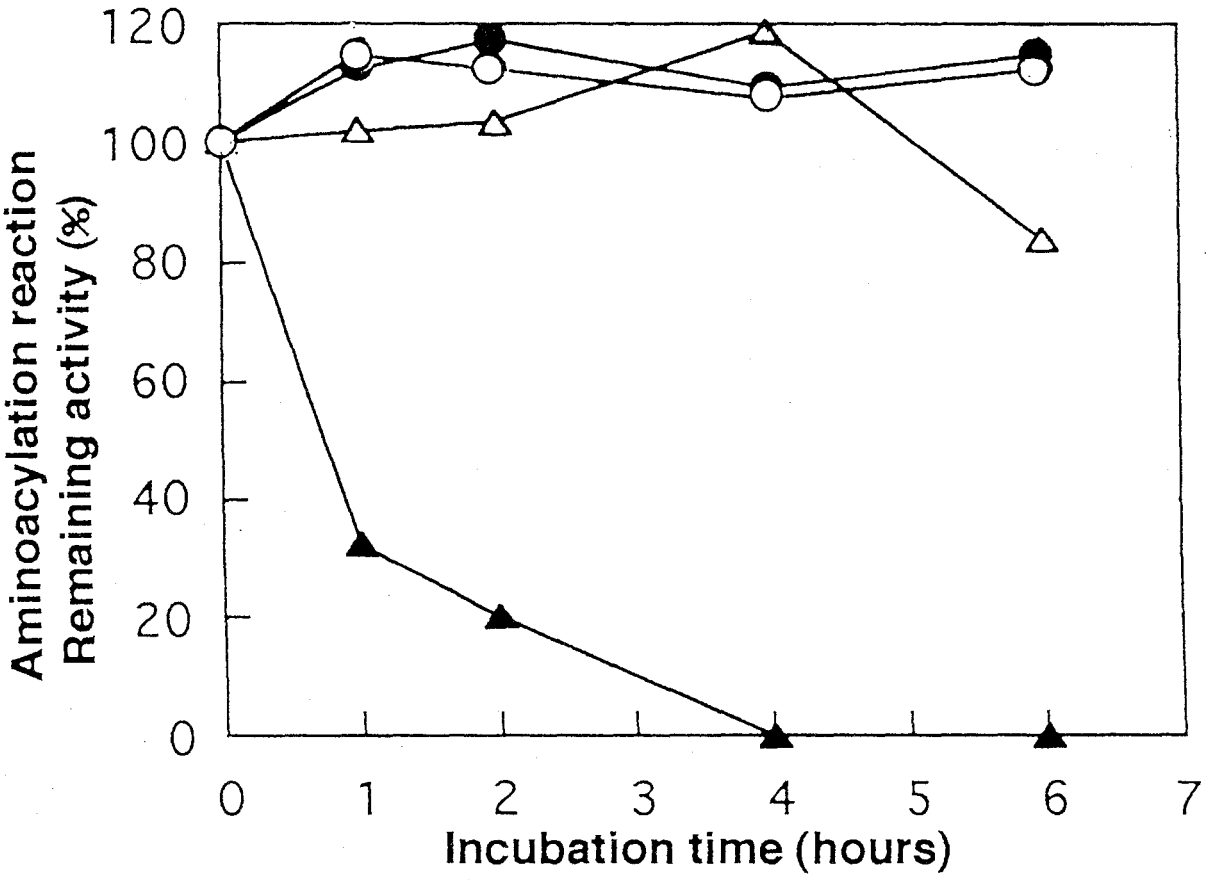

Thermostability of *B.s.* LysRS

The enzyme solution (11nM in 10mM piperazine-glycylglycine buffer (pH8.0) containing 0.1M NaCl and 10mM $MgCl_2$) was incubated in the range of 20 to 60°C for 1~6 hours. The remaining activity was measured in the aminoacylation reaction under the conditions described above at pH 8.0, 37°C; (○), 20°C; (●), 40°C; (△), 50°C; (▲), 60°C.

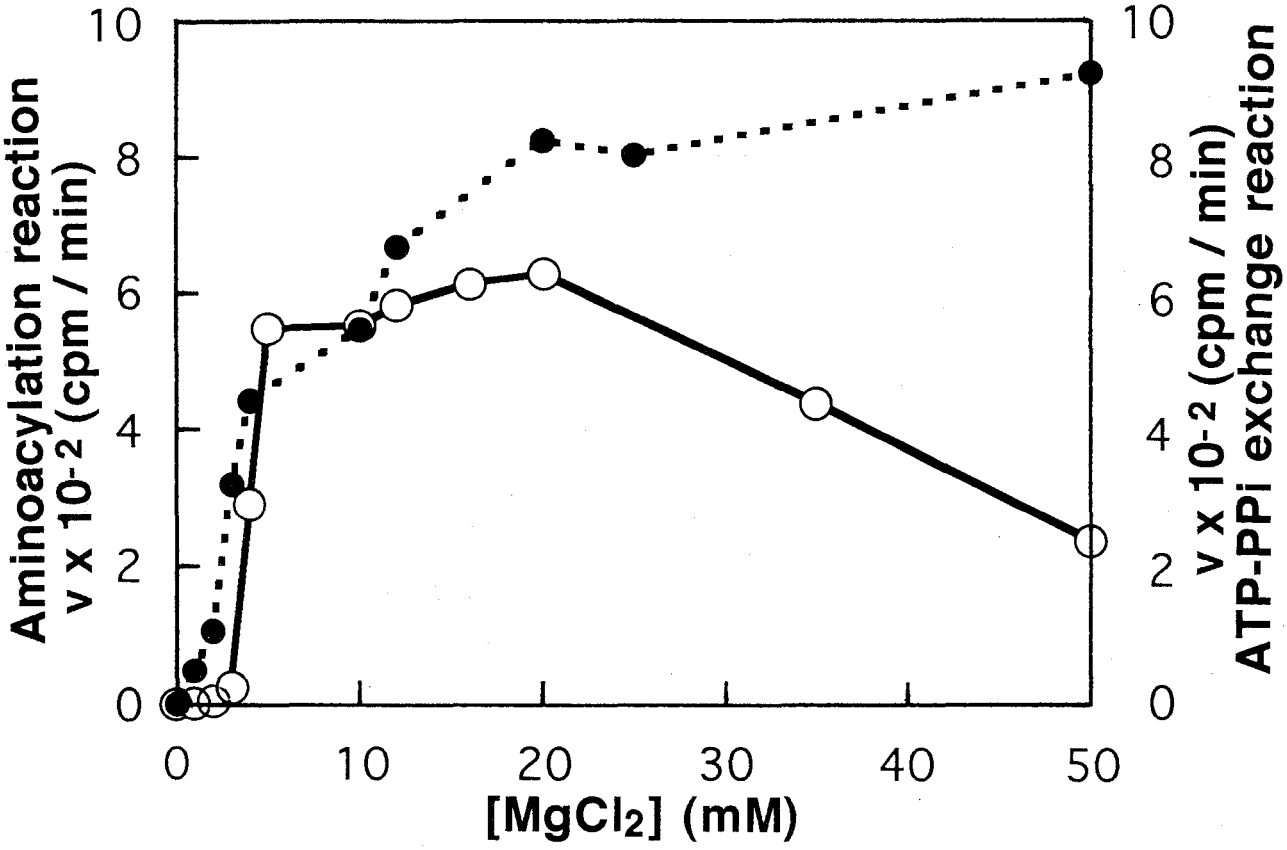

Effect of $MgCl_2$ concentration on the aminoacylation reaction and the ATP-PPi exchange reaction catalyzed by *B.s.* LysRS

Aminoacylation reaction, $[E]_0$=0.47nM, pH 8.0, 37°C, (—○—); ATP-PPi exchange reaction, $[E]_0$=4.0nM, pH 8.0, 37°C, (··· ● ···).

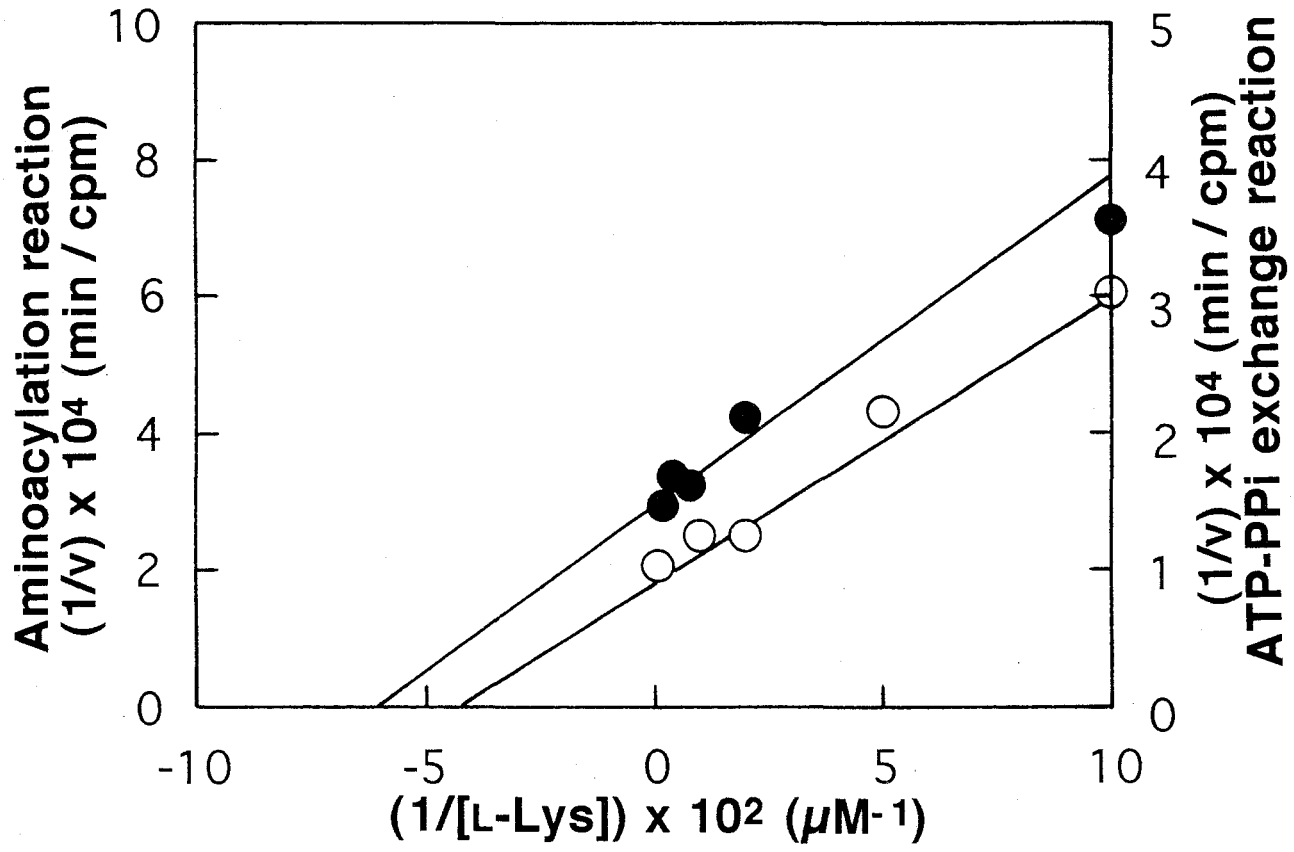

Effect of L-lysine concentration on the aminoacylation reaction and the ATP-PPi exchange reaction catalyzed by *B.s.* LysRS

Aminoacylation reaction, $[E]_0$=0.52nM, ^{3}H-L-lysine (200mCi/mmol), $[ATP]_0$=1mM, pH 8.0, 37°C, (●); ATP-PPi exchange reaction, $[E]_0$=4.0nM, $[ATP]_0$=1mM, $[PPi]_0$=1mM, pH 8.0, 37°C,(○). The solid lines are the theoretical line drawn with K_m=16.4μM & V_{max}=3,380.6cpm/min (-●-●-) and K_m=20.9μM & V_{max}=10,364.0cpm/min (-○-○-).

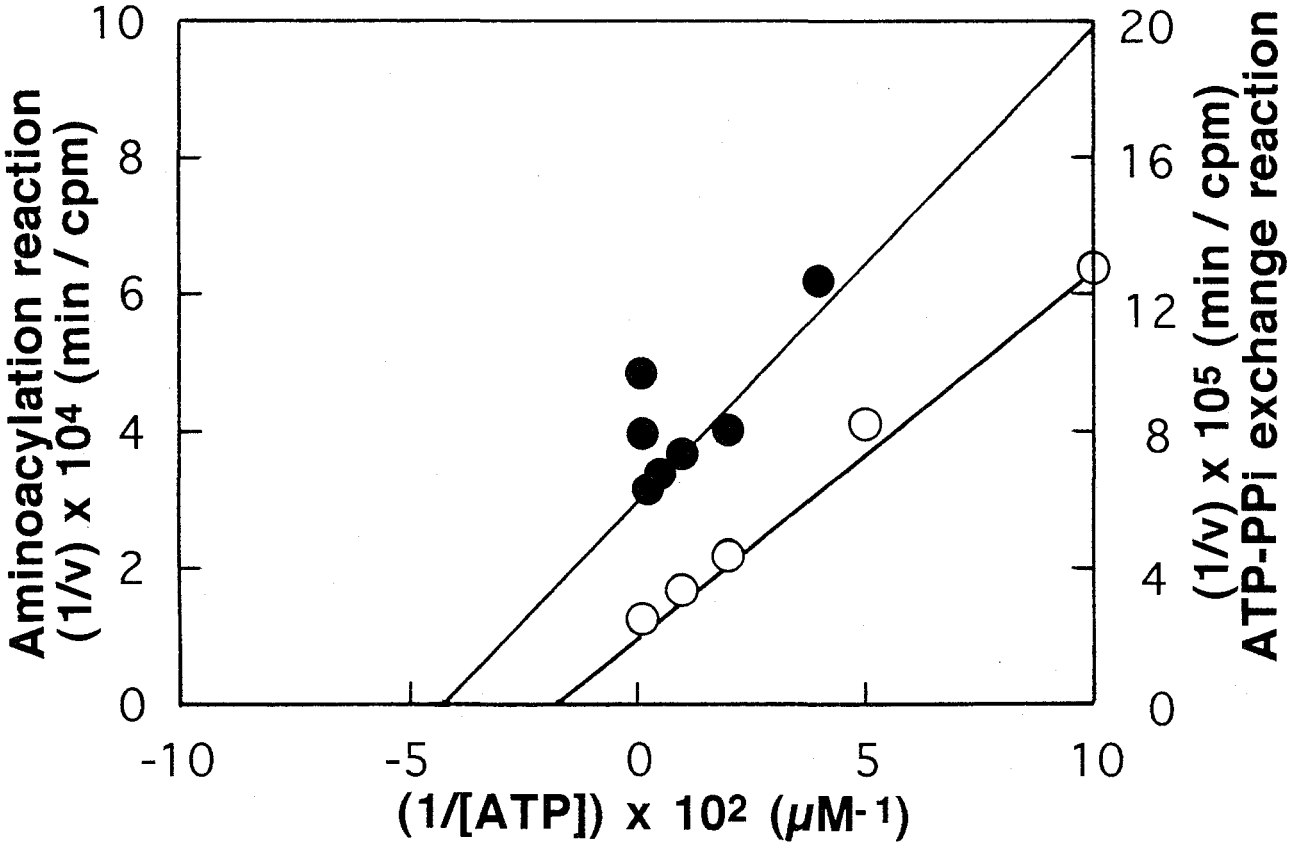

Effect of ATP concentration on the aminoacylation reaction and ATP-PPi exchange reaction catalyzed by *B.s.* LysRS

Aminoacylation reaction, $[E]_0$=0.52nM, [^{3}H-L-lysine]$_0$=200μM (200mCi/mmol), pH 8.0, 37°C, (●). The line is obtained by neglecting the data at 800μM and 1,000μM; ATP-PPi exchange reaction, $[E]_0$=4.0nM, [L-lysine]$_0$=1mM, $[PPi]_0$=1mM, pH 8.0, 37°C, (○). The solid lines are the theoretical line drawn with K_m=23.2μM & V_{max}=3,406.5cpm/min (-●-●-) and K_m=41.6μM & V_{max}=40,601.7cpm/min (-○-○-).

Chapter 2
Formation and Isolation of the Enzyme•lysyladenylate Complex and its Analogue

An aminoacyl-tRNA synthetase **(abbreviated to ARS)** is a key figure to endorse the accuracy of translation of the genetic message into the protein structure *(1)*. A high degree of substrate specificity is required for the reaction of ARS. Elucidation of the molecular mechanism by which this high degree of substrate specificity is exerted should be important in understanding the process of life.

The aminoacylation of tRNA involves usually two main steps *(1)*: the activation of amino acid with ATP forming an enzyme-aminoacyl adenylate complex (Equation 1) and the transfer of the amino acid to tRNA from the enzyme-aminoacyl adenylate complex (Equation 2).

$$E + AA + ATP \rightleftharpoons E{\bullet}AA{\sim}AMP + PPi \qquad (1)$$

$$E{\bullet}AA{\sim}AMP + tRNA \rightleftharpoons E + AMP + AA\text{-}tRNA \qquad (2)$$

where AA denotes an amino acid; E, the enzyme; and PPi, inorganic pyrophosphate. Individual ARS specific for one of the 20 amino acids constituting proteins has strictly to discriminate its cognate amino acid and tRNA among like compounds *in vivo*.

ARSs are classified into two groups (Class I and Class II) by characteristic sequences in the primary structure. The catalytic domain of Class I enzymes is different from that of Class II enzymes *(2, 3, 4)*. The three dimensional structures of eleven out of twenty ARSs have been or are being resolved by X-ray crystallographic analysis *(5)*.

I have been interested in elucidating the molecular mechanism of substrate recognition by ARS, and have chosen as the target LysRS (L-lysine:$tRNA^{Lys}$ ligase (AMP forming)), EC6.1.1.6, of

Bacillus stearothermophilus (**abbreviated to *B.s.* LysRS**), a Class II enzyme. A comprehensive review article on LysRS has recently appeared ***(6)***. In the previous paper ***(7)***, I revealed, based on the fluorometric analysis, the equilibrium dialysis, and kinetic analysis of the L-lysine dependent ATP-PPi exchange reaction, that the binding of the substrates, L-lysine and ATP, proceeded in the sequential ordered mechanism in which L-lysine was bound first to the enzyme. Accordingly, I have assumed that Equation 1 should be expanded at least to Equations 3, 4, and 5 in the case of *B.s.* LysRS:

$$E + \text{L-Lysine} \rightleftharpoons E\bullet\text{L-Lysine} \quad (3)$$

$$E\bullet\text{L-Lysine} + ATP \rightleftharpoons E\bullet\text{L-Lysine}\bullet ATP \quad (4)$$

$$E\bullet\text{L-Lysine}\bullet ATP \rightleftharpoons E\bullet\text{L-Lys}\sim AMP + PPi \quad (5)$$

In the present study, I have examined the formation of the enzyme•lysyladenylate complex by fluorometric measurements of the binding of ATP and L-lysine or its analogues. I have also tried to isolate the enzyme•lysyladenylate complex and an enzyme•lysinehydroxamate-AMP complex to find the binding stoichiometry.

MATERIALS AND METHODS

Enzymes: *B.s.* LysRS was purified from *B. stearothermophilus* according to the methods described previously ***(7)***. The enzyme is a homodimer of which the molecular weight of the subunit is 57,700. The enzyme concentration was determined with the molar absorption coefficient ε at 280nm of 71,600 $M^{-1}cm^{-1}$ at pH 8.0.

L-Lysine and lysine analogues:

L-Lysine and *S*-(2-aminoethyl)-L-cysteine (**abbreviated to SAEC**) was the product of Wako Pure Chemical Industries.

Cadaverine, 6-amino-*n*-hexanoic acid, L-norleucine, L-ornithine, and D-lysine were purchased from Nakarai Tesque. L-Lysine hydroxamate **(abbreviated to L-Lyshxt)**, L-lysine amide, 5-hydroxylysine (mixed DL and DL-allo) were obtained from Sigma Chemical Co. *Threo*-4-hydroxy-L-lysine was purchased from Fluka Fine Chemicals.

Others: Anthraniloyl-ATP was synthesized according to the methods of Hiratsuka *et al.* ***(8)***. Adenosine 5'-[γ-^{32}P]triphosphate was the product of Amersham International; [2,8-^{3}H] adenosine 5'-triphosphate (tetraammonium salt), of Moravek Biochemicals; [4,5-^{3}H] L-lysine, of NEN Research Products; ATP (disodium salt) and α,β-methyleneATP, of Sigma Chemical Co.; glass microfiber filter (GF/C), of Whatman Ltd.; nitrocellulose membrane filters (pore size, 100nm and 1000nm) and DEAE-cellulose filter, of Advantec Toyo Co. Sephacryl S-200 and NAP-10 columns (prepacked columns with Sephadex G-25) were purchased from Pharmacia Fine Chemicals. Unfractionated tRNA from *Escherichia coli* MRE 600 was purchased from Boehringer Mannheim. All other chemicals were of reagent grade.

Fluorescence titration: The purified LysRS was dialyzed, before the fluorescence measurement, against 100mM Tris-HCl buffer (pH 8.0) containing 10mM $MgCl_2$. Fluorometric titration was conducted at 30°C in the same buffer with a Hitachi Fluorescence Spectrophotometer 850. The excitation wavelength and emission wavelength were 295nm and 340nm, respectively. When the fluorometric titration of a ligand was done in the absence of the other ligand, K_d and ΔF_{max1} were determined by the method previously reported ***(7)***. When the fluorometric titration of a ligand L_1 was carried out in the presence of a saturating amount of the

other ligand L_2, the apparent K_d **(abbreviated to $K_{d,\ app}$)** and ΔF_{max1} were determined according to the Equations 6~8 using the nonlinear least-squares method ***(9)***.

$E \bullet L_2 + L_1 \rightleftharpoons E \bullet L_2 \bullet L_1$ (6)

$K_{d,\ app} = [E \bullet L_2][L_1] / [E \bullet L_2 \bullet L_1]$ (7)

$\Delta F\ (\%) = \Delta F_{max1}[L_1]_0 / (K_{d,\ app} + [L_1]_0)$ (8)

where $\Delta F\ (\%) = 100(F_{E \bullet L_2 \bullet L_1} - F_{E \bullet L_2}) / F_E$,; and $F_{E \bullet L_2 \bullet L_1}$, $F_{E \bullet L_2}$ and F_E are the fluorescence intensities at 340nm of the enzyme-ligand$_2$-ligand$_1$ complex, the enzyme-ligand$_2$ complex, and the free enzyme, respectively.

Enzyme assay: The activity of *B.s.* LysRS was measured by either the ATP-PPi exchange reaction or the aminoacylation of tRNA. The ATP-PPi exchange reaction with [^{32}P]-PPi and the aminoacylation of tRNA with [4, 5-^{3}H]-L-lysine were measured as described previously ***(7)***.

Filter assay: Glass microfiber filters were immersed in 100mM Tris-HCl buffer (pH 8.0) containing 10mM $MgCl_2$ over night. After preincubation of the reaction mixture without the enzyme (20μl) at 37°C for 2min, the enzyme solution (20μl) was added to it. The final reaction mixture contained in 40μl: 100mM Tris-HCl (pH 8.0), 10mM $MgCl_2$, 4.65μM LysRS, and either 200μM [4,5-^{3}H] L-lysine (abbreviated to ^{3}H-L-lysine) (0.5 Ci/mmol) plus 1mM ATP or 1mM L-lysine plus 200μM [2,8-^{3}H] ATP **(abbreviated to ^{3}H-ATP)** (0.5 Ci/mmol). After incubation at 37°C for several different time intervals, the reaction mixture was placed in an ice bath for 5min to stop the reaction. An aliquot (up to 40μl) of the reaction mixture was filtered through Whatman GF/C glass fiber filter and the filter was washed six times with each 3ml of ice-cold 100mM Tris-HCl buffer (pH 8.0) containing 10mM $MgCl_2$. After the filter was dried

under an IR lamp, the radioactivity remaining on the filter was measured in a Packard Liquid Scintillation Spectrometer Tri Carb 3255 similarly as the case of tRNA aminoacylation. When adenosine 5'-[γ-^{32}P]triphosphate **(abbreviated to ^{32}P-ATP)** was to be used, ^{3}H-ATP was substituted by ^{32}P-ATP.

Isolation of the enzyme•lysyladenylate complex with gel-filtration: The reaction mixture contained in 0.4ml: 100mM Tris-HCl buffer (pH 8.0) containing 10mM $MgCl_2$, 25μM ^{3}H-L-lysine (1.0 Ci/mmol), 1mM ATP, and 2.2μM *B.s.* LysRS. After incubation at 37°C for 4min, the reaction mixture was applied to a Sephacryl S-200 column (ϕ 2 x 50cm) equilibrated with 100mM Tris-HCl buffer (pH 8.0) containing 10mM $MgCl_2$ and eluted with the same buffer at 4°C. Each fraction of the eluate was subjected to the filter assay, the measurement of the absorbance at 260nm, and the total radioactivity measurement. The total radioactivity was measured as follows: the sample solution was spotted on the glass fiber filter, which was dried under an IR lamp without washing, and the radioactivity on the filter was measured as in the case of filter assay.

RESULTS

Fluorescence change of B.s LysRS by the addition of ATP in the presence of L-lysine or lysine analogues: Addition of ATP to *B.s* LysRS that had been saturated with L-lysine caused apparent increase of protein fluorescence; this may be expressed alternatively as that the fluorescence quenching of LysRS caused by the binding of L-lysine *(7)* was restored by the addition of ATP **(Fig. 1)**. This is different from the observation with *B.s.* ValRS (a monomer, Class I enzyme) reported previously, in which the addition of either L-

valine or ATP lead to a quenching of protein fluorescence and the effects were additive ***(10, 11)***. This restoration may be regarded as a reflexion of either ATP binding to LysRS (Equation 4) or the formation of lysyl adenylate on the enzyme (Equation 5), or both, because the conditions employed were the same as those for the L-lysine dependent ATP-PPi exchange reaction except the absence of added PPi. The apparent dissociation constant of ATP and LysRS•L-lysine complex, $K_{d,app,A}$, was obtained by fitting to Equation 8 to be 15.5μM, which is one fourth of K_m for ATP, 65.1μM, in the ATP-PPi exchange reaction ***(7)***.

Such phenomena of fluorescence restoration by ATP were also observed in the cases that the enzyme was saturated with SAEC, substrate of *B.s.* LysRS in the ATP-PPi exchange reaction, and with L-Lyshxt and L-lysine amide, strong inhibitor of *B.s.* LysRS in the L-lysine dependent ATP-PPi exchange reaction **(Fig.2)**, although the degree of restoration was different in each case. The values of $K_{d,app,A}$ are 47.3μM with SAEC, 3.0μM with L-Lyshxt, and 4.0μM with L-lysine amide **(Table I)**.

The presence of EDTA inhibited the fluorescence restoration by ATP of the L-lysine-saturated enzyme **(Fig. 3)**. α,β-MethyleneATP and anthraniloyl-ATP, neither of which is substrate of the L-lysine-dependent ATP-PPi exchange reaction, did not cause fluorescence restoration of *B.s.* LysRS saturated with L-lysine **(data not shown)**.

Fluorometric titration of LysRS with L-lysine and lysine analogues in the presence of excess ATP: On the other hand, the addition of L-lysine to *B.s.* LysRS in the presence of 1mM ATP caused quenching of the protein fluorescence to a lesser extent **(Fig. 1)** than the case of the absence of ATP **(Table I)**. The final

level of the relative fluorescence intensity coincided more or less with the level after the fluorescence restoration by ATP of the L-lysine-saturated LysRS (**Fig. 1**). The apparent dissociation constant of L-lysine in the presence of excess amount of ATP calculated with Equation 8, $K_{d, app, L}$, is 50.9μM (**Table I**), while K_m for L-lysine was 23.6μM in the ATP-PPi exchange reaction *(7)*.

The fluorometric titration of LysRS were carried out also with lysine analogues in the presence of 1mM ATP (**Fig. 4**). Estimated $K_{d, app, L}$ and ΔF_{max} are listed in **Table I** together with K_d obtained in the absence of ATP as reported previously *(7)*. SAEC and threo-4-hydroxy L-lysine, which were substrate in the ATP-PPi exchange reaction, caused quenching of fluorescence of LysRS in the presence of ATP, though to a lesser extent than in the absence of ATP. Each $K_{d, app, L}$, 421μM for SAEC, 11.2mM for threo-4-hydroxy L-lysine, is slightly larger than the respective K_d obtained in the absence of ATP. 5-Hydroxy-L-lysine and L-ornithine did not cause fluorescence change in the presence of ATP, although they were substrate of the ATP-PPi exchange reaction. The fluorescence change was not detected, in the presence of ATP, either with D-lysine, 6-amino-n-hexanoic acid, or norleucine, which were inhibitor of the ATP-PPi exchange reaction. All the α-carboxyl group-modified analogues of L-lysine tested: cadaverine, L-Lyshxt, and L-lysine amide, which were inhibitor of the ATP-PPi exchange reaction, caused fluorescence quenching of LysRS in the presence of ATP, and each estimated $K_{d, app, L}$ is considerably smaller than respective K_d obtained in the absence of ATP (**Table I**).

Filter assay: The formation of lysyladenylate on *B.s.* LysRS was examined with ^{3}H-L-lysine or ^{3}H-ATP by trapping the complex on the filter. An appreciable radioactivity was detected on the filter

only when LysRS, L-lysine, and ATP are present together **(Fig. 5)**. The glass fiber filter held more radioactivity than did either cellulose nitrate filter or DEAE-cellulose filter at pH 8.0 **(Fig. 6)**. The radioactivity trapped on the glass fiber filter was proportional to the enzyme concentration used **(Fig. 6, inset)**.

When the enzyme was added to the reaction mixture containing ^{3}H-ATP and either L-lysine or L-Lyshxt, an appreciable radioactivity was detected on the filter in the both cases **(Fig. 7)**. However, when ^{3}H-ATP was replaced by [γ-^{32}P] ATP **(abbreviated ^{32}P-ATP)**, no radioactivity was detected in either cases **(Fig. 7)**. This implies that the enzyme•lysyladenylate complex (LysRS•L-Lys~AMP) or an enzyme • lysinehydroxamate-AMP (or -ADP) complex has been formed and trapped on the filter.

Isolation of the LysRS•lysyladenylate complex by gel filtration, and transfer of lysine from the complex to tRNA: The enzyme•lysyladenylate complex labelled with ^{3}H-lysine was isolated by gel filtration with a Sephacryl S-200 column. The eluate fractions that were active in the filter assay described above could be completely separated from those of free L-lysine and ATP at pH 8.0, 4°C **(data not shown)**. The isolated LysRS•lysyladenylate complex was kept at 0°C at pH 8.5 for 12 hours, during which the filter-assay activity was intermittently examined. The activity decreased gradually **(Fig. 8)**, and the halflife time of the complex decomposition was about 700min (k = 9.87x10^{-4} sec^{-1}) under these conditions. The transfer of ^{3}H-lysine from the complex to tRNA was followed as shown in **Fig. 8 (inset)**. The k_{app} of the transfer reaction was 0.012sec^{-1} at 0°C, pH 8.5.

Chasing the radioactivity out of the LysRS•lysyladenylate complex: The radioactivity of the LysRS•lysyladenylate complex

labelled with ^{3}H-ATP was chased out by cold ATP added to the elution buffer during gel filtration, but not by the added cold L-lysine (**Fig. 9A**). When the complex was labelled with ^{3}H-lysine, the radioactivity was chased out by the added cold L-lysine but not by the added cold ATP (**data not shown**). However, for the *B.s.* LysRS•lysinehydroxamate-AMP complex labelled with ^{3}H-ATP, the radioactivity was not chased out either by cold Lyshxt added to the buffer or by the added cold ATP (**Fig. 9B**). These results show that the formation of LysRS•lysyladenylate complex is reversible, whereas , the formation of LysRS•lysinehydroxamate-AMP complex is practically irreversible. The latter coincides with that I could not detect the L-Lyshxt dependent ATP-PPi exchange reaction *(7)*.

Binding stoichiometry of L-Lyshxt-AMP and B.s. LysRS: *B.s.* LysRS was titrated with ATP with the fluorescence change as probe in the presence of excess L-Lyshxt, and titrated with L-Lyshxt in the presence of excess ATP. In both cases the fluorescence changed linearly and reached a plateau (**Fig. 10**), and from the inflexion points of each curve, the stoichiometry of binding is estimated as one mole of each L-Lyshxt and ATP, consequently Lyshxt-AMP, per mole of dimer LysRS.

DISCUSSION

Substrate induced fluorescence change of B.s. LysRS in the presence of both L-lysine and ATP: The addition of ATP to *B.s.* LysRS that was saturated with either L-lysine (**Fig. 1**), SAEC (**Fig. 2**), or threo-4-hydroxy-L-lysine (**data not shown**), the substrates of the ATP-PPi exchange reaction, resulted in an apparent increase of

protein fluorescence or the restoration of protein fluorescence from the quenched state caused by the binding of the amino acid substrates. The fluorescence restoration thus observed reflects the binding of ATP to LysRS complexed with the amino acid substrate, and is consistent with the previous conclusion of the substrate binding shown as Equation 3 & 4.

Similar fluorescence restoration by ATP was found when it was added to the enzyme complexed with those lysine analogues of which α-carboxyl group was modified. They were cadaverine **(data not shown)**, L-Lyshxt, and L-lysine amide **(Fig. 2)**; All were inhibitor of the L-lysine dependent ATP-PPi exchange reaction by *B.s.* LysRS ***(7)***. These results may suggest that the observed fluorescence restoration accompanies with the step of ATP binding (Equation 4) rather than the formation of the lysyladenylate complex (Equation 5). The fact that the addition of EDTA to remove Mg ions decreased the binding strength of ATP **(Fig. 3)**, and that the addition, in place of ATP, of α,β-methyleneATP, an inhibitor, in which the triphosphate moiety seems to take a streched conformation, did not cause the fluorescence change **(data not shown)** may suggest that the triphosphate moiety of ATP must be in the right conformation to be properly bound to the enzyme to cause the fluorescence restoration. The observed values of $K_{d,\,app,\,A}$ **(Table I)** are smaller for the α-carboxyl modified analogues than for the substrates of the ATP-PPi exchange reaction. This is probably due to the lack of the repulsion between the negative electrostatic charges of carboxylate and phosphate in the former case.

The addition of L-lysine to *B.s.* LysRS in the presence of ATP resulted in a slight decrease in the protein fluorescence **(Fig. 1)**. There must have been no enzyme-ATP complex to start with in this

case according to the order of binding of the two substrates as proved previously, and as soon as the enzyme•L-lysine complex was formed by the addition of L-lysine, ATP should have been bound to this complex (Equations 3 & 4). The smaller degree of fluorescence quenching, thus, must be the outcome of the binding of both substrates.

The difference in the magnitude of $K_{d,\,app,\,L}$ thus obtained in the presence of ATP and of K_d obtained in the absence of ATP **(Table I)** should be a measure of the effect of ATP to the binding of L-lysine and the analogues. The ratio of the two dissociation constants ($K_{d,\,app,\,L}$ / K_d) are compared in **Table I**. For L-lysine, SAEC, and threo-4-hydroxy-L-lysine, $K_{d,\,app,\,L}$ is 2 to 3 fold larger than the respective K_d; thus, the effect of ATP even results in reduction of the binding strength of the amino acid substrate, which may be favorable for the following reactions. On the other hand, for those lysine analogues in which α-carboxyl group is modified, $K_{d,\,app,\,L}$ is much smaller (0.5-5%) than respective K_d **(Table I)**. Thus, the presence of ATP greatly enhances the apparent binding of those inhibitors.

The LysRS•lysyladenylate complex: **Figures 5 & 6** show that filtration using glass fiber filter can be used for the detection and quantitative analysis of the LysRS• lysyladenylate complex at pH 8.0. The radioactivity was trapped only when all LysRS, L-lysine, and ATP were present together in the reaction mixture **(Fig.5)**. Nitrocellulose filter and DEAE-cellulose filter have been used to trap other enzyme•aminoacyladenylate complexes ***(12, 13)***; however, under my conditions glass fiber filter exhibits higher trapping efficiency of the LysRS•lysyladenylate complex than either nitrocellulose or DEAE-cellulose filter **(Fig. 6)**. The trapping mechanism of glass fiber filter is not clear at present, but I speculate

that glass, silicate by nature, may have some ionic interaction with the complex. The LysRS•lysyladenylate complex can be isolated by gel filtration by detection with the filter assay. The half-time of the complex decomposition was about 11 hours at 0°C, pH 8.5 (**Fig. 8**), which is shorter than the value reported for *E. coli* LysRS•lysyladenylate complex: 30 hours at 4°C, pH 8.0 ***(14)***. Estimated k_{app} of the transfer reaction (**Fig. 8, inset**), 0.012sec^{-1}, is similar to the value for *E. coli* IleRS under comparable conditions ***(15)***.

A complex formed from LysRS, ATP, and L-Lyshxt: The above results with the filter assay (**Fig. 7**) indicate that the filter-trapped complex with L-Lyshxt was LysRS•L-Lyshxt-AMP or LysRS•L-Lyshxt-ADP. By analogy to LysRS•lysyladenylate complex, I may assume that the complex is LysRS•L-Lyshxt-AMP. Then, it looks contradictory, at least superficially, with the fact that I can not detect the L-Lyshxt dependent ATP-PPi exchange reaction ***(7)***. However, this apparent inconsistency is solved by assuming that the formation of the LysRS•Lyshxt-AMP complex is practically irreversible (Equation 9) as suggested by the results of radioactivity chasing-out experiments (**Fig. 9A & B**).

$$E + \text{L-Lyshxt} + ATP \longrightarrow E\bullet\text{Lyshxt-AMP} + PPi \qquad (9)$$

A recent study on the structure of *T. thermophilus* SerRS complexed with seryladenylate analogues ***(16)*** showed that serinehydroxamate-AMP complex was formed enzymatically in the enzyme crystal from ATP and serinehydroxamate, that the linkage between serinehydroxamate and AMP was -P-O-N(H)- rather than -P-N(OH)- as deduced from the results of ^{31}P-NMR studies, and that the enzyme serinehydroxamate-AMP complex was more stable to hydrolysis than the enzyme seryladenylate complex. These results

are suggestive for the interpretation of my observation on the reaction products of *B.s.* LysRS, ATP, and L-Lyshxt.

If one takes it into consideration that a stable covalent bond may have been formed between L-Lyshxt and AMP, the linear change of fluorescence in **Fig. 10** is rational. It is shown that one mole of L-Lyshxt-AMP is formed per mole of dimer LysRS under these conditions. Accordingly, "half of the sites" of the enzyme reactivity seems to have started at this step.

Structural considerations: *B.s.* LysRS and *E. coli* LysRS (u) have more than 50% homology in the primary structure **(Takita, *et al.*, to be published)**, and the three dimentional structure of *B.s.* enzyme is expected very similar to those of *E. coli* enzyme. The structure of *E. coli* LysRS (u) complexed with L-lysine has been resolved at 2.8Å resolution ***(17)***. Onesti *et al.* ***(17)*** describe that a model of ATP binding to *E. coli* LysRS (u) can be built easily although no experimental data of X-ray crystallography is available. The structure of ATP bound to yeast AspRS•$tRNA^{Asp}$•ATP complex ***(18)*** can be simply pasted into the structure of *E. coli* LysRS (u) without any mannual adjustment. This is likely to mean that the ATP binding site is in an open state in LysRS complexed with L-lysine. This agrees with my conclusion that the first binding of L-lysine to *B.s.* LysRS enables ATP to enter the binding site of the enzyme.

The triphosphate back bone of this ATP molecule is said in a bent conformation ***(18)*** which is stabillized by charged residues of the enzyme and Mg ion. My results of fluorometric study in the presence of EDTA (**Fig. 3**) and with α, β-methylene ATP in place of ATP seems to be in accordance with this aspects of ATP conformation.

LysRS is classified into the same subclass with AspRS among the Class II enzymes ***(3, 4, 19, 20)***. The amino acid residues bound to ATP and L-aspartic acid substrate in yeast AspRS are functionally well conserved in *E. coli* LysRS. It was reported with yeast AspRS that the postulated binding site of L-aspartic acid should be blocked when ATP was in its binding site and that the substrate binding should be the sequential ordered mechanism in which L-aspartic acid was bound first ***(18)***. This agrees with my conclusion on the order of substrate binding in *B.s.* LysRS as reported in the previous paper (Equation 3 & 4) and with the observation on ATP binding presented in this paper, implying that the topology of the substrate binding site of *B.s.* LysRS is similar to that of yeast AspRS.

REFERENCES

1) Berg, P. (1961) Specificity in protein synthesis. *Annu. Rev. Biochem.* **30**, 293-324

2) Eriani, G., Delarue, M., Poch, O., Gangloff, J., and Moras, D. (1990) Partition of tRNA synthetases into two classes based on mutually exclusive sets of sequence motifs. *Nature*, **347**, 203-206

3) Delarue, M. and Moras, D. (1992) "Nucleic Acid and Molecular biology", **6**, ed. by F. Eckstein and D. M. J. Lilley, Springer-Verlag Berlin, Heidelberg, pp.203-224.

4) Carter, C. W. Jr. (1993) Cognition, mechanism, and evolutionary relationships in aminoacyl-tRNA synthetases. *Annu. Rev. Biochem.* **62**, 715-748

5) Cusack, S. (1995) Eleven down and nine to go. *Nature Structual Biology*, **2**, 824-831

6) Freist, W. and Gauss, D. H. (1995) Lysyl-tRNA synthetase. *Biol. Chem. Hoppe-Seyler*, **376**, 451-472

7) Takita, T., Ohkubo, Y., Shima, H., Muto, T., Shimizu, N., Sukata, T., Ito, H., Saito, Y., Inouye, K., Hiromi, K., and Tonomura, B. (1996) Lysyl-tRNA synthetase from *Bacillus stearothermophilus*. Purification, and fluorometric and kinetic analysis of the binding of substrates, L-lysine and ATP. *J. Biochem.*, (in press).

8) Hiratsuka, T. (1983) New ribose-modified fluorescent analogues of adenine and guanine nucleotides available as substrates for various enzymes. *Biochim. Biophys. Acta* **742**, 496-508

9) Sakoda, M. and Hiromi, K. (1976) Determination of the best-fit values of kinetic parameters of the Michaelis-Menten equation by the method of least squares with Taylor expansion. *J. Biochem.* **80**, 547-555

10) Kakitani, M., Tonomura, B., and Hiromi, K. (1986) Valyl-tRNA synthetase from *Bacillus stearothermophilus*. Purification and binding with the substrate L-valine and ATP. *Agric. Biol. Chem.* **50**, 2437-2444

11) Kakitani, M., Tonomura, B., and Hiromi, K. (1987) Fluorometric study on the interaction of amino acids and ATP with valyl-tRNA synthetase from *Bacillus stearothermophilus*. *J. Biochem.* **101**, 477-484

12) Yarus, M. and Berg, P. (1970) On the properties and utility of a membrane filter assay in the study of isoleucyl-tRNA synthetase. *Anal. Biochem.* **35**, 450-465

13) Bartmann, P., Hanke, T., and Holler, E. (1976) Rapid determination of an amino acid:tRNA ligase•aminoacyl

adenylate complex on DEAE-cellulose filter disks. *Anal. Biochem.* **70**, 174-180

14) Waldenström, J. (1968) Some properties of lysyl ribonucleic acid synthetase from *Escherichia coli. Eur. J. Biochem.* **5**, 239-245

15) Eldred, E., W. and Schimmel P., R. (1972) Investigation of the transfer of amino acid from a transfer ribonucleic acid synthetase-aminoacyl adenylate complex to transfer ribonucleic acid. *Biochemistry*, **11**, 17-23

16) Belrhali, H., Yaremchuk, A., Tukalo, M., Larsen, K. Berthet-Colominas, C., Leberman, R., Beijer, B., Sproat, B. Als-Nielsen, J., Grübel, G., Legrand, J-F., Lehmann, M. and Cusack, S. (1994) Crystal structure at 2.5 angstrom resolution of seryl-tRNA synthetase complexed with two analogues of seryl adenylate. *Science*, **263**, 1432-1436

17) Onesti, S., Miller, A. D., and Brick, P. (1995) The crystal structure of the lysyl-tRNA synthetase (LysU) from *Escherichia coli. Structure*, **3**, 163-176

18) Cavarelli, J., Eriani, G., Rees, B., Ruff, M., Boeglin, M. Mitschler, A., Martin, F., Gangloff, J., Thierry, J. C. and Moras, D. (1994) The active site of yeast aspartyl-tRNA synthetase: structual and functional aspects of the aminoacylation reaction. *EMBO J.* **13**, 327-337

19) Eriani, G., Dirheimer, G., and Gangloff, J. (1990) Aspartyl-tRNA synthetase from *Escherichia coli*: cloning and characterisation of the gene, homologies of its translated amino acid sequence with asparaginyl- and lysyl-tRNA synthetases. *Nucl. Acids Res.* **18**, 7109-7118

20) Cusack, S., Härtlein, M., and Leberman R. (1991) Sequence, structual and evolutionary relationships between class 2 aminoacyl-tRNA synthetases. *Nucl. Acids Res.* **19**, 3489-3498

Table I
Fluorometric parameters of the binding of ATP, L-lysine, and its analogues with *B.s.* LysRS

	In the absence of ATP[a]		In the presence of ATP				$K_{d,app,L}/K_d$
			A[b]		B[c]		
	K_d (μM)	ΔF_{max} (%)	$K_{d,app,L}$ (μM)	ΔF_{max} (%)	$K_{d,app,A}$ (μM)	ΔF_{max} (%)	(%)
L-lysine	20.4 ± 1.8[d]	16.1	50.9 ± 3.2	5.0	15.5 ± 0.9	12.8	250
α-carboxyl group modified							
cadaverine	19,900 ± 900	15.6	120 ± 18	4.1	/[e]	/	0.60
L-lysine hydroxamate	704 ± 79	11.0	4.0 ± 0.6	4.8	2.98 ± 0.54	9.31	0.57
L-lysine amide	4,260 ± 210	16.6	48.9 ± 3.7	10.2	3.98 ± 0.55	5.51	0.12
α-amino group modified							
6-amino-*n*-hexanoic acid	21,000 ± 2,160	8.2	—[f]	0	-	0	-
ε-amino group modified							
L-norleucine	—	0	—	0	-	0	-
Others							
S-(2-aminoethyl)-L-cysteine	197 ± 24	14.1	421 ± 35	5.6	47.3 ± 2.6	9.13	213
L-ornithine	14,700 ± 900	8.2	—	0	/	/	-
D-lysine	3,180 ± 180	10.2	—	0	-	0	-
5-hydroxylysine (mixed DL and DL-allo)	18,600 ± 600	19.0	—	0	-	0	-
threo-4-hydroxy-L-lysine	3,230 ± 170	8.9	11,200 ± 1,300	6.1	/	/	347

$[E]_0$=4.2μM, λ_{ex}=295nm, λ_{em}=340nm, pH 8.0, 30°C.
a), Cited from the previous report *(7) B.s.* LysRS was titrated with L-lysine and its analogues.
b), *B.s.* LysRS was titrated with L-lysine and its analogues in the presence of 1mM ATP.
c), *B.s.* LysRS was titrated with ATP in the presence of excess L-lysine and its analogues.
d), $[E]_0$=0.88μM
e), Not measured.
f), — indicates that the fluorescence change could not be detected.

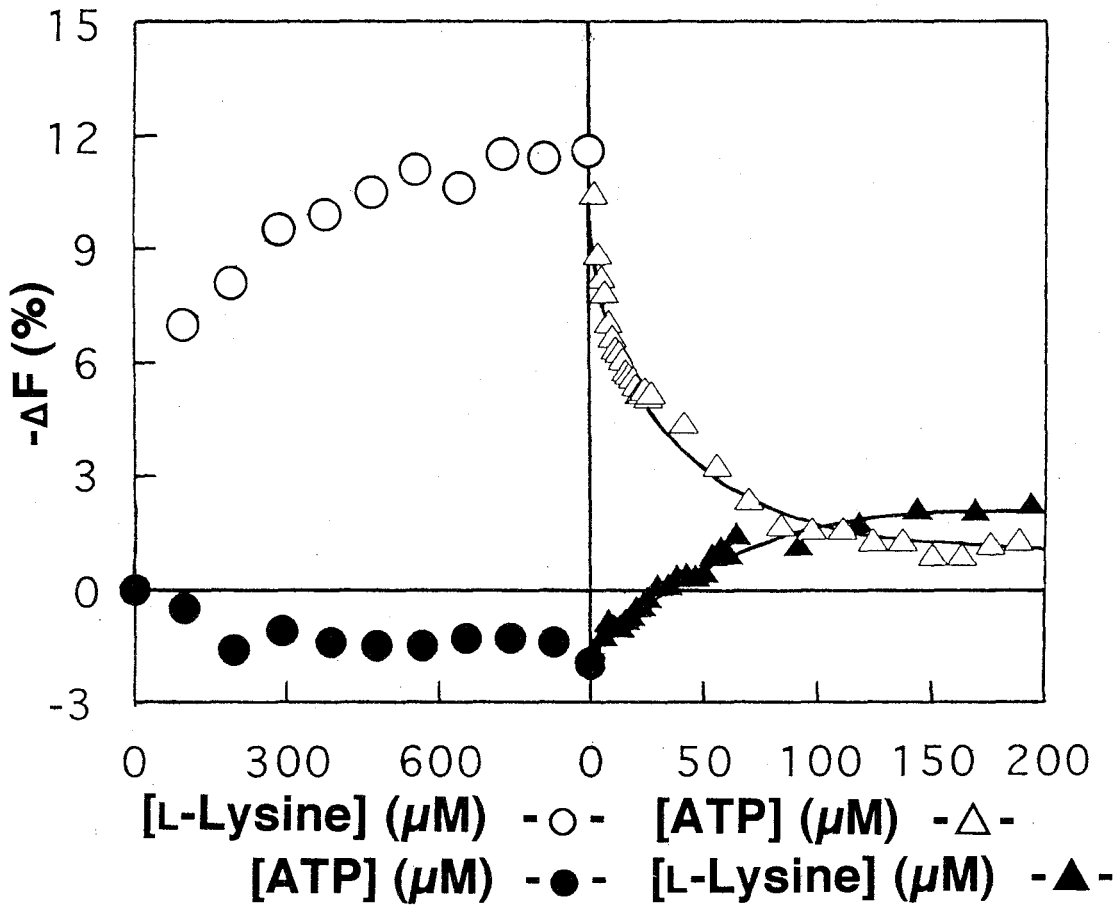

Figure 1

Fluorescence titration of *B.s.* LysRS with L-lysine and ATP

(A) Titration with L-lysine (○) followed by ATP (△).
(B) Titration with ATP (●) followed by L-lysine (▲).
The reaction mixture contained 100mM Tris-HCl buffer, pH 8.0, 10mM $MgCl_2$, and 4.2μM LysRS.
λ_{ex}=295nm, λ_{em}=340nm, at 30°C.
$K_{d,\,app,\,A}$=15.5±0.9μM (△) $K_{d,\,app,\,L}$=50.6±3.1μM (▲).
The solid curves are the threoretical ones obtained according to Equation 8 with respective dissociation constants.

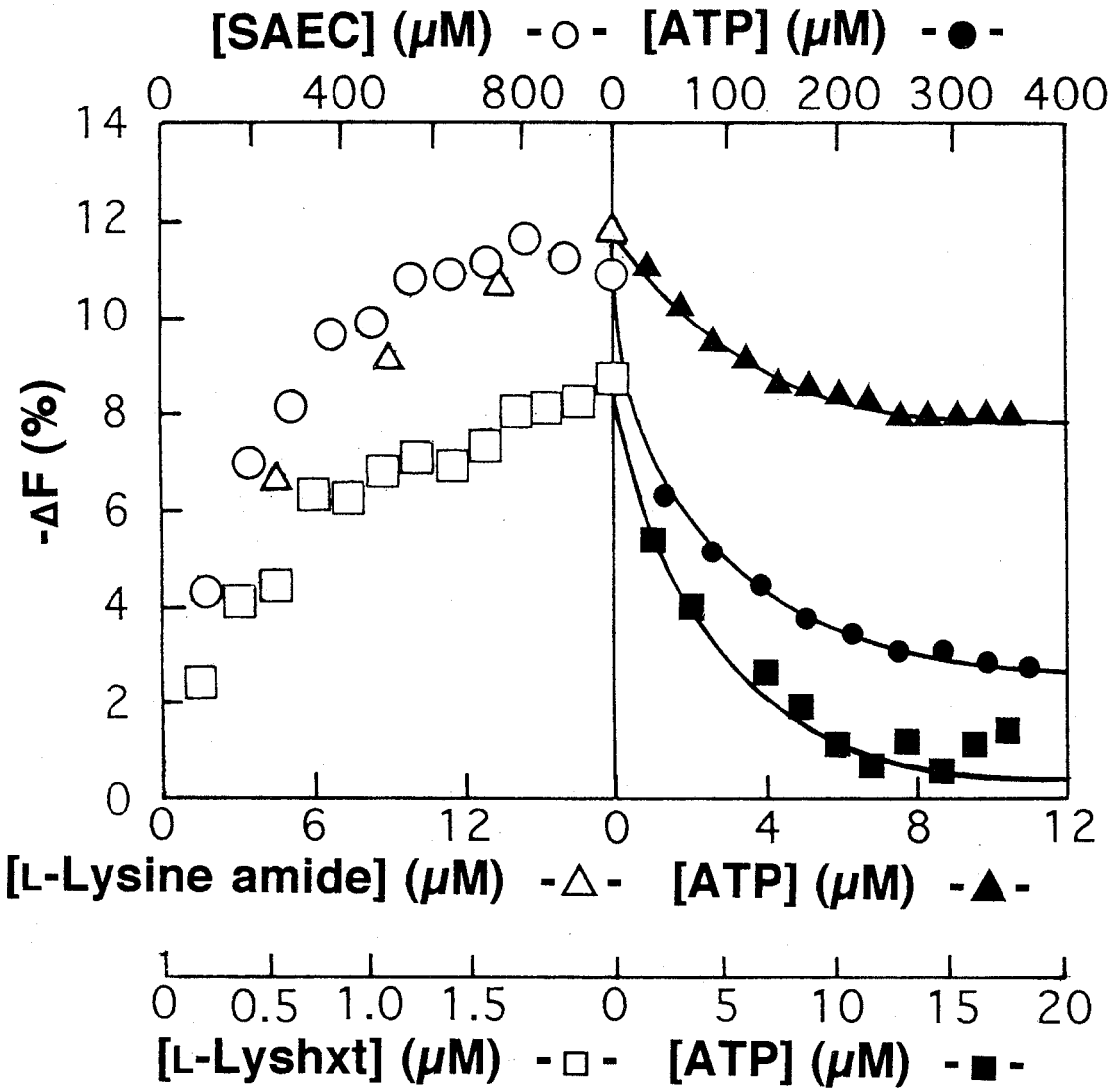

Figure 2

Fluorescence titration of *B.s.* LysRS with lysine analogues and ATP

The reaction mixture contained 100mM Tris-HCl buffer, pH 8.0, 10mM $MgCl_2$, and 4.2μM LysRS. λ_{ex}=295nm, λ_{em}=340nm, at 30°C. Titration with SAEC (○) followed by ATP (●). $K_{d,\,app,\,A}$=47.3±2.6μM (●). Titration with L-Lyshxt (□) followed by ATP (■). $K_{d,\,app,\,A}$= 2.97±0.54μM (■). Titration with L-lysineamd (△) followed by ATP (▲). $K_{d,\,app,\,A}$= 3.98±0.55μM (▲). The solid curves are the threoretical ones obtained according to Equation 8 with respective dissociation constants.

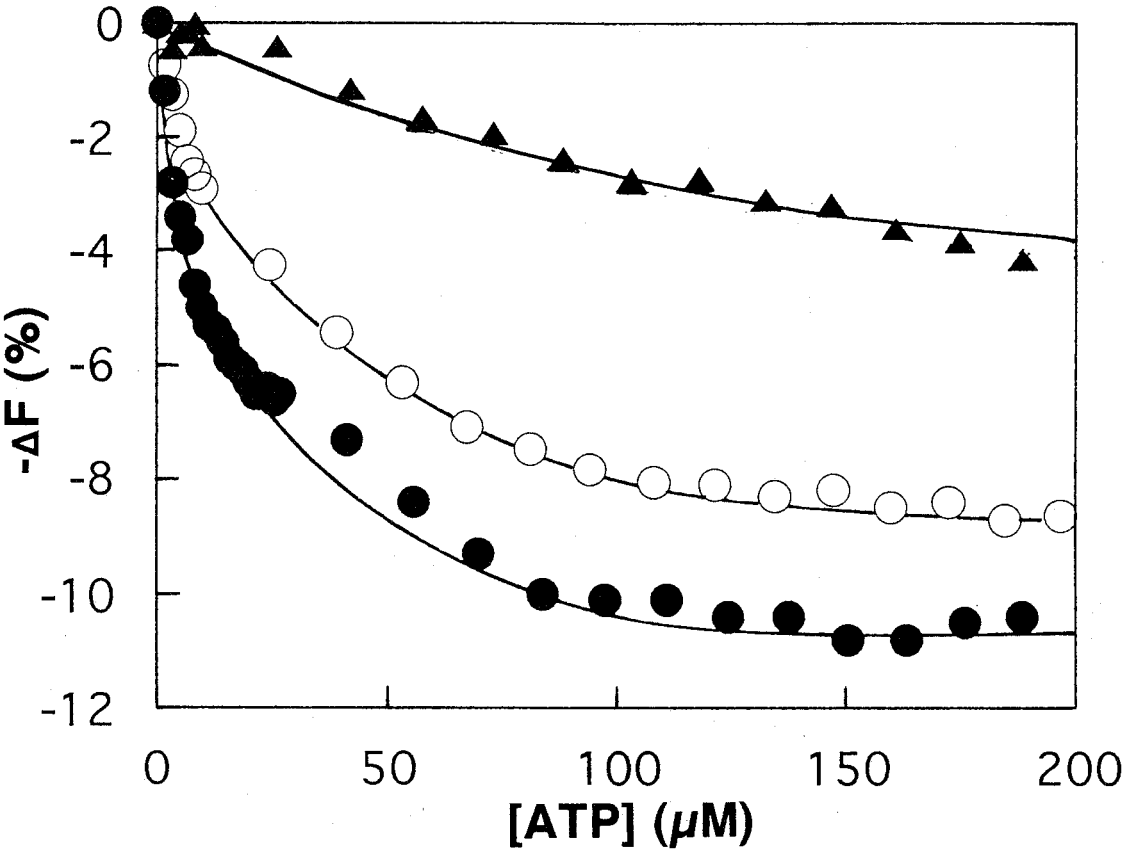

Figure 3

Effect of EDTA on the fluorescence titration with ATP of *B.s.* LysRS saturated with L-lysine

Titration of LysRS with ATP in the presence of L-lysine and EDTA (-●-, 0M; -○-, 500μM; -▲-, 5mM). Estimated $K_{d,\,app,\,A}$´s are as follows: -●-, 15.5±0.9μM; -○-, 25.7±1.6μM; -▲-, 443.3±22.7μM. The reaction mixture contained 100mM Tris-HCl buffer, pH 8.0, 10mM $MgCl_2$, 4.0μM LysRS, 1mM L-lysine, and various concentration of EDTA. λ_{ex}=295nm, λ_{em}=340nm, at 30°C.

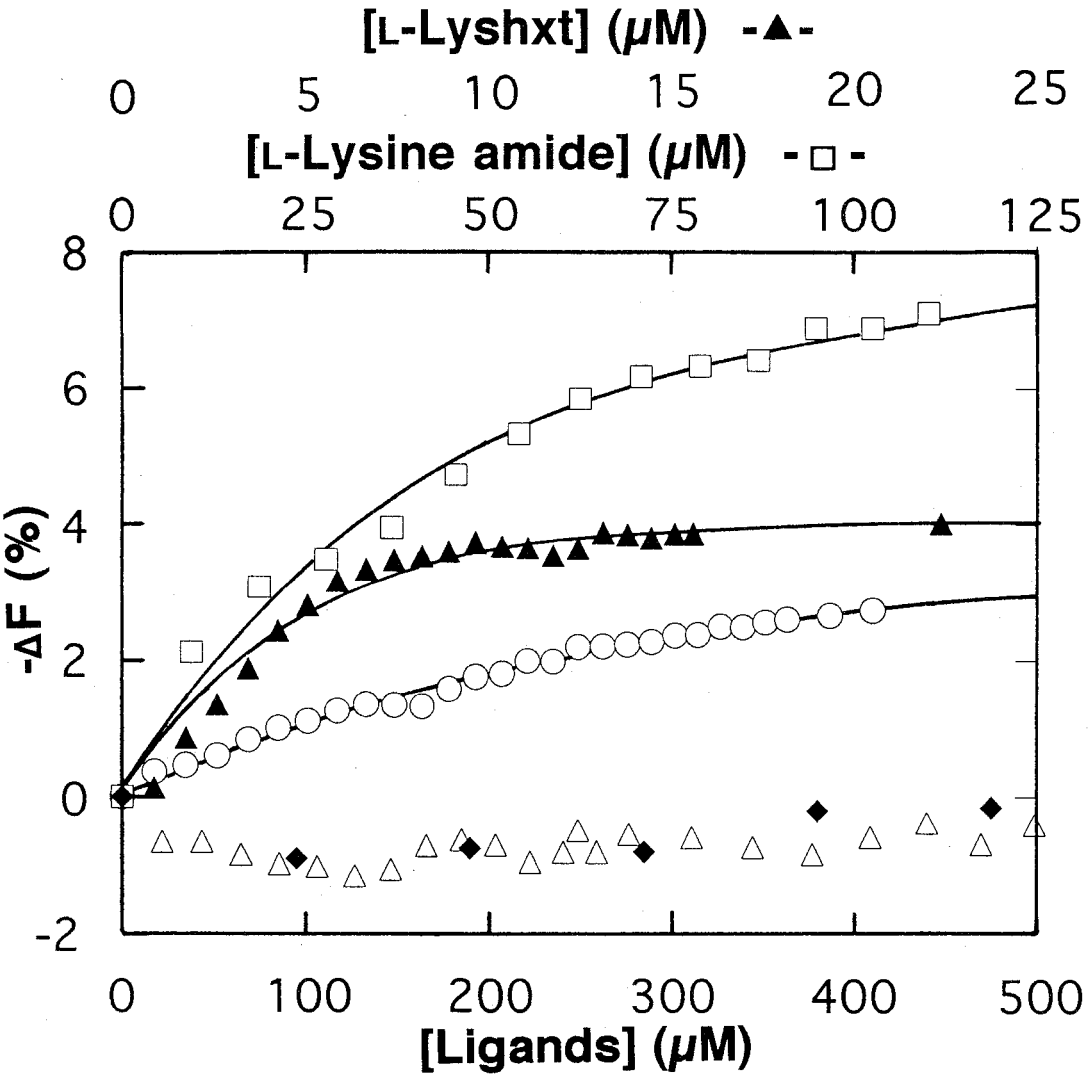

Figure 4

Flulorescence titration of *B.s.* LysRS with lysine analogues in the presence of excess ATP

Titration of LysRS with lysine analogues in the presence of 1mM ATP. SAEC (○), L-Lyshxt (▲), L-Lysamd (□), D-lysine (△), and 6-amino-*n*-hexanoic acid (◆). The reaction mixture contained 100mM Tris-HCl buffer, pH 8.0, 10mM $MgCl_2$, 1mM ATP, and 4.2μM LysRS. λ_{ex}=295nm, λ_{em}=340nm, at 30°C. The solid curves are the threoretical ones obtained according to Equation 8 with $K_{d,\,app,\,L}$ of 421±35μM (○), 4.0±0.6μM (▲), and 49.0±3.7μM (□).

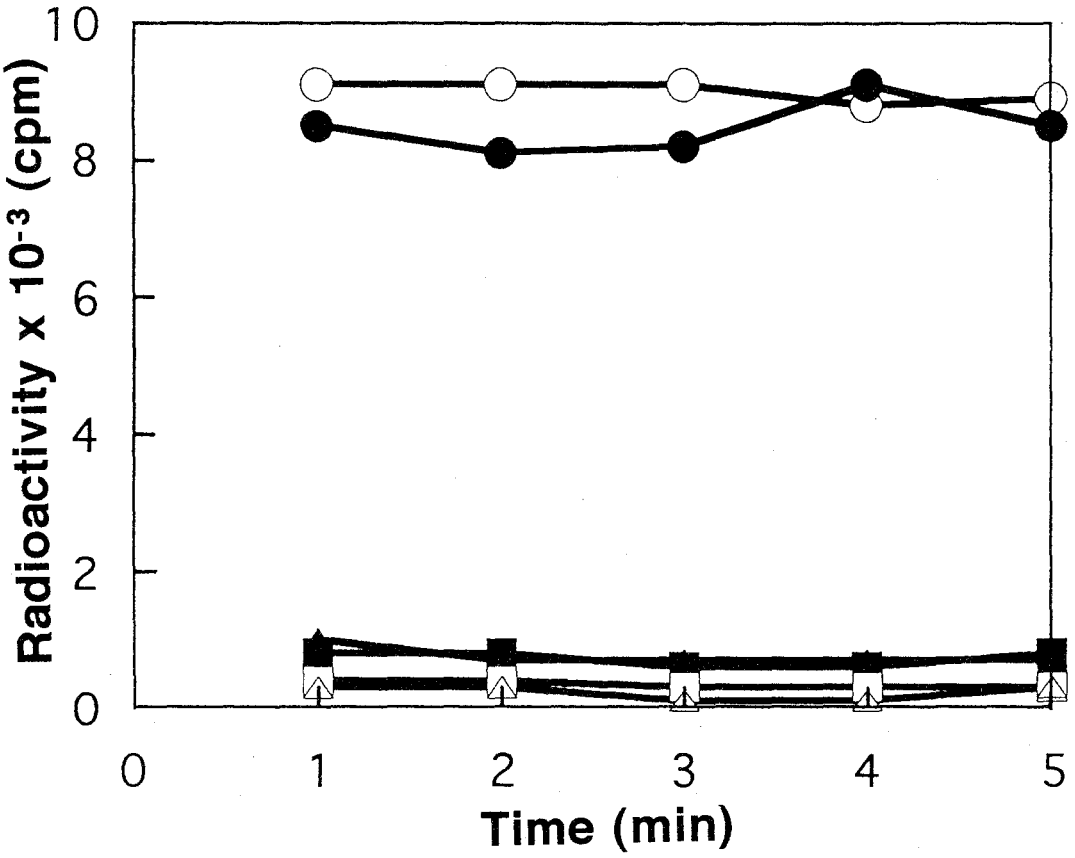

Figure 5

Filter assay of *B.s.* LysRS using glass fiber filter

The reaction mixture contained 100mM Tris-HCl buffer, pH 8.0, and either of the following: (4.7μM LysRS + 200μM ^{3}H-L-lysine + 1mM ATP; -●-), (4.7μM LysRS + 200μM ^{3}H-L-lysine; -■-), (200μM ^{3}H-L-lysine + 1mM ATP; -▲-), (4.7μM LysRS + 1mM L-lysine + 200μM ^{3}H-ATP; -○-), (4.7μM LysRS + 200μM ^{3}H-ATP; -□-), or (1mM L-lysine + 200μM ^{3}H-ATP; -△-).

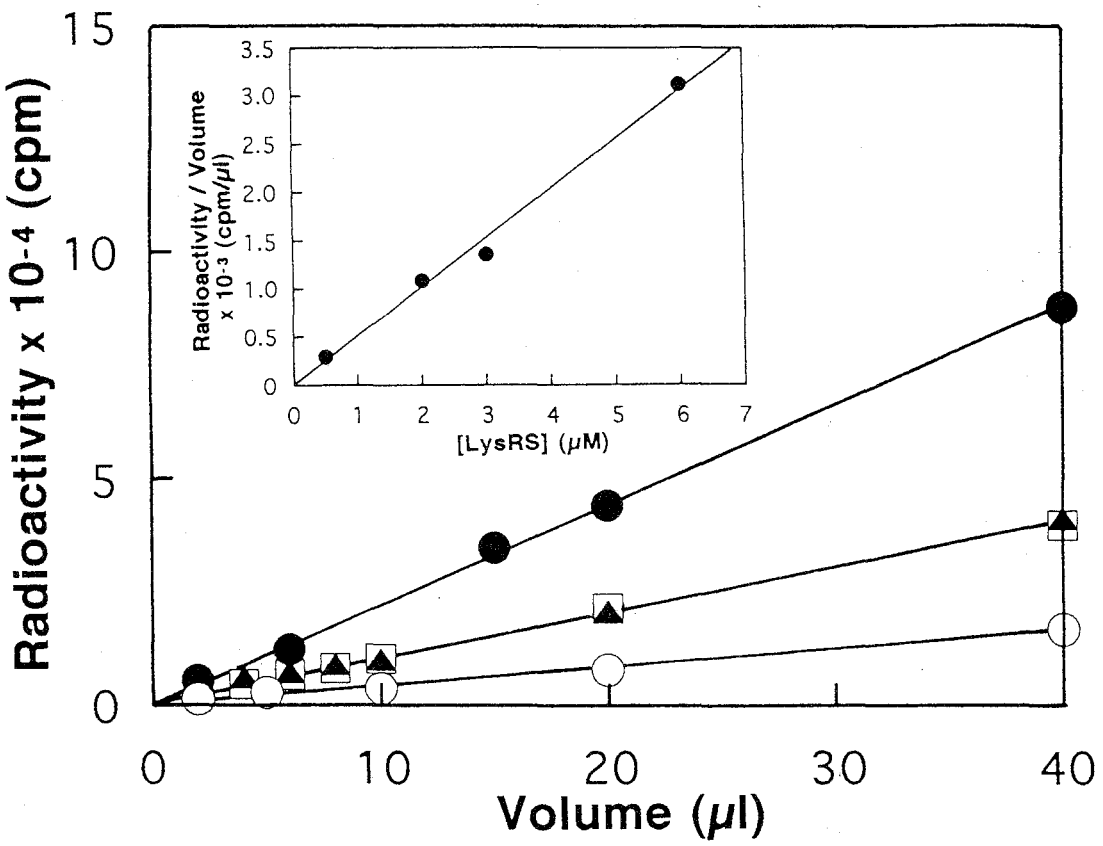

Figure 6

The comparison of glass fiber, nitrocellulose, and DEAE-cellulose filters in the filter assay

The reaction mixture contained 100mM Tris-HCl buffer, pH 8.0, 10mM $MgCl_2$, 4.7μM LysRS, 200μM [4,5-^{3}H] L-lysine (0.5 Ci/mmol), and 1mM ATP. Various volumes of the reaction mixture were subjected to the filter assays using each glass fiber filter (●), nitrocellulose filter (-□-, pore size 100nm and -▲-, pore size 1000nm), and DEAE-cellulose filter (○). Inset shows the replot of the slope of the main figure with glass fiber filter against the enzyme concentration used.

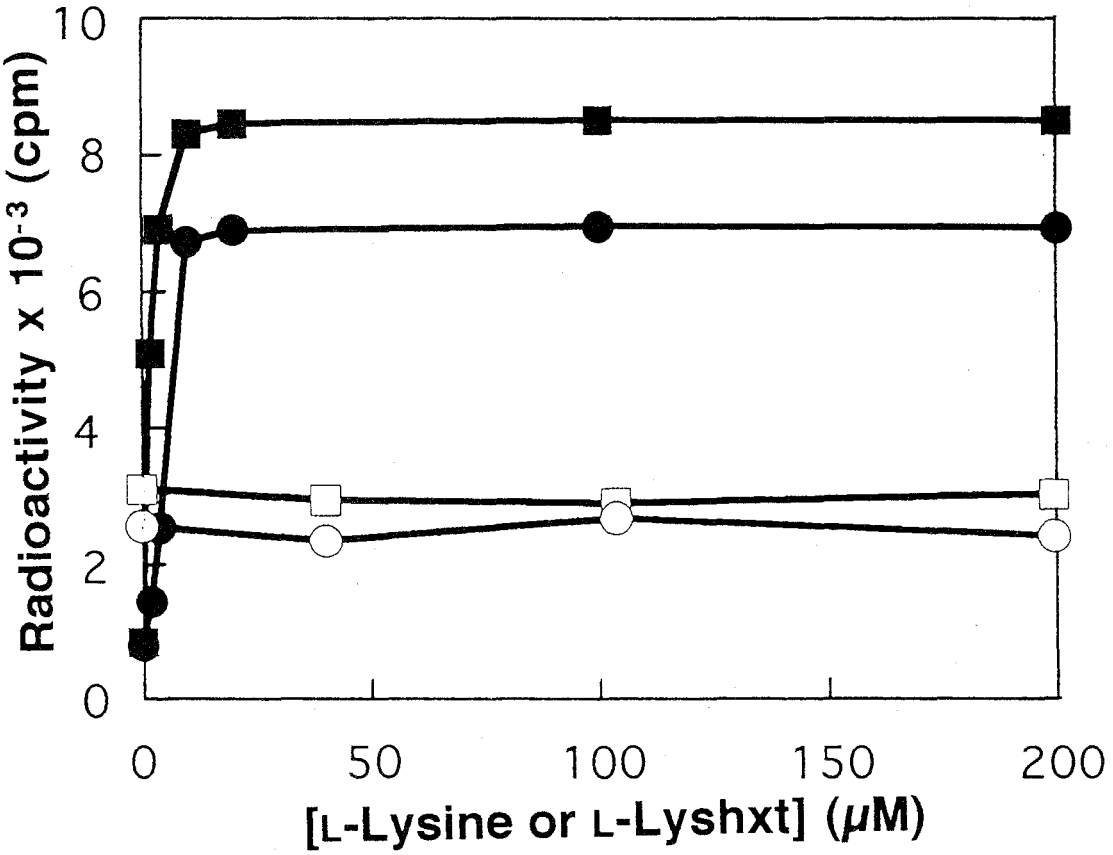

Figure 7

Formation of a *B.s.* LysRS•Lyshxt-AMP complex as judged by the filter assay

The reaction mixture contained 100mM Tris-HCl buffer, pH 8.0; 10mM $MgCl_2$; 4.2μM LysRS; either L-lysine or L-Lyshxt; 200μM ATP labelled with either [2, 8 ^{3}H]-ATP or [γ-^{32}P]-ATP. (●) and (○) represent the trapped radioactivity when L-lysine was used with ^{3}H-ATP and ^{32}P-ATP, respectively. (■) and (□) represent the trapped radioactivity when L-Lyshxt was used with ^{3}H-ATP and ^{32}P-ATP, respectively.

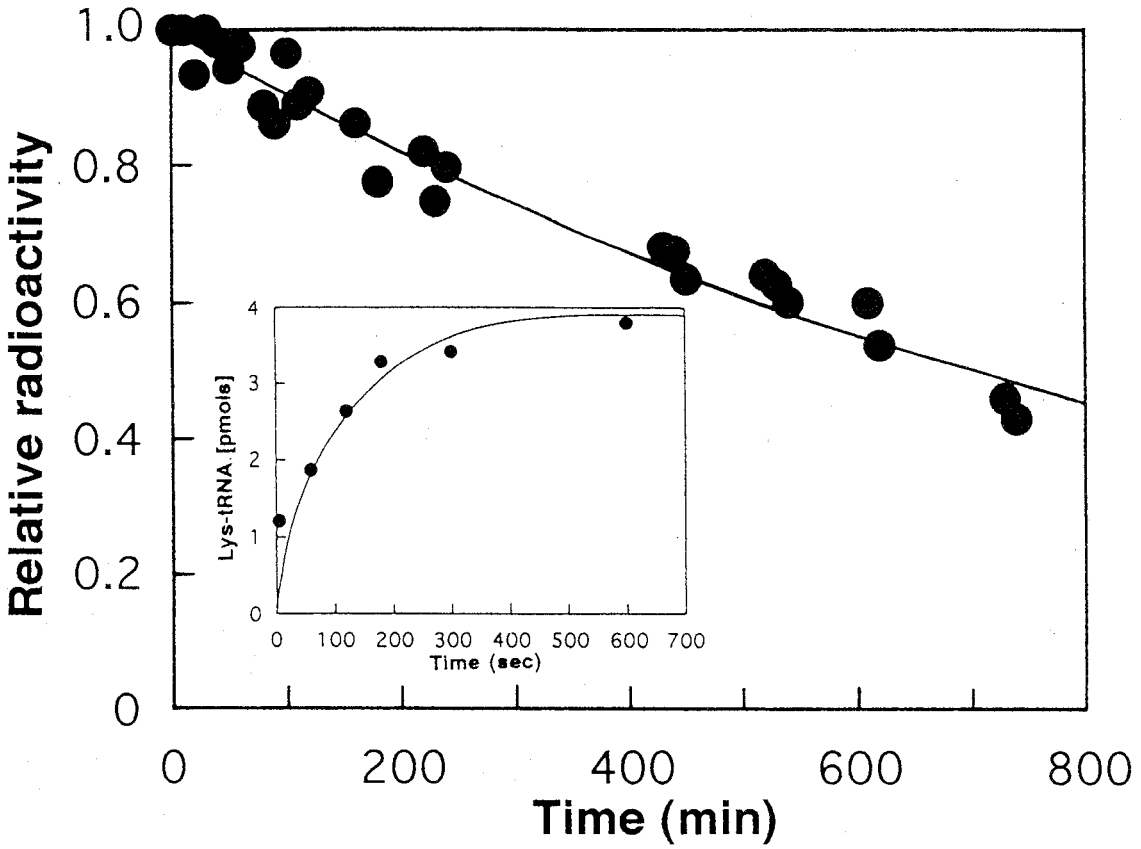

Figure 8

Stability of the *B.s.* LysRS•lysyladenylate complex and the transfer of lysine to tRNA

The LysRS• lysyladenylate complex labelled with ^{3}H-lysine was obtained by chromatographic separation at pH 8.5 on a Sephacryl S-200 column and reserved in an ice bath. At different time intervals, aliquots of the complex solution were used for the filter assay. The solid cirve is the theoretical first-order reaction curve with k_{app}=9.87x10^{-4} sec^{-1} ($t_{1/2}$=702min). The inset figure shows the transfer of ^{3}H-lysine from the LysRS•lysyladenylate complex to tRNA. Unfractionated *E. coli* tRNA was added to the above mentioned LysRS•lysyladenylate complex at 0°C, pH 8.5. The reaction was stopped by adding 6 volumes of 5% trichloroacetic acid at different time intervals. [LysRS•lysyladenylate]$_0$=18.5nM, [tRNA]$_0$=63.5μM. The solid line is the theoretical first-order reaction curve with k_{app} = 0.012sec^{-1}.

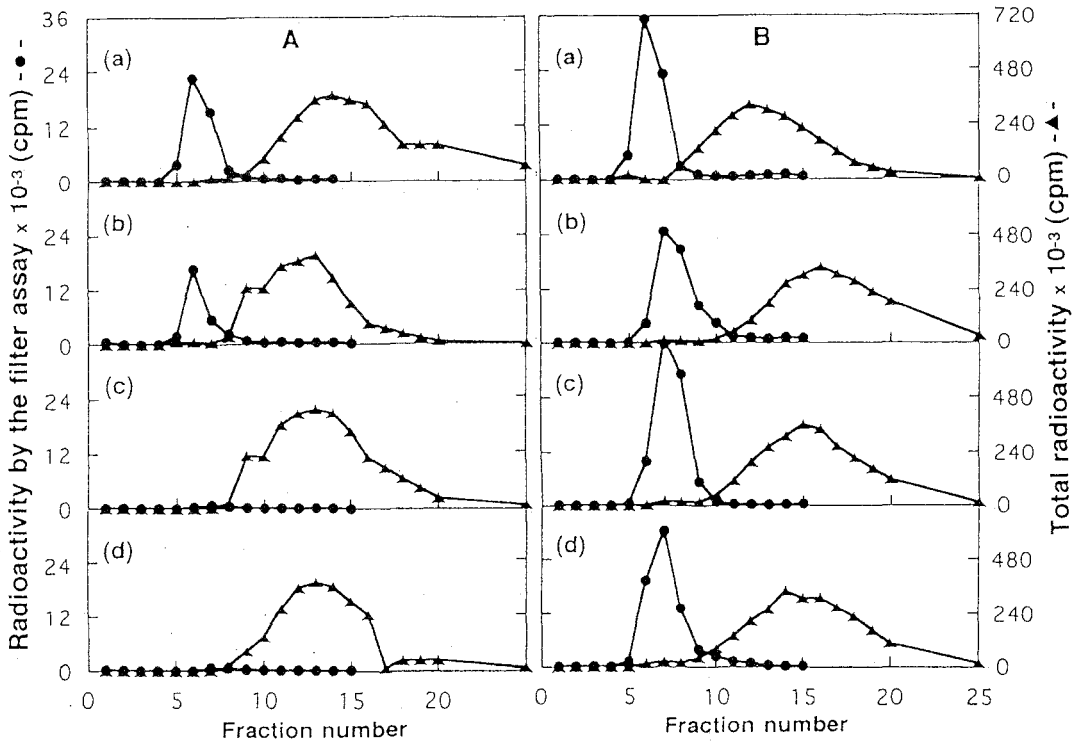

Figure 9

Chasing out of the radioactivity of the ^{3}H-AMP labeled *B.s.* LysRS•amino acid•AMP complex

(A) LysRS•lysyladenylate complex

The reaction mixture contained 100mM Tris-HCl buffer (pH 8.0), 10mM $MgCl_2$, 1mM L-lysine, 200μM ^{3}H-ATP (1.2 Ci/mmol), and 1.85μM LysRS. The reaction mixture was incubated at 37°C for 3min and reserved in an ice bath, and it was applied to each NAP-10 column equilibrated with the following buffers: (a), 100mM Tris-HCl buffer (pH 8.0) containing 10mM $MgCl_2$;(b), (a) + 1mM L-lysine;(c), (a) + 1mM ATP;(d), (a) + 1mM L-lysine + 200μM ATP. The elution buffer was the same as the equilibrating buffer in every case.

(B) LysRS•L-Lyshxt-AMP complex

The reaction mixture is the same as in **(A)** except for replacement of 1mM L-lysine by 1mM L-Lyshxt. The reaction mixture was treated similarly as in (A). Equilibration and elution bufferes were: (a), 100mM Tris-HCl buffer (pH 8.0) containing 10mM $MgCl_2$; (b), (a) + 1mM L-Lyshxt; (c), (a) + 1mM ATP; (d), (a) + 1mM L-Lyshxt + 200μM ATP.

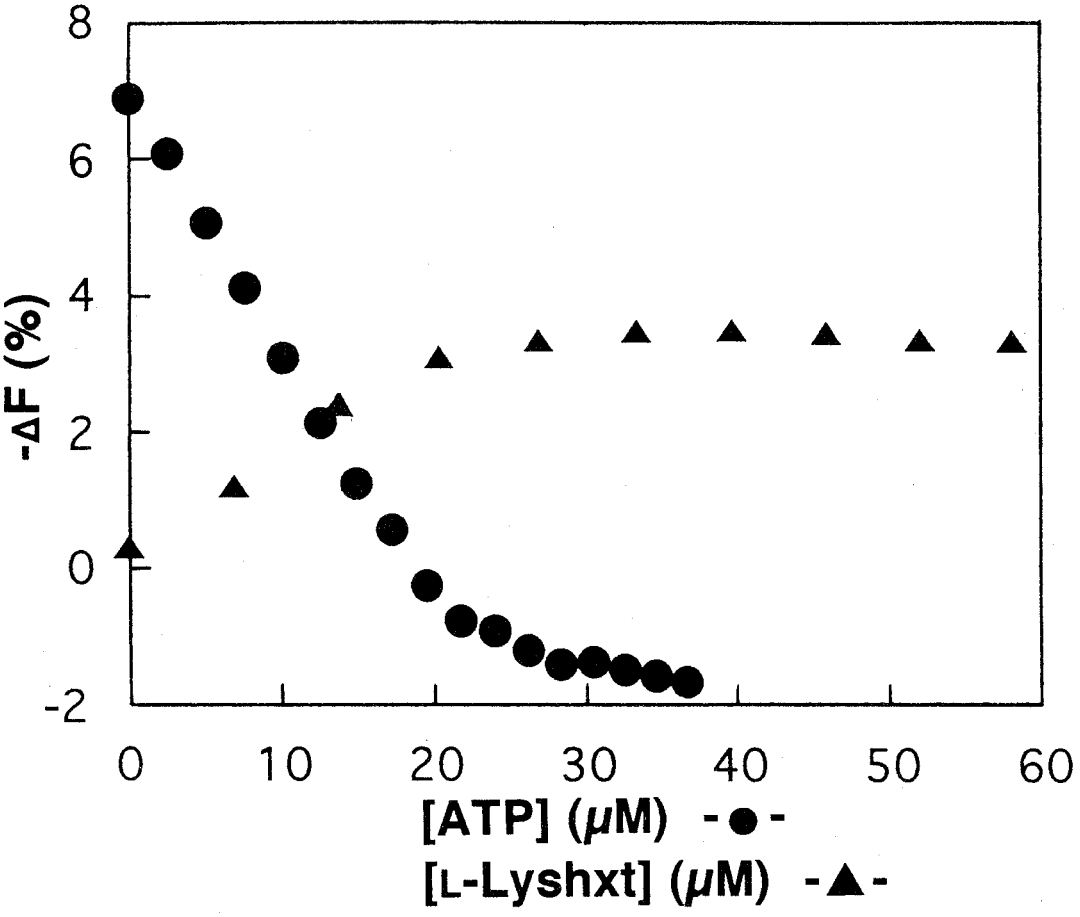

Figure 10

Binding stoichiometry of L-Lyshxt-AMP to *B.s.* LysRS by fluorescence titration.

Titration of LysRS with ATP in the presence of 2.4mM L-Lyshxt (▲). Titration of LysRS with L-Lyshxt in the presence of 1mM ATP (●). The reaction mixture contained 100mM Tris-HCl buffer, pH 8.0, and 10mM $MgCl_2$. λ_{ex}=295nm, λ_{em}=340nm, at 30°C. $[E]_0$=22.1μM as dimer.

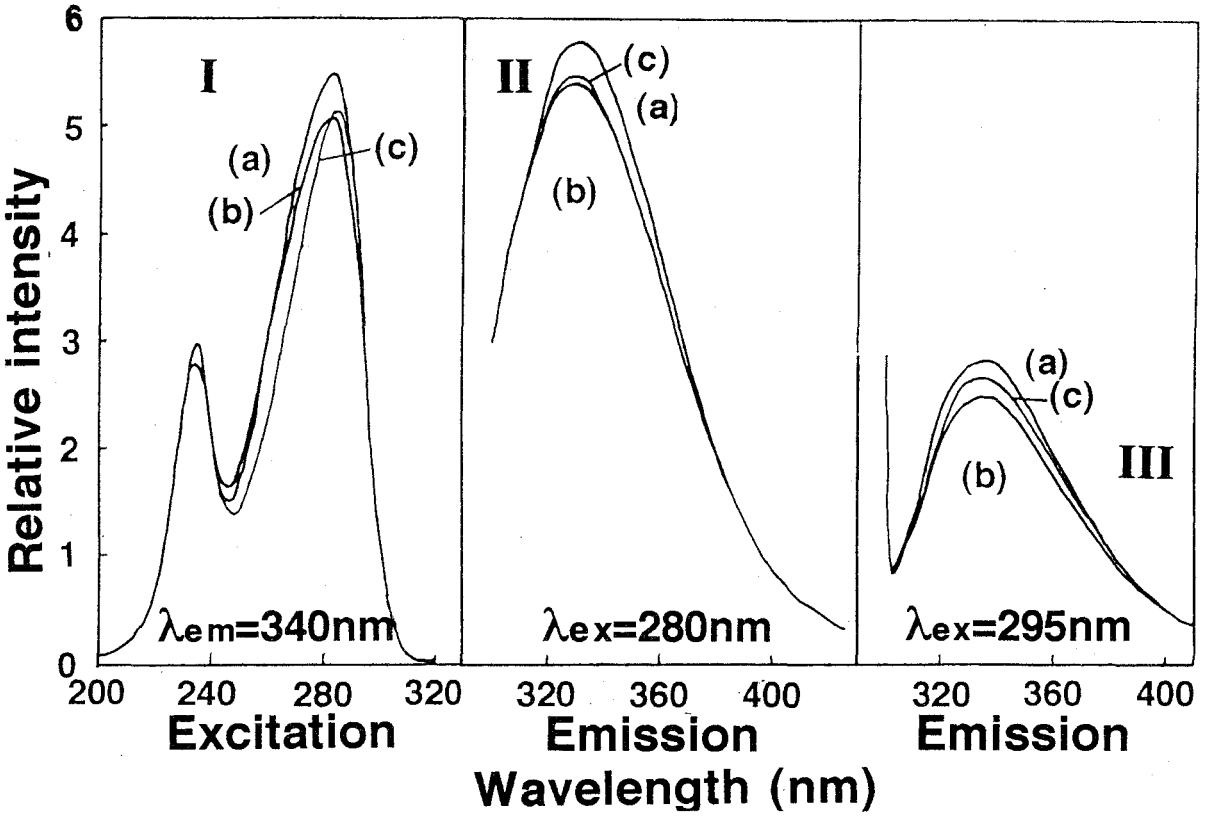

Fluorescence spectra of *B.s.* LysRS and effects of adding L-lysine and ATP

I, excitation spectra for the emission at 340nm.
II, emission spectra with excitation at 280nm.
III, emission spectra with excitation at 295nm.
$[E]_0$=4.9μM; pH 8.0, 30°C;
(a), [L-lysine]=0μM; (b), [L-lysine]=227μM;
(c), [L-lysine]=227μM and [ATP]=30μM.

Chapter 3
Stopped-Flow Analysis of Enzyme•lysyladenylate Formation

An aminoacyl-tRNA synthetase (abbreviated to ARS) catalyzes the binding of an amino acid to the cognate tRNA, generally according to the following reaction scheme ***(1)***.

$$E + AA + ATP \rightleftharpoons E{\bullet}AA{\sim}AMP + PPi \quad (1)$$

$$E{\bullet}AA{\sim}AMP + tRNA \rightleftharpoons E + AMP + AA\text{-}tRNA \quad (2)$$

where AA denotes the amino acid; E, ARS; PPi, inorganic pyrophosphate; and E•AA~AMP, an aminoacyl-adenylate-ARS complex. The first reaction is called amino acid activation reaction. In previous papers, I reported that *B.s.* LysRS obeys a sequential ordered mechanism in which L-Lys binds first ***(2)*** and that the binding of L-Lys to *B.s.* LysRS caused the protein fluorescence decrease ***(2)***, but following addition of ATP restored the decrease of the fluorescence ***(3)***. Then, in this paper, I tried to investigate by stopped-flow apparatus the two processes, the L-Lys binding process to *B.s.* LysRS and the ATP binding process to the *B.s.* LysRS•L-Lys complex. As far as I know, there was four reports investigating the preequilibrium kinetics of the amino acid activation reaction in which two measured fluorescence change indirectly with a reversibly binding fluorescent reporter group, 2-p-toluidinylnaphthalene-6-sulfonate (abbreviated to TNS) ***(4, 5)***, while two measured protein-fluorescence directly ***(6, 7)***.

MATERIALS AND METHODS

Enzymes: B.s. LysRS was purified from *B. stearothermophilus* according to the methods described previously ***(2)***. The enzyme is a homodimer of which the

molecular weight of the subunit is 57,700. The enzyme concentration was determined with the molar absorption coefficient ε at 280nm of 71,600 $M^{-1}cm^{-1}$ at pH 8.0.

Chemicals: L-Lysine hydroxamate (abbreviated to L-Lyshxt) and L-lysine amide (abbreviated to L-Lysamd) were obtained from Sigma Chemical Co. ATP (disodium salt) was the product of Sigma Chemical Co. All other chemicals were of reagent grade.

Stopped-flow kinetic study of the binding of L-lysine to B.s. LysRS: The purified LysRS was dialyzed, before the fluorescence measurement, against 100mM Tris-HCl buffer (pH 8.0) containing 10mM $MgCl_2$. Binding of L-lysine to *B.s.* LysRS was studied kinetically by monitoring the decrease of fluorescence intensity of LysRS by the stopped-flow method. The excitation wavelength was 295nm and the fluorescence change was monitored by use of a cut-off filter that cuts 50% of the fluorescence at 310nm. The enzyme concentration in the reaction mixture was fixed at 2.6μM as dimer when L-lysine concentration is in the range of 30μM to 1mM. The standard buffer was 100mM Tris-HCl buffer (pH8.0) containing 10mM $MgCl_2$. The reaction was carried out at 30°C. In order to obtain reaction progress curves accurately, the reaction under the same condition was repeated more than ten times. Each reaction curve was accumulated and averaged by using a kinetic data processor, Union Giken RA-451, to improve the signal-to-noise ratio.

Stopped-flow kinetic study of the binding of ATP to B.s. LysRS•L-lysine complex: The reaction was carried out under the same condition as described above except for mixing the solution containing *B.s.* LysRS•L-lysine complex and the solution containing L-lysine and ATP. Each solution contained 1mM ATP.

On the other hand, the reaction was carried out by mixing the solution containing *B.s.* LysRS and the solution containing 2mM or 200μM L-lysine and ATP.

Stopped-flow kinetic study of the binding of ATP to B.s. LysRS•L-lysine analogue complex: The reaction was carried out under the same condition as described above except for mixing the solution containing *B.s.* LysRS•L-lysine analogue complex and the solution containing L-lysine analogue and ATP. The concentration of L-lysine analogue in each solution was more than 10-fold of the *K*d value as estimated previously by fluorometric titration.

Estimation of kinetic parameters: The apparent first-order rate constant, k_{app}, (the reciprocal of the relaxation time) was calculated with the accumulated and averaged reaction progress curve by the use of Guggenheim plot from the progress curve.

RESULTS

The binding of L-lysine to B.s. LysRS: As **Fig.1** shows, the fluorescence change was not detected in the process of the binding of L-lysine to *B.s.* LysRS. It suggests that the L-lysine binding process is completed within about 3msec.

The binding of ATP to B.s. LysRS•L-lysine complex: As **Fig.2** shows, the restoration of fluorescence change was detected in the process of ATP-binding to *B.s.* LysRS•L-lysine complex. The dependence of k_{app} on the initial ATP concentration showed that k_{app} deviates hyperbolically from the linearity but appears to become independent as the concentration of ATP increases (**Fig. 3**).

The type of curve is consistent with the two-step binding scheme *(8)* shown in equation (3),

$$\mathrm{E \bullet L\text{-}Lys} \underset{k_{-1}}{\overset{k_{+1}}{\Leftrightarrow}} \mathrm{E \bullet L\text{-}Lys \bullet ATP} \underset{k_{-2}}{\overset{k_{+2}}{\Leftrightarrow}} \mathrm{X} \qquad (3)$$

where X is an isomerized form of the E•L-Lys•ATP complex, and k_{+1}, k_{-1}, k_{+2}, and k_{-2} are the rate constants for the elementary process as indicated (see Appendix 3). The first step is fast and always in preequilibrium. For this mechanism, values for the observed apparent first-order rate constant, k_{app}, follow the equation (4) under the condition that $[S]_0 >> [E]_0$

$$k_{app} - k_{-2} = \frac{k_{+2}[S]_0}{K_{-1} + [S]_0} \qquad (4)$$

where K_{-1} is the dissociation constant of E•L-Lys•ATP complex defined as

$$K_{-1} = [\mathrm{E \bullet L\text{-}Lys}][\mathrm{ATP}] / [\mathrm{E \bullet L\text{-}Lys \bullet ATP}] = k_{-1} / k_{+1} \qquad (5)$$

The value of k_{-2} can be evaluated by fitting the equation (4) to the experimental measurements in **Fig. 3**, in the plot of (k_{app}-k_{-2}) against $[S]_0$. When the k_{-2} value obtained is used as a constant, K_{-1} and k_{+2} can be evaluated by the non linear least-squares method according to the equation (6) obtained by the conversion of the equation (4)

$$k_{app} - k_{-2} = k_{+2} + \frac{k_{app} - k_{-2}}{[S]_0} K_{-1} \qquad (6)$$

The values obtained were:K_{-1}=356μM, k_{+2}=42s^{-1}, and k_{-2}=3.1s^{-1} at pH 8.0 and 30°C. The solid line in **Fig.3** was drawn according to the equation (6) with these values. Further, the overall dissociation constant, K_d, was calculated according to the equation (7).

$$K_d = \frac{[E \bullet L\text{-}Lys][ATP]}{[E \bullet L\text{-}Lys \bullet ATP] + [X]} = \frac{K_{-1}}{1 + K_{+2}} \qquad (7)$$

where K_{+2} is the equilibrium constant between E•L-Lys and X defined as

$$K_{+2} = \frac{[E \bullet L\text{-}Lys \bullet ATP]}{[X]} = \frac{k_{+2}}{k_{-2}}$$

The calculated overall dissociation constant was $K_d = 24.5\ \mu M$. This value is well agreed with previously estimated $K_{d,\,app,\,A}$ value, 15.5μM.

On the other hand, the results of the reaction by mixing the solution containing *B.s.* LysRS and the solution containing 2mM or 200μM L-lysine and ATP were the similar to that of the reaction by mixing the solution containing *B.s.* LysRS•L-Lys complex and the solution containing L-Lys and ATP (**Fig. 3**). It supports that the L-Lys binding process is adequate faster than the following the ATP binding process.

The binding of ATP to B.s. LysRS•L-lysine analogue complex: In the cases using L-Lyshxt and L-Lysamd, the restoration of fluorescence change was detected in the process of ATP-binding to *B.s.* LysRS•L-lysine analogues complex. The dependence of k_{app} on the initial ATP concentration also showed that k_{app} deviates hyperbolically from the linearity but appears to become independent as the concentration of ATP increases (**data not shown**). Estimated kinetic parameter is shown in **Table I**.

DISCUSSION

The binding of L-lysine to B.s. LysRS: There are three reports in which the amino acid-binding process was investigated by stopped-flow apparatus. The first is the case for *E. coli* IleRS (Class I ARS) ***(4)*** where the binding of L-Ile to the enzyme was measured by use of fluorescence change of TNS, indicating that L-Ile-binding obeys such a two-step process as shown in Equation (3) with K_{-1}=0.093 mM, k_{+2}=125 s^{-1}, and k_{-2}=3 s^{-1} by a plot of k_{app} *vs.* $[L\text{-Ile}]_0$. It was reported that though the reaction for L-Ile appears to become bimolecular (a one-step process) ***(8)*** when the temperature is raised from 13°C to 25°C, the rate of association reaction is too slow to be a diffusion-controlled process. The second is the case for *B.s.* TyrRS (Class I ARS) ***(6)*** where the binding of L-Tyr to the enzyme was measured by use of the protein-fluorescence change, indicating that L-Tyr binding obeys a one-step process with $k_{+1}=2.4 \times 10^6$ s^{-1} and $k_{-1}=24 \times 10^6$ s^{-1} by a plot of k_{app} *vs.* $[L\text{-Tyr}]_0$. It was also reported that the k_{+1} value estimated is some two to three orders of magnitude below that of a diffusion controlled reaction. These two reports suggest that the bindings of L-Ile and L-Tyr involve a conformational change of each ARS since the reactions are slow and fluorescence changes are involved. However, the third for the case for *E. coli* MetRS (Class I ARS) ***(7)*** where the binding of L-Met to the enzyme was measured by use of the protein-fluorescence change, indicating that 60μM L-Met (a concentration equal to the dissociation constant) reacts with enzyme within the dead time (2.5ms) of the stopped-flow apparatus used. It suggests the possibility that the binding of L-Met to the enzyme is very fast or that no fluorescence change occurs in a slow process. It can be applied to the case for *B.s.* LysRS.

The binding of ATP to B.s. LysRS•L-lysine complex: There are four reports in which the amino acid-activation process was investigated by stopped-flow apparatus ***(4~7)***. Since used ARSs are Class I enzymes that obey a random ordered mechanism in the ATP-PPi exchange reaction, it is difficult to analyze the amino acid-activation process. In fact, in order to analyze the process of the ARS obeying a random ordered mechanism, it will be necessary, the first, to investigate the association-dissociation equilibrium between substrates and enzyme in preequilibrium, the second, to assume that the rate constants in the association-dissociation equilibrium under noncatalytic conditions can be applied to those under catalytic conditions, and the third, to control the association-dissociation processes to be in rapid preequilibrium. If these three difficult problems are solved, the expression of k_{app} is very complicated. For estimation of the forward rate constant, k_f and the backward one, k_b in the following reaction E•AA•ATP $\rightleftharpoons$ E•AA~AMP•PPi, several expressions were applied to observed k_{app}s for each condition used ***(4)***. On the other hand, the advantages of kinetic analysis of the process for *B.s.* LysRS are as follows. (1) The protein-fluorescence of *B.s.* LysRS is decreased by the addition of L-lysine but restored by the following addition of ATP. (2) The observed fluorescence change is considered to be deprived from Trp residues and only two Trp residues exist in a subunit of *B.s.* LysRS. (3) *B.s.* LysRS obeys a sequential ordered mechanism in which L-lysine binds first. (4) The binding of L-lysine to *B.s.* LysRS is considered to be adequately faster than the following ATP binding. These advantages will make it possible to analyze the amino acid-activation process more directly, simply, and precisely.

Estimated k_f and k_b E•AA•ATP $\rightleftharpoons$ E•AA~AMP•PPi are 135 s^{-1} and 670 s^{-1} for *E. coli* IleRS ***(4)***, 12~32 s^{-1} and 42~77 s^{-1} for *E. coli* PheRS ***(5)***, 342 s^{-1} and 226 s^{-1} for *E. coli* MetRS ***(7)***, respectively at 25°C. In the case for *B.s.* TyrRS, estimated $k_f + k_b$ value is 17.8 s^{-1} at 25°C ***(6)***. The value of the equilibrium constant ([E•AA~AMP•PPi] / [E•AA•ATP]=k_f / k_b) is 0.2 for *E. coli* IleRS ***(4)***, 0.16~0.76 for *E. coli* PheRS ***(5)***, 1.5 for *E. coli* MetRS ***(7)***, respectively at 25°C. However, corresponding value (k_{+2} / k_{-2}) is for *B.s.* LysRS is 14. The difference remains unknown but may reflect the difference in the catalytic mechanism between Class I and Class II enzymes.

The binding of ATP to B.s. LysRS•L-lysine analogue complex: "Slow" fluorescence-changing process observed in preequilibrium of the amino acid activation process are considered to be attributable to the aminoacyladenylate formation either by the comparison of k_{cat} in the ATP-PPi exchange reaction with the corresponding rate constant, k_{-2}, for the similar reaction monitored by stopped-flow apparatus ***(5, 6)*** or by the comparison of the rate constant of quenched-flow experiment with that of stopped-flow experiment ***(7)***. In this paper, we tried to identify the product "X" in the slow process by use of L-lysine analogues. I reported that L-Lysamd and L-Lyshxt are strong inhibitors for *B.s.* LysRS under the condition of amino acid activation reaction and that under such condition, *B.s.* LysRS•L-Lyshxt-AMP complex is formed almost irreversibly ***(3)***. The amino acid activation processes with L-lysine or L-Lyshxt involves the covalent-bond formation, while it is considered that corresponding process with L-Lysamd does not involve it. **Table I** shows that the k_{+2} value for L-Lysamd is apparently larger than those for L-lysine and L-Lyshxt. It suggests

that the observed fluorescence change in the process with L-Lysamd is the ATP binding process, while the fluorescence changes observed with L-lysine and L-Lyshxt are the formation processes of L-Lys~AMP and L-Lyshxt-AMP. It should be noted that K_{-1} value for L-Lyshxt is smaller than those for L-lysine and L-Lysamd. The calculated overall dissociation constants, K_ds, for L-Lyshxt and L-Lysamd are 9.8μM and 7.2μM, respectively. These values are essentially agreed with previously estimated $K_{d,\ app,\ A}$ value for L-Lyshxt, 2.98μM and that for L-Lysamd, 3.98μM, respectively.

REFERENCES

1) Berg, P. (1961) Specificity in protein synthesis. *Annu. Rev. Biochem.* **30**, 293-324

2) Takita, T., Ohkubo, Y., Shima, H., Muto, T., Shimizu, N., Sukata, T., Ito, H., Saito, Y., Inouye, K., Hiromi, K., and Tonomura, B. (1996) Lysyl-tRNA synthetase from *Bacillus stearothermophilus*. Purification, and fluorometric and kinetic analysis of the binding of substrates, L-lysine and ATP. *J. Biochem.*, (in press).

3) Takita *et al.*

4) Holler, E. and Calvin, M. (1972) Isoleucyl transfer ribonucleic acid synthetase of *Escherichia coli* B. A rapid kinetic investigation of the L-isoleucine-activating reaction. *Biochemistry*, **11**, 3741-3752

5) Bartmann, P., Hanke, T., and Holler, E. (1975) L-Phenylalanine:tRNA ligase of *Escherichia coli* K10. A rapid kinetic investigation of the catalytic reaction. *Biochemistry*, **14**, 4777-4786

6) Fersht, A. R., Mulvey, R. S., and Koch, G., L., E. (1975) Ligand binding and enzyme catalysis coupled through subunits in tyrosyl-tRNA synthetase. *Biochemistry*, **14**, 13-18

7) Hyafil, F., Jacques, Y., Fayat, G., Fromant, M., Dessen, P., and Blanquet, S. (1976) Methionyl-tRNA synthetase from *Escherichia coli:* Active stoichiometry and stopped-flow analysis of methionyl adenylate formation. *Biochemistry*, **15**, 3678-3685

8) Czerlinski, G. H. (1966) Chemical relaxation, an introduction to theory and application of stepwise perturbation. New York, N. Y., Marcel Dekker.

Table I
Kinetic parameters in the ATP binding process

LysRS · LA	$\underset{K_{-1}}{\overset{fast}{\rightleftharpoons}}$	LysRS · LA · ATP	$\underset{k_{-2}}{\overset{slow\ k_{+2}}{\rightleftharpoons}}$	X
LysRS · L-Lys	$\underset{356\,\mu M}{\overset{ATP}{\rightleftharpoons}}$	LysRS · L-Lys · ATP	$\underset{3.1(s^{-1})}{\overset{42(s^{-1})\ PPi}{\rightleftharpoons}}$	LysRS · L-Lys~AMP
LysRS · L-Lyshxt	$\underset{77\,\mu M}{\overset{ATP}{\rightleftharpoons}}$	LysRS · L-Lyshxt · ATP	$\underset{1.9(s^{-1})}{\overset{13(s^{-1})\ PPi}{\rightleftharpoons}}$	LysRS · L-Lyshxt-AMP
LysRS · L-Lysamd	$\underset{574\,\mu M}{\overset{ATP}{\rightleftharpoons}}$	LysRS · L-Lysamd · ATP	$\underset{2.9(s^{-1})}{\overset{230(s^{-1})}{\rightleftharpoons}}$	LysRS · L-Lysamd · ATP*

The excitation wavelength was 295nm and the fluorescence change was monitored by use of a cut-off filter which cuts 50% of the fluorescence at 310nm. The enzyme concentration in the reaction mixture was fixed at 2.6μM as dimer. The standard buffer was 100mM Tris-HCl buffer (pH8.0) containing 10mM $MgCl_2$. The reaction were carried out at 30°C.

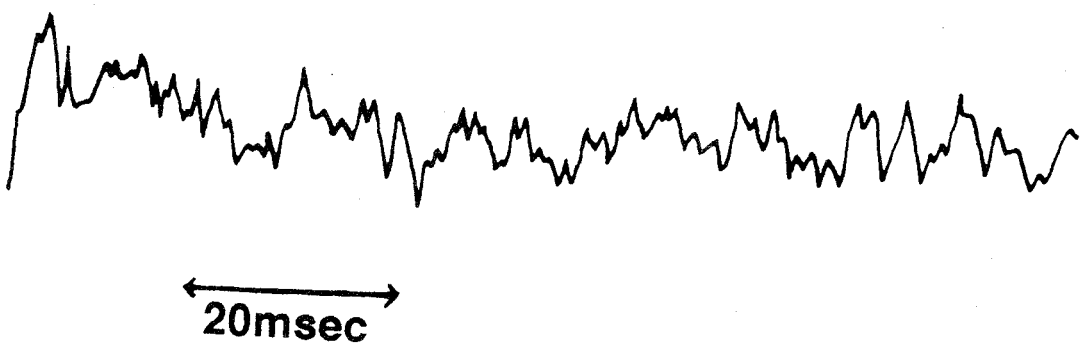

Figure 1
Stopped-flow analysis of the binding of L-lysine to *B.s.* LysRS
The standard buffer was 100mM Tris-HCl buffer (pH 8.0) containing 10mM $MgCl_2$. The reaction was started by mixing the solution containing 5.2μM LysRS and that containing 1mM L-lysine at 30°C. The excitation wavelength was 295nm and the fluorescence change was monitored by use of a cut-off filter which cuts 50% of the fluorescence at 310nm.

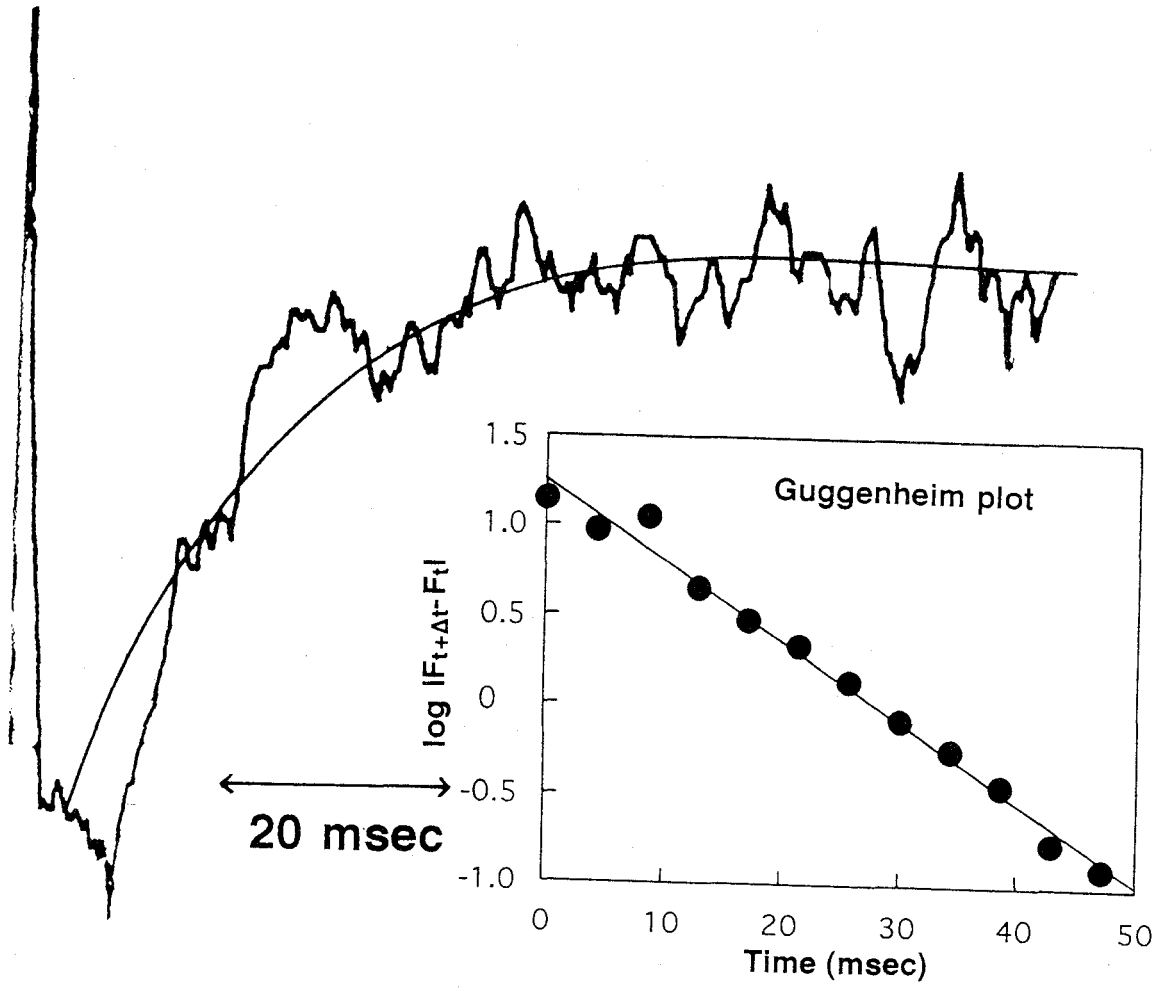

Figure 2

Stopped-flow analysis of the binding of ATP to *B.s.* LysRS•L-lysine complex

The standard buffer was 100mM Tris-HCl buffer (pH 8.0) containing 10mM $MgCl_2$. The reaction was started by mixing the solution containing 5.2μM LysRS and 1mM L-lysine and that containing 1mM L-lysine and 6mM ATP at 30°C. Inset shows the Guggenheim plot of the solid curve.

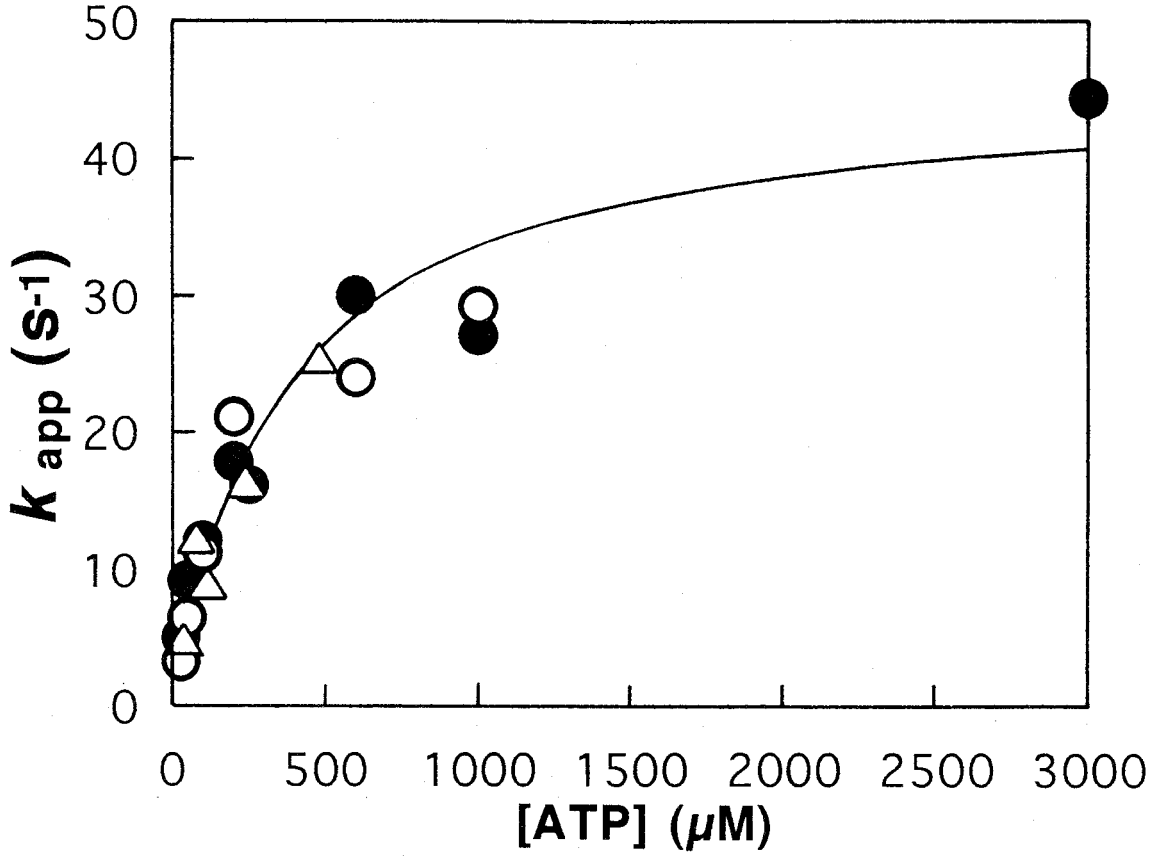

Figure 3

ATP concentration dependence of *k*app in the ATP binding process to *B.s.* LysRS•L-lysine complex

The standard buffer was 100mM Tris-HCl buffer (pH 8.0) containing 10mM $MgCl_2$. Reactions by mixing the solution containing 5.2μM LysRS and 1mM L-lysine, and that containing 1mM L-lysine and ATP (●), by mixing the solution containing 5.2μM LysRS, and 2mM L-lysine and ATP (○), and by mixing the solution containing 5.2μM LysRS and 100μM L-lysine, and that containing 100μM L-lysine and ATP (△). The solid curves are the threoretical ones obtained from the points (●) with K_{-1}=356μM, k_{+2}=42s^{-1}, and k_{-2}=3.1s^{-1}.

Chapter 4
A Continuous Fluorophotometric Assay and Examination of the Proof-reading Mechanism of the Aminoacylation Reaction

An aminoacyl-tRNA synthetase **(abbreviated to ARS)** is important group of enzymes that catalyze the following two-part reaction ***(1)***.

$$E + AA + ATP \rightleftharpoons E{\bullet}AA{\sim}AMP + PPi \quad (1)$$

$$E{\bullet}AA{\sim}AMP + tRNA \rightleftharpoons E + AMP + AA\text{-}tRNA \quad (2)$$

where AA denotes an amino acid; E, the enzyme; and PPi, inorganic pyrophosphate. The reaction expressed by equation (1) is called amino acid activation reaction. The overall equilibrium reaction is usually represented as in equation (3).

$$E + AA + ATP + tRNA \rightleftharpoons E + AMP + AA\text{-}tRNA + PPi \quad (3)$$

The reaction expressed by equation (3) is called aminoacylation reaction. The method generally employed to assay the aminoacylation activity, what is called, the aminoacylation reaction assay involves the use of radioactive amino acids and measurement of the quantity of the aminoacyl-tRNA formed. Though the aminoacylation assay is highly sensitive, I was confronted with a problem under investigation of the specificity of lysyl-tRNA synthetase **(abbreviated to LysRS)** from *Bacillus stearothermophilus* towards lysine analogues in the aminoacylation reaction ***(2, 3)***, because it is hard to supply noncommercial radioactive compounds to this assay.

Two continuous spectrophotometric assays for ARS were reported ***(4~6)***. However, it is considered that the effect of the presence of ATP and tRNA under my condition on the detection at 340nm considerably large. In order to reduce the effect and enlarge the sensitivity of the detection, I measured the AMP production

fluorophotometrically. In this paper, the development of a new assay procedure of ARS in the aminoacylation reaction that does not need an isotopic labeled compound was tried. This method uses three other enzymes, adenylate kinase, pyruvate kinase, and lactate dehydrogenase. AMP production can be measured by coupling the aminoacylation reaction with those catalyzed by these enzymes as follows.

$$\text{AMP} + \text{ATP} \xrightleftharpoons{\text{adenylate kinase}} 2\ \text{ADP}$$

$$2\ \text{ADP} + 2\ \text{PEP} \xrightleftharpoons{\text{pyruvate kinase}} 2\ \text{ATP} + 2\ \text{pyruvate}$$

$$2\ \text{pyruvate} + 2\ \text{NADH} \xrightleftharpoons{\text{lactate dehydrogenase}} 2\ \text{lactate} + 2\ \text{NAD}$$

where PEP denotes a phosphoenolpyruvate.

This procedure is based on the quantitative analysis of AMP reported by Shimizu *et al.* in fatty acid determination ***(7)***. The conversion of NADH to NAD can be measured with the guidance of fluorometry. In the presence of excess coupling enzymes and substrates, the rate of NADH oxidation will reflect the rate of AMP production.

By use of this continuous assay, we try to investigate the specificity of *B.s.* LysRS towards lysine analogues in the aminoacylation reaction and the existence of editing mechanism.

MATERIALS AND METHODS

Enzymes and tRNA: *B. stearothermophilus* NCA 1503 cells were generally supplied by Unitika, Ltd., and stored at -20°C until use. LysRS was purified according to the methods described

previously ***(2)***. The enzyme is consisted of two apparently identical subunits of which the minimum molecular weight is 57,900. The enzyme concentration was determined with the molar absorption coefficient, ε , 71,600 $M^{-1}cm^{-1}$ at pH 8.0. Unfractionated tRNA from *E. coli* MRE 600 and *E. coli* $tRNA^{Lys}$ were purchased from Boehringer Mannheim and Sigma Chemical Co., respectively. Adenylatekinase from yeast (EC2.7.4.3), pyruvate kinase from rabbit muscle (EC2.7.1.40), and lactate dehydrogenase from pig heart (EC1.1.1.27), were the products of Oriental Yeast Co..

Others: L-[4,5-^{3}H] lysine was the product of of NEN Research Products; ATP (disodium salt), of Sigma Chemical Co.; glass microfiber filter (GF/C), of Whatman; NADH and phosphoenolpyruvate, of Oriental Yeast Co.; sodium metaperiodate, of Nakarai tesque; DC-Alufolien Kiselgel 60 F_{254}, of E. Merck. All other chemicals were of reagent grade.

L-Lysine and lysine analogues: L-Lysine and *S*-(2-aminoethyl)-L-cysteine **(abbreviated to SAEC)** were the product of Wako Ltd. L-Ornithine was purchased from Nakarai tesque. 5-Hydroxylysine (mixed DL and DL-allo), L-lysine hydroxamate **(abbreviated to L-Lyshxt)**, and L-lysine amide were obtained from Sigma Chemical Co. *Threo*-4-hydroxy-L-lysine was purchased from Fluka Fine Chemicals.

Periodate oxidation of free tRNA and lysyl-tRNA: 100 A_{260} units of the mixture of *E. coli* tRNA in 100mM sodium acetate buffer (pH 4.5) containing 10mM $MgCl_2$ was incubated with 10mM sodium metaperiodate at 25°C for 3hours. For protection experiment of $tRNA^{Lys}$ in the tRNA mixture against periodate cleavage, I added acetic acid to the reaction mixture after aminoacylation reaction, adjusting pH to 4.5 and reacted it with

sodium metaperiodate under the condition described above. The reaction mixture in the aminoacylation reaction contained in 0.2ml: 100mM Tris-HCl buffer (pH 8.0), 10mM $MgCl_2$, 1mM ATP, 100μM ^{3}H-L-lysine (500mCi/mmol), and 370nM LysRS. After the incubation with sodium metaperiodate, I added KCl to be 0.2M and 3 volumes of ethanol (-20°C) in this order, precipitating tRNA at -80°C for 30min. After centrifugation at 12,000 x g for 10 min at 4°C and decantation of the supernatant, I added 80% ethanol (-20°C) and centrifuged again. After decanting, the precipitant was dried under reduced pressure. After deacylation of L-lysine at pH 10 (50mM glycine-NaOH buffer), remaining L-lysine-acceptance activity of tRNA was checked by the aminoacylation reaction with ^{3}H-lysine.

Continuous assay: The purified LysRS was dialyzed, before the fluorescence measurement, against 100mM Tris-HCl buffer (pH 8.0) containing 10mM $MgCl_2$. The standard reaction mixture used for the measurement contained in 0.19ml: 100mM Tris-HCl buffer (pH 8.0), 10mM $MgCl_2$, 50μM NADH, 200μM phosphoenolpyruvate, 200μM ATP, 140A_{260} units of tRNA from *E. coli* MRE 600, 10nM LysRS, 30U/ml adenylate kinase, 18U/ml pyruvate kinase, and 18U/ml lactate dehydrogenase. The reaction mixture was placed in a quartz microcell (optical path length, 0.5cm) thermostated at 30°C, and the reaction was initiated by adding 10μl of L-lysine solution at different concentrations. The oxidation of NADH to NAD was measured by monitoring the decrease of fluorescence intensity with a Hitachi Fluorescence Spectrophotometer 850. The excitation wave length and the emission wave length were 365nm and 460nm, respectively. The

initial velocity ($-\Delta F \bullet sec^{-1}$) was calculated from the decrease of the fluorescence intensity *versus* time.

Aminoacylation reaction assay: The aminoacylation reaction assay was conducted with radioactive L-lysine as described previously ***(2)***. For the measurement of the aminoacylation reaction under the condition of the continuous assay, the aminoacylation reaction assay was conducted in the same manner as the continuous assay except that the addition of 10μl of ^{3}H-L-lysine initiated the reaction and the addition of 1.2ml of 5% trichloroacetic acid terminated the reaction. The concentrations of L-lysine were varied differently at the same specificity (1.0Ci/mmol). The terminated mixture was treated in the same manner as the aminoacylation reaction assay.

Back-titration experiment: The first aminoacylation reaction was carried out by 10nM B.s. LysRS with 1mM L-lysine, 10mM SAEC, and 10mM 5-hydroxylysine at different times at 37°C. The standard reaction mixture of aminoacylation reaction contained in 500μl: 100mM Tris-HCl buffer (pH 8.0), 10mM $MgCl_2$, 1mM ATP, and $40A_{260}$ units of *E. coli* tRNA. The reaction was stopped by the addition of 275μl of 1.6M potassium acetate buffer (pH 4.0) and 150μl of it was transferred to a fresh tube. After the addition of 100μl of acetic anhydride, 125μl of 0.6M NaCl and 1,000μl of ethanol (-20°C) were added and precipitated at -80°C for 30min. After the centrifugation at 12,000 x g for 10 min at 4°C and decantation of the supernatant, I added 1,000μl of 70% ethanol (-20°C) and centrifuged again. After decanting and drying under reduced pressure, the precipitant was dissolved in the same reaction mixture (500μl) as described above except containing 10μM ^{3}H-lysine (160mCi/mmol) and none of tRNA and the second

aminoacylation reaction (back-titration reaction) was carried out for 5min. The charging percentage of the first reaction was calculated as follows;

Charging (%)=(R_0-R_x) x $100/R_0$ (4)

where R_0 and R_x denote the final radioactivity of the solution reacted for 0 min and x min in the first reaction.

TLC analysis: I investigated different sets of reaction mixture containing either L-lysine or its analogues by a TLC system. After silicagel plates are developed with n-buthanol : acetic acid : water, 4 : 1 : 1 and dried, products were detected by ninhydrin reaction.

RESULTS

Calibration of fluorescence decrease with AMP concentration in the continuous assay: Under the same condition as the continuous assay except in the absence of LysRS and AMP, AMP at different concentrations was added and the fluorescence decrease was measured. Estimated correction value, $-\Delta F / [AMP]_0$ was determined as 0.0186±0.0005 (μM^{-1}) (**Fig. 1**).

Continuous assay in the absence of tRNA: In order to detect slight amounts of fluorescence decrease, I increased the concentration of LysRS 10-fold (100nM) over that in the standard condition of the continuous assay in the presence of tRNA. Appreciable fluorescence decrease could not be detected in the case with L-lysine, L-Lyshxt, and L-lysine amide, while fluorescence decrease was observed in the case with 5-hydroxylysine, L-ornithine, and SAEC with estimated k_{cat} values, 9.08 x 10^{-2} s^{-1}, 2.16 x 10^{-2} s^{-1}, and 7.65 x 10^{-2} s^{-1}, respectively (**Fig. 2** and **Table I**).

Continuous assay with L-lysine in the presence of tRNA:

The inset of **Fig. 3** shows the reaction curves observed with different concentrations of L-lysine (0~90μM). The plot of V_0 *versus* the concentration of L-lysine is shown in **Fig. 3**. Estimated K_m and k_{cat} are 29.4 ± 2.7μM and 6.95 ± 0.23s^{-1}, respectively.

Comparison of the continuous assay with the aminoacylation reaction assay: In order to compare the kinetic parameters in the continuous assay with those in the aminoacylation reaction, I added ^{3}H-lysine to the reaction mixture of the continuous assay and measured the transfer of ^{3}H-lysine to tRNA at 30°C in the same way as in the aminoacylation reaction assay (precipitation with 5% trichloroacetic acid), while the same reaction was measured in the continuous assay (fluorescence decrease). **Figure 4** shows the plot of V_0 *versus* the concentration of L-lysine in the two kinds of assays in the concentration range of L-lysine, 2.5~40μM. Estimated K_ms in the aminoacylation assay and in the continuous assay are similar, 52.2μM and 46.5μM, respectively. On the other hand, observed V_0s are different by a factor of about 2, where the latter V_0 (k_{cat}=5.1)value is larger than the former one (k_{cat}=2.9).

Continuous assay with L-lysine analogues in the presence of tRNA: I conducted the continuous assay with L-lysine analogues. As typical reaction curves are shown in **Fig. 5**. When SAEC, L-ornithine, *threo*-4-hydroxy-L-lysine were used, the reaction, coming to an equilibrium state, or fully aminoacylation of tRNA, was almost stopped apparently (**Fig. 5**). However, on using 5-hydroxylysine, the reaction continued linearly until NADH was converted into NAD completely (**Fig. 5**). Kinetic parameters (K_m and k_{cat}) of these analogues are listed as follows; SAEC (145μM, 1.79s^{-1}), L-ornithine (2,630μM, 1.92s^{-1}), threo-4-hydroxy-L-lysine (2,540μM, 3.94s^{-1}), and 5-hydroxylysine (8,540μM, 2.22s^{-1}) (**Table I**).

Back-titration experiments with L-lysine, SAEC, and 5-hydroxylysine: **Figure 6** shows that though tRNA was charged with L-lysine and SAEC, it was not with 5-hydroxylysine. Estimated chargings (%) of L-lysine and SAEC were about 70% and 40%, respectively.

Preparation of periodate-oxidated tRNA and lysyl-tRNA: L-Lysine-acceptance activity of free tRNA disappeared completely by the periodate oxidation (**Fig. 7B**). On the other hand, the acceptance activity of lysyl-tRNA was almost maintained as shown in **Fig. 7A** that shows relative radioactivity of ^{3}H-lysyl-tRNA precipitated with 6 volume of 5% trichloroacetic acid at each step. It was reproducible the finding that the relative radioactivities at the pH 4.5 step and the periodate-oxidation step were larger than the initial step. **Figure 7A** also shows the relative radioactivity at deacylation process at 25°C. Deacylation could not be detected at pH 5.0 but detected at pH 8.0 and 10.0. In both cases, final L-lysine-acceptance activity of lysyl-tRNA was maintained more than 80% of the initial value.

Continuous assay with L-lysine and 5-hydroxylysine using periodate-oxidated free tRNA and lysyl-tRNA: **Figure 7B** and **7C** are the reaction curves (2nM LysRS) with 10μM L-lysine and 10mM 5-hydroxylysine, respectively. In both cases, appreciable fluorescence decrease could not be detected by use of periodate-oxidated free tRNA (70 A_{260} unit) but detected by use of periodate-oxidated lysyl-tRNA and intact tRNA.

Relationship between V_0 and V_S in the continuous assay with L-lysine and threo-4-hydroxy-L-lysine: In the case for 300μM L-lysine, I found that though the aminoacylation reaction using ^{3}H-lysine was apparently in an equilibrium state, a linear line

continuing until NADH is completely converted into NAD could be observed in the continuous assay (**Fig. 8**). This linear line following a curve could be also confirmed in the cases with SAEC (150μM), L-ornithine (2mM), and threo-4-hydroxy-L-lysine (10mM) (**Table I**). The velocity of the linear line (abbreviated to V_s) for 10mM threo-4-hydroxy-L-lysine estimated was about two times V_s for 300μM L-lysine (**Fig. 8**). I conducted the continuous assay with different concentrations of threo-4-hydroxy-L-lysine in order to investigate the relationship between V_0 and V_s (**Fig. 9B**). **Figure 9C** shows the plots of relative V_0 and V_s *versus* the concentration of threo-4-hydroxy-L-lysine, in which V_s was almost constant while V_0 changed extensively in the concentration range used.

Comparison of the aminoacylation reaction with E. coli tRNA with that with E. coli tRNA^{Lys}: With either of the same L-lysine-acceptance activity of *E. coli* tRNA ($20A_{260}$ units) or *E. coli* tRNA^{Lys} ($0.35A_{260}$ units), the aminoacylation reaction was measured at different concentrations of L-lysine (**Fig. 10**). Estimated K_m and k_{cat} with *E. coli* tRNA were 23.5±1.5μM, 2.29±0.07s^{-1}, respectively, while those with *E. coli* tRNA^{Lys} were 14.1±3.0μM, 1.98±0.16s^{-1}, respectively.

TLC analysis: In the case with 5-hydroxylysine, new spot appeared only under the condition of aminoacylation reaction (in the presence of B.s. LysRS, ATP, 5-hydroxylysine, and *E. coli* tRNA) (**Fig. 11**), while in the case with L-ornithine, new spot appeared under the condition of aminoacyladenylate formation (in the presence of B.s. LysRS, ATP, and L-ornithine) besides under the condition of aminoacylation reaction (**Fig. 11**). In the other cases, no appreciable new spot could be detected (**Fig. 11**).

DISCUSSION

Calibration of fluorescence decrease with AMP concentration in the continuous assay: **Figure 1** indicates that a linear relationship between the AMP concentration produced and observed fluorescence decrease was at least held up to $[AMP]_0$=10μM, or $-\Delta F$=0.186. Accordingly, I conducted the continuous assay in this range of fluorescence and estimated initial velocity ($-\Delta F \bullet sec^{-1}$) was converted with the correction value 0.0186 into the initial velocity (AMPμM$\bullet sec^{-1}$) for the calculation of k_{cat} value.

Discrimination mechanism of B.s. LysRS towards L-lysine from its analogues: **Scheme I** represents the possible pathways producing AMP in the aminoacylation reaction; (a) pre-transfer editing reaction, (b) tRNA dependent pre-transfer editing reaction, (c) tRNA dependent post-transfer editing reaction, and (d) aminoacylation reaction. At first, I tried to investigate the pre-transfer editing reaction with L-lysine and its analogues in **Fig. 2**. In the cases with SAEC, L-ornithine, and 5-hydroxylysine, the existence of this editing reaction was confirmed. The ratios of the k_{cat}s of the pre-transfer editing reaction for these analogues against the k_{cat} for L-lysine were 7.81, 22.1, and 92.7, respectively. However, these k_{cat}s are considerably smaller than estimated k_{cat}s of the main reactions following this editing reaction (0.0141% for L-lysine~4.09% for 5-hydroxylysine), as reported previously Jakubowski *et al.* except the cases of *E. coli* IleRS against L-cysteine and homocysteine and of *E. coli* MetRS against homocysteine ***(8)***.

Estimated K_m and k_{cat} for L-lysine in **Fig. 3** are 29.4 ± 2.7μM and 6.95 ± 0.23s^{-1}, respectively, while those determined in the aminoacylation reaction using ^{3}H-lysine in previous paper (**Takita**

et al.) are 16.4μM, 3.2s^{-1}, respectively. I particularly noted the ratio, 2.2 (6.95 / 3.2) in k_{cat} and considered that it reflects the number of mole of AMP produced per a mole of lysyl-tRNA formed. Therefore, the same reaction mixture was subjected to the continuous assay for the determination of AMP produced and the aminoacylation reaction assay using ^{3}H-lysine for that of lysyl-tRNA formed. **Figure 4** indicates that about two moles of AMP are produced when one mole of lysyl-tRNA formed. This difference can not be explained by the pre-transfer editing reaction in **Table I** but by either of tRNA dependent pre-transfer editing reaction or tRNA dependent post-transfer editing reaction. In **Scheme I**, the initial velocities of the tRNA dependent pre-transfer editing reaction, the tRNA dependent post-transfer editing reaction, and the aminoacylation are denoted as V_1, V_2, and V_3. Since I can neglect the pre-transfer editing reaction, the initial velocity (V_0) in the continuous assay is the sum of V_1, V_2, and V_3, and the initial velocity in the aminoacylation reaction is equal to V_3.

$$V_0=V_1 + V_2 + V_3 \qquad (5)$$

$$2=V_0/V_3=(V_1 + V_2 + V_3)/V_3$$

$$\therefore\ V_1 + V_2=V_3 \qquad (6)$$

It is shown here that in the case with L-lysine, the initial velocity of the sum of tRNA dependent pre-transfer editing reaction and tRNA dependent post-transfer editing reaction is similar to that of aminoacylation reaction. The reason why such energetically wasteful reaction occurs in my system remains unknown. However, this result is consistent with the result of direct measurement of the transfer of L-lysine from the LysRS•lysyladenylate complex to tRNA described previously ***(3)***. Freist *et al.* reported that the ratio of AMP against lysyl-tRNA is 3.95 in a yeast system ***(9)***. The ratio is

higher than the ratios determined by them, 1.1 for *E. coli* IleRS ***(10)***, 1.2 for yeast ValRS ***(11)***, 1.7 for yeast ArgRS ***(12)***, and 2.2 for ThrRS ***(13)*** except 5.5 for yeast IleRS ***(10)***. These results suggested that the tRNA dependent pre-transfer or/and the tRNA dependent post-transfer editing reaction occurred more or less even against cognate amino acid besides against non-cognate amino acid ***(14~17)***.

As shown in **Fig. 5**, when SAEC, L-ornithine, threo-4-hydroxy-L-lysine were used, the reaction apparently stopped, which indicates that tRNA was charged with these analogues by B.s. LysRS. However, the result of 5-hydroxylysine strongly indicates the possibility that tRNA was not charged with 5-hydroxylysine, in other words, $V_1 + V_2 >> V_3$ (see **Scheme I**). Then, I tried to investigate the charging of tRNA with 5-hydroxylysine by the back-titration method. **Figure 6** indicates that tRNA was not charged with 5-hydroxylysine. This is consistent with the result of Stern *et al.* with *E.coli* LysRS ***(18)***. In order to investigate a role of 2'- and 3'-hydroxy groups of the 3'-terminal adenosine of tRNA in the tRNA dependent editing mechanism towards 5-hydroxylysine, I prepared periodate-oxidated tRNA and periodate-oxidated lysyl-tRNA besides intact tRNA. After the deacylation of the periodate-oxidated lysyl-tRNA, I could detect L-lysine-acceptance activity fully from it **(Fig. 7A)**. Therefore, I call it $tRNA^{Lys}$ with periodate-oxidated tRNA. In **Fig. 7B** with L-lysine and **7C** with 5-hydroxylysine, both reactions with the intact tRNA and the $tRNA^{Lys}$ with periodate-oxidated tRNA occurred. However, the reactions with the periodate-oxidated tRNA did not occur (**Fig. 7B** and **7C**). It indicates the requirement of the 2'- and 3'-hydroxy groups of tRNA for the tRNA dependent pre-transfer editing reaction and the tRNA dependent

post-transfer editing reaction towards 5-hydroxylysine and may suggest a possibility that main editing reaction against 5-hydroxylysine is the tRNA dependent post-transfer editing reaction. Since 5-hydroxylysine used contained DL-type and DL-allo type, I may consider the effect of D- types on the post-transfer editing reaction. However, by considering that the detected activity with 10mM D-lysine was significantly small (5.8% of that with 1mM L-lysine) (**data not shown**), it is rational to explain that the post-transfer editing reaction is driven by L- and L-allo types.

Vs shows the existence of esterase activity of B.s. LysRS towards aminoacyl- tRNA: Only in the case with L-lysine, it was confirmed that the continuous AMP production was occurred in an apparent equilibrium state of the aminoacylation reaction. However, I have considered that it is applied to the cases with SAEC, L-ornithine, and threo-4-hydroxy-L-lysine because the chase of the continuous reaction with these analogues shows a clear curve followed by linear line as is seen in that with L-lysine (**Fig. 5**). Since k_{cat}s estimated from V_S of the continuous AMP production in the continuous assay are at least 14 times larger than those of the pre-transfer editing reaction (in the case with L-ornithine), I can not explain it by the pre-transfer editing reaction (**Table I**). Since the continuous AMP production was occurred in an apparent equilibrium state of the aminoacylation reaction, I can not also explain it by the tRNA dependent pre-transfer editing reaction and the tRNA dependent post-transfer editing reaction. It is difficult to explain the continuous AMP production by the reverse reaction in Equation (2) essentially or because of the presence of three continuous reactions following the aminoacylation reaction. Further, though the k_{app}s of the continuous AMP production were

estimated with L-lysine analogues at the concentration that was about 4~10 times larger than K_m in the continuous assay, the values are different in all cases. It is difficult to explain only by a spontaneous deacylation of aminoacyl-tRNA. Then, I have considered an esterase activity of *B.s.* LysRS towards aminoacyl-tRNA as described in other ARSs ***(19, 20)***. The production of free tRNA from aminoacyl-tRNA through a spontaneous deacylation and a hydrolytic reaction by *B.s.* LysRS is considered to be rate-determining step in the apparent equilibrium state in the aminoacylation reaction. Therefore, the velocity of the continuous AMP production, V_s is the sum of the velocity of a spontaneous deacylation and that of a hydrolytic reaction by *B.s.* LysRS (**Scheme II**). If this assumption is proper, V_s is dependent on the concentration of aminoacyl-tRNA in an apparent equilibrium state in the aminoacylation reaction. In order to confirm this, I tried to estimate relative concentration of tRNA aminoacylated with threo-4-hydroxy-L-lysine in an apparent equilibrium state with the guidance of the concentration of AMP formed until the reaction come to an equilibrium state by the method as shown in **Fig. 9A**. Though the value of $(V_1+V_2)/V_3$ for threo-4-hydroxy-L-lysine is unknown, it is rational to consider the linear relationship between V_1+V_2 and V_3 as is the case with L-lysine (Equation 7). Then, I can estimate the relative concentration of aminoacyl-tRNA in an equilibrium state, $[\text{aminoacyl-tRNA}]_{eq}$ from **Fig. 9B**. Estimated relative concentration of tRNA aminoacylated with threo-4-hydroxy-L-lysine is shown in **Fig. 9C**. Evidently, the concentration of aminoacyl-tRNA at 0.5mM threo-4-hydroxy-L-lysine is lower than those at higher concentrations. It agrees with the plot of relative V_s against the concentration of threo-4-hydroxy-L-lysine

(**Fig. 9C**). Then, when I calculated the relative values of V_s and divided it by corresponding [aminoacyl-tRNA]$_{eq}$ (**Fig. 9C**), estimated values are all close to 1. It strongly proves the property of our assumption. By comparing k_{cat}s in **Table I**, the hydrolytic reaction by B.s. LysRS is not considered important for the substrate specificity of *B.s.* LysRS.

Why such a high frequency of post-transfer editing occurs in our system with L-lysine?: Equation (7) indicates that in my system, even in the case with L-lysine, the tRNA dependent pre-transfer editing reaction or/and the tRNA dependent post-editing reaction proceeds at the same rate as the aminoacylation does. Since I used *E. coli* tRNA mixture in the reaction catalyzed by *B.s.* LysRS, I must investigate the effects of non-cognate *E. coli* tRNA and *E. coli* $tRNA^{Lys}$ on the tRNA dependent editing reactions. I compared the aminoacylation reaction with *E. coli* tRNA mixture with that with *E. coli* $tRNA^{Lys}$ (**Fig. 10**). I, however, could not detect appreciable difference in both cases. Especially, the observation of similar values of k_{cat} suggests that *B.s.* LysRS does not mischarge *E. coli* non-cognate tRNA with L-lysine. Therefore, I consider that the difference of k_{cat} in two assays used is not deprived from the editing of such a mischarged tRNA but from that of tRNA charged properly with L-lysine. On using tRNA from *B. stearothermophilus* towards *B.s.* LysRS, however, it is unknown whether such an energetically wasteful editing reaction occurs or not. If we consider two types of reaction (charging and non-charging reactions) at the step of transfer of amino acid from the ARS•aminoacyladenylate complex to tRNA in the same origin system, it will turn out that ARS guarantees a high degree of substrate specificity at the sacrifice of energy costs.

X-spots from 5-hydroxylysine and L-ornithine: When the second development of the different sets of reaction mixture containing either 5-hydroxylysine or L-ornithine at right angle was conducted after the first development followed by drying under an alkaline condition, we could detect the conversion of X-spots to the starting spot (**data not shown**). It was reported that though hydroxy analogues of amino acid not only can form the aminoacyladenylate intermediate but also transferred to tRNA, the misactivated hydroxy analogues are hydrolytically removed in the cases of the Class I enzymes specific for hydrophobic residues ***(21, 22)***. These results agree with the observation that the post-transfer editing reaction prevents the charging of tRNA with 5-hydroxylysine. It is considered not fortuitous the fact that an editing or proofreading mechanism exists for correction of misaminoacylation for hydrophobic residues and explained tentatively as follows: ARS specific for hydrophobic residues are the ones which need this correction mechanism more, because their active site is bound to be less specific than the one for polar residues ***(23)***. However, it is shown in this study that a Class II enzyme specific for charged residue, LysRS also has such an editing mechanism. At present, though it is unknown whether the X-spot from 5-hydroxylysine is a lactone, the easy conversion under a natural condition to 5-hydroxylysine suggests the possibility that the X-spot formed in a lactonisation. Further, since we could detect the X-spot only under the condition of aminoacylation reaction, it is considered that the tRNA dependent editing reactions produce the X-spot from 5-hydroxylysine. On the other hand, since we could detect X-spot from L-ornithine under the condition of the aminoacyladenylate formation, it is considered that the pre-transfer editing reaction

(possibly post-transfer editing reaction) produces the X-spot from L-ornithine. At present, the X-spot from L-ornithine is unknown but may be considered to be formed in a lactamisation. Jakubowski reported that *E coli* MetRS misactivated very efficiently homocysteine but prevents a charging of tRNA by the pre-transfer editing reaction, resulting in the production of homoserine thiolactone by cyclization of homocysteine, while *E coli* MetRS deacylates methionyl-tRNA by tRNA dependent post-transfer editing reaction and, to a lesser extent, pre-transfer editing reaction, resulting in the production of *S*-methyl homocysteine thiolactone by cyclization of methionine because the limited ability of the enzyme to discriminate against the cognate L-methionine at the editing site designed for non-cognate homocysteine ***(24)***. Jakubowski reported that *E. coli* CysRS also deacylates cysteinyl-tRNA by tRNA dependent post-transfer editing reaction, resulting in the production of cysteine thiolactone, while non-enzymatic deacylation of cysteinyl-tRNA yields cysteine ***(25)***. By considering that the nucleophilicity of the side chain of amino acid and the presence of α-carboxyl group are essential for these cyclization editing reactions, the lactamisation of L-ornithine may be possible because of the weak binding of 5-amino group of its side-chain to the enzyme ***(2, 3)***. We could detect no new appreciable spot in other cases involving the one with L-lysine. However, we could detected the difference in k_{cat} of AMP production and lysyl-tRNA formation in the case with L-lysine. It makes us considering tRNA dependent post-transfer editing reaction in which lysyl-tRNA is hydrolyzed, resulting in the production of L-lysine.

REFERENCES

1) Berg, P. (1961) Specificity in protein synthesis. *Annu. Rev. Biochem.* **30**, 293-324

2) Takita *et al.*

3) Takita *et al.*

4) Roy, S. (1983) A continuous spectrophotometric assay for *Escherichia coli* alanyl-transfer RNA synthetase. *Analytical Biochem.* **133**, 292-295

5) Wu, M. X. and Hill, K. A. W. (1993) A continuous spectrophotometric assay for the aminoacylation of transfer RNA by alanyl-transfer RNA synthetase. *Analytical Biochem.* **211**, 320-323

6) Lloyd, A. J., Thomann, H-U., Ibba, M., and Söll D. (1995) A broadly applicable continuous spectrophotometric assay for measuring aminoacyl-tRNA synthetase activity. *Nucleic Acid Res.* **23**, 2886-2892

7) Shimizu, S., Inoue, K., Tani, Y., and Yamada, H. (1979) Enzymatic microdetermination of serum free fatty acids. *Analytical Biochem.* **98**, 341-345

8) Jakubowski, H., Fersht, A. R. (1981) Alternative pathways for editing non-cognate amino acids by aminoacyl-tRNA synthetases. *Nucleic Acid Res.* **9**, 3105-3117

9) Freist, W., Sternbach, H., and Cramer, F. (1992) Lysyl-tRNA synthetase from yeast. Discrimination of amino acids by native and phosphorylated species. *Eur. J. Biochem.* **204**, 1015-1023

10) Freist, W., Sternbach, H., and Cramer, F. (1987) Isoleucyl-tRNA synthetase from baker's yeast and from *Escherichia coli* MRE 600. Discrimination of 20 amino acids in

aminoacylation of $tRNA^{Ile}$-C-C-A(3'NH_2). *Eur. J. Biochem.* **169**, 33-39

11) Freist, W. and Cramer, F. (1990) Valyl-tRNA synthetase from yeast. Discrimination of 20 amino acids in aminoacylation of $tRNA^{Val}$-C-C-A and $tRNA^{Val}$-C-C-A(3'NH_2). *Eur. J. Biochem.* **191**, 123-129

12) Freist, W., Sternbach, H., and Cramer, F. (1989) Arginyl-tRNA synthetase from yeast. Discrimination of 20 amino acids in aminoacylation of $tRNA^{Arg}$-C-C-A and $tRNA^{Arg}$-C-C-A(3'NH_2). *Eur. J. Biochem.* **186**, 535-541

13) Freist, W., Sternbach, H., and Cramer, F. (1994) Threonyl-tRNA synthetase from yeast. Discrimination of 20 amino acids in aminoacylation of $tRNA^{Thr}$-C-C-A and $tRNA^{Thr}$-C-C-A(3'NH_2). *Eur. J. Biochem.* **220**, 745-752

14) Norris, A. and Berg. P. (1965) Mechanism of aminoacyl RNA synthesis: studies with isolated aminoacyl adenylate complexes of isoleucyl RNA synthetase. *Proc. Natl. Acad. Sci. USA.* **52**, 330-337

15) Fersht, A. R. and Kaethner, M. M. (1976) Enzyme hyperspecificity rejection of threonine by the valyl-tRNA synthetase by misacylation and hydrolytic editing. *Biochemistry* **15**, 3342-3346

16) Fersht, A. R. and Dingwall, C. (1979) Establishing the misacylation/deacylation of the tRNA pathway for the editing mechanism of prokaryotic and eukaryotic valyl-tRNA synthetase. *Biochemistry* **18**, 1238-1245

17) Fersht, A. R. and Dingwall, C. (1979) An editing mechanism for the methionyl-tRNA synthetase in the selection of amino acids in protein synthesis. *Biochemistry* **18**, 1250-1256

18) Stern, R. and Mehler, A. H. (1965) Lysyl-tRNA synthetase from *Escherichia coli. Biochem. Z.* **342**, 400-409

19) Eldred, E. W. and Schimmel, P. R. (1972) Rapid deacylation by isoleucyl transfer ribonucleic acid synthetase of isoleucine-specific transfer ribonucleic acid aminoacylated with valine. *J. Bio. Chem.* **247**, 2961-2964

20) Yarus. M. (1972) Phenylalanyl-tRNA synthetase and isoleucyl-$tRNA^{Phe}$: A possible verification mechanism for aminoacyl-tRNA. *Proc. Natl. Acd. Sci. USA* **69**, 1915-1919

21) English, S., English, U., Haar, F. von der, and Cramer, F. (1986) The proofreading of hydroxy analogues of leucine and isoleucine by leucyl-tRNA synthetases from *E. coli* and yeast. *Nucleic. Acid. Res.* **14**, 7529-7539

22) English-Perters, S., Haar, von der F. , and Cramer, F. (1990) Fidelity in the aminoacylation of $tRNA^{Val}$ with hydroxy analogues of valine, leucine, and isoleucine by valyl-tRNA synthetases from Saccharomyces cerevisiae and *E. coli. Biochemistry* **29**, 7953-7958

23) Delarue, M. and Moras, D. (1992) "*Nucleic Acid and Molecular Biology*", **6**, ed. by Eckstein, F. and Lilley, D. M. J., Springer-Verlag, Berlin, Heidelberg, pp.203-224

24) Jakubowski H. (1993) Proofreading and the evolution of a methyl donor function. *J. Biol. Chem.* **268**, 6549-6553

25) Jakubowski H. (1994) Editing function of *Escherichia coli* cysteinyl-tRNA synthetase: cyclization of cysteine to cysteine thiolactone. *Nucleic Acid Res.* **22**, 1155-1160

Table I
Continuous assay with L-lysine analogues

	In the absence of tRNA	In the presence of tRNA			
		V_0			V_S
	k_{cat} (s^{-1})	K_m (μM)	k_{cat} (s^{-1})	k_{cat}/K_m ($s^{-1} \cdot M^{-1}$)	k_{cat} (s^{-1})
L-lysine	9.79×10^{-4}	29.4 ± 2.7	6.95 ± 0.23	2.36×10^5	0.268
α-carboxyl group modified					
L-lysine hydroxamate	9.18×10^{-4}	/	/	/	/
L-lysine amide	0	/	/	/	/
Others					
S-(2-aminoethyl)-L-cysteine	7.65×10^{-3}	145 ± 12.4	1.79 ± 0.06	1.23×10^4	0.1756
L-ornithine	2.16×10^{-2}	2,630 ± 235	1.92 ± 0.07	7.30×10^2	0.312
5-hydroxylysine (mixed DL and DL-allo)	9.08×10^{-2}	8,540 ± 754	2.22 ± 0.10	2.60×10^2	/
threo-4-hydroxy-L-lysine	—	2,540 ± 185	3.94 ± 0.12	1.55×10^3	0.456

The standard reaction mixture used for the measurement contained in 0.19ml: 100mM Tris-HCl buffer (pH 8.0), 10mM $MgCl_2$, 50μM NADH, 200μM phosphoenolpyrubate, 200μM ATP, $140A_{260}$ units of tRNA from *E. coli* MRE 600, 10nM LysRS, 30U/ml adenylate kinase, 18U/ml pyuruvate kinase, and 18U/ml lactate dehydrogenase. The excitation wave length and the emission wave length were 365nm and 460nm, respectively. The initial velocity, V_0 ($-\Delta F \cdot sec^{-1}$) was calculated from the decrease of the fluorescence intensity *versus* time.
V_0, initial velocity
V_s, the velocity estimated in a linear line following a curve observed in the continuous assay.

Scheme I

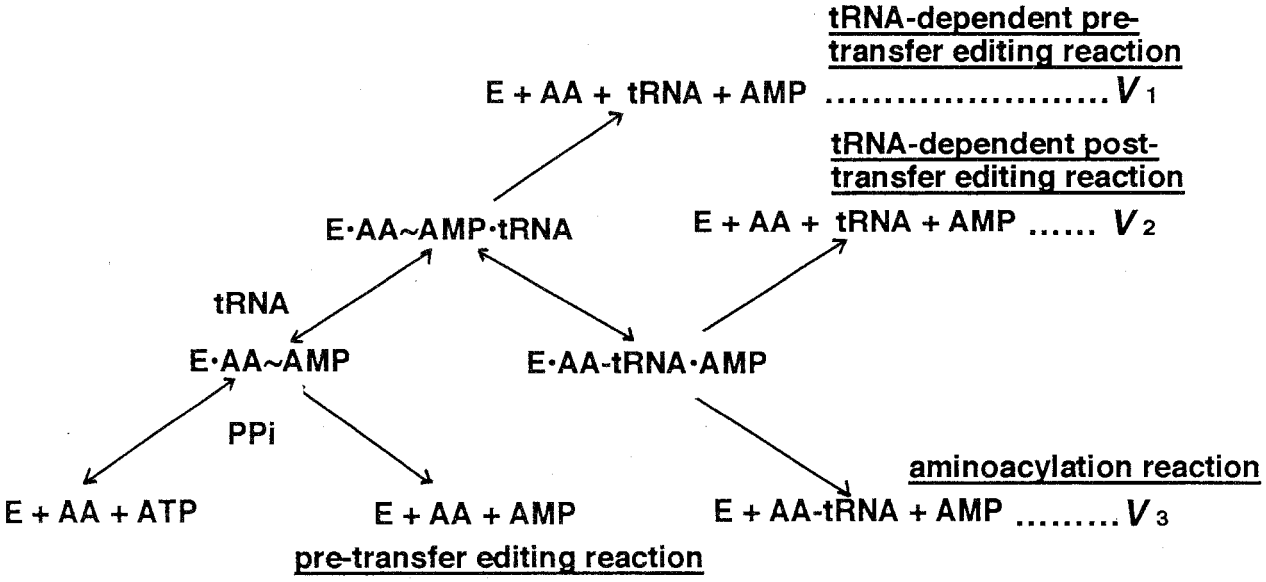

Scheme II

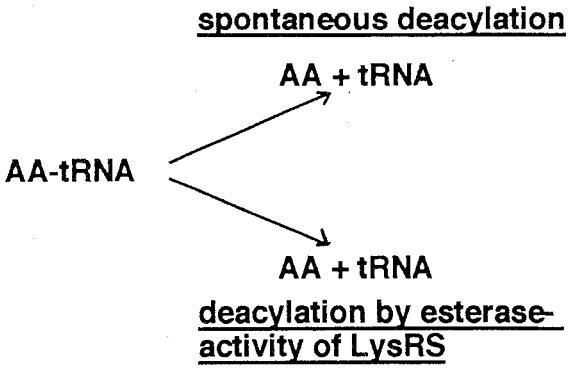

Scheme III

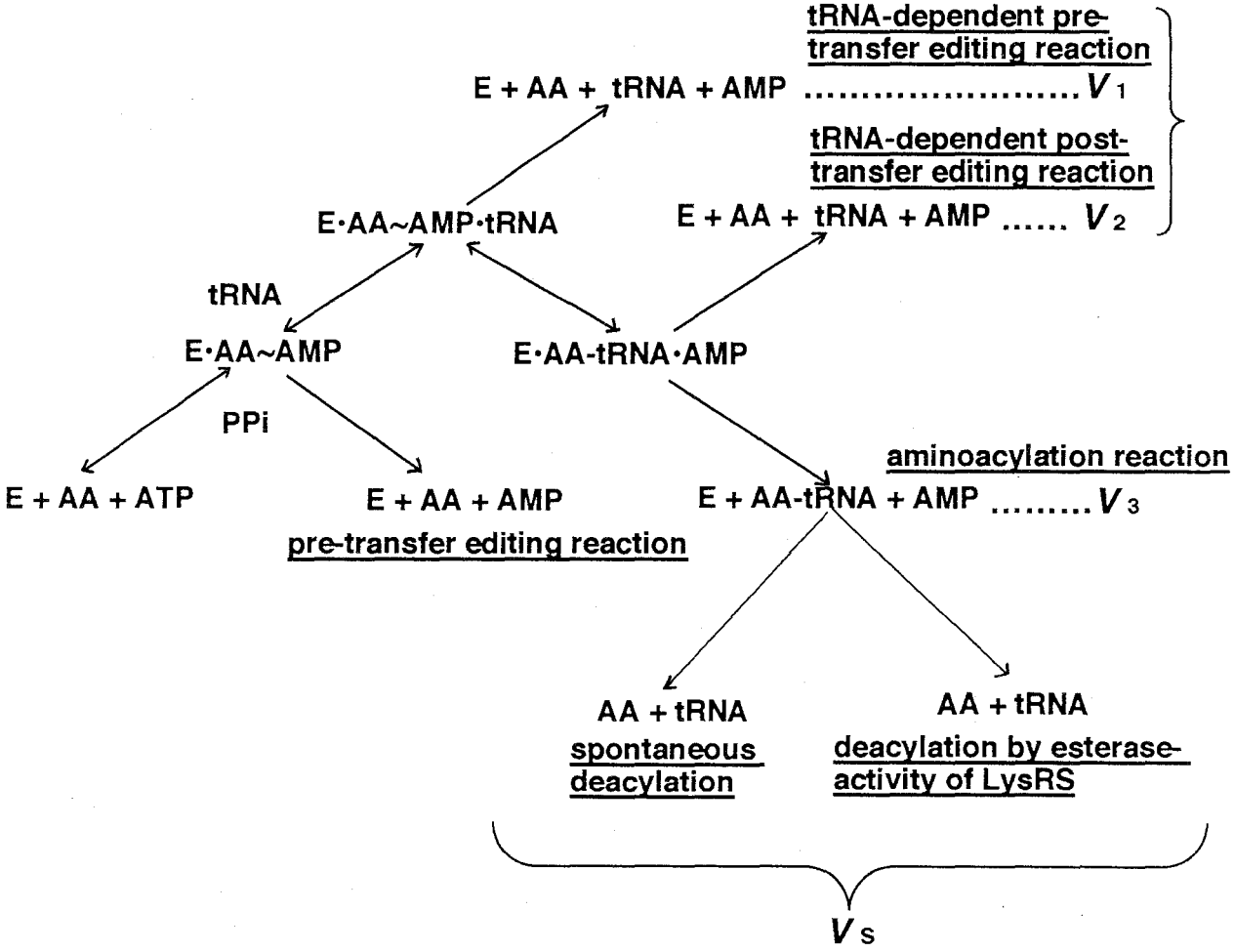
tRNA-dependent pre-transfer editing reaction
E + AA + tRNA + AMP V1
tRNA-dependent post-transfer editing reaction
E·AA~AMP·tRNA
E + AA + tRNA + AMP V2
tRNA
E·AA~AMP
E·AA-tRNA·AMP
PPi
aminoacylation reaction
E + AA + ATP
E + AA + AMP
pre-transfer editing reaction
E + AA-tRNA + AMP V3
AA + tRNA
spontaneous deacylation
AA + tRNA
deacylation by esterase-activity of LysRS
Vs

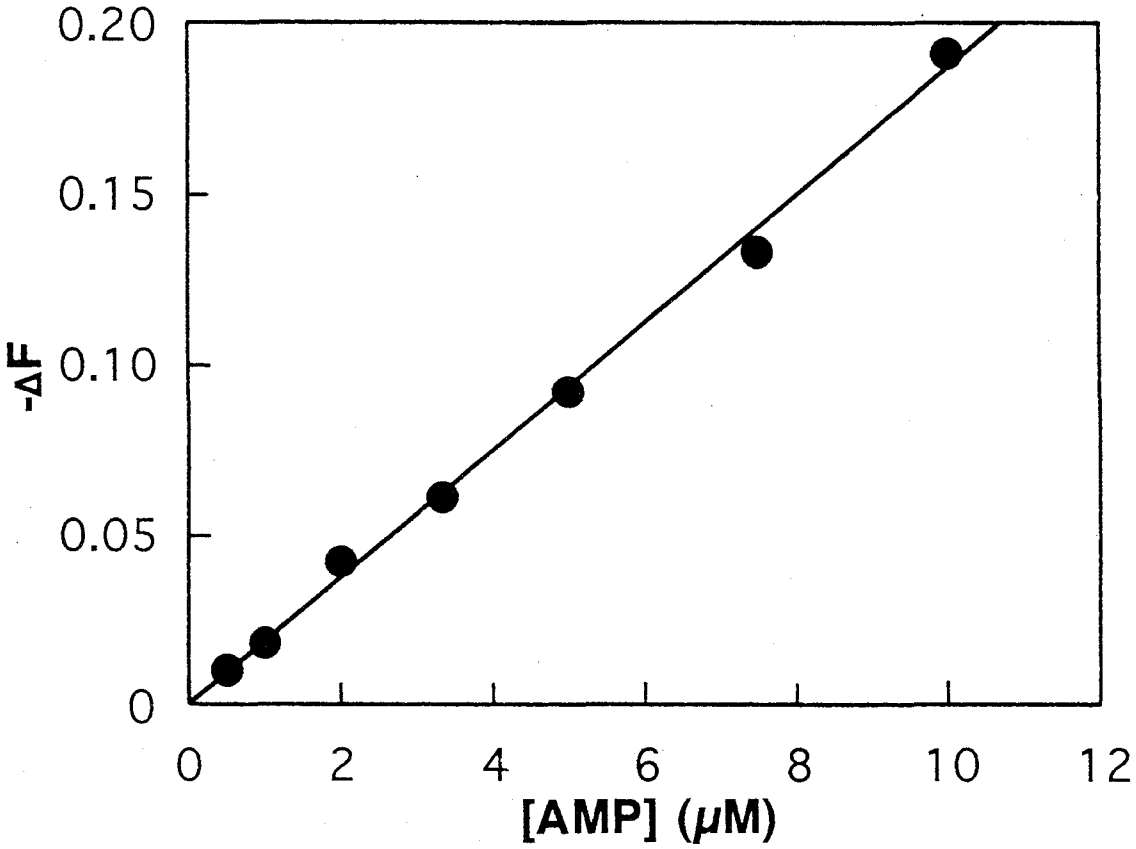

Figure 1

Calibration of fluorescence decrease with AMP concentration in the continuous assay

The standard reaction mixture used for the measurement contained in 0.19ml: 100mM Tris-HCl buffer (pH 8.0), 10mM $MgCl_2$, 50μM NADH, 200μM phosphoenolpyruvate, 200μM ATP, 140A_{260} units of tRNA from *E. coli* MRE 600, 30U/ml adenylate kinase, 18U/ml pyruvate kinase, and 18U/ml lactate dehydrogenase. After the addition of 10μl of AMP, fluorescence change was measured at pH 8.0, 30°C, λ_{ex}=365nm, and λ_{em}=460nm. The solid line is drawn by the least squares method.

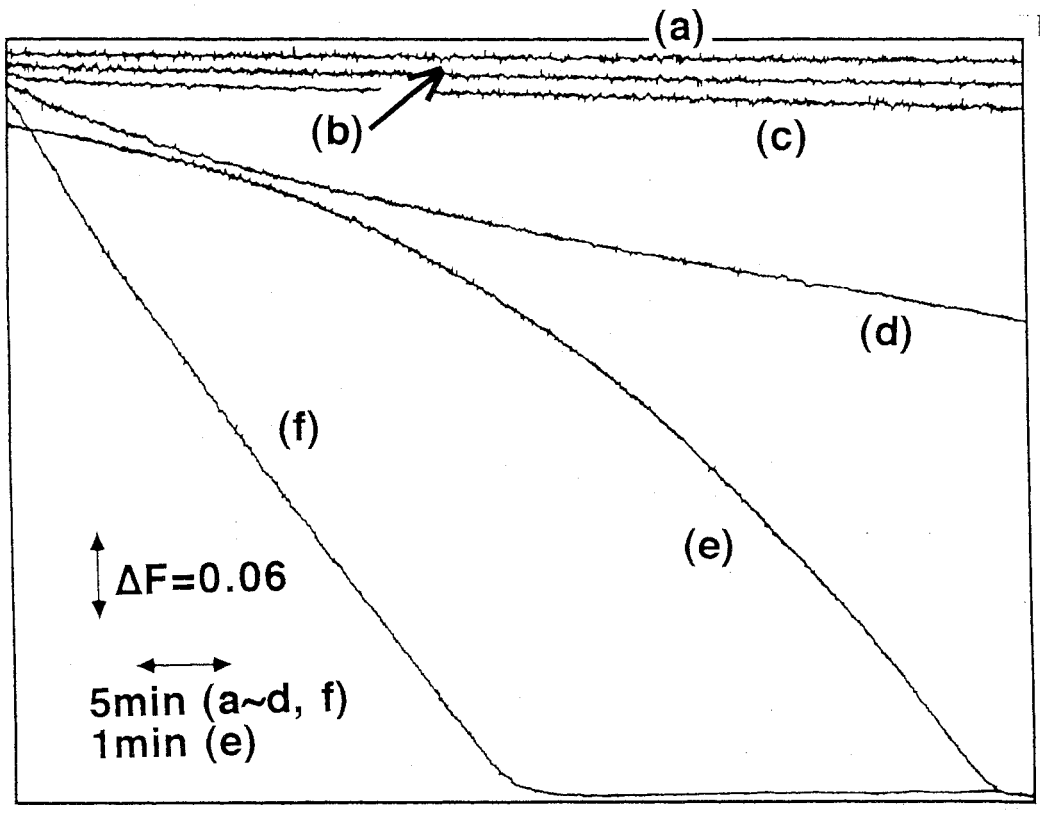

Figure 2
Continuous assay in the absence of tRNA
$[E]_0$=100nM, λ_{ex}=365nm, λ_{em}=460nm, at pH 8.0, 30°C. (a) 300μM L-lysine, (b) 300μM L-Lyshxt, (c) 300μM L-Lysamd, (d) 3mM SAEC, (e) 50mM L-ornithine, and (f) 170mM 5-hydroxylysine.

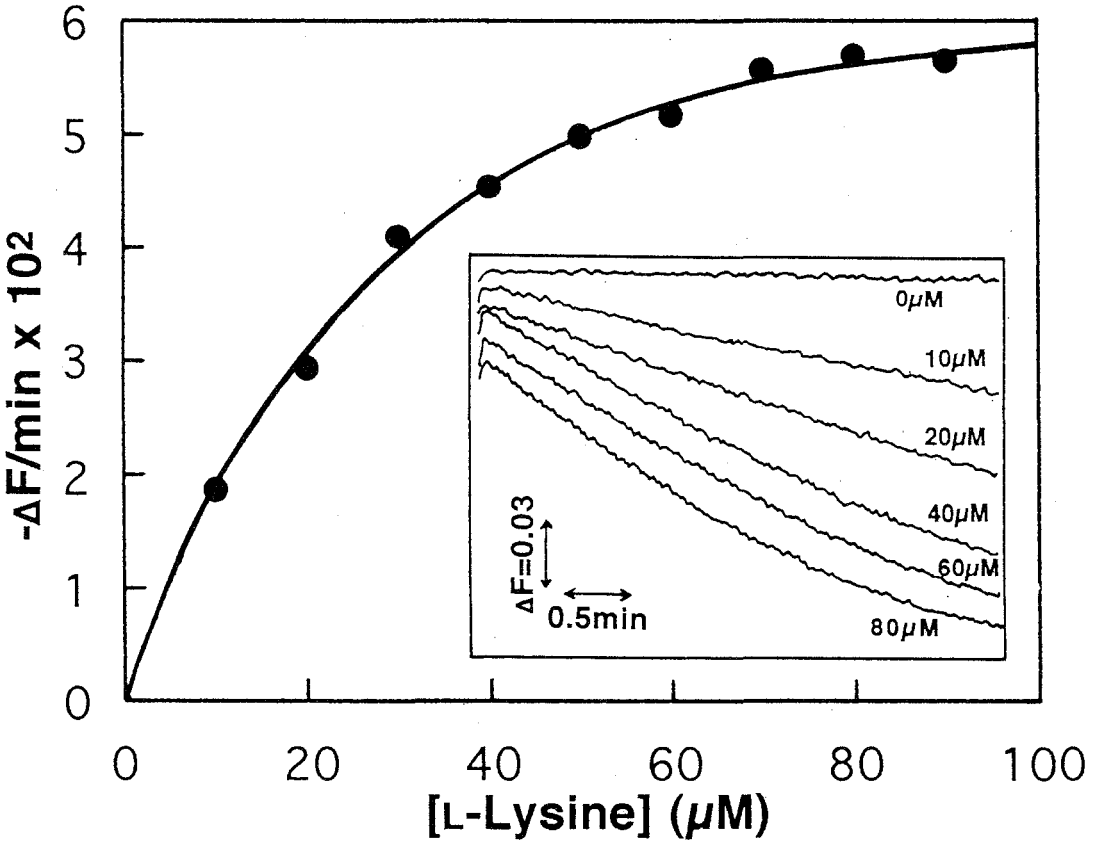

Figure 3

Continuous assay with L-lysine in the presence of tRNA

$[E]_0$=10nM, λ_{ex}=365nm, λ_{em}=460nm, at pH 8.0, 30°C. The solid line is the theoretical curve drawn according to an equation of Michaelis-Menten with K_m=29.4±2.7μM and k_{cat} =6.95±0.23s^{-1}. The inset shows the reaction curves observed with different concentrations of L-lysine (0~90μM).

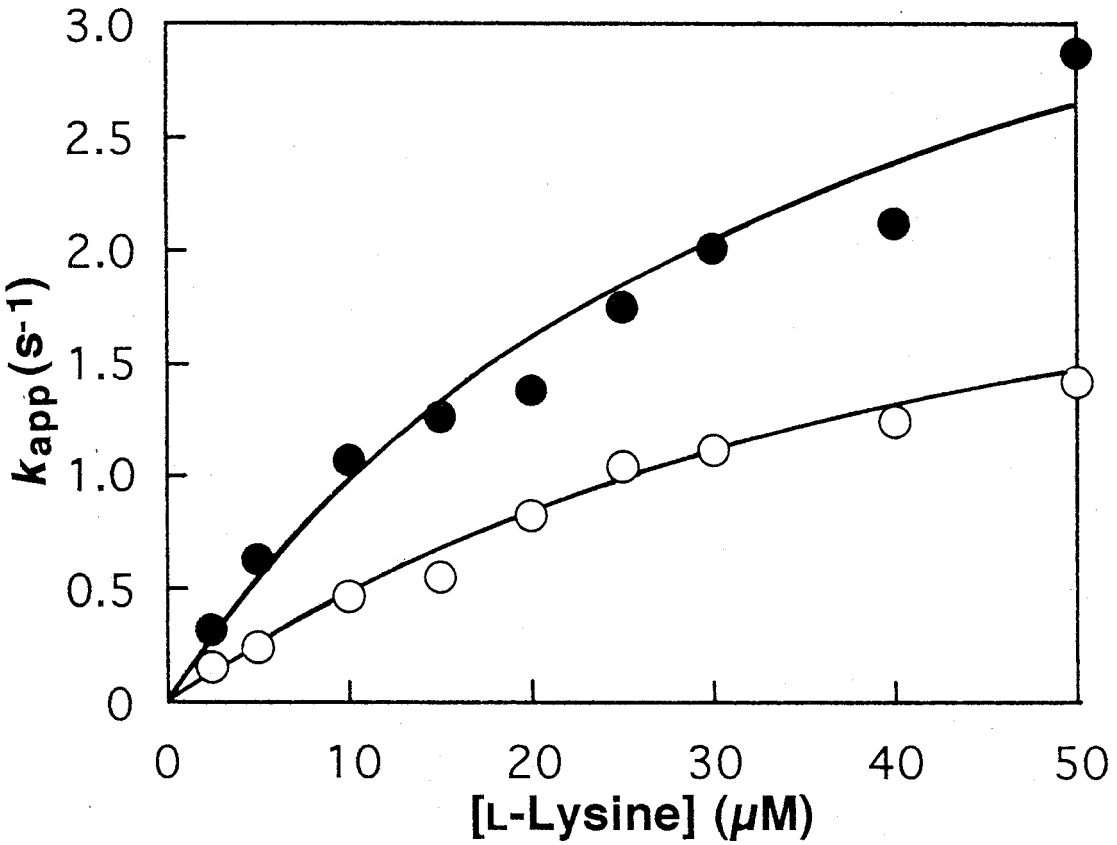

Figure 4

Comparison of the continuous assay with the aminoacylation reaction assay

$[E]_0$=10nM, λ_{ex}=365nm, λ_{em}=460nm, at pH 8.0, 30°C. The solid lines for the continuous assay (●) and for the aminoacylation reaction (○) are the theoretical curves drawn according to an equation of Michaelis-Menten with K_m=46.5±13.9μM and k_{cat} =5.10±0.91s^{-1} and with K_m=52.2±11.1μM and k_{cat} =2.94±0.39s^{-1}, respectively.

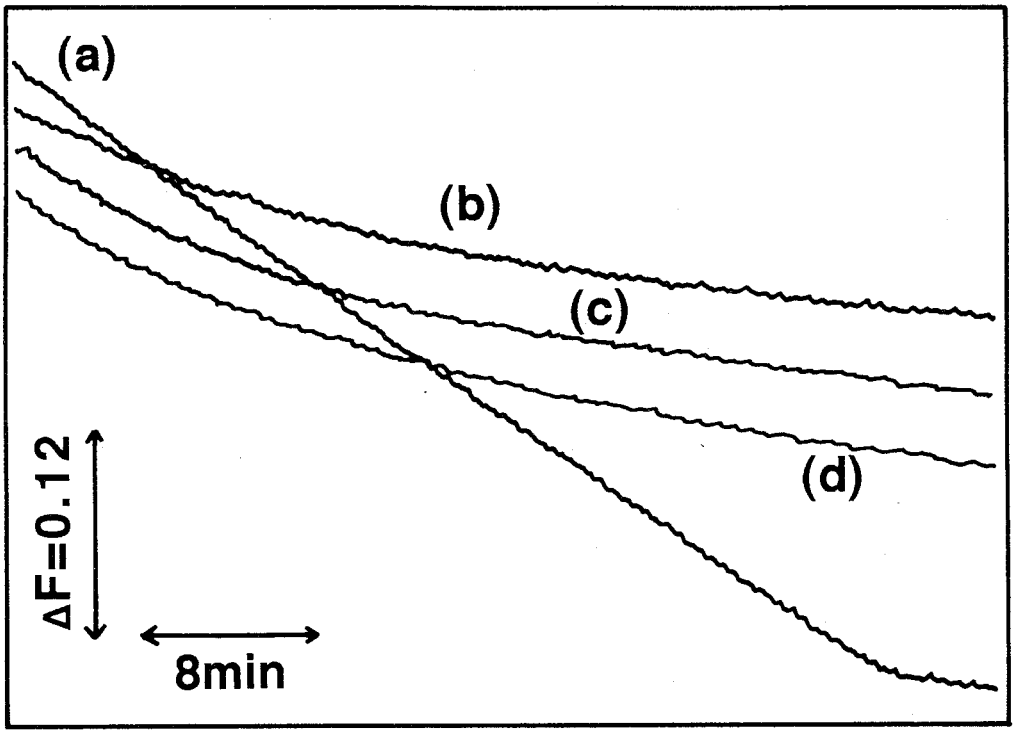

Figure 5

Continuous assay with L-lysine analogues in the presence of tRNA

$[E]_0$=10nM, λ_{ex}=365nm, λ_{em}=460nm, at pH 8.0, 30°C. (a) 10mM 5-hydroxylysine, (b) 150μM SAEC, (c) 2mM L-ornithine, and (d) 2mM *threo*-4-hydroxy-L-lysine.

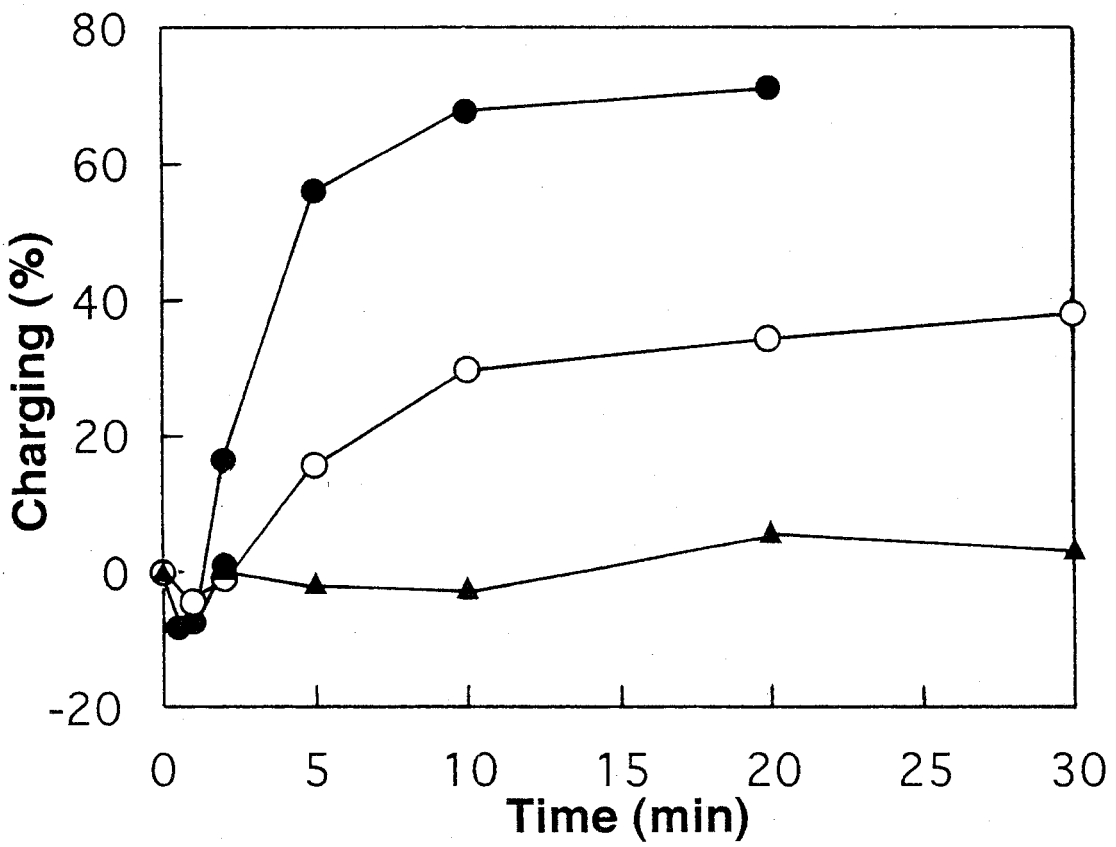

Figure 6

Back-titration experiments with L-lysine, SAEC, and 5-hydroxylysine

The first aminoacylation reaction was carried out by 10nM *B.s.* LysRS with 1mM L-lysine, 10mM SAEC, and 10mM 5-hydroxylysine at different times at pH 8.0, 37°C. The charging percentage of the first reaction was calculated as shown by Equation (4).

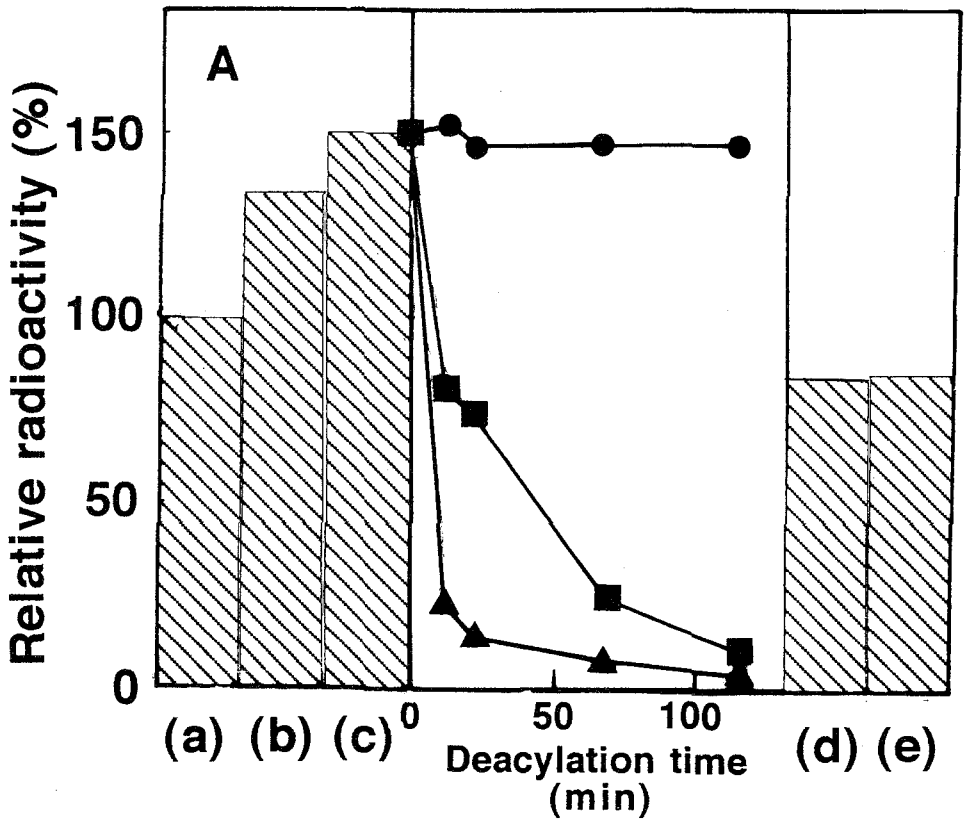

Figure 7

A role of 2'- and 3'-hydroxy groups of the 3'-terminal adenosine of tRNA in tRNA dependent editing mechanism

A: Preparation of periodate-oxidated tRNA and lysyl-tRNA. Fig. 7A shows relative radioactivity of ^{3}H-lysyl-tRNA precipitated with 5% trichloroacetic acid at each step, (a) aminoacylation reaction, (b) + acetic acid (pH 4.5), (c) + $NaIO_4$ cleavage, (d) reaminoacylation of the tRNA deacylated at pH 10.0, and (e) reaminoacylation of the tRNA deacylated at pH 8.0 in addition to the deacylation step, (●) at pH 5.0, (■) at pH 8.0, and (▲) at pH 10.0.

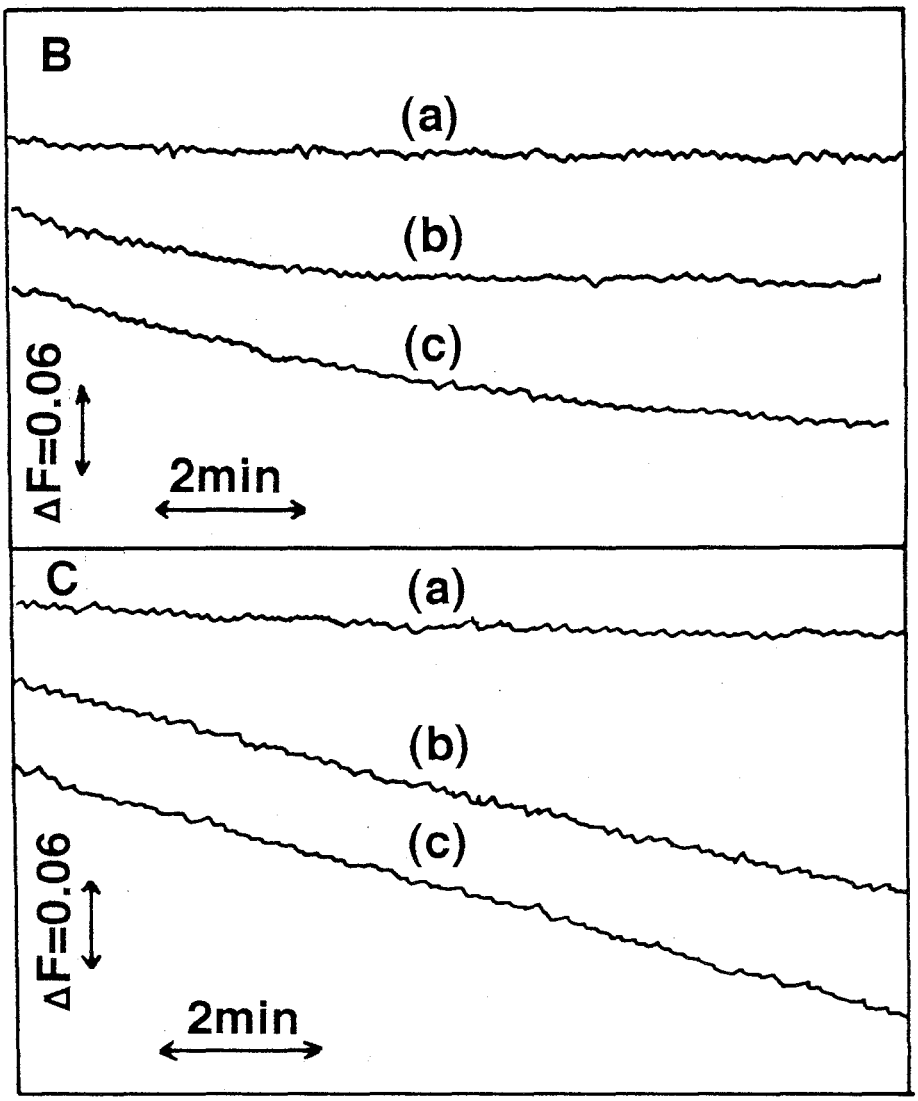

B: Continuous assay with L-lysine using periodate-oxidated free tRNA and lysyl-tRNA. $[E]_0$=2nM, [L-lysine]=10μM, [tRNA]=70A_{260} units, λ_{ex}=365nm, λ_{em}=460nm, at pH 8.0, 30°C. (a) periodate-oxidated free tRNA, (b) periodate-oxidated lysyl-tRNA, and (c) intact tRNA.

C: Continuous assay with 5-hydroxylysine using periodate-oxidated free tRNA and lysyl-tRNA. Used conditions were the same as **B** except [5-hydroxylysine]=10mM.

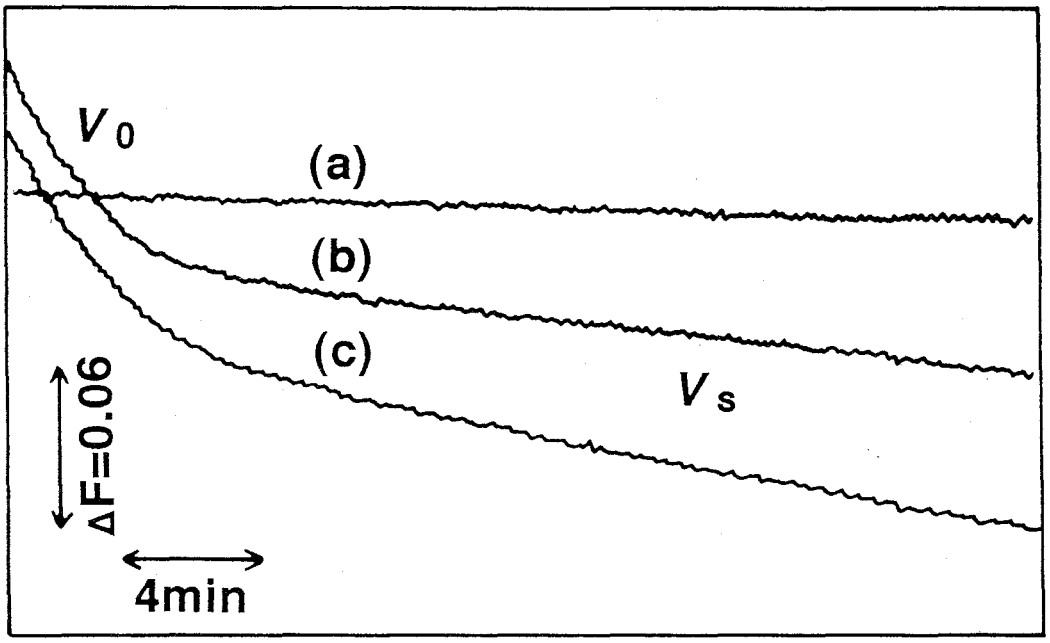

Figure 8

Reaction curves in the continuous assay with L-lysine and *threo*-4-hydroxy-L-lysine

$[E]_0$=10nM, λ_{ex}=365nm, λ_{em}=460nm, at pH 8.0, 30°C. V_0 and V_s denote the initial velocity of the continuous assay and the velocity estimated in a linear line following a curve, respectively. (a) blank, (b) [L-lysine]=300μM, and (c) [*threo*-4-hydroxy-L-lysine]=10mM.

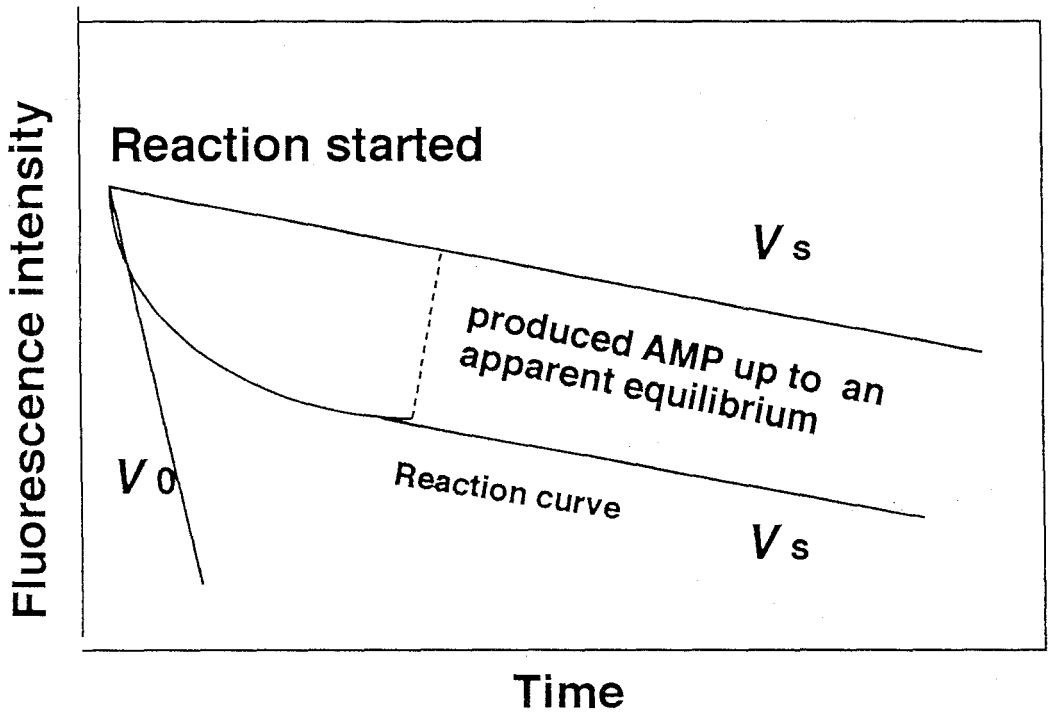

Figure 9

A possible explanation of V_S in the continuous assay

A: A method estimating the concentration of AMP formed until aminoacylation reaction come to an equilibrium state.

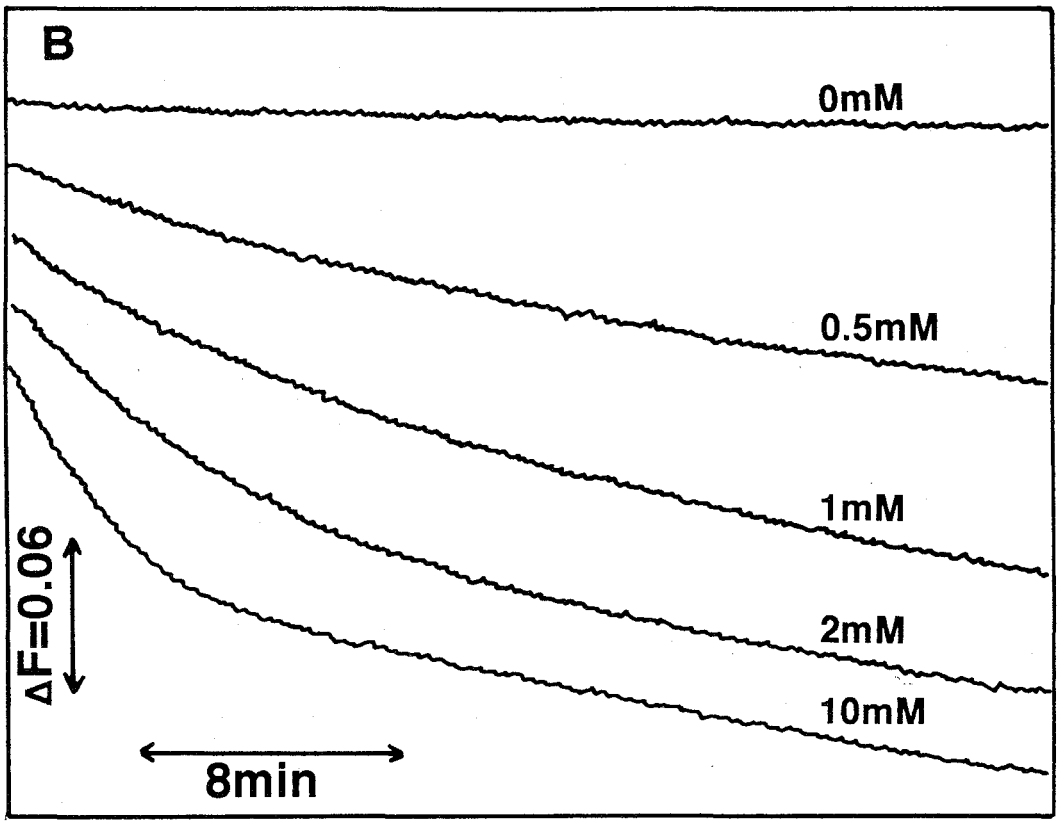

B: Reaction curves with different concentrations of *threo*-4-hydroxy-L-lysine. $[E]_0$=10nM, λ_{ex}=365nm, λ_{em}=460nm, pH 8.0, 30°C.

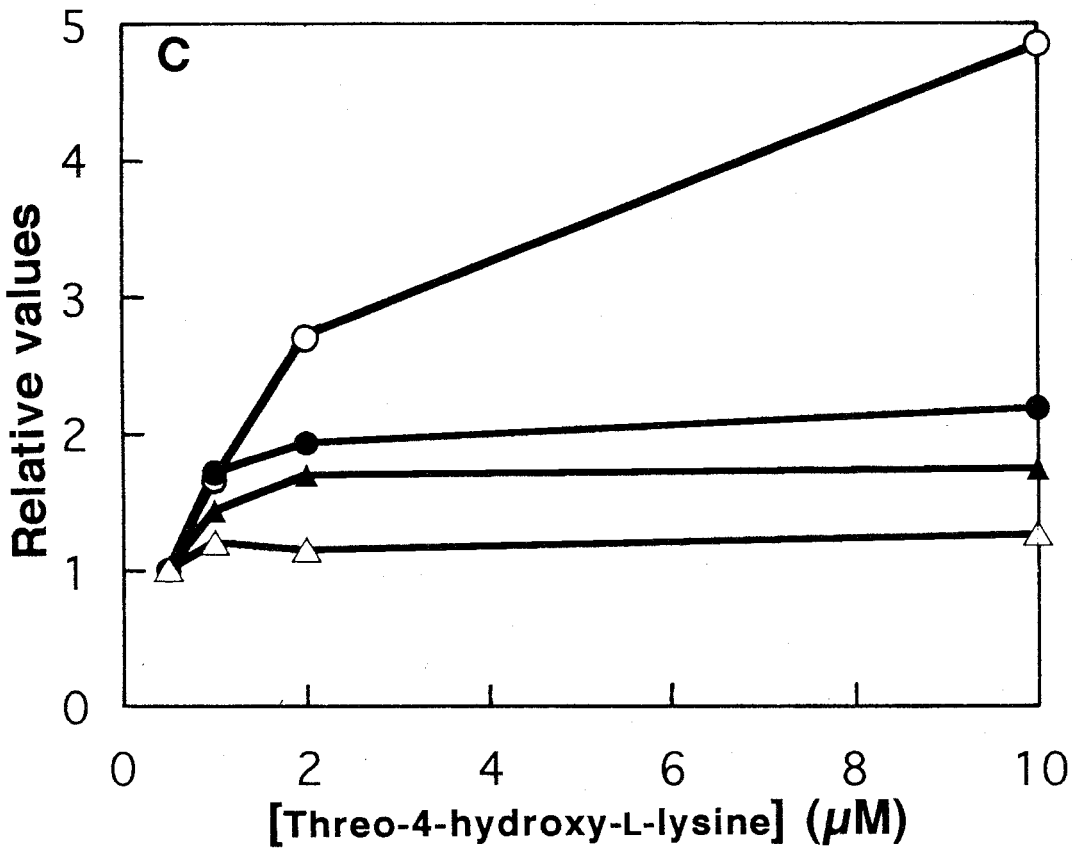

C: Relative values of V_0 (○), V_s (●), [aminoacyl-tRNA]$_{eq}$ (▲), and V_s / [aminoacyl-tRNA]$_{eq}$ (△). In all cases, the value at [*threo*-4-hydroxy-L-lysine]=0.5mM is defined as 1.

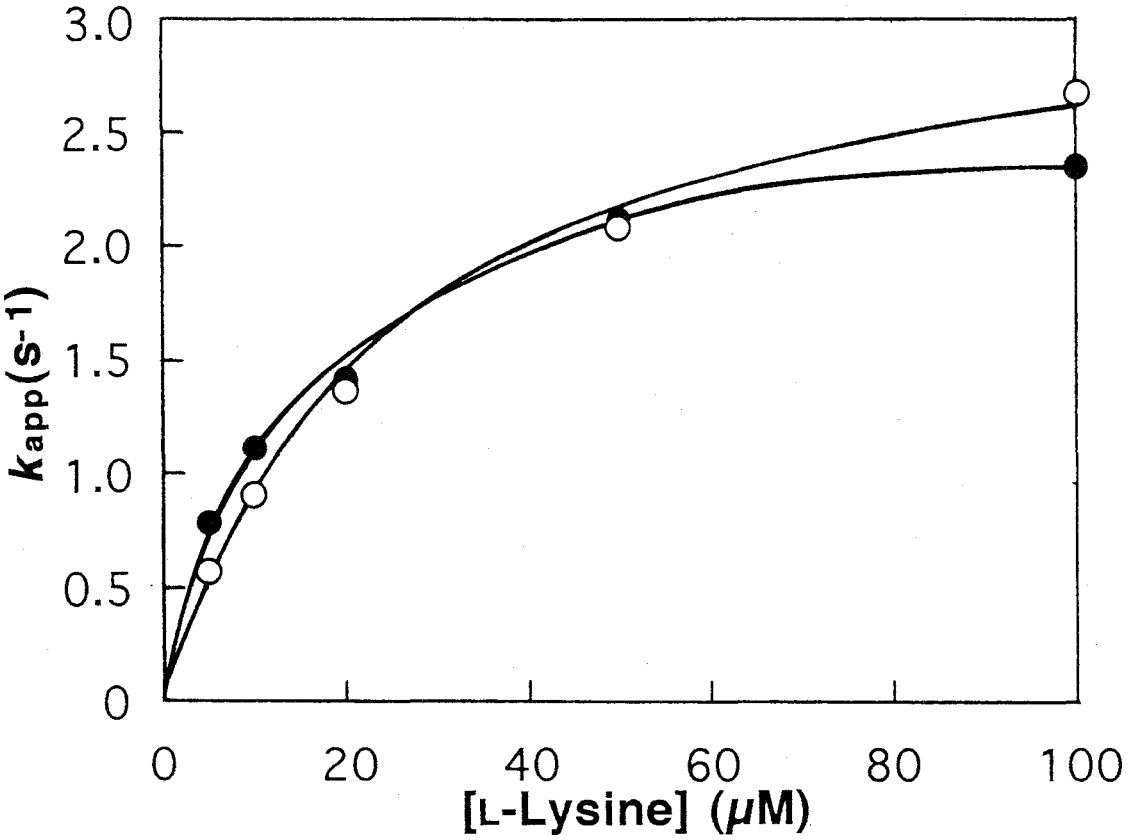

Figure 10

Comparison of the aminoacylation reaction with *E. coli* tRNA with that with *E. coli* $tRNA^{Lys}$

$[E]_0$=0.5nM, 100mM Tris-HCl buffer (pH 8.0), 10mM $MgCl_2$, 1mM ATP, 100μM ^{3}H-L-lysine (40mCi/mmol), and either of $20A_{260}$ units of *E. coli* tRNA (○) or $0.35A_{260}$ units of *E. coli* $tRNA^{Lys}$ (●), at 37°C. The solid lines with *E. coli* tRNA (○) and *E. coli* $tRNA^{Lys}$ (●) are the theoretical curves drawn according to an equation of Michaelis-Menten with K_m=23.5±1.5μM and k_{cat} =2.29±0.07s^{-1} and with K_m=14.1±3.0μM and k_{cat} =1.98±0.16s^{-1}, respectively.

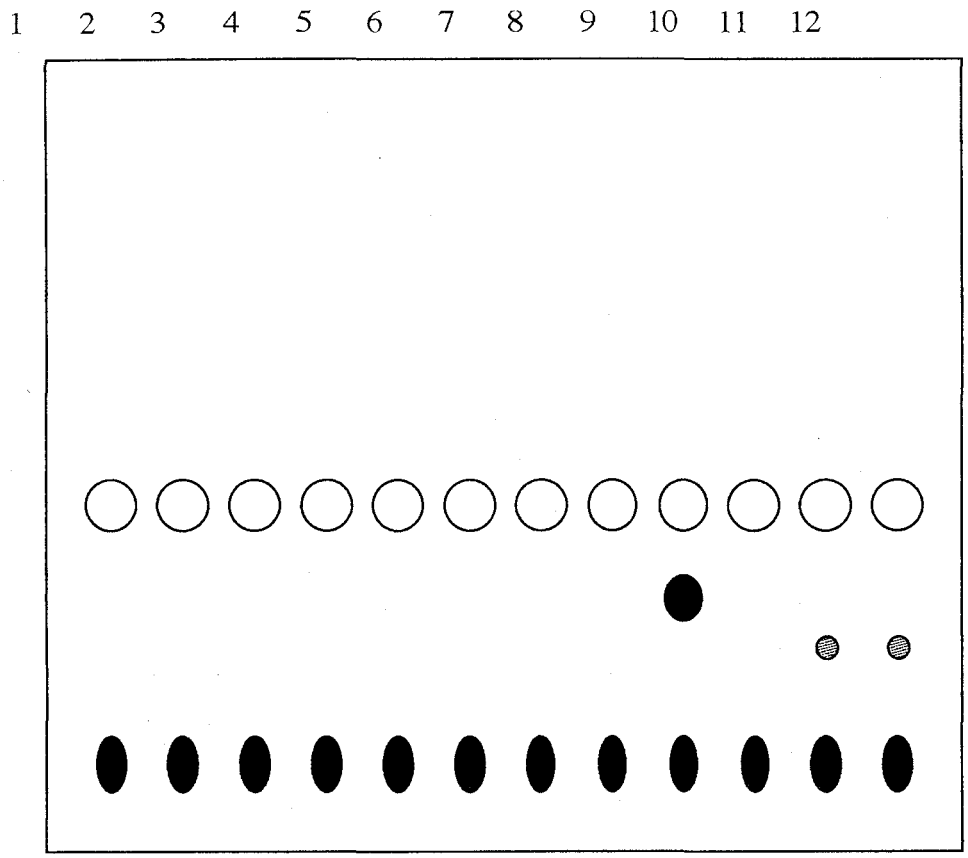

Figure 11
TLC analysis of the product catalyzed by LysRS with either L-lysine or its analogues
The reaction mixture was 100mM Tris-HCl buffer (pH 8.0), 10mM $MgCl_2$, 100nM LysRS, 1mM ATP, 20mM either L-lysine or its analogues , and 36 A_{260} units of *E. coli* tRNA. After the incubation at 37°C for 6 hours, the reaction mixture was spotted to silicagel plate, developed with n-buthanol : acetic acid : water, 4 : 1 : 1, dried, and colored by ninhydrin reaction. Lanes 1, 2, and 3 are the case with L-lysine; lanes 4, 5, and 6, SAEC; lanes 7, 8, and 9, 5-hydroxylysine; lanes 10, 11, and 12, L-ornithine; lanes 13, no L-lysine analogues. Lanes 3, 6, 9, and 12, in the presence of amino acid, ATP, tRNA; lanes 2, 5, 8, and 11, without tRNA; lanes 1, 4, 7, and 10, without ATP and tRNA.

Chapter 5
The Effect of Sodium Chloride on the Aminoacylation Reaction

An aminoacyl-tRNA synthetase (abbreviated to ARS) catalyzes the following reaction *(1)*;

$$AA + ATP + tRNA \rightleftharpoons AA\text{-}tRNA + AMP + PPi \qquad (1)$$

where AA denotes an amino acid. ARSs catalyze this aminoacylation reaction very accurately, which warrants the relations between genetic codes and amino acid. Each ARS recognizes a specific amino acid and cognate tRNAs in aminoacylation reaction. Explanation of this accuracy will requires the study of the recognition mechanism of ARS for cognate tRNA. One approach is the establishment of "tRNA identity", the features of a tRNA molecule making it recognizable to one ARS and preventing to the others *(2)*. These results imply that several nucleotides on each tRNA are major identity elements. The other is the elucidation of the functionally important structure of tRNA. Though the solution structures of various tRNAs were similar to the crystal structure of yeast $tRNA^{Phe}$ *(3~5)*, there were several reports that the presence of salt diminished the rate of aminoacylation reaction *(6, 7)* and the amount of aminoacyl-tRNA in an apparent equilibrium state *(7, 8)*. Some of them suggested the possibility of the conformational changes in the tertiary structure of tRNA *(7, 8)*. It was also suggested that tRNA could assume different conformational states under the near-physiological solution conditions, for example, by changing salt-concentration, pH, and Mg^{2+} concentration *(9)*. The changes, however, were not related to amino acid acceptance activity of tRNA. In order to elucidate a functionally important tertiary structure, it is indispensable to

investigate the relationship between the change of the tertiary structure and the amino acid acceptance activity.

For this purpose, we noted the diminution of the final level of aminoacyl-tRNA in the aminoacylation reaction that was reported previously ***(7, 8)*** and tried to investigate a salt-dependent conformational change of tRNA with a guidance of amino acid acceptance activity. In this study, we considered $K_{eq \cdot tRNA}$, an equilibrium constant between active tRNA and inactive tRNA, or $[tRNA_A]/[tRNA_I]$ and K_{eq}, an equilibrium constant for the reaction Lys + ATP + tRNA $\rightleftharpoons$ Lys-tRNA +AMP +PPi at different sodium chloride concentrations by use of lysyl-tRNA synthetase from *Bacillus stearothermophilus* (abbreviated to *B.s.* LysRS; L-lysine:tRNA ligase (AMP forming); EC6.1.1.6) and *E. coli* tRNA.

MATERIALS AND METHODS

Enzymes: *B.s.* LysRS was purified from *B. stearothermophilus* according to the methods described previously ***(10)***. The enzyme is a homodimer of which the molecular weight of the subunit is 57,700. The enzyme concentration was determined with the molar absorption coefficient ,ε at 280nm, 71,600 $M^{-1}cm^{-1}$ at pH 8.0.

Others: *E. coli* tRNA mixture was purified accordingly to the method described previously ***(10)***. L-[4,5-^{3}H] lysine was the product of NEN Research Products; L-lysine (dihydrochloride) and sodium chloride, of Wako Pure Chemical Industries; ATP (disodium salt), of Sigma Chemical Co.; glass microfiber filter (GF/C), of Whatman.

Enzyme activity assay: Enzyme activities of the aminoacylation reaction and the ATP-PPi exchange reaction were measured

according to the method described previously ***(10)*** unless otherwise noted.

RESULTS

The effect of sodium chloride on the initial velocities in two enzyme activity assays: The initial velocities of the aminoacylation reaction and the ATP-PPi exchange reaction were affected by the sodium chloride concentration (**Fig. 1**). The aminoacylation activity was inhibited larger than the ATP-PPi exchange reaction. In the presence of 1 (M) sodium chloride, we could not detect the aminoacylation activity but the ATP-PPi exchange activity.

Final level of lysyl-tRNA in an apparent equilibrium state: **Figure 2** shows that the final level of lysyl-tRNA in an apparent equilibrium state of the aminoacylation reaction did not depend on the enzyme concentration. The final level of lysyl-tRNA, however, decreased as the concentration of sodium chloride increased (**Fig. 3**).

Enzyme activity in an apparent equilibrium state: We could detect an increase of lysyl-tRNA up to 0.6 (M) sodium chloride when the additional reaction mixture containing tRNA was added, while we could not when that containing none of tRNA was added (**Fig. 4**). These indicate that up to 0.6 (M) sodium chloride, *B.s.* LysRS remained still active in an apparent equilibrium state.

Accordance of the final level of lysyl-tRNA prepared by different processes: **Figure 5** shows that the final level of lysyl-tRNA once formed at 0M sodium chloride was decreased by the addition of sodium chloride, resulting in an agreement with that of formed initially at the same concentration of sodium chloride, 0.4

(M). It indicates that it is regarded as reversible the effect of sodium chloride on the final level of lysyl-tRNA.

Shift of the equilibrium of aminoacylation reaction by changing ATP concentration: **Figure 6** shows that the final level of lysyl-tRNA decreased as the concentration of sodium chloride increased but increased as the ATP concentration increased at 0~0.6 (M)ATP.

DISCUSSION

Smith *(7)* reported that a L-leucine dependent ATP-PPi exchange activity is not completely inhibited, even by very high salt concentration, while in the presence of sufficiently high salt concentrations, tRNA is entirely unable to accept amino acids. It agrees our result of **Fig. 1**. However, the pattern of decrease in the leucine dependent ATP-PPi exchange activity is different from that in the L-lysine dependent ones.

On the basis of results of **Figs. 2~5**, we conclude that in the presence of 0~0.6 (M) sodium chloride, aminoacylation reaction catalyzed by *B.s.* LysRS attains equilibrium under our condition. In order to evaluate the effect of sodium chloride on the structure of tRNA, I investigated the effects of sodium chloride on equilibrium's of both the conformational change reaction of tRNA, $tRNA_A$ ("active tRNA") $\rightleftharpoons$ $tRNA_I$ ("inactive tRNA") and the aminoacylation reaction Lys + ATP + $tRNA_A$ $\rightleftharpoons$ Lys-$tRNA_A$ +AMP +PPi as shown in Scheme I, with the guidance of L-lysine acceptance activity in the aminoacylation reaction. $tRNA_A$ and $tRNA_I$ indicate active tRNA that can be charged with L-lysine by *B.s.* LysRS and inactive tRNA that can not, respectively. $K_{eq \cdot tRNA \cdot x}$

and $K_{eq\bullet x}$ denote an equilibrium constant at x (M) sodium chloride for the conformational change reaction of tRNA and for the aminoacylation reaction.

At 0 (M) sodium chloride in **Fig. 6**

$$1/[ATP]_0=K_{eq\bullet 0}[Lys]_0([tRNA]_0-[Lys\text{-}tRNA_A])/[AMP]_0[PPi]_0[Lys\text{-}tRNA_A]$$
$$=(K_{eq\bullet 0}[Lys]_0/[AMP]_0[PPi]_0)([tRNA]_0/[Lys\text{-}tRNA_A]-1)$$
$$=A[tRNA]_0/[Lys\text{-}tRNA_A]-A \quad (6)$$

Here,

$$A=K_{eq\bullet 0}[Lys]_0/[AMP]_0[PPi]_0$$

(see Appendix 4A)

According to Equation (6), we can obtain **Fig. 7** (- ● -), a replot of the result at 0 (M) sodium chloride in **Fig. 6** and theoretical line by at least squares method. From the intercept of **Fig. 7** (- ● -), we can calculate $K_{eq\bullet 0}$ with Equation (7). With estimated value of $K_{eq\bullet 0}$, 1.95±0.16, from the slope of **Fig. 7** (- ● -), we can also calculate $[tRNA]_0$ with Equation (6) and (7). Estimated value of $[tRNA]_0$ is 5.68±0.14μM, which indicates that 7.24% of used unfractionated tRNA has a L-lysine acceptance activity by calculating with 1 A_{260} unit = 50 (μg/ml) tRNA.

At x (M) sodium chloride in **Fig. 6**,

$$1/[ATP]_0=B[tRNA]_0K_{eq\bullet A/0\bullet x}(1/[Lys\text{-}tRNA_A])-B \quad (11)$$

Here,

$$B=[Lys]_0K_{eq\bullet x}/[AMP]_0[PPi]_0$$

(see Appendix 4B)

According to Equation (11), we can obtain **Fig. 7** (- ○ -, - ▲ -, - △ -, and - ■ -), replots of the results at 0.2~0.6 (M) sodium chloride in **Fig. 6** and theoretical lines by at least squares method. From the intercept of **Fig. 7** (- ○ -, - ▲ -, - △ -, and - ■ -), we can calculate $K_{eq\bullet x}$

with Equation (12). With estimated value of $K_{eq\bullet X}$ and $[tRNA]_0$=5.68μM, from the slope of **Fig. 7** (-○-, -▲-, -△-, and -■-), we can also calculate $K_{eq\bullet A/0\bullet X}$ with Equation (11) and (12). Estimated values of $K_{eq\bullet X}$ and $K_{eq\bullet A/0\bullet X}$ at 0.2, 0.3, 0.4, 0.6 (M) sodium chloride are 1.75±0.24 and 0.769±0.028, 2.64±0.45 and 0.508±0.031, 2.00±0.26 and 0.384±0.015, and 1.44±0.23 and 0.109±0.010, respectively (**Fig. 8**).

In our condition, estimated $K_{eq\bullet X}$s were larger than the $K_{eq\bullet X}$s previously obtained, 0.37 ***(11)*** and 0.32 ***(12)***. On the other hand, **Figure 8** shows that $K_{eq\bullet A/0\bullet X}$ changed significantly where $tRNA_A$ decreased as the concentration of sodium chloride increased. The concentration of sodium chloride where $K_{eq\bullet A/0\bullet X}$ equals 0.5 is about 0.3~0.4 (M) (**Fig. 8**). It agrees with the results of 0.35 (M) in **Fig. 3** and 0.3 (M) and 0.4 (M) in **Fig. 6**. Accordingly, it is considered that the diminution of the final level of aminoacyl-tRNA by the presence of sodium chloride is due to the salt-dependent conformational change of tRNA to inactive form. This can explain the finding that in the presence of 1 (M) sodium chloride, we could not detect the aminoacylation activity but the ATP-PPi exchange activity. The fact that $K_{eq\bullet X}$ did not change so much suggests that the decrease in the initial velocity of aminoacylation as would be expected because of the increase of K_m for tRNA by the addition of sodium chloride is proportional to the decrease in that of deacylation.

Many detailed studies on the analysis of the solution structure of the tRNA were conducted intensively with a view toward the elucidation of the solution structure and identification of important structure-function relationships. Reported studies on the structure of the tRNA may be divided into two groups. One is a group

investigating the structural changes between aminoacyl-tRNA and free tRNA, which must be recognized for discriminating aminoacyl-tRNA and free tRNA in a number of biological synthesis. Results from these, however, were in disagreement (see the references of *(13)*). Potts *et al.* suggested the possibility that the apparent contradictory results were related to differences in solution conditions, individual tRNAs, and physical properties being evaluated *(13)* and that tRNA conformational changes can occur with aminoacylation but may be dependent upon solution conditions, particularly upon the effects Mg^{2+} *(13~16)*. The other is a group investigating the structural changes in free tRNA, which must be recognized by aminoacyl-tRNA synthetase on aminoacylation *(17~37)*. The absence of Mg^{2+} greatly destabilized the tertiary structure of tRNA *(20, 22, 28~32)*. Cole *et al. (9, 30)* showed the general conformation equilibrium of tRNA when the Na^{+} concentration is varied in the absence of Mg^{2+}. Since the electrostatic free energy of native tRNA increases as lowering ionic strength, tRNA probably adopts a non-native conformation, the extended form. Under the condition in the aminoacylation reaction, tRNA is considered to be intact. As raising ionic strength, however, tRNA adopts a non-native conformation, the compact form. It was also suggested that at high salt concentration and medium temperature, the tertiary structure of tRNA is hypothesized to be cloverleaf or close variant *(30)*.

Olson *et al.* investigated the conformational change in *E. coli* bulk tRNA and yeast $tRNA^{Phe}$ at different ionic strength in the presence of either 1mM Mg^{2+} or 10mM Mg^{2+} using the technique of a laser light scattering *(24)* and indicated as follows: (1) the structure of tRNA is an extended one in low ionic strength but a

compact one in high ionic strength; (2) readily reversible association of bulk tRNA occurred at 10mM Mg^{2+} at high ionic strength; (3) a more compact structure exists in the transition from the extended structure to the compact structure only in the case at 1mM Mg^{2+}; (4) calculating average charge at different concentrations of sodium chloride, there are ten electrons per tRNA molecule in 1mM Mg^{2+} and eight electrons per tRNA molecule in 10mM Mg^{2+}, and the net charge is clearly a function of magnesium concentration. Further, Rhee *et al.* investigated the effects of Mg^{2+} and ionic strength on the solution structures of seven tRNA species using the same technique, and showed that the responses of all except $tRNA^{fMet}$ were qualitatively similar to each other and to that of unfractionated tRNA though significant quantitative differences were detected ***(25)***. Noninhibitor tRNAs ***(25)*** and bulk tRNA ***(24)*** underwent similar salt-dependent conformational change in diffusivity where a transition to faster-diffusing conformer is observed as the ionic strength increases at 1mM Mg^{2+}. These results indicate that different tRNAs undergo the same transitions in response to changes in Mg^{2+} concentration and ionic strength. In our experiments, it seems likely that this salt-dependent conformational change occurs, resulting in the decrease in $K_{eq \bullet tRNA \bullet x}$.

Olson *et al.* ***(24)*** also reported the possibility of a readily reversible association of monomeric tRNAs in the experiment with bulk tRNA at not 1mM but 10mM Mg^{2+}, while Rhee *et al.* ***(25)*** reported that little or no association occurred at 10mM Mg^{2+} in the experiment with the purified tRNA. The relationship between the decrease in $K_{eq \bullet tRNA \bullet x}$ and the association of bulk tRNA was remains unknown.

Peterkovsky *et al.* reported that the homologous reactions of yeast LeuRS with yeast $tRNA^{Leu}$ or *E. coli* LeuRS with *E. coli* $tRNA^{Leu}$ were almost insensitive to the presence of 0.12 (M) sodium chloride, but that in the corresponding heterogeneous reactions, the initial velocity of the aminoacylation was depressed by half ***(8)***. If weaker binding of tRNA to the enzyme in the heterogeneous reactions is the reason why the heterogeneous ones are easily affected by the presence of salt, it may be applied to our system using *E. coli* tRNA and *B.s.* LysRS.

In this study, we have studied the effect of sodium chloride on the L-lysine acceptance activity of tRNA statically and proposed that the decrease of it is mainly due to the conformational change of tRNA not but to the shift of the equilibrium in the aminoacylation reaction. For elucidation of a functionally important tertiary structure, it will be needed to find the conformational change of tRNA that corresponds to the change of the amino acid acceptance activity.

REFERENCES

1) Berg, P. (1961) Specificity in protein synthesis. *Annu. Rev. Biochem.* **30**, 293-324

2) Normanly, J. and Abelson, J. (1989) tRNA identity. *Annu. Rev. Biochem.* **58**, 1029-1049

3) Jack, A., Ladner, J. E., and Klug, A. (1976) Crystallographic refinement of yeast phenylalanine transfer RNA at 2.5Å resolution. *J. Mol. Biol.* **108**, 619-649

4) Clark, B. F. C. (1977) Correlation of biological activities with structural features of transfer RNA. *Progress in nucleic acid research and molecular biology*, **20**, 1-19

5) Rich, A. and RajBhandary, U. L. (1976) Transfer RNA: Molecular structure, sequence, and properties. *Annu. Rev. Biochem.* **45**, 805-852

6) Loftfield, R. B. and Einger, E. A. (1967) Ionic strength effects in the aminoacylation of valine transfer ribonucleic acid. *J. Biol. Chem.* **242**, 5355-5359

7) Smith, D. W. E. The effect of salt solutions on the acceptance of amino acids by transfer ribonucleic acid. (1969) **244**, 896-901

8) Peterkofsky, A., Gee, S. J., and Jesensky, C. (1966) The effect of sodium chloride on esterification of leucine to transfer ribonucleic acid by heterologous aminoacyl transfer ribonucleic acid synthetases. *Biochemistry* **5**, 2789-2799

9) Crothers, D. M. (1979) *Trasfer RNA: Structure, Properties and Recognition* (Abelson, J., Schimmel, P., and Söll, D., eds.) pp163-170, Cold Spring Harbor Laboratory, Cold Spring Harbor, NY.

10) Takita et al.

11) Leahy, J., Glassman, E., and Schweet, R. S. (1960) Incorporation of amino acids into ribonucleic acid. *J. Biol. Chem.* **235**, 3209-3212

12) Berg, P., Bergmann, F. H., Ofengand, E. J., and Dieckmann, M. (1961) The enzymic synthesis of amino acyl derivatives of ribonucleic acid. *J. Biol. Chem.* **236**, 1726-1734

13) Potts, R. O., Ford, N. C. Jr., and Fournier, M. J. (1981)

Changes in the solution structure of yeast phenylalanine transfer ribonucleic acid associated with aminoacylation and magnesium binding. *Biochemistry*, **20**, 1653-1659

14) Potts, R. O., Fournier, M. J., and Ford, N. C. Jr. (1977) Effect of aminoacylation on the conformation of yeast phenylalanine tRNA. *Nature*, **268**, 563-564

15) Potts, R. O., Wang, C. C., Fritzinger, D. C., Ford, N. C. Jr., and Fournier, M. J. (1979) *Trasfer RNA: Structure, Properties and Recognition* (Abelson, J., Schimmel, P., and Söll, D., Eds.) pp207-220, Cold Spring Harbor Laboratory, Cold Spring Harbor, NY.

16) Sprinzl, M. and Cramer, F. (1979) The-C-C-A end of tRNA and its role in protein biosynthesis. *Progress in nucleic acid research and molecular biology*, **22**, 1-69

17) Riesner, D. and Buenemann, H. (1973) A stopped-flow apparatus with light-scattering detection and its application to biochemical reactions. *Proc. Natl. Acad. Sci. USA*, **70**, 890-893

18) Bina-Stein, M. and Crothers, D. M. (1974) Conformational changes of transfer ribonucleic acid. The pH phase diagram under acidic conditions. *Biochemistry*, **13**, 2771-2775

19) Stein, A. and Crothers, D. M. (1976) Equilibrium binding of magnesium (II) by *Escherichia coli* $tRNA^{fMet}$. *Biochemistry*, **15**, 157-160

20) Stein, A. and Crothers, D. M. (1976) Conformational changes of transfer RNA. The role of magnesium (II). *Biochemistry*, **15**, 160-168

21) Filimonov, V. V. and Privalov, P. L. (1976) Calorimetric investigation on thermal stability of $tRNA^{Ile}$ (yeast) and $tRNA^{Ser}$ (yeast). *Eur. J. Biochem.* **70**, 25-31

22) Hinz, H. J., Filimonov, V. V., and Privalov, P. L. (1977) Calorimetric studies on melting of $tRNA^{Phe}$ (yeast). *Eur. J. Biochem.* **72**, 79-86

23) Rhodes, D. (1977) Initial stages of the thermal unfolding of yeast phenylalanine transfer RNA as studied by chemical modification: the effect of magnesium. *Eur. J. Biochem.* **81**, 91-101

24) Olson, T., Fournier, M. J., Langley, K. H., and Ford, N. C. Jr. (1976) Detection of a major conformational change in transfer ribonucleic acid by laser light scattering. *J. Mol. Biol.* **102**, 193-203

25) Rhee, K. W., Potts, R. O., Wang, C. C., Fournier, M. J., and Ford, N. C. Jr. (1981) Effects of magnesium and ionic strength on the diffusion and charge properties of several single tRNA species. *Nucleic Acid Res.* **9**, 2411-2420

26) Chu, W. C., Feiz, V., Derrick, W. B., and Horowitz. J. (1992) Fluorine-19 nuclear magnetic resonance as a probe of the solution structure of mutants of 5-fluorouracil-substituted *Escherichia coli* valine tRNA. *J. Mol. Biol.* **227**, 1164-1172

27) Chu, W. C., Kintanar, A., Horowitz. J. (1992) Correlations between Fluorine-19 nuclear magnetic resonance chemical shift and the secondary and tertiary structure of 5-fluorouracil-substituted tRNA. *J. Mol. Biol.*, **227**, 1173-1181

28) Römer, R. and Hach, R. (1975) tRNA conformation and Magnesium binding. A study of yeast phenylalanine-specific

tRNA by a fluorescent indicator and differential melting curves. *Eur. J. Biochem.* **55**, 271-284

29) Jack, A., Ladner, J. E., Brown, R. S., and Klug, A. (1977) A crystallographic study of metal-binding to yeast phenylalanine transfer RNA. *J. Mol. Biol.* **111**, 315-328

30) Cole, P. E., Yang, S. K., and Crothers, D. M. (1972) Conformational changes of transfer ribonucleic acid. Equilibrium phase diagrams. *Biochemistry*, **11**, 4358-4368

31) Rialdi, G., Levy, J., and Biltonen, R. (1972) Thermodynamic studies of transfer ribonucleic acids. I. Magnesium binding to yeast phenylalanine transfer ribonucleic acid. *Biochemistry*, **11**, 2472-2479

32) Lynch, D. C. and Schimmel, P. R. (1974) Cooperative binding of magnesium to transfer ribonucleic acid studied by a fluorescent probe. *Biochemistry*, **13**, 1841-1852

33) Bina-Stein, M. and Stein A. (1976) Allosteric interpretation of Mg^{2+} binding to the denaturable *Escherichia coli* $tRNA^{Glu2}$. *Biochemistry*, **15**, 3912-3917

34) Jones, C. R. and Kearns, D. R. (1974) Investigation of the structure of yeast $tRNA^{Phe}$ by nuclear magnetic resonance: paramagnetic rare earth ion probes of structure. *Proc. Natl. Acad. Sci. USA.* **71**, 4237-4240

35) Danchin, A. and Guéron, M. (1970) Cooperative binding of manganese (II) to transfer RNA. *Eur. J. Biochem.* **16**, 532-536

36) Karpel, R. L., Miller, N. S., Lesk, A. M., and Fresco, J. R. (1975) Stabilization of the native tertiary structure of yeast $tRNA^{Leu_3}$ by cationic metal complexes. *J. Mol. Biol.* **97**, 519-532

37) Wolfson, J. M. and Kearns, D. R. (1975) Europium as a fluorescent probe of transfer RNA structure. *Biochemistry*, **14**, 1436-1444

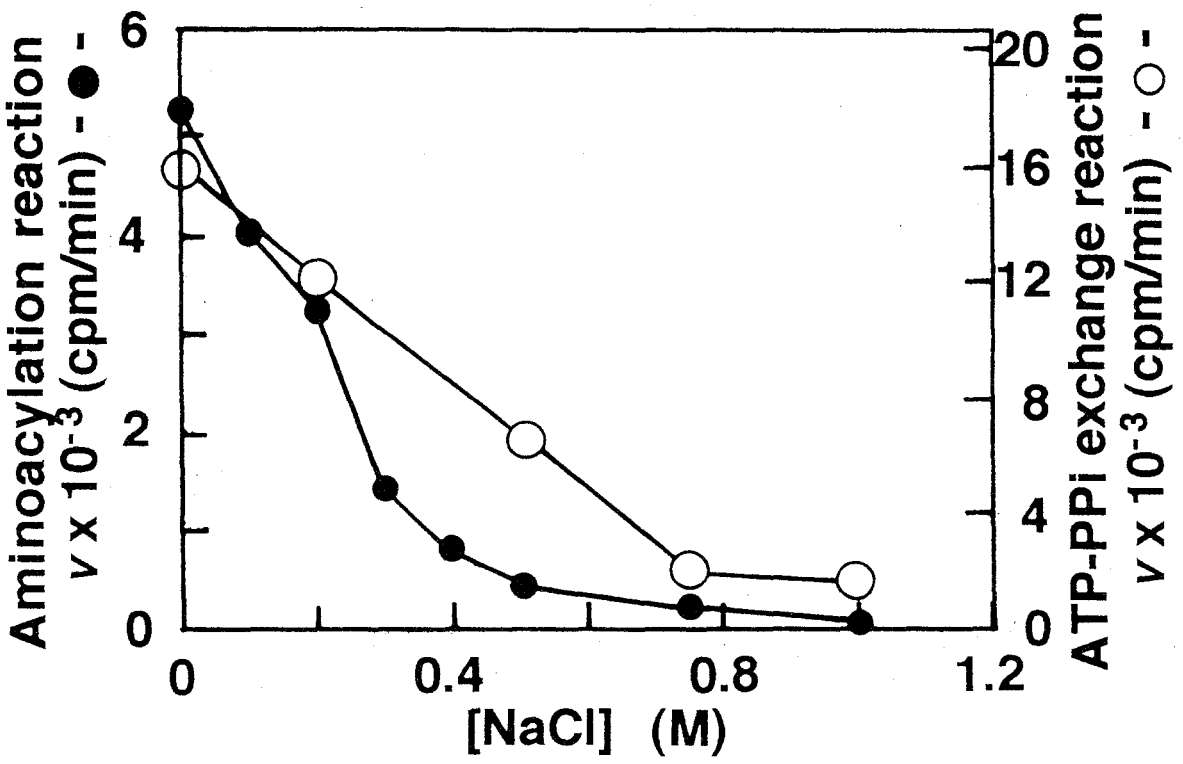

Figure 1

The effect of sodium chloride on the initial velocities in two enzyme activity assay

Aminoacylation reaction (●) and ATP-PPi exchange reaction (○) were measured at 37°C, pH 8.0 at different sodium chloride concentrations.

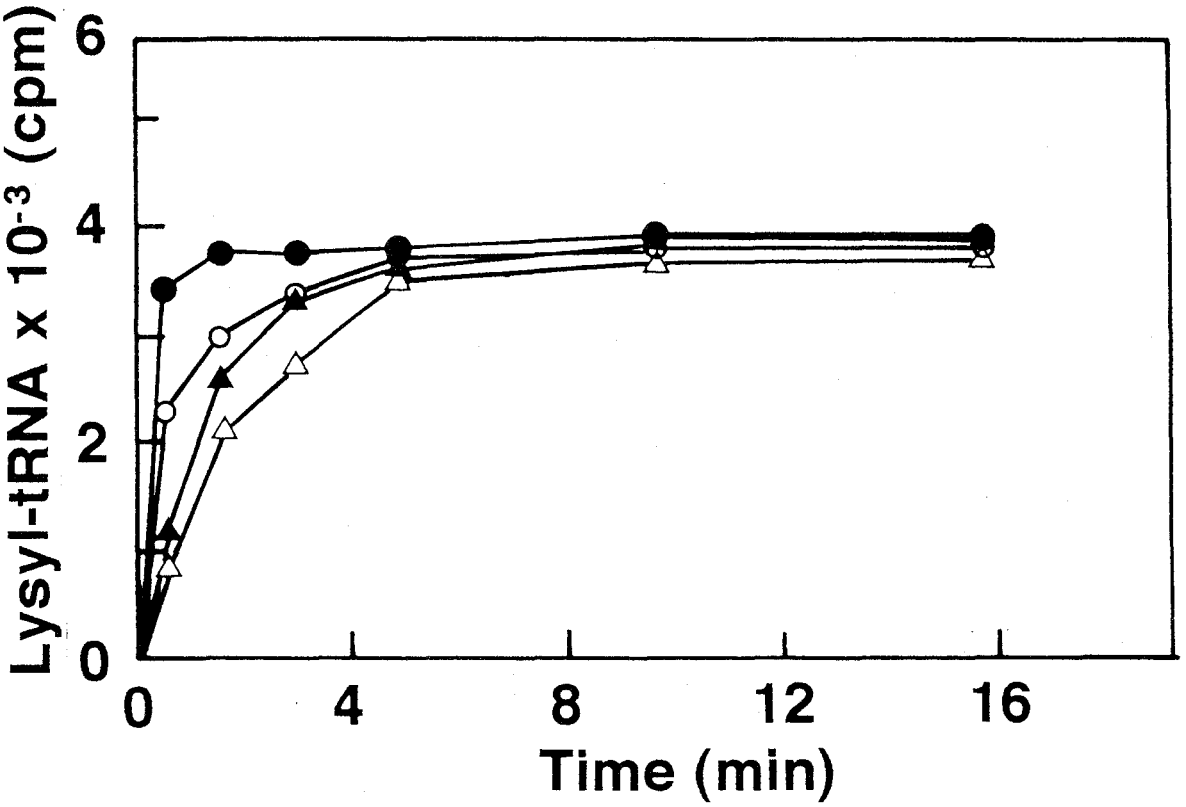

Figure 2

Final levels of lysyl-tRNA in an apparent equilibrium state by different concentrations of *B.s.* LysRS

The standard reaction mixture contained in 0.5ml: 100mM Tris-HCl buffer (pH 8.0), 10mM $MgCl_2$, 50μM L-lysine, 1mM ATP, and 11A_{260} units of *E. coli* tRNA. The reactions were carried out at 37°C by the addition of different concentrations of *B.s.* LysRS; 6.2nM (-●-), 3.1nM (-○-), 1.5nM (-▲-), and 0.77nM (-△-).

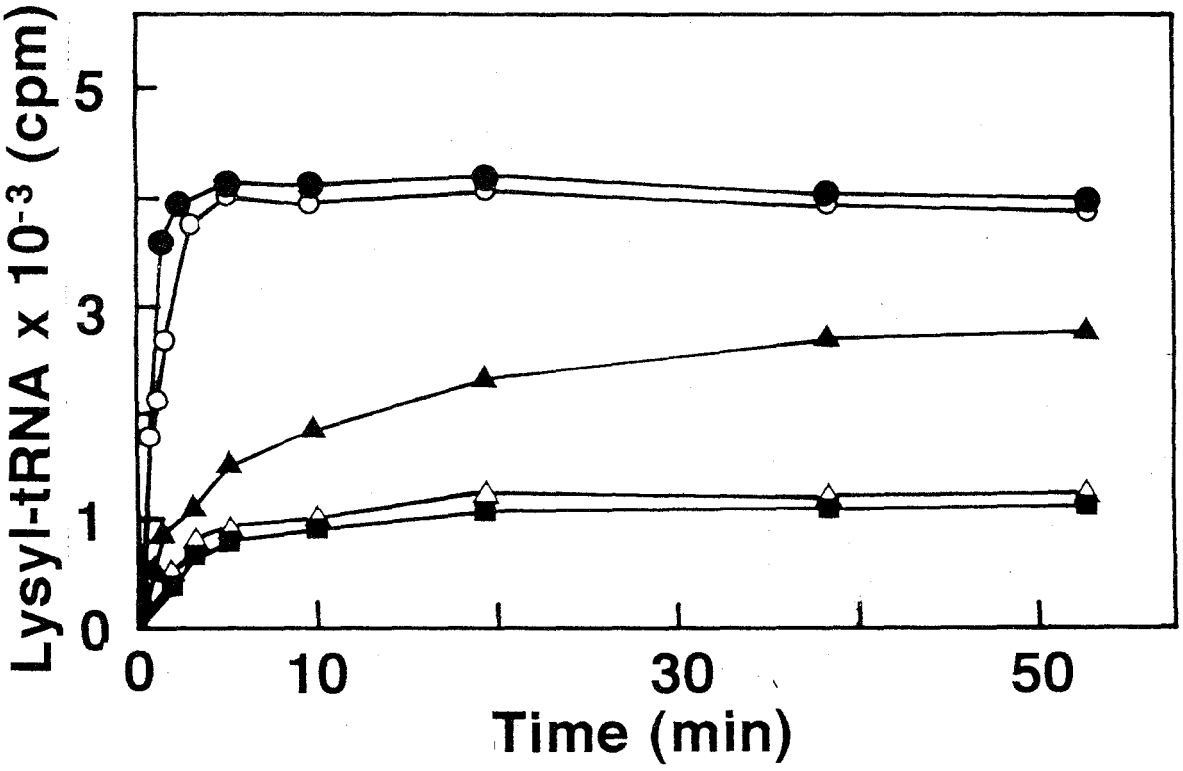

Figure 3

Final levels of lysyl-tRNA in an apparent equilibrium state at different concentrations of sodium chloride

The reaction mixture was the same as in **Fig. 2** except the presence of sodium chloride; 0M (-●-), 0.12M (-○-), 0.36M (-▲-), 0.6M (-△-), and 0.72M (-■-). The reactions were carried out at 37°C by the addition of 3.1nM *B.s.* LysRS

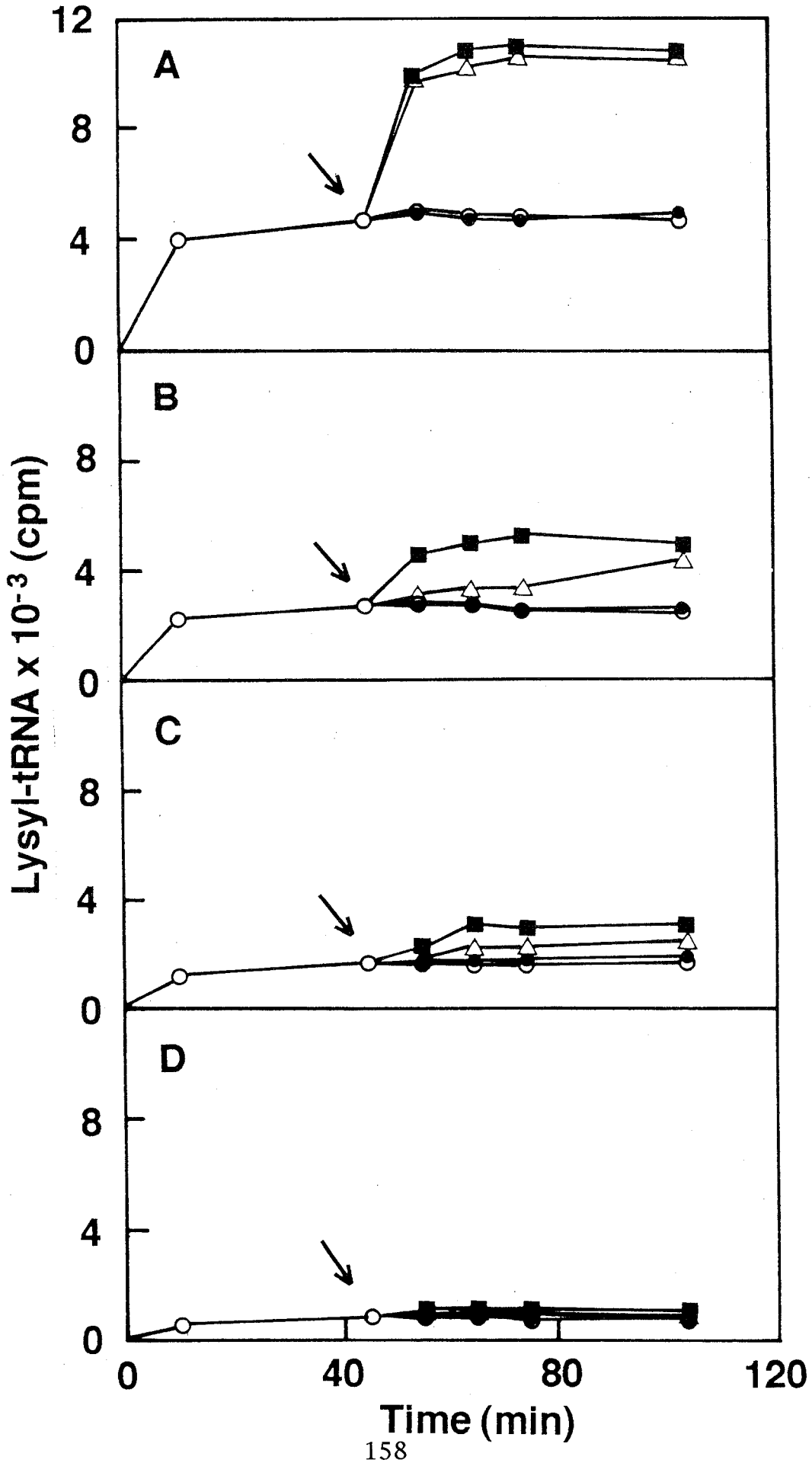
A
B
C
D
12
8
4
0
Lysyl-tRNA x 10-3 (cpm)
0
40
80
120
Time (min)

Figure 4

Enzyme activity in an apparent equilibrium state at different concentrations of sodium chloride

The arrow indicates the addition of the second reaction mixture after the first aminoacylation reaction at 37°C, pH 8.0. The first reaction mixture (0.5ml) was the same as in **Fig. 3** except the presence of sodium chloride; 0M (A), 0.4M (B), 0.6M (C), and 0.8M (D). 0.5ml of second reaction mixture was added to the first one with the concentration of sodium chloride not changed; none (-●-), 3.1nM, 50μM L-lysine, and 1mM ATP(-○-), 50μM L-lysine, 1mM ATP, and 33A_{260} units of *E. coli* tRNA (-△-), and 3.1nM, 50μM L-lysine, 1mM ATP, and 33A_{260} units of *E. coli* tRNA (-■-). After precipitation with 6 volume of 5% trichloroacetic acid, radioactivity of lysyl-tRNA was measured.

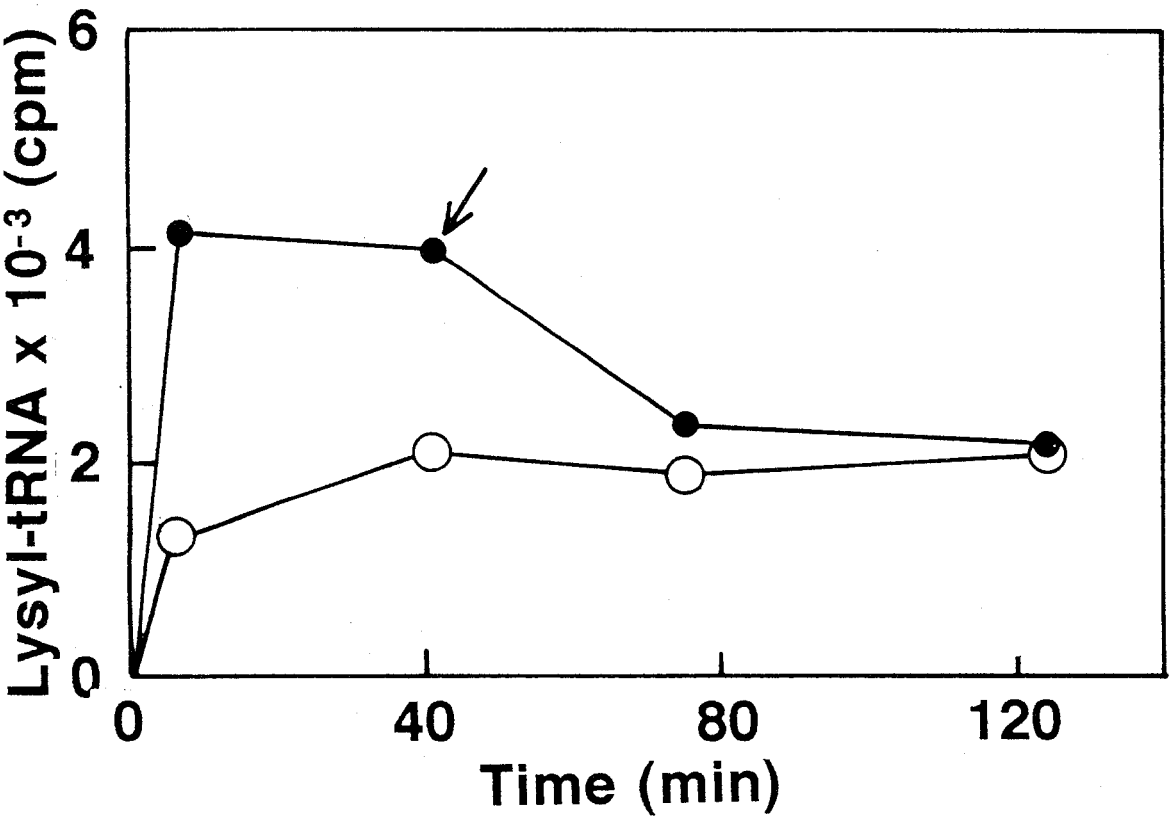

Figure 5

Accordance of the final level of lysyl-tRNA prepared by different processes

The reaction curve (-○-) shows the aminoacylation reaction at 0.4M sodium chloride, 37°C, pH 8.0. Onthe other hand, The reaction curve (-●-) shows the aminoacylation reaction at 0M sodium chloride followed by the addition of sodium chloride, where the arrow indicates the addition of sodium chloride resulting in 0.4 M sodium chloride. The first reaction mixture (0.5ml) was the same as in **Fig. 3** except the concentration of sodium chloride. After precipitation with 6 volume of 5% trichloroacetic acid, radioactivity of lysyl-tRNA was measured.

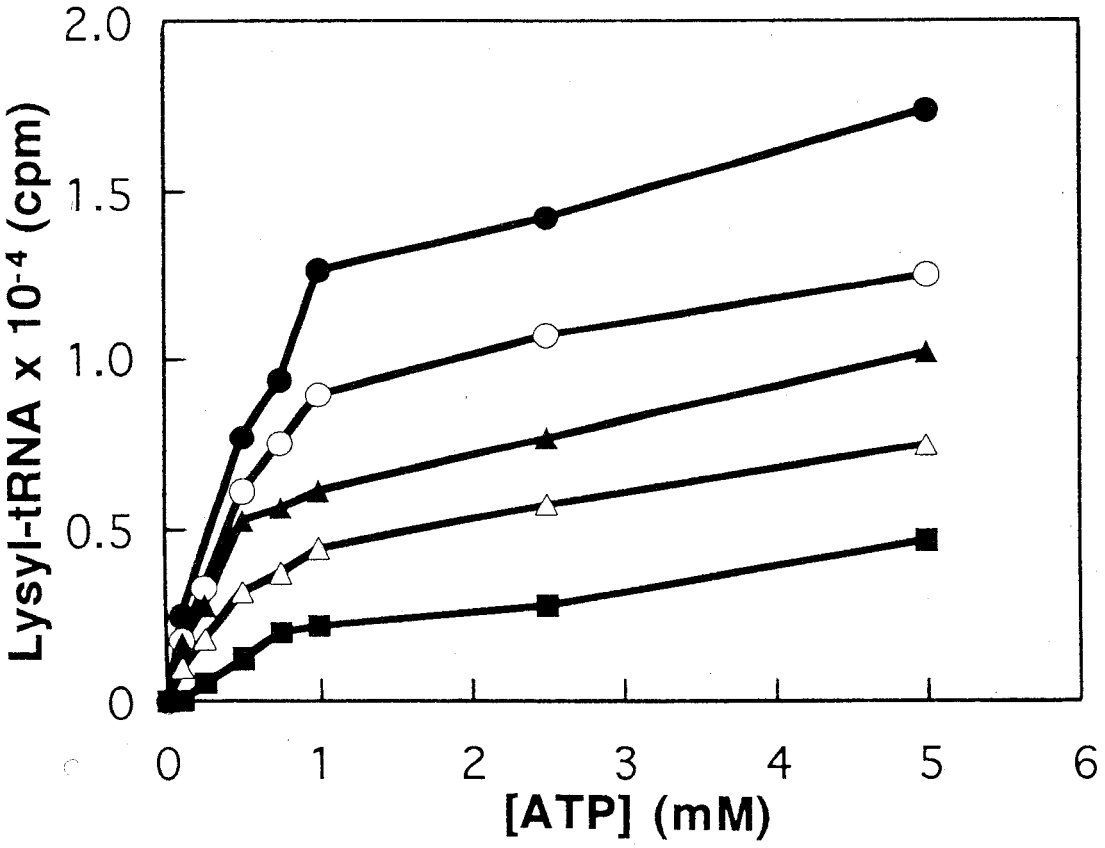

Figure 6

Shift of the equilibrium of aminoacylation reaction by changing ATP concentration

The reaction mixture was all the same except the concentration of sodium chloride; 0M (-●-), 0.2M (-○-), 0.3M (-▲-), 0.4M (-△-), and 0.6M (-■-). The standard reaction mixture contained in 0.5ml: 100mM Tris-HCl buffer (pH 8.0), 10mM $MgCl_2$, 200μM L-lysine (80mCi/mmol), 500μM AMP, 500μM PPi, 33A_{260} units of *E. coli* tRNA, and 0.1~5mM ATP. The reactions were carried out at 37°C by the addition of 3.1nM *B.s.* LysRS. After precipitation with 6 volume of 5% trichloroacetic acid, radioactivity of lysyl-tRNA was measured.

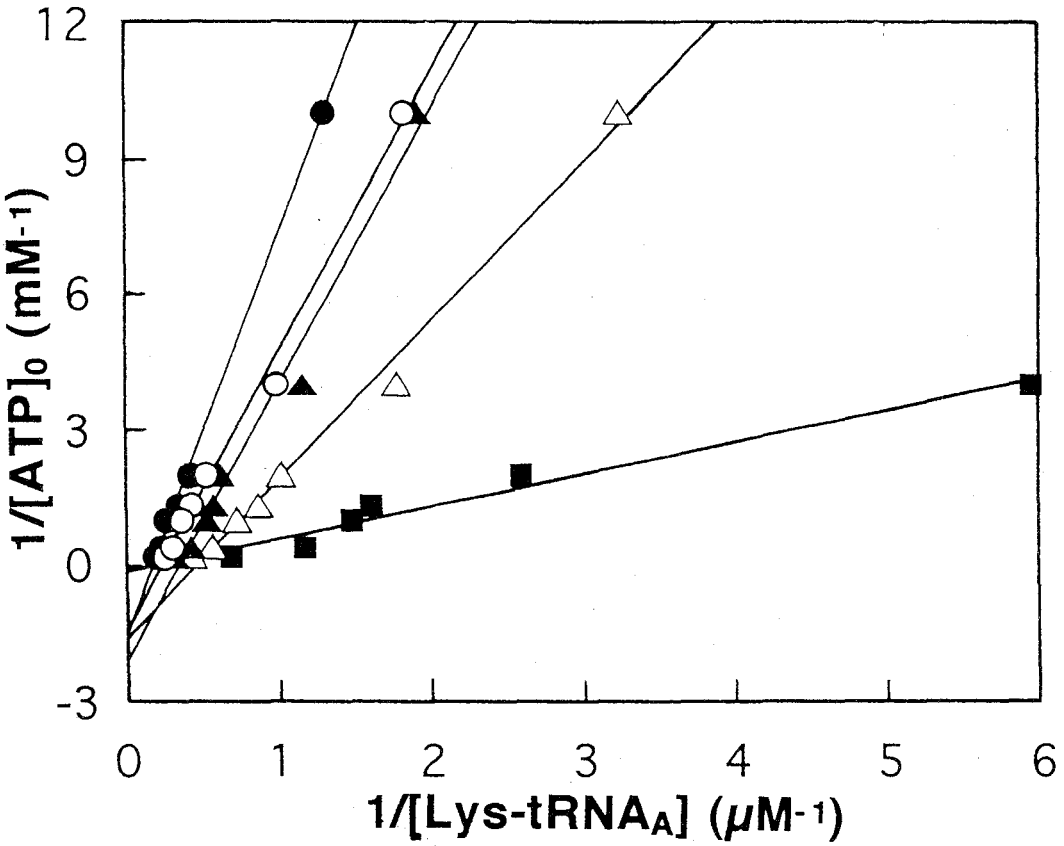

Figure 7

Estimation of $K_{eq \cdot x}$ and $K_{eq \cdot A/0 \cdot x}$

The results of Fig. 6 were reploted according to Equation (6) or (11). The solid lines are the theoretical curves drawn according to at least squares method. The concentration of sodium chloride is as follows; 0M (- ● -), 0.2M (- ○ -), 0.3M (- ▲ -), 0.4M (- △ -), and 0.6M (- ■ -).

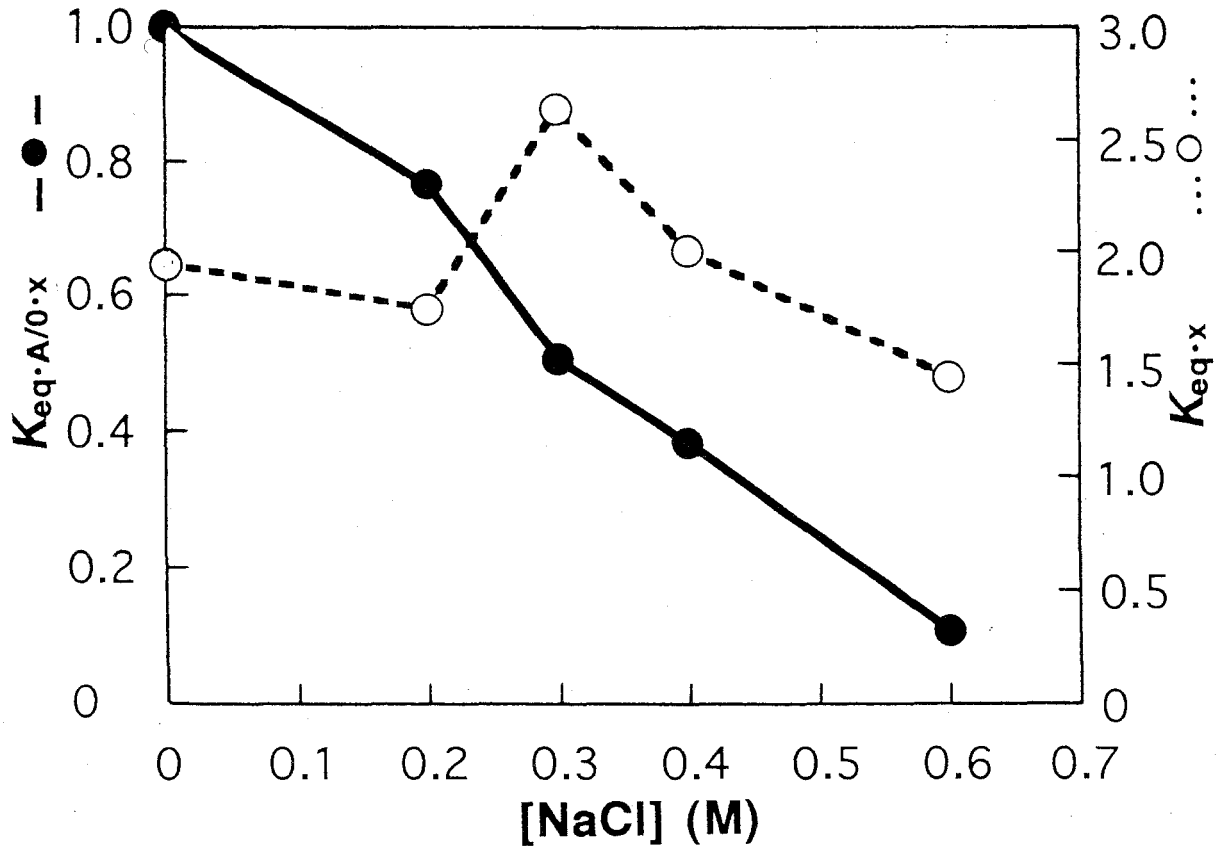

Figure 8

The effect of sodium chloride on $K_{eq\cdot x}$ and $K_{eq\cdot A/0\cdot x}$

Estimated $K_{eq\cdot x}$ (··· ○ ···) and $K_{eq\cdot A/0\cdot x}$ (- ● -) at each concentration of sodium chloride are shown.

Chapter 6
Molecular Cloning, Nucleotide Sequence, and Expression of the Lysyl-tRNA Synthetase Gene

Aminoacylation reaction, the binding of an amino acid to the cognate tRNA is generally catalyzed by an aminoacyl-tRNA synthetase (abbreviated to ARS) according to the following reaction scheme *(1)*.

$$E + AA + ATP \rightleftharpoons E{\bullet}AA{\sim}AMP + PPi \quad (1)$$

$$E{\bullet}AA{\sim}AMP + tRNA \rightleftharpoons E + AMP + AA\text{-}tRNA \quad (2)$$

where AA denotes the amino acid; E, ARS; PPi, inorganic pyrophosphate; and E•AA~AMP, an aminoacyl-adenylate-ARS complex. In order to guarantee the fidelity of translation of the genetic information into the structure of a protein, ARS has a high degree of substrate specificity for each heterogeneous substrate: amino acids, nucleotides, and tRNAs.

Though all ARSs catalyze the aminoacylation reaction and the sizes of tRNAs are similar, ARSs exhibit a wide diversity in subunit size and quarternary structure. For example, in *E. coli*, the subunit sizes range from 303 amino acids for α subunit of GlyRS to 951 amino acids for ValRS and the diversity of quarternary structure involves α, α_2, α_4, and $\alpha_2\beta_2$, and the native molecular weight range from 52,000 for CysRS to 380,000 for AlaRS. Based on the sequence alignment analysis, the twenty ARSs were divided into two classes, Class I and Class II, consisting of ten ARSs each, and this is supported by the three dimensional structure of ARSs revealed by X-ray crystallographic analysis *(2)*.

I have strong interest in elucidating the molecular mechanism for the strict substrate specificity of ARSs. Therefore, we chose lysyl-tRNA synthetase (L-lysine:$tRNA^{Lys}$ ligase (AMP

forming);EC6.1.1.6) (abbreviated to LysRS) from *Bacillus stearothermophilus* as the target for the consideration of the availability of amino acid analogues and the appropriate stability of the enzyme and investigated the mechanism of substrate specificity ***(3, 4)***. The has not been cleared with LysRS of any origin ***(5)***. In order to study more detailed reaction mechanism of LysRS of *Bacillus stearothermophilus* (abbreviated to *B.s.* LysRS), I need to obtain adequate amount of the enzyme and the structural information about it.

In the present study, I tried to isolate the *B.s.* LysRS gene and overexpress the enzyme. Thus far LysRS gene was determined for *E. coli* (*lysS and lysU*) ***(6)***, yeast cytoplasmic ***(7)*** and mitochondrial forms ***(8)***, *Mycoplasma hominis* ***(9)***, *Campylobacter jwjuni* ***(10)***, and *Thermus thermophilus* ***(11)***. Recently, the three dimensional structures of the *E. coli* LysRS (*lysU*-encoded) complexed with L-lysine ***(12)*** and of the *T. thermophilus* LysRS complexed with tRNA ***(13)*** have been determined by X-ray crystallography.

MATERIALS AND METHODS

Enzymes: *B.s.* LysRS was purified from *B. stearothermophilus* according to the methods described previously ***(3)***. The enzyme concentration was determined with the molar absorption coefficient ,ε at 280nm, 71,600 $M^{-1}cm^{-1}$ at pH 8.0. Carboxypeptidase Y was purchased from Oriental Yeast Co. T4 DNA ligase and *Pfu* DNA polymerase were purchased from Stratagene. *Xho* I and *Taq* DNA polymerase were obtained from Boehringer Mannheim and from Pharmacia Biotech. The other restriction endonucleases, Mung Bean Nuclease, and Klenow Fragment were the products of Takara Shuzo Co.

Plasmids, helper Phage, and λ phage: The plasmid pCR II was obtained from Invitrogen for cloning PCR products. λDASH II, λZAP II, ExAssist Helper Phage, VCSM13 Helper Phage were purchased from Stratagene. The expression vectors, pTrc 99A and pKK223-3 were the products of Pharmacia Biotech; pET 11a, of Novagen.

Bacterial strains and growth media: pCR II was transformed to *E. coli* TA One Shot Competent Cells (Invitrogen) and the cells were grown in SOC medium at 37°C. λDASH II and λZAP II was infected to *E. coli* XL-1 Blue MRS (P2) and XL-1 Blue MRF' strains (Stratagene) grown in LB medium containing 0.2% (v/v) maltose and 10mM $MgCl_2$, respectively and amplified in NZCYM medium. For *in vivo* excision of the Bluescript SK(-) from the λZAP II, *E. coli* SOLR, ABLE C, and ABLE K strains (Stratagene) were used. *E. coli* JM 109 (TOYOBO Co.) was used in the transformation of the derivatives of pTrc 99A and pKK223-3 and *E. coli* JM 105 was used for the expression. Other transformations were done to *E. coli* JM109 competent cells (TOYOBO Co.) unless otherwise mentioned. For the expression of *B.s.* LysRS from the derivative of pET 11a, *E. coli* BL21 (DE3) competent cells (Novagen) was used.

Chemicals: ATP (disodium salt) was the product of Sigma Chemical Co.; dansyl chloride, Nakarai Tesque; [4,5-^{3}H] L-lysine and [α-^{32}P] CTP, of NEN Research Products; [γ-^{32}P] ATP, Amersham Co.; glass microfiber filter (GF/C), of Whatman. Unfractionated tRNA from *E. coli* MRE 600 was purchased from Boehringer Mannheim. All other chemicals were of reagent grade. Gigapack II XL Packaging Extract (Stratagene) and Ready-To Go Lambda Packaging Kit (Pharmacia Biotech) were used to package recombinant λDASH II and λZAP II, respectively. Ready-To Go

DNA Labeling Kit (-dCTP) and T4 polynucleotide kinase (TOYOBO Co.) was used for the preparation of the probe in southern hybridization and plaque hybridization. The GENECLEAN II Kit (BIO 101 Inc.) was used for the recovery of DNA fragment from agarose gel. DNA sequencing was performed by the dideoxy chain termination method of Sanger et al. ***(?)*** with *Bca*BEST Dideoxy Sequencing Kit (-dCTP) (Takara Shuzo Co.).

Amino acid sequence analysis: The phenylthio-hydantoin (abbreviated to PTH) amino acids were separated and identified by an on-line PTH analyzer with a PTH-C column.

Digestion of B.s. LysRS by cyanogen bromide or lysylendopeptidase and purification of the peptide fragments: Purified LysRS was dialyzed against very dilute aqueous ammonia, lyophilized, and subjected to the N-terminal and the peptide fragment analysis. In the case for the preparation of cyanogen bromide fragments, 6mg of the purified LysRS was dissolved in 0.6ml of 70% (v/v) formic acid containing about 10mg cyanogen bromide. The tube was sealed and incubated at 30°C for 30 hours. The reaction mixture was diluted ten times by water and lyophilized. This was dissolved in 10mM ammonia bicarbonate and centrifuged at 12,000 x g 10min. The supernatant was applied to a Mono Q HR5/5 column equilibrated with 10mM ammonia bicarbonate in a Pharmacia FPLC system and eluted with a linear gradient from 10mM to 1M ammonia bicarbonate with the flow rate of 0.3 ml/min. Each fraction detected at the wavelength of 280nm were pooled and applied to a Cosmosil C_{18} column. The elution was done with a linear gradient from 0.1% trifluoroacetic acid to 60% acetonitrile with the flow rate of 0.75 ml/min and the detection was done at the wavelength of 220nm. Some fractions separated

incompletely were applied to the same column and eluted with a linear gradient from 10mM triethylamine-acetate buffer to 60% acetonitrile with the flow rate of 0.5 ml/min. In the case for the preparation of lysylendopeptidase fragments, 2mg of the purified LysRS was dissolved in 2ml of 100mM Tris-HCl (pH 9.0) and dialyzed to the same buffer containing 8M urea for 3days. After the addition of equal volume of 100mM Tris-HCl (pH 9.0), 1/200 of lysylendopeptidase against *B.s.* LysRS was added and the reaction mixture was incubated 35°C for 12 hours. After the centrifugation at 12,000 x g 20min, the supernatant was applied to a Shimadzu ODS-II column and eluted with a linear gradient from 0.1% trifluoroacetic acid to 60% acetonitrile with the flow rate of 1.0 ml/min. Further, each fraction was applied to the same column and eluted with a linear gradient from 10mM triethylamine-acetate buffer to 60% acetonitrile with the flow rate of 1.0 ml/min.

Extraction of plasmid DNA and λ phage DNA: Plasmid DNA was extracted with Wizard Minipreps DNA Purification system (Promega). λ Phage DNA was extracted by the method of Yamamoto *et al.* ***(14)*** except that the CsCl step gradient centrifugation was omitted.

Hybridization: For Southern hybridization and colony hybridization, Hybond N^+ membranes (Amersham Co.) were used. The oligonucleotide probes were labeled using T4 polynucleotide kinase with [γ-^{32}P] ATP. The hybridizations with the labeled oligonucleotide probes were done at 42°C in 6x SSC (0.9M NaCl and 0.09M sodium citrate) containing 5x Denhardt's solution (0.1% Ficoll 400, 0.1% polyvinylpyrrolidone, 0.1% bovine serum albumin (Fraction V)), 0.1mg/ml of denatured salmon sperm DNA, and 0.5% SDS. The hybridizations with PCR fragment labeled by random

oligonucleotides primers were done at 65°C in 0.5M $NaHPO_4$ (pH 7.2) containing 1mM EDTA, 1% crystalline bovine serum albumin (Fraction V), and 7% SDS.

Preparation of genomic DNA from B. stearothermophilus: *Bacillus stearothermophilus* NCA 1503 cells were harvested by centrifugation (12,000 x g, 2min). The genomic DNA of the microorganism was extracted with the method using hexadecyltrimethyl ammonium bromide.

PCR reaction for amplifying B.s. LysRS gene from genomic DNA and cloning of the amplified fragments: Mixed oligonucleotide primers were chemically synthesized. The PCR products were obtained with a DNA thermal cycler. The reaction mixture (100μl) consisted of 10mM Tris-HCl (pH 9.0 at 20°C), 50mM KCl, 1.5mM $MgCl_2$, 200μM dNTP, 0.4μM primers, 10.2μg/ml genomic DNA, and 2.5U of *Taq* DNA polymerase. The PCR reaction was done for 30cycles. One cycle consisted of 94°C for 90sec, 52°C for 120sec, and 72°C for 180sec. Amplified DNA fragments were cloned into pCR II and sequenced.

Partial digestion of genomic DNA by Sau3A I: Reaction mixture (100μl) consisted of 50mM Tris-HCl buffer (pH 7.5) containing 10mM $MgCl_2$, 1mM dithiothreitol, 100mMKCl, and 100μg of *B. stearothermophilus* genomic DNA. After the incubation for 5min at 37°C, the digestion was started by the addition of 0.15U of *Sau*3A I and stopped after 1 hour by the addition of buffered phenol (pH 8.0). After centrifugation, the supernatant was subjected to the phenol-chloroform and chloroform extraction, and the supernatant was precipitated with 2 volumes of ethanol at -80°C. After the centrifugation at 12,000 x g for 10min followed by the next centrifugation of 70% ethanol, the precipitate was dried and

ligated to *Bam*H I digested λDASH II. It was packaged and amplified once for the construction of a *B. stearothermophilus* λDASH II genome DNA library.

Molecular cloning of B.s. LysRS gene and trying of expression of B.s. LysRS: Strategy for molecular cloning of *B.s.* LysRS gene is shown in **Fig. 4**. For expression of *B.s.* LysRS, I used four new oligonucleotide primers (**Table III**), conducted PCR reaction with 4.5kbp Xho I fragment of pBLX45 as DNA template. Amplified fragments were digested with restriction endonucleases and introduced into plasmids as shown in **Fig. 12**.

RESULTS AND DISCUSSION

Amino acid sequence analysis of N-terminus and the peptide fragments by cyanogen bromide or lysylendopeptidase digestion: The amino acid sequence analysis of N-terminus of *B.s.* LysRS revealed 36 amino acid sequence, ?HEELNDQLRVRREKLKKIE?LGVD???KRFER-THK (**Table I**). The N-terminal amino acid was likely to be Ser. However, unknown peak comparable to that of Ser was observed at the close position of Gln. Further, the sequence analysis of 7 peptide fragments by cyanogen bromide and that of 6 fragments by lysylendopeptidase revealed 110 amino acid sequence (**Table I**).

PCR reaction for amplifying B.s. LysRS gene from genomic DNA and cloning of the amplified fragments: On the basis of the amino acid sequence of N-terminus, HEELNDQ and the peptide fragment which was considered to be close C-terminus by the sequence alignment, MLWTNSP, mixed oligonucleotide primers were chemically synthesized (**Table II**). With N-terminal region

primer (N-1 and N-2) and C-terminal region primer (C-1, C-2, C-3, and C-4), 8 set of PCR reactions were performed under the condition described in MATERIALS and METHODS. As is shown in **Fig. 1**, significantly amplified 1.4kbp DNA fragment was observed in the set of PCR reaction with N-1 and C-3. This fragment was cloned into pCR II vector and 3 recombinants containing 1.4kbp fragment were sequenced. These 3 recombinants have the same amplified fragment that is significantly agreed with the amino acid sequence of purified enzyme and digested peptide fragments **(data not shown)**.

Analysis of B. stearothermophilus genomic DNA: In order to determine the complete sequence of *B.s.* LysRS gene, genomic DNA was digested by several restriction endonucleases and the digested DNA was subjected to southern hybridization analysis with the 1.4kbp PCR fragment labeled by random oligonucleotides primers. There was possibility that 3.5 kbp *Sac* I fragment and 4.5kbp *Xho* I fragment involve complete *B.s.* LysRS gene (**Fig. 2**). In order to investigate it, on the basis of the identified nucleotide sequence (**Fig. 2**), we newly synthesized N-terminal region probes, N-A (sense primer, 58 -77), GAGGAATTGG-GTGTCGATCC and C-terminal region primer, C-A (sense primer, 1408 -1427), AGGTTAGTCATGCTTTGGAC, and conducted southern hybridization again by using these probes. The result indicated that both fragments contain at least 77-1408 nucleotides (**data not shown**).

Molecular cloning of B.s. LysRS gene: Screening of λDASH II recombinants having *B.s.* LysRS gene from the library was conducted with the 1.4kbp PCR fragment probe. This screening procedure was repeated 3 times and 13 positive clones were

obtained and one of them was amplified. After the extraction of the λDASH II recombinant DNA, it was digested by *Xho* I and subjected to southern hybridization with the 1.4kbp PCR fragment probe. The result indicated that the inserted *Sau*3A I fragment involves the 4.5kbp *Xho* I (**Fig. 3**). Then, this recombinant λDASH II was digested by *Xho* I and the 4.5kbp *Xho* I fragment was ligated to the *Xho* I site of λZAP II. After packaging and amplification, plaque hybridization was conducted with the 1.4kbp PCR fragment probe. After the extraction of the λZAP II recombinant DNA, it was digested by *Xho* I and subjected to southern hybridization with the 1.4kbp PCR fragment probe. The result indicated that 4.5kbp *Xho* I fragment exists (**Fig. 3**). After the amplification of a positive λZAP II, single stranded circular Bluescript SK(-) phagemid was excised with ExAssist helper phage in *E. coli* XL1-Blue MRF'. After the heat treatment and centrifugation, the supernatant was mixed with SOLR cells and incubated. Then, the mixtures were plated LB-ampicillin plates. However, none of positive clone was obtained in spite of several challenges. On the other hand, when we used ABLE C, a positive clone was obtained having Bluescript SK(-) phagemid in which 4.5kbp *Xho* I fragment was inserted (**Fig. 4**). This phagemid was termed as pBLX45 and sequenced. **Figure 5** shows the identified nucleotide sequence of *B.s.* LysRS which has 1479bp of structural gene with initiation codon, ATG and termination codon, TAA. **Figure 6** shows the amino acid sequence of *B.s.* LysRS which has 493 amino acid residues. Deduced amino acid sequence of *B.s.* LysRS shows about 53% homology with *E. coli* LysRS (**Fig. 7**).

10 amino acid residues which are thought to be involved in the interaction with the substrate, L-lysine were well conserved except

that one the Tyr460 of *E. coli* LysRS is changed to Phe451 of *B.s.* LysRS (**Fig. 8**).

Though the 3D-structure of LysRS•ATP complex remains unknown, two complexes with ATP of two Class II ARSs, SerRS of *T. thermophilus* ***(15)*** and yeast AspRS ***(16)*** are available, though the 3D-structure of LysRS•ATP complex remains unknown. They indicate that ATP is bound to these enzymes in a bent-conformation (**Fig. 9**), while an ATP analogue, α,β-methyleneATP with a methlene group between the β– and γ–phosphates is bound in a extended conformation. Of 10 amino acid residues which are thought to be involved in the interaction with the substrate, ATP in the system for yeast AspRS (25% homology to *E. coli* LysRS) belonging to the same subclass as LysRS, 8 residues are conserved in *E. coli* LysRS with Met335 and Ser481 of yeast AspRS changed into Asn271 and Asn424, respectively in *E. coli* LysRS. The difference between *E. coli* LysRS and *B.s.* LysRS is only one residues at the position of Ile479 of yeast AspRS making interaction with 3'-OH group, which is conserved in *E. coli* LysRS but not in *B.s.* LysRS (**Fig. 9**). Taking it into consideration that the ATP binding sites of yeast AspRS, *E. coli* LysRS, and *B.s.* LysRS are similar to each other, it is interesting the properties of these enzymes for ATP binding. I reported that *B.s.* LysRS does not bind to ATP in the absence of L-lysine ***(3)***, while Rymo *et al.* reported that *E. coli* LysRS has very low affinity for ATP (probably K_d for ATP is about 3~4mM) by equilibrium dialysis experiments ***(17)***. Hountondji *et al.* conducted affinity labeling with adenosine di- and triphosphopyridoxals to identify the ATP-binding site of *E. coli* MetRS ***(18)***, *E. coli* ValRS ***(18)***, and *E. coli* LysRS ***(19)***. Comparing the results of the Class I ARSs, *E. coli* MetRS and *E. coli* ValRS with that of Class II ARS, *E. coli* LysRS may support

the very low affinity for ATP of *E. coli* LysRS since many Lys residues are labeled in *E. coli* LysRS with a low specificity. As far as I know, AspRS is not investigated directly for the ATP binding. However, a hypothesis is presented by Cavarelli *et al.* on the basis of the results of site-directed mutagenesis ***(16)*** that in yeast AspRS, the presence of ATP on the enzyme a prerequisite for aspartic acid binding in spite of their own result of 3D-structure (L-aspartic acid binds first). It indicates the possibility that the binding process of L-aspartic acid and ATP for yeast AspRS is different from that for *B.s.* LysRS. It should be also noted that the K_m value for L-aspartic acid, 2.5mM (in the ATP-PPi exchange reaction) is extremely larger than that for ATP, 30μM (in the aminoacylation reaction) ***(16)***.

For speculation of the 3D-structure of LysRS•lysyladenylate complex, two complexes with aminoacyladenylate of two Class II ARSs, SerRS of *T. thermophilus* ***(20)*** and yeast AspRS ***(16)*** are available. Amino acid sequence alignment of Class II ARSs involving SerRS, AspRS, AsnRS, and LysRS is shown in **Fig. 10**. Comparing the aminoacyladenylate-binding site between SerRS of *T. thermophilus* ***(20)*** and yeast AspRS ***(16)*** (**Fig. 11**), amino acid residues interacting with adenosine moiety are essentially the same except that there are additional residues, Glu 258 (interaction with amino group of adenine moiety) and Glu345 (interaction with 3'-OH of glucose moiety) in *T. thermophilus* SerRS, and Gly528 (interaction with 3'-OH of glucose moiety), in yeast AspRS. However, some residues at the same positions in the alignment (**Fig. 10**) recognized different positions of aminoacyladenylate, especially, 2'- and 3'-OH of glucose moiety (Thr346 and Arg386 in *T. thermophilus* SerRS, Ile479 and Arg531 in yeast AspRS). The residue interacting with α-phosphate, Arg256 in *T. thermophilus*

SerRS and Arg325 in yeast AspRS and the residue interacting with α-amino group of amino acid moiety, Glu279 in *T. thermophilus* SerRS and Asp342 in yeast AspRS are conserved. It should be noted and interesting that the Glu279 also make interaction with the OH group in side-chain of Ser moiety of the seryladenylate analogue in SerRS system, while additional Arg485 does with the COO^- group in side-chain of Asp moiety of aspartyladenylate in AspRS system. The amino acid sequence alignment (**Fig. 10**) suggests such lysyladenylate binding site in *E. coli* LysRS as is shown in **Fig. 11 C**, where the recognition mechanism for adenylate moiety is the same as in yeast AspRS except that for the side-chain of amino acid moiety. It should be noted that the residue interacting with the COO^- group in side-chain of Asp moiety of aspartyladenylate in yeast AspRS system, Arg485 is the same position of the residue interacting with the amino group in side-chain of substrate, L-lysine in *E. coli* LysRS system with L-lysine, Glu 428. The difference between *B.s.* LysRS and *E. coli* LysRS is only one residue, His412 in *B.s.* LysRS and Ile422 in *E. coli* LysRS which make interaction with 3'-OH of glucose moiety.

Expression of B.s. LysRS: Thus far amplified PCR fragment (used primers, N-B and C-B) digested by *EcoR* I and *Pst* I was introduced into pKK223-3 and pTrc 99A. However, I could not detect expression of *B.s.* LysRS. Then, I am trying to introduce PCR fragment (used primers, N-C and C-C) digested by *Nde* I and *BamH* I into pET-11a.

REFERENCES

1) Berg, P. (1961) Specificity in protein synthesis. *Annu. Rev. Biochem.* **30**, 293-324

2) Cusack, S. (1995) Eleven down and nine to go. *Nature Structural Biology*, **2**, 824-831

3) Takita, T., Ohkubo, Y., Shima, H., Muto, T., Shimizu, N., Sukata, T., Ito, H., Saito, Y., Inouye, K., Hiromi, K., and Tonomura, B. (1996) Lysyl-tRNA synthetase from *Bacillus stearothermophilus.* Purification, and fluorometric and kinetic analysis of the binding of substrates, L-lysine and ATP. *J. Biochem.*, (in press).

4) Takita *et al.*

5) Freist, W. and Gauss, D. H. (1995) Lysyl-tRNA synthetase. *Biol. Chem. Hoppe-Seyler*, **376**, 451-472

6) Lévêque, F., Plateau, P., Dessen, P., and Blanquet, S. (1990) Homology of lysS and lysU, the two *Escherichia coli* genes encoding distinct lysyl-tRNA synthetase species. *Nucleic Acids Res.* , **18**, 305-312

7) Mirande, M and Waller, J. P. (1988) The yeast lysyl-tRNA synthetase gene. *J. Bio. Chem.* **263**, 18443-18451

8) Gatti, D. L. and Tzagoloff, A. (1991) Structure and evolution of a group of related aminoacyl-tRNA synthetase. *J. Mol. Biol.* , **218**, 557-568

9) Özkökmen, D., Birkelund, S., and Christiansen, G. (1994) Characterization of a *Mycoplasma hominis* gene encoding lysyl-tRNA synthetase (LysRS). *FEMS Microbiology Letters*, **116**, 277-282

10) Chan, V. L. and Bingham, H. L. (1992) Lysyl-tRNA synthetase gene of *Campyrobacter jejuni. J. Bacteriol*, **174**, 695-701

11) Chen, J., Brevet, A., Lapadat-Tapolsky, M, Blanquet, S., and Plateau, P. (1994) Properties of the lysyl-tRNA synthetase gene and product from the extreme thermophile *Thermus thermophilus. J. Bacteriol*, **176**, 2699-2705

12) Onesti, S., Miller, A. D., and Brick, P. (1995) The crystal structure of the lysyl-tRNA synthetase (LysU) from *Escherichia coli. Structure*, **3**, 163-176

13) Yaremchuk, A. D., Krikliviy, I. A., Cusack, S., and Tukalo, M. A. (1995) Cocrystallization of lysyl-tRNA synthetase from *Thermus thermophilus* with its cognate $tRNA^{lys}$ and with *Escherichia coli* $tRNA^{lys}$. *Proteins*, **21**, 261-264

14) Yamamoto, K. R., Alberts, B. M., Benzinger, R., Lawhorne, L., and Treiber, G. (1970) Rapid bacteriophage sedimentation in the presence of polyethylene glycol and its application to large-scale virus purification. *Virology*, **40**, 734

15) Biou, A., Yaremchuk, A., Tukalo, M., and Cusack, S. (1994) The 2.9 Å crystal structure of T. thermophilus seryl-tRNA synthetase complexed with $tRNA^{Ser}$. Science, 263, 1404-1410

16) Cavarelli, J., Eriani, G., Rees, B., Ruff, M., Boeglin, M., Mitschler, A., Martin, F., Gangloff, J., Thierry, J. C., and Moras, D. (1994) The active site of yeast aspartyl-tRNA synthetase: structural and functional aspects of the aminoacylation reaction. *EMBO J.*, **13**, 327-337

17) Rymo, L., Lundvik, L., and Lagerkvist, U. (1972) Subunit structure and binding properties of three amino acid transfer ribonucleic acid ligases. (1972) *J. Biol. Chem.*, **247**, 3888-3899

18) Hountondji, C., S., Schmitter, Fukui, T., Tagaya, M., and Blanquet, S. (1990) Affinity labeling of Aminoacyl-tRNA synthetases with adenosine triphosphopyridoxal: Probing the Lys-Met-Ser-Lys-Ser signature sequence as ATP-binding site in *Escherichia coli* methionyl- and valyl-tRNA synthetases., **29**, 11266-11273

19) Hountondji, C., Gillet, S., Schmitter, J. M., Fukui, T., and Blanquet, S. Affinity labeling of the two species of *Escherichia coli* lysyl-tRNA synthetase with adenosine di- and triphosphopyridoxals. (1994), *J. Biochem.*, **116**, 493-501

20) Belrhali, H., Yaremchuk, A., Tukalo, M., Larsen, K., Berthet-Colominas, C., Leberman, R., Beijer, B., Sproat, B. , Als-Nielsen, J., Grübel, G., Legrand, J-F., Lehmann, M., and Cusack, S. (1994) Crystal structure at 2.5 angstrom resolution of seryl-tRNA synthetase complexed with two analogues of seryl adenylate. *Science*, **263**, 1432-1436

Table I
Amino acid sequence analysis

(a) N-terminus

?HEELNDQLRVRREKLKKIE?LGVD???KRFERTHK

(b) Peptide fragments by

BrCN	lysyl endopeptidase
NP(I?)(I?)KKTFIT	TELNDPIDQRQRFEEQLK
(?)KYLDSHGYLEVE	RFERTHK
HAVAGGAAARPFITHHNALD	MHAV
(K?)LTENLIAHIATEVL	FWRQM
SDEEARELAKEHGVEVAP	LIQPT
PPTGGLGIGV	EHGVEVAPH
L(W?)TNSPSIRDVLLFPQ	

Table II
Synthetic oligonucleotide primers for amplification of *B.s.* LysRS gene from genomic DNA by PCR reaction

N-terminus region

	H	E	E	L	N	D	Q
N-1	CA(T/C)	GA(A/G)	GA(A/G)	TT(A/G)	AA(T/C)	GA(T/C)	CA(A/G)
N-2	CA(T/C)	GA(A/G)	GA(A/G)	CT(A/G/T/C)	AA(T/C)	GA(T/C)	CA(A/G)

C-terminus region

	M	L	W	T	N	S	P
C-1	TAC	AA(T/C)	ACC	TG(A/G/T/C)	TT(A/G)	AG(A/G/T/C)	GG
C-2	TAC	AA(T/C)	ACC	TG(A/G/T/C)	TT(A/G)	TC(A/G)	GG
C-3	TAC	GA(A/G/T/C)	ACC	TG(A/G/T/C)	TT(A/G)	AG(A/G/T/C)	GG
C-4	TAC	GA(A/G/T/C)	ACC	TG(A/G/T/C)	TT(A/G)	TC(A/G)	GG

Table III
Synthetic oligonucleotide primers for amplification of *B.s.* LysRS gene

N-terminus region

	GTGAATGAGGTATGAGCCATGAAGAATT
N-B	GGGAATTCGGTATGAGCCATGAAGAATT
	Eco RI
N-C	GTGAATGACATATGAGCCATGAAG
	Nde I

C-terminus region

	TTCGCAACAGGGGACGATCGTGGTTATT
C-B	TTCGCTGCAGGGGACGATCGTGGTTATT
	Pst I
C-C	CGCAACAGGGGAGGATCCTGGTTA
	Bam HI

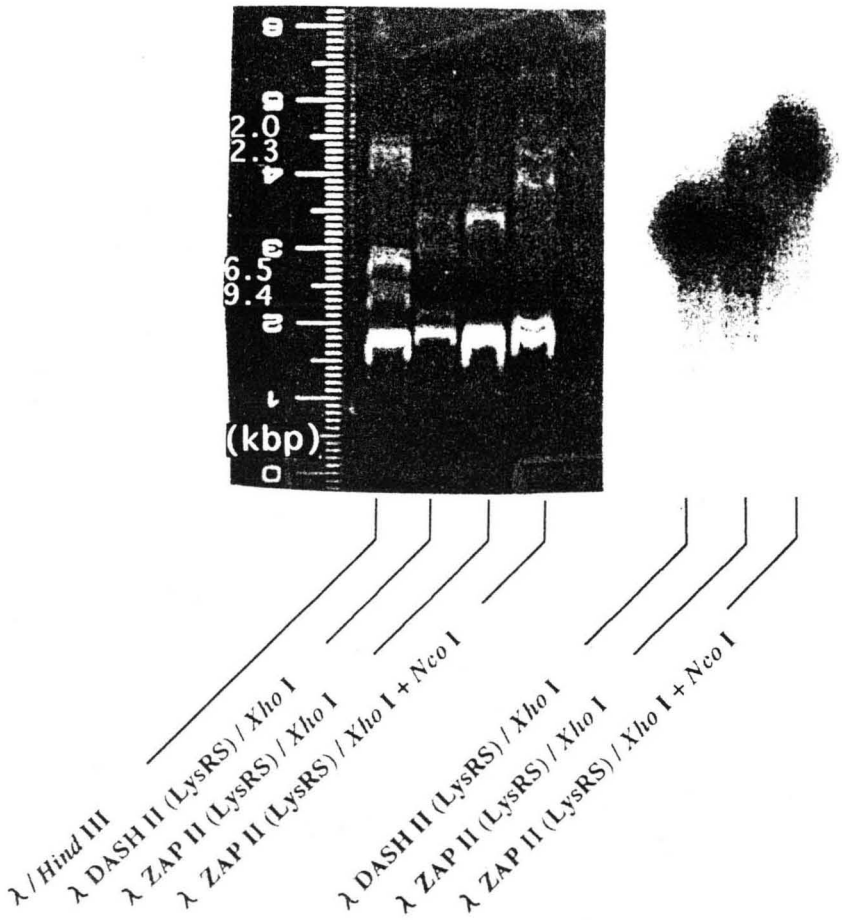

Figure 3
Southern hybridization for analysis of λ phages containing *B.s.* LysRS gene

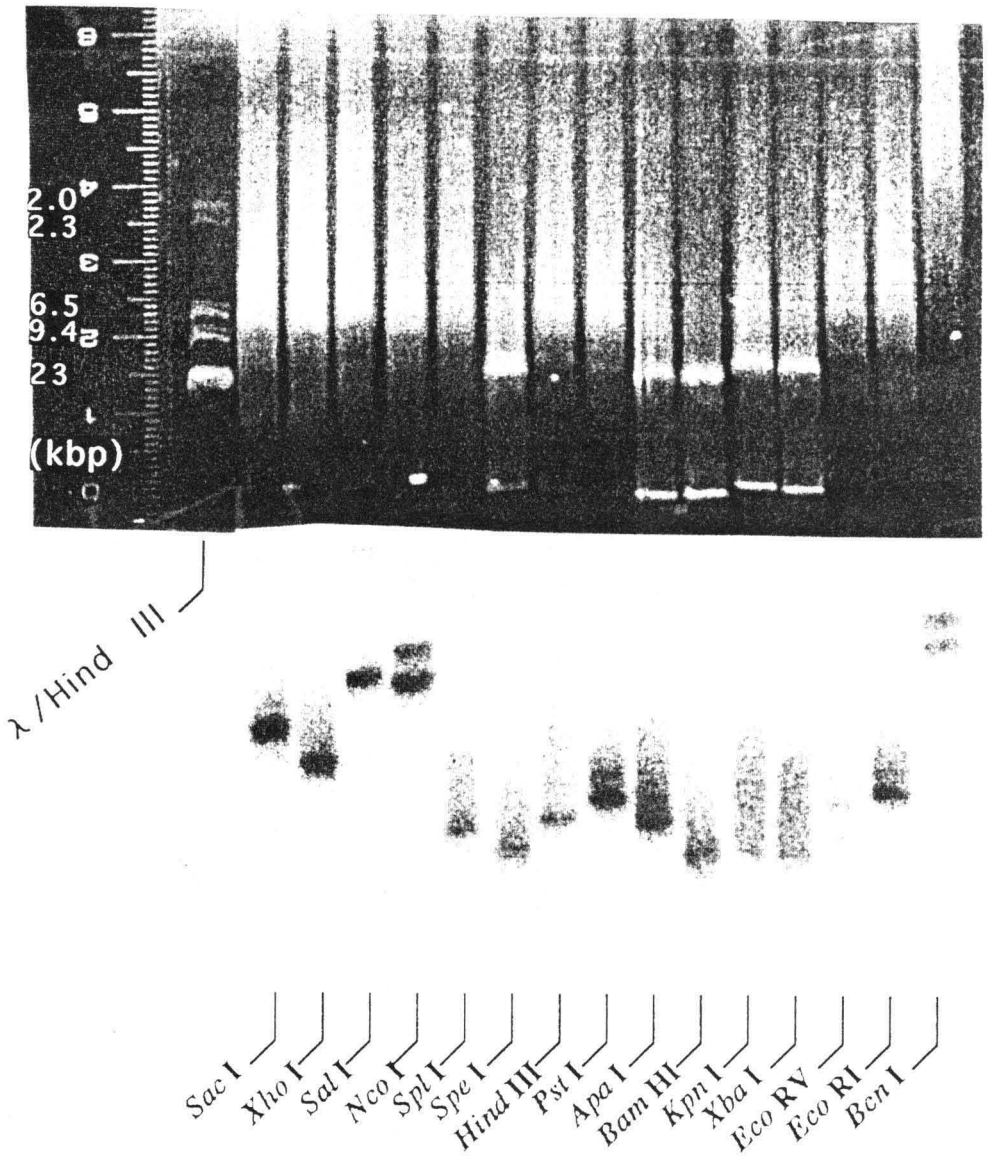

Figure 2
Southern hybridization for analysis of *B.s.* genomic DNA

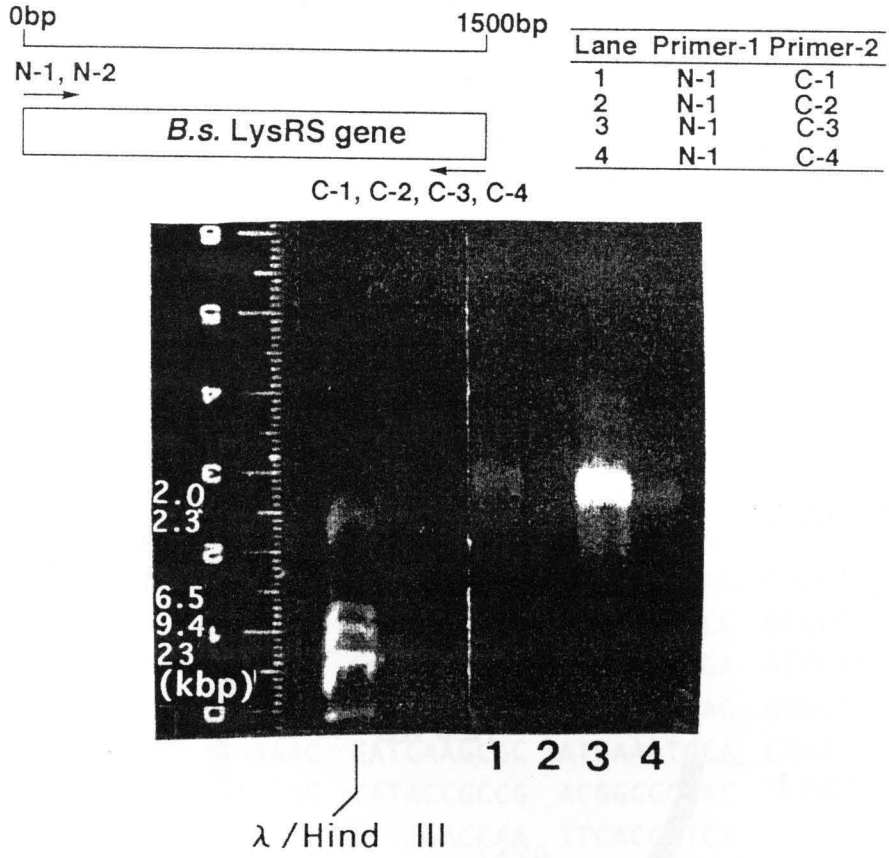

Figure 1

PCR reaction for amplification of *B.s.* LysRS gene

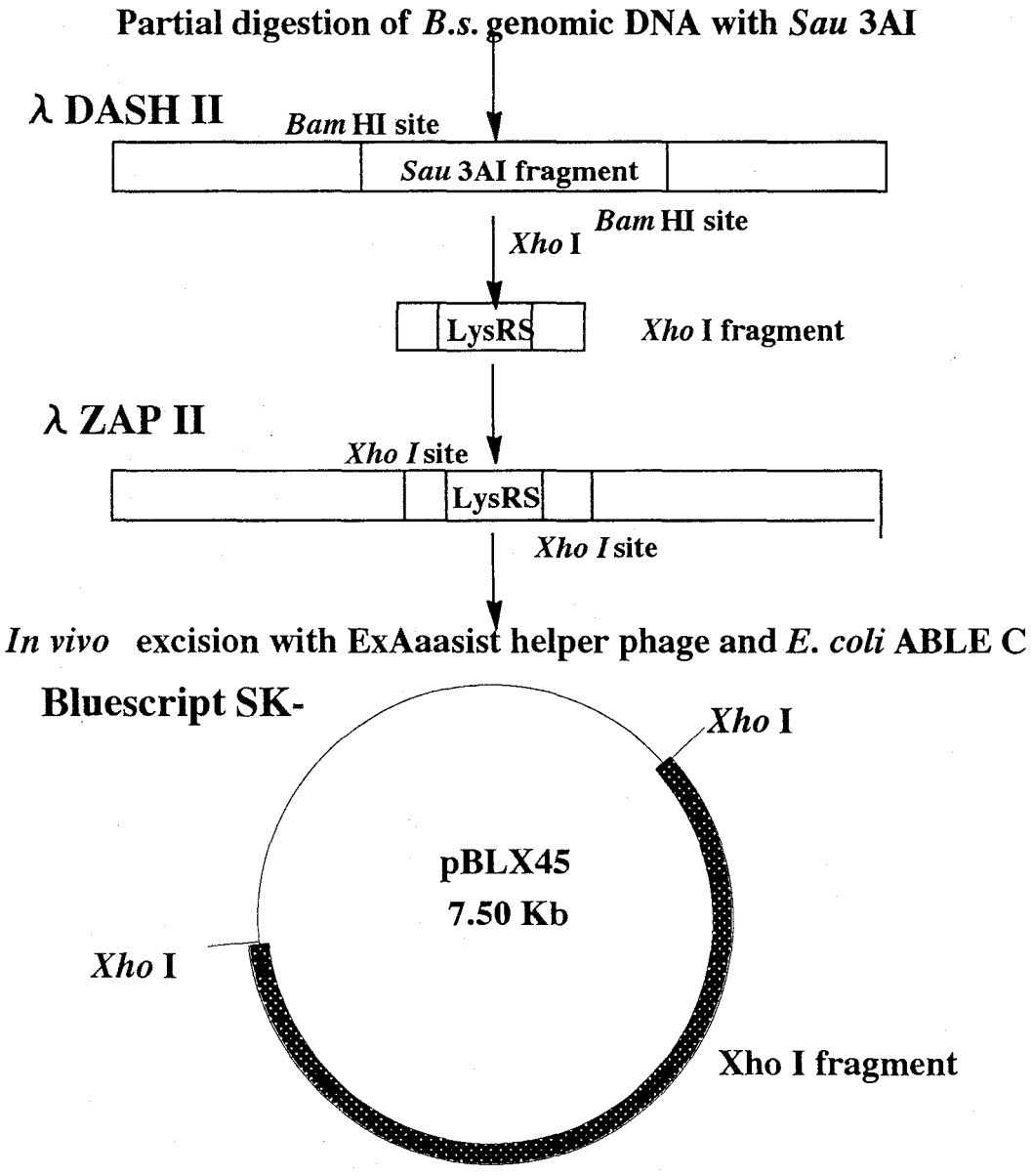

Figure 4
Strategy for cloning of *B.s.* LysRS gene

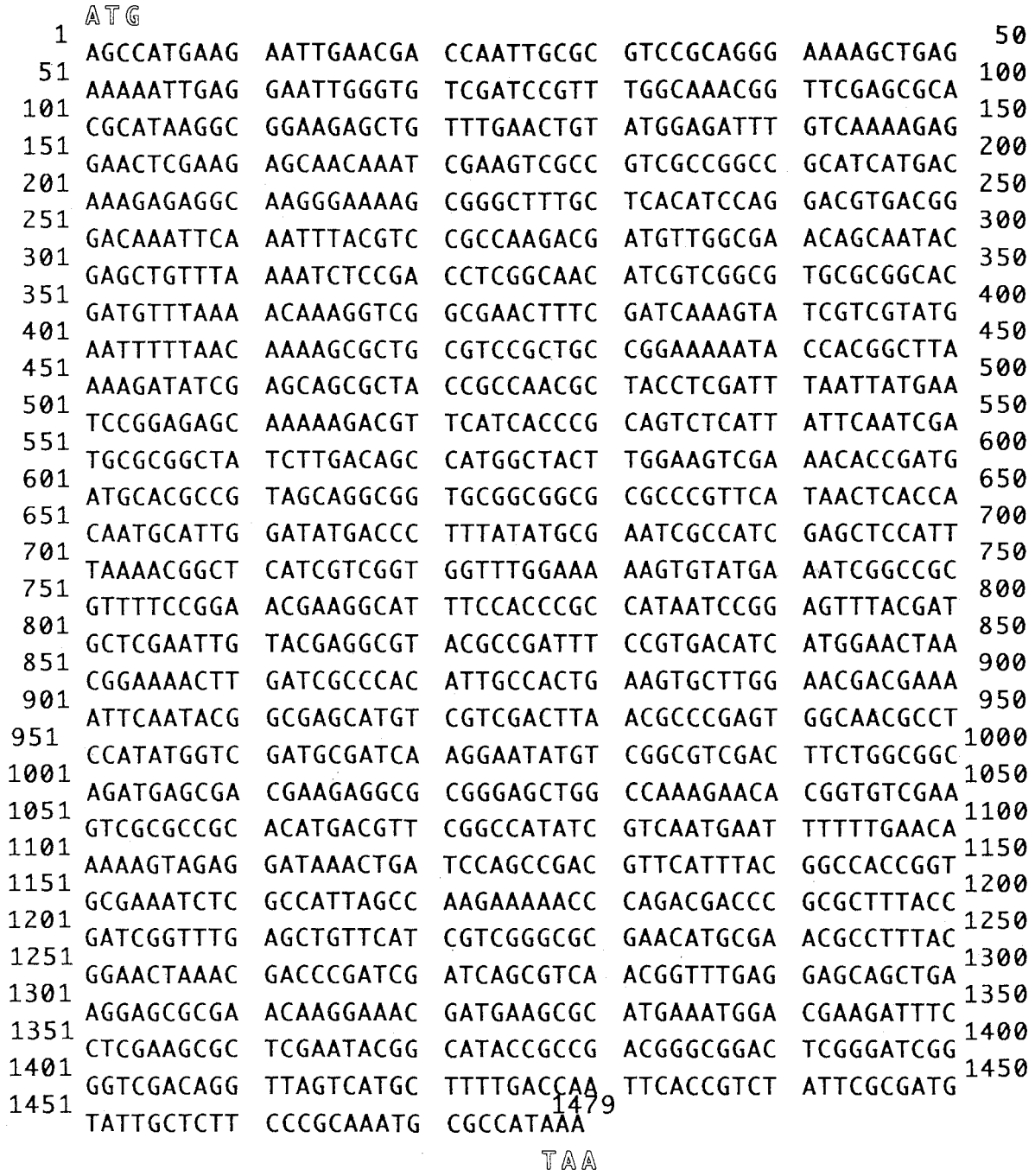

Figure 5
Nucleotide sequence of *B.s.* LysRS gene

```
  1                                                                   50
    SHEELNDQLR  VRREKLKKIE  ELGVDPFGKR  FERTHKAEEL  FELYGDLSKE
 51                                                                  100
    ELEEQQIEVA  VAGRIMTKRG  KGKAGFAHIQ  DVTGQIQIYV  RQDDVGEQQY
101                                                                  150
    ELFKISDLGN  IVGVRGTMFK  TKVGELSIKV  SSYEFLTKAL  RPLPEKYHGL
151                                                                  200
    KDIEQAYRQR  YLDLIMNPES  KKTFITRSLI  IQSMRGYLDS  HGYLEVETPM
201                                                                  250
    MHAVAGGAAA  RPFITHHNAL  DMTLYMRIAI  ELHLKRLIVG  GLEKVYEIGR
251                                                                  300
    VFRNEGISTR  HNPEFTMLEL  YEAYADFRDI  MELTENLIAH  IATEVLGTTK
301                                                                  350
    IQYGEHVVDL  TPEWRRLHMV  DAIKEYVGVD  FWRQMSDEEA  RELAKEHGVE
351                                                                  400
    VAPHMTFGHI  VNEFFEQKVE  DKLIQPTFIY  GHRCEISPLA  KKNPDDPRFT
401                                                                  450
    DRFELFIVGR  EHANAFTELN  DPIDQRQRFE  EQLKEREQGN  DEAHEMDEDF
451                                                                  494
    LEALEYGIPP  TGGLGIGVDR  LVMLLTNSPS  IRDVLLFPQM  RHK
```

Figure 6
Amino acid sequence of *B.s.* LysRS gene

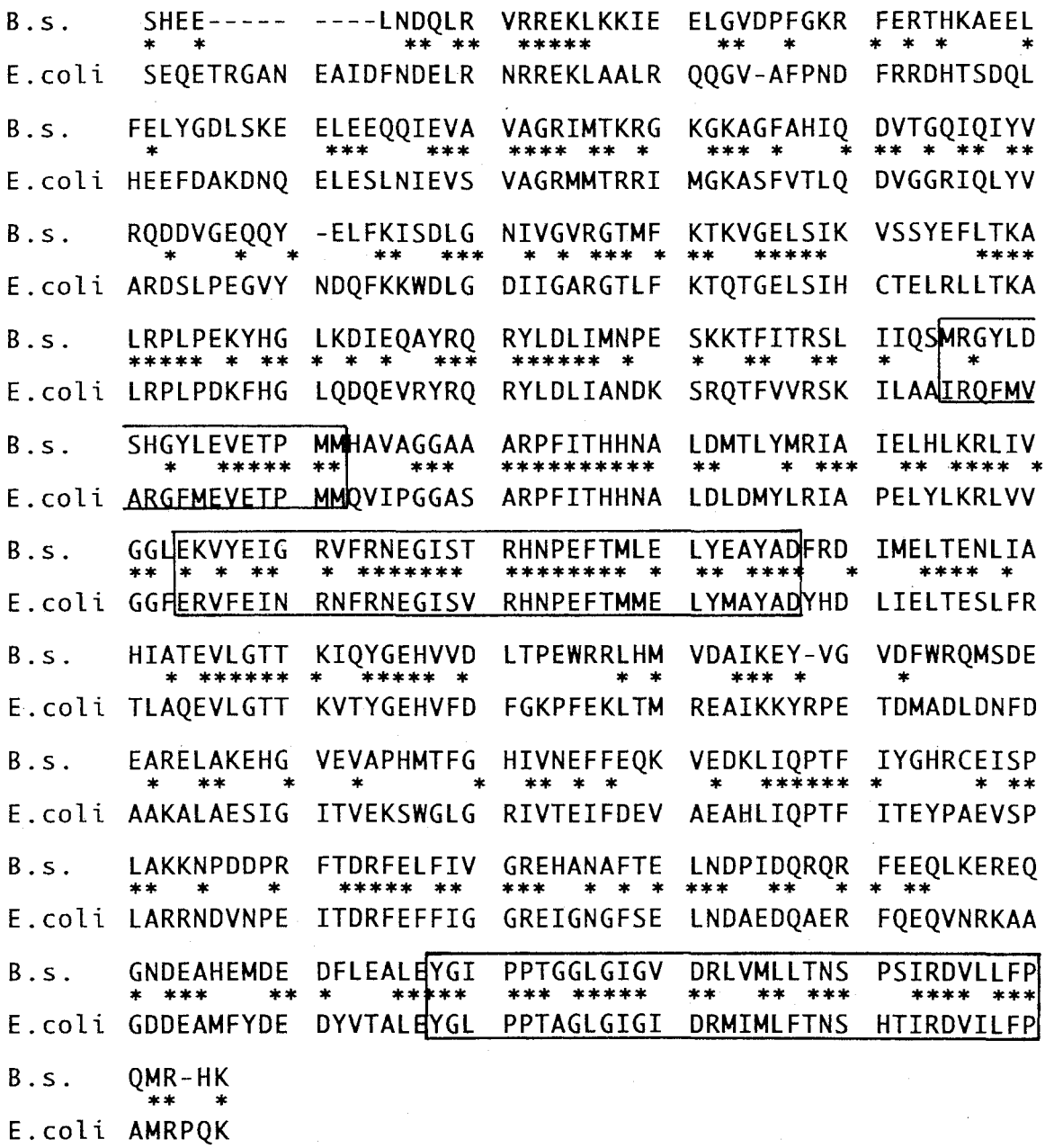

Figure 7

Amino acid sequence homology between *B.s.* LysRS and *E. coli* LysRS U

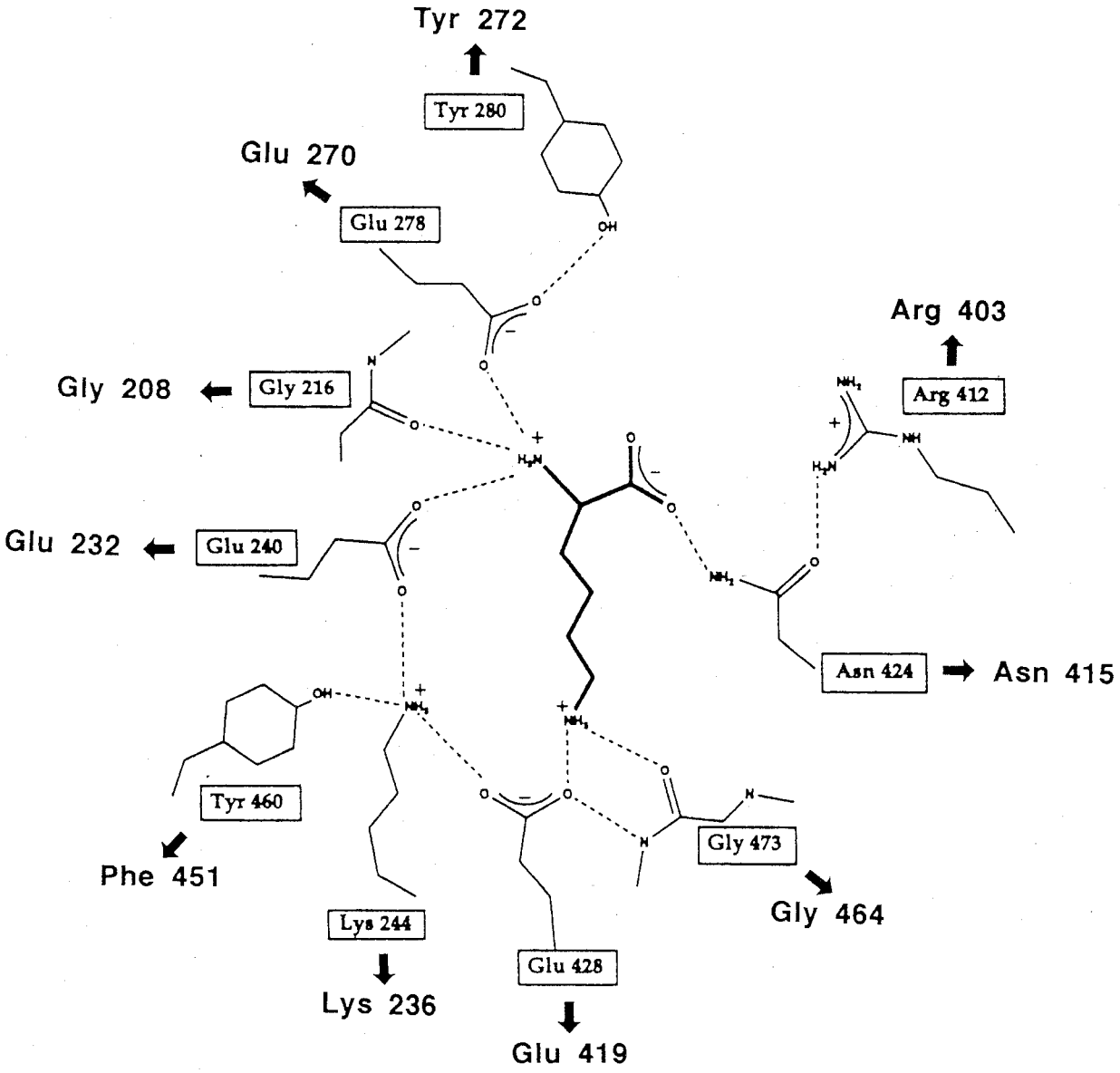

Figure 8

Schematic representation of the interactions at the L-lysine binding pocket

The boxes contain amino acid residues interacting with L-lysine in 3D-structure of *E. coli* LysRS. Residues in bold are those observed in the primary structure of *B.s.* LysRS.

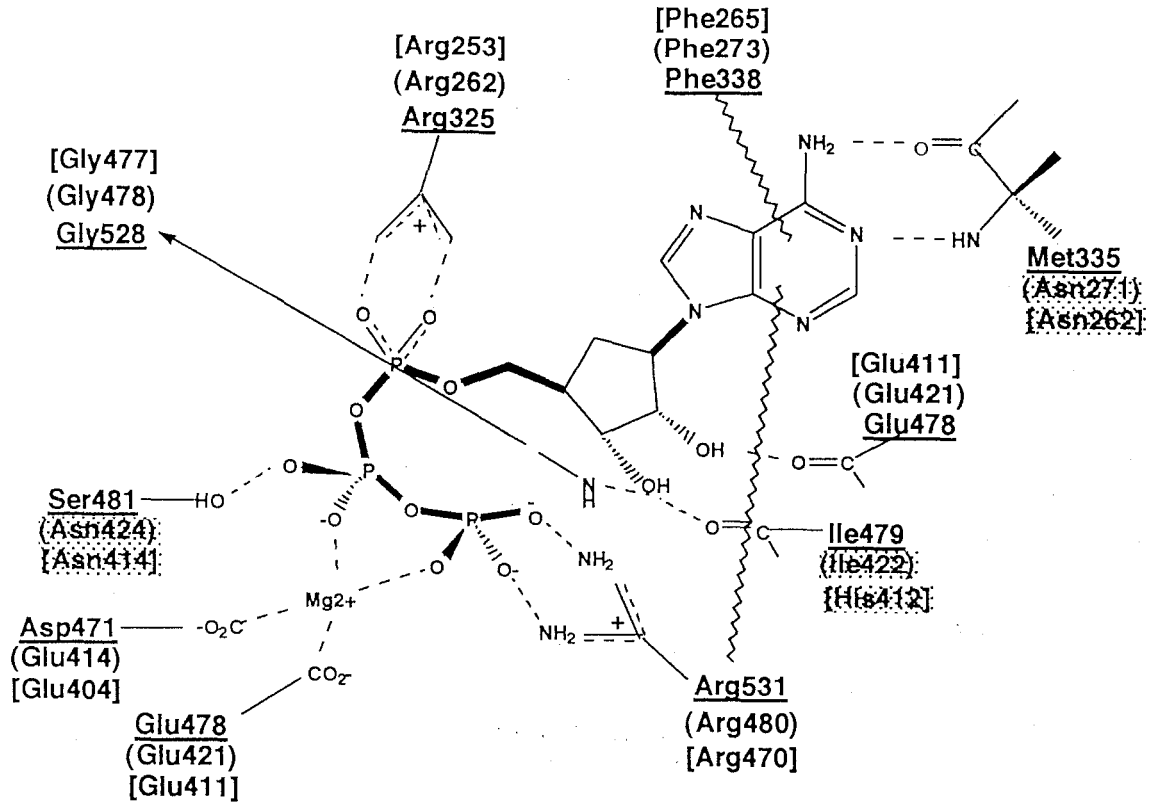

Figure 9

Schematic representation of the interactions at the ATP binding pocket

Residues with underline are those interacting with ATP in 3D-structure of yeast AspRS. Residues in ( ) and in [ ] are those observed in the primary structure of *E. coli* LysRS and in that of *B.s.* LysRS.

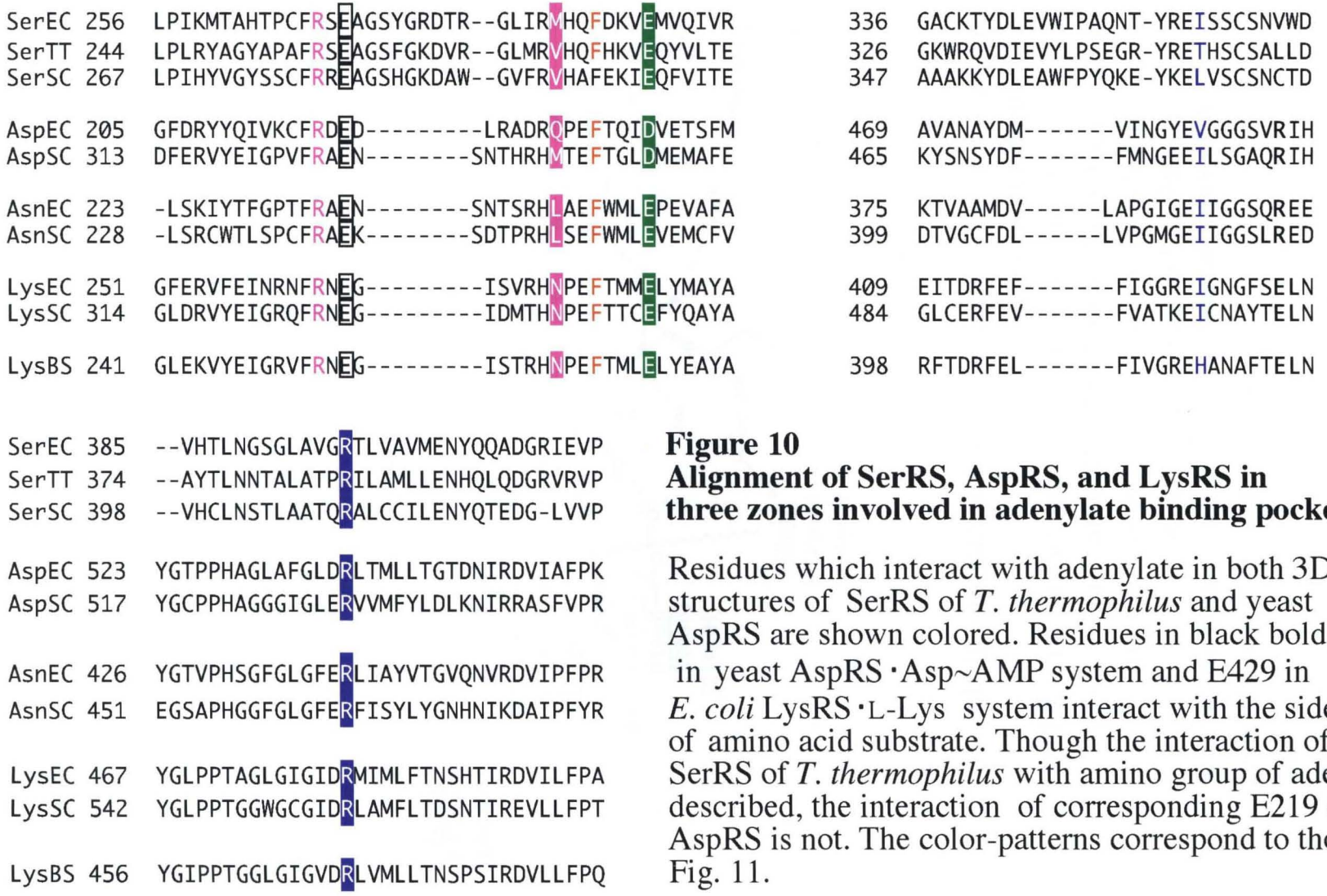

Figure 10
Alignment of SerRS, AspRS, and LysRS in three zones involved in adenylate binding pocket

Residues which interact with adenylate in both 3D-structures of SerRS of *T. thermophilus* and yeast AspRS are shown colored. Residues in black bold, R485 in yeast AspRS·Asp~AMP system and E429 in *E. coli* LysRS·L-Lys system interact with the side-chain of amino acid substrate. Though the interaction of E258 of SerRS of *T. thermophilus* with amino group of adenylate is described, the interaction of corresponding E219 of yeast AspRS is not. The color-patterns correspond to those in Fig. 11.

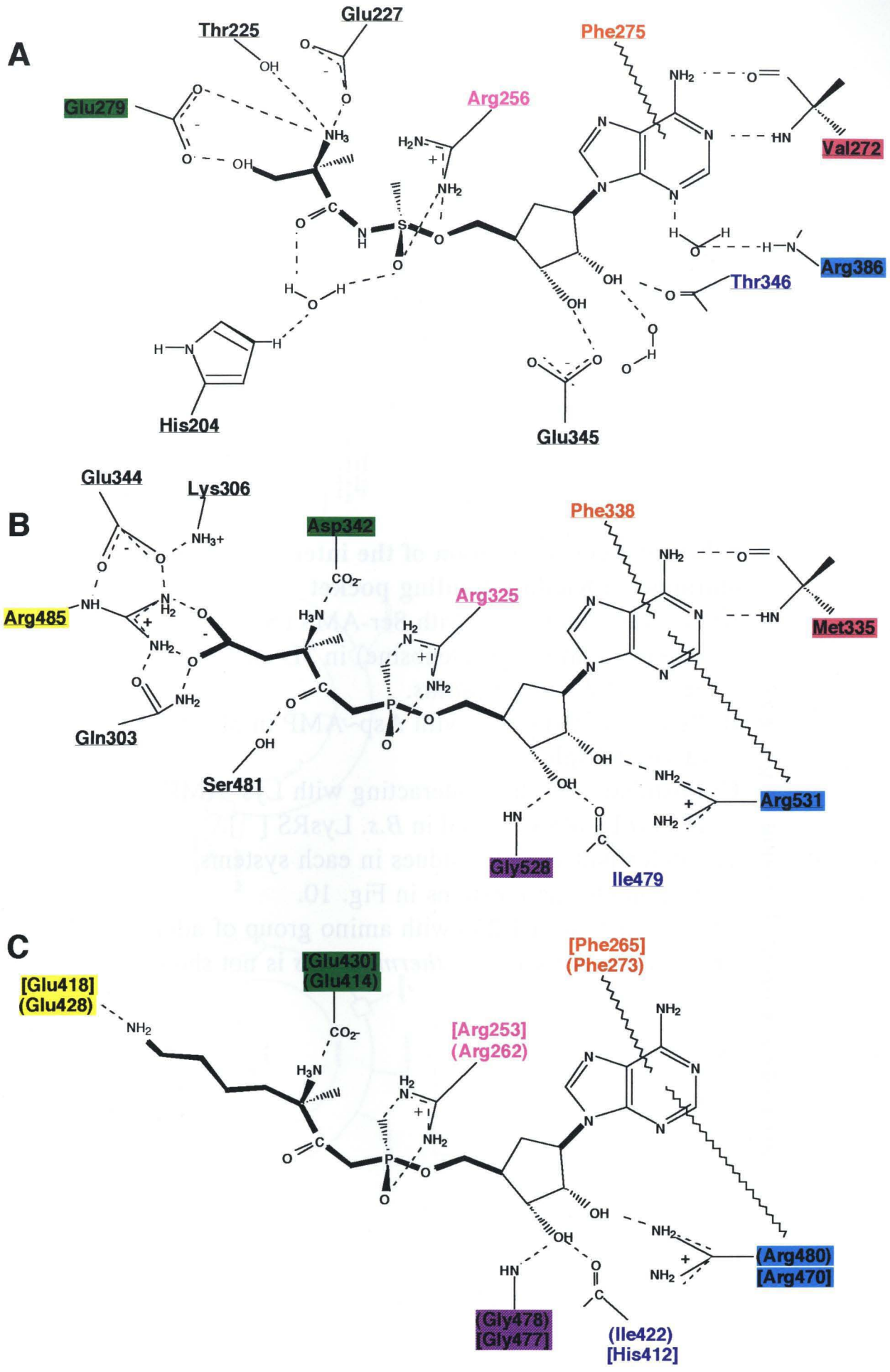
A
Glu227
Thr225
Phe275
Glu279
Arg256
Val272
Arg386
Thr346
His204
Glu345
B
Glu344
Lys306
Asp342
Phe338
Arg485
Arg325
Met335
Gln303
Ser481
Arg531
Gly528
Ile479
C
[Glu430]
(Glu414)
[Glu418]
(Glu428)
[Phe265]
(Phe273)
[Arg253]
(Arg262)
(Arg480)
[Arg470]
(Gly478)
[Gly477]
(Ile422)
[His412]

Figure 11

Schematic representation of the interactions at the aminoacyladenylate binding pocket

A; Residues interacting with Ser-AMS (5'-*O*-[*N*-(L-seryl)-sulfamoyl]adenosine) in 3D-structure of SerRS of *T. thermophilus*.

B; Residues interacting with Asp~AMP in 3D-structure of yeast AspRS.

C; Postulated residues interacting with Lys~AMP in *E. coli* LysRS ( ) and in *B.s.* LysRS [ ].

The color-patterns of residues in each systems correspond to the positions in Fig. 10.

The interaction of E258 with amino group of adenylate described in SerRS of *T. thermophilus* is not shown.

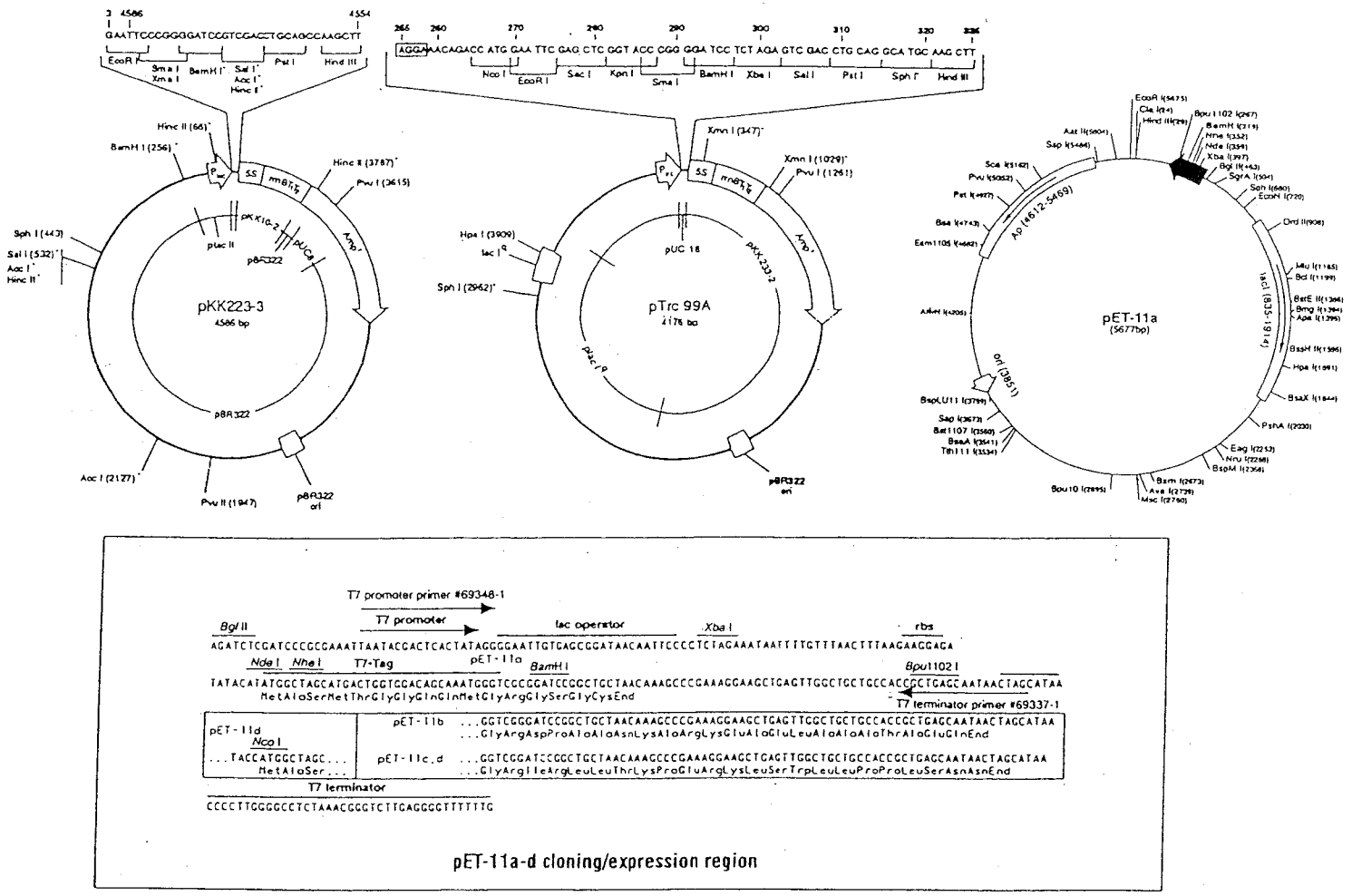

Figure 12

Strategy for overexpression of *B.s.* LysRS in *E. coli*

Appendix 1

Rate Laws of ATP-PPi Exchange Reaction for the Sequential Ordered Mechanism in which Amino Acid Binds First

$$E + AA + ATP \rightleftharpoons E\bullet AA\sim AMP + PPi$$

$$v = k_{app}[PPi][E\bullet AA\sim AMP]$$

$$E + AA \underset{k_{-1}}{\overset{k_1}{\rightleftharpoons}} E\bullet AA$$

$$E\bullet AA + ATP \underset{k_{-2}}{\overset{k_2}{\rightleftharpoons}} E\bullet AA\bullet ATP$$

$$E\bullet AA\bullet ATP \underset{k_{-3}}{\overset{k_3}{\rightleftharpoons}} E\bullet AA\sim AMP + PPi$$

$$\frac{d[ATP^*]}{dt} = \frac{d[PPi^*]}{dt} = 0 = -k_3[X^*] + k_{-3}[PPi^*][E\bullet AA\sim AMP] \quad \text{.....(1)}$$

$$\frac{d[E\bullet AA]}{dt} = 0 = k_1[E][AA] + k_{-2}[X^*] - k_{-1}[E\bullet AA] - k_2[ATP^*][E\bullet AA] \quad \text{.....(2)}$$

$$\frac{d[X^*]}{dt} = 0 = k_2[ATP^*][E\bullet AA] + k_{-3}[PPi^*][E\bullet AA\sim AMP] - k_{-2}[X^*] - k_3[X^*] \quad \text{.....(3)}$$

from (2)

$$0 = k_1[E][AA] + k_{-2}[X^*] - (k_{-1} + k_2[ATP^*])[E\bullet AA]$$

$$[E\bullet AA] = \frac{k_1[E][AA] + k_{-2}[X^*]}{k_{-1} + k_2[ATP^*]} \quad \text{.....(4)}$$

Subsutituting (4) into (3) gives

$$0 = k_2[ATP^*]\left(\frac{k_1[E][AA] + k_{-2}[X^*]}{k_{-1} + k_2[ATP^*]}\right) + k_{-3}[PPi^*][E\bullet AA\sim AMP] - k_{-2}[X^*] - k_3[X^*]$$

$$[X^*]\left\{k_{-1}k_{-2}+k_{-1}k_3+\left(k_2k_{-2}+k_2k_3-k_2k_{-2}\right)[ATP^*]\right\}$$

$$=k_1k_2[E][AA][ATP^*]+k_{-1}k_{-3}[PPi^*][E\bullet AA\sim AMP]$$

$$+k_2k_{-3}[ATP^*][PPi^*].....(5)$$

When t=0, $[ATP^*]=0$, (5) gives

$$[X^*]=\frac{k_{-3}[PPi^*][E\bullet AA\sim AMP]}{k_{-2}+k_3}.....(6)$$

Substituting (6) into (1) gives

$$\left.\frac{d[\mathrm{ATP}^*]}{dt}\right|_{t=0} = \left.\frac{d[\mathrm{PPi}^*]}{dt}\right|_{t=0} = -k_3[\mathrm{X}^*] + k_{-3}[\mathrm{PPi}^*][\mathrm{E}\bullet\mathrm{AA}\sim\mathrm{AMP}]$$

$$= \frac{k_{-2}k_{-3}[\mathrm{PPi}^*][\mathrm{E}\bullet\mathrm{AA}\sim\mathrm{AMP}]}{k_{-2}+k_3} \quad \ldots\ldots(7)$$

$$R_o = \frac{[\mathrm{PPi}^*]}{[\mathrm{PPi}]}$$

$$v = \frac{\left.\frac{d[\mathrm{ATP}^*]}{dt}\right|_{t=0}}{R_o} = \frac{1}{R_o}\frac{k_{-2}k_{-3}[\mathrm{PPi}^*][\mathrm{E}\bullet\mathrm{AA}\sim\mathrm{AMP}]}{k_{-2}+k_3}$$

$$= \frac{[\mathrm{PPi}]}{[\mathrm{PPi}^*]}\frac{k_{-2}k_{-3}[\mathrm{PPi}^*][\mathrm{E}\bullet\mathrm{AA}\sim\mathrm{AMP}]}{k_{-2}+k_3}$$

$$= \frac{k_{-2}k_{-3}[\mathrm{PPi}][\mathrm{E}\bullet\mathrm{AA}\sim\mathrm{AMP}]}{k_{-2}+k_3}$$

$$= \frac{k_{-2}k_{-3}}{k_{-2}+k_3}[\mathrm{PPi}][\mathrm{E}\bullet\mathrm{AA}\sim\mathrm{AMP}]$$

$$= k_{app}[\mathrm{PPi}][\mathrm{E}\bullet\mathrm{AA}\sim\mathrm{AMP}]$$

$$\therefore k_{app} = \frac{k_{-2}k_{-3}}{k_{-2}+k_3}$$

$$[\mathrm{E}]_0 = [\mathrm{E}] + [\mathrm{E}\bullet\mathrm{AA}] + [\mathrm{X}] + [\mathrm{E}\bullet\mathrm{AA}\sim\mathrm{AMP}]$$

$$= [\mathrm{E}\bullet\mathrm{AA}\sim\mathrm{AMP}]\left(\frac{[\mathrm{E}]+[\mathrm{E}\bullet\mathrm{AA}]+[\mathrm{X}]}{[\mathrm{E}\bullet\mathrm{AA}\sim\mathrm{AMP}]}+1\right) \quad \ldots\ldots\ldots\ldots(8)$$

$$v = k_{app}[\mathrm{PPi}][\mathrm{E}\bullet\mathrm{AA}\sim\mathrm{AMP}] \quad \ldots\ldots\ldots\ldots(9)$$

from (8) , (9)

$$\frac{[\mathrm{E}]_0}{v} = \frac{1}{k_{app}}\left(\frac{[\mathrm{E}]+[\mathrm{E}\bullet\mathrm{AA}]+[\mathrm{X}]}{[\mathrm{PPi}][\mathrm{E}\bullet\mathrm{AA}\sim\mathrm{AMP}]}+\frac{1}{[\mathrm{PPi}]}\right) \quad \ldots\ldots\ldots\ldots(10)$$

$$K_{eq} = \frac{[\mathrm{E}][\mathrm{AA}][\mathrm{ATP}]}{[\mathrm{PPi}][\mathrm{E}\bullet\mathrm{AA}\sim\mathrm{AMP}]}$$

$$K_{AA} = \frac{[\mathrm{E}][\mathrm{AA}]}{[\mathrm{E}\bullet\mathrm{AA}]}$$

$$K_X = \frac{[\mathrm{PPi}][\mathrm{E}\bullet\mathrm{AA}\sim\mathrm{AMP}]}{[\mathrm{X}]}$$

$$\frac{[E]}{[PPi][E \bullet AA \sim AMP]} = \frac{K_{eq}}{[AA][ATP]} \text{.....(11)}$$

$$\frac{[E \bullet AA]}{[PPi][E \bullet AA \sim AMP]} = \frac{K_{eq}}{K_{AA}} \frac{1}{[ATP]} \text{.....(12)}$$

$$\frac{[X]}{[PPi][E \bullet AA \sim AMP]} = \frac{1}{K_X} \text{.....(13)}$$

Substituting (11), (12), (13) into (10) gives

$$\frac{[E]_0}{v} = \frac{1}{k_{app}}\left(\frac{1}{K_X} + \frac{1}{[PPi]} + \frac{K_{eq}}{K_{AA}[ATP]} + \frac{K_{eq}}{[AA][ATP]}\right)$$

$$\frac{1}{v} = \frac{1}{k_{app}K_X[E]_0}\left(1 + \frac{K_X}{[PPi]} + \frac{K_X K_{eq}}{K_{AA}[ATP]} + \frac{K_X K_{eq}}{[AA][ATP]}\right)$$

$$= \frac{1}{\Phi_1}\left(\frac{\Phi_2}{[PPi]} + \frac{\Phi_3}{[ATP]} + \frac{\Phi_4}{[AA][ATP]}\right)$$

$$\Phi_1 = k_{app}K_X[E]_0$$

$$\Phi_2 = K_X$$

$$\Phi_3 = \frac{K_X K_{eq}}{K_{AA}}$$

$$\Phi_4 = K_X K_{eq}$$

$$\frac{1}{v} = \frac{1}{\Phi_1}\left(\frac{\Phi_2}{[PPi]} + \frac{\Phi_3}{[ATP]} + \frac{\Phi_4}{[AA][ATP]}\right) \text{.....(14)}$$

When S is AA, (14) is presented below in this form

$$\frac{1}{v} = \left(\frac{1}{\Phi_1}\frac{\Phi_4}{[ATP]}\right)\frac{1}{[AA]} + \frac{1}{\Phi_1}\left(1 + \frac{\Phi_2}{[PPi]} + \frac{\Phi_3}{[ATP]}\right) \text{.....(15)}$$

When S is ATP, (14) is presented below in this form

$$\frac{1}{v} = \frac{1}{\Phi_1}\left(\Phi_3 + \frac{\Phi_4}{[AA]}\right)\frac{1}{[ATP]} + \frac{1}{\Phi_1}\left(1 + \frac{\Phi_2}{[PPi]}\right) \text{.....(16)}$$

Inhibition studies

(A) Inhibition patterns in the presence of cadaverine as analogue of L-lysine

$$[E]_0 = [E] + [E \bullet I] + [E \bullet AA] + [X] + [E \bullet AA \sim AMP] \quad \text{.....(17)}$$

$$K_i = \frac{[E][I]}{[E \bullet I]} \quad \text{.....(18)}$$

from (17), (18)

$$[E]_0 = [E] + \frac{[E][I]}{K_i} + [E \bullet AA] + [X] + [E \bullet AA \sim AMP]$$

$$= [E]\left(\frac{1+[I]}{K_i}\right) + [E \bullet AA] + [X] + [E \bullet AA \sim AMP]$$

$$= [E \bullet AA \sim AMP]\left\{\frac{[E]\left(\frac{1+[I]}{K_i}\right) + [E \bullet AA] + [X]}{[E \bullet AA \sim AMP]} + 1\right\} \quad \text{.....(19)}$$

from (9), (19)

$$\frac{[E]_0}{v} = \frac{1}{k_{app}}\left\{\frac{[E]\left(\frac{1+[I]}{K_i}\right) + [E \bullet AA] + [X]}{[PPi][E \bullet AA \sim AMP]} + \frac{1}{[PPi]}\right\}$$

$$= \frac{1}{k_{app}}\left\{\frac{1}{K_X} + \frac{1}{[PPi]} + \frac{K_{eq}}{K_{AA}[ATP]} + \frac{K_{eq}\left(\frac{1+[I]}{K_i}\right)}{[AA][ATP]}\right\}$$

$$\frac{1}{v} = \frac{1}{k_{app}K_X[E]_0}\left\{1 + \frac{K_X}{[PPi]} + \frac{K_{eq}K_X}{K_{AA}[ATP]} + \frac{K_{eq}K_X\left(\frac{1+[I]}{K_i}\right)}{[AA][ATP]}\right\}$$

$$= \frac{1}{\Phi_1}\left\{1 + \frac{\Phi_2}{[PPi]} + \frac{\Phi_3}{[ATP]} + \frac{\Phi_4\left(\frac{1+[I]}{K_i}\right)}{[AA][ATP]}\right\} \quad \text{.....(20)}$$

When S is AA, (20) is presented below in this form

$$\frac{1}{v}=\left(\frac{1}{\Phi_1}\frac{\Phi_4}{[ATP]}\right)\left(\frac{1+[I]}{K_i}\right)\frac{1}{[AA]}+\frac{1}{\Phi_1}\left(\frac{\Phi_2}{[PPi]}+\frac{\Phi_3}{[ATP]}\right).....(21)$$

When S is ATP, (20) is presented below in this form

$$\frac{1}{v}=\frac{1}{\Phi_1}\left\{\Phi_3+\frac{\Phi_4\left(\frac{1+[I]}{Ki}\right)}{[AA]}\right\}\frac{1}{[ATP]}+\frac{1}{\Phi_1}\left(1+\frac{\Phi_2}{[PPi]}\right).....(22)$$

(A) Inhibition patterns in the presence of adenosine as analogue of ATP

$$[E]_0=[E]+[E\bullet AA]+[E\bullet AA\bullet I]+[X]+[E\bullet AA\sim AMP].....(23)$$

$$K_i=\frac{[E\bullet AA][I]}{[E\bullet AA\bullet I]}.....(24)$$

from (23), (24)

$$[E]_0=[E]+[E\bullet AA]+\frac{[E\bullet AA][I]}{K_i}+[X]+[E\bullet AA\sim AMP]$$

$$=[E]+[E\bullet AA]\left(1+\frac{[I]}{K_i}\right)+[X]+[E\bullet AA\sim AMP]$$

$$=[E\bullet AA\sim AMP]\left\{\frac{[E]+[E\bullet AA]\left(1+\frac{[I]}{Ki}\right)+[X]}{[E\bullet AA\sim AMP]}+1\right\}.....(25)$$

from (9), (25)

$$\frac{[E]_0}{v}=\frac{1}{k_{app}}\left\{\frac{[E]+[E\bullet AA]\left(1+\frac{[I]}{Ki}\right)+[X]}{[PPi][E\bullet AA\sim AMP]}+\frac{1}{[PPi]}\right\}$$

$$=\frac{1}{k_{app}}\left\{\frac{1}{K_X}+\frac{1}{[PPi]}+\frac{K_{eq}\left(\frac{1+[I]}{K_i}\right)}{K_{AA}[ATP]}+\frac{K_{eq}}{[AA][ATP]}\right\}$$

$$\frac{1}{v}=\frac{1}{k_{app}K_X[E]_0}\left\{1+\frac{K_X}{[PPi]}+\frac{K_{eq}K_X\left(\frac{1+[I]}{K_i}\right)}{K_{AA}[ATP]}+\frac{K_{eq}K_X}{[AA][ATP]}\right\}$$

$$=\frac{1}{\Phi_1}\left\{1+\frac{\Phi_2}{[PPi]}+\frac{\Phi_3\left(\frac{1+[I]}{K_i}\right)}{[ATP]}+\frac{\Phi_4}{[AA][ATP]}\right\}.....(26)$$

When S is AA, (26) is presented below in this form

$$\frac{1}{v}=\left(\frac{1}{\Phi_1}\frac{\Phi_4}{[ATP]}\right)\frac{1}{[AA]}+\frac{1}{\Phi_1}\left\{1+\frac{\Phi_2}{[PPi]}+\frac{\Phi_3\left(\frac{1+[I]}{K_i}\right)}{[ATP]}\right\}.....(27)$$

When S is ATP, (26) is presented below in this form

$$\frac{1}{v}=\frac{1}{\Phi_1}\left\{\Phi_3\left(\frac{1+[I]}{K_i}\right)+\frac{\Phi_4}{[AA]}\right\}\frac{1}{[ATP]}+\frac{1}{\Phi_1}\left\{1+\frac{\Phi_2}{[PPi]}\right\}.....(28)$$

Kinetic analysis of ATP-PPi exchange reaction catalyzed by LysRS

Rate patterns

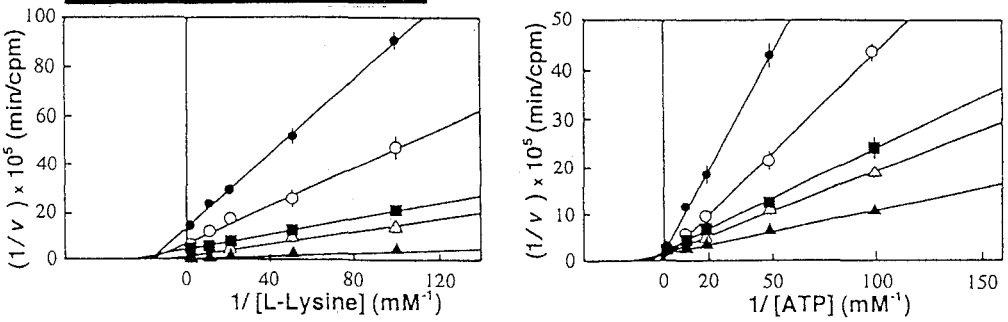

Inhibition patterns with cadaverine

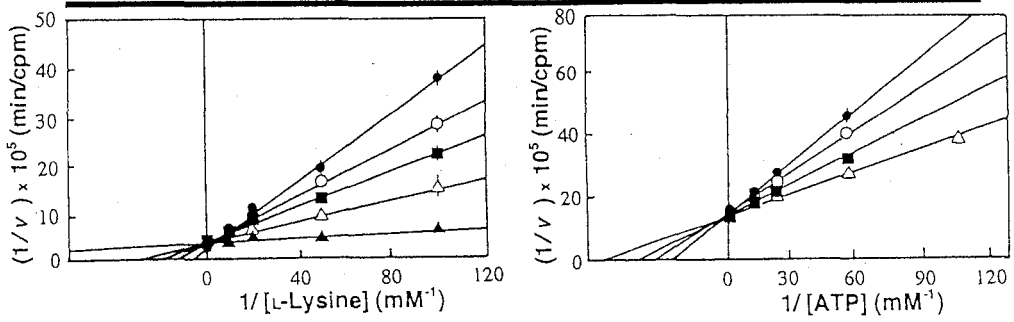

Inhibition patterns with adenosine

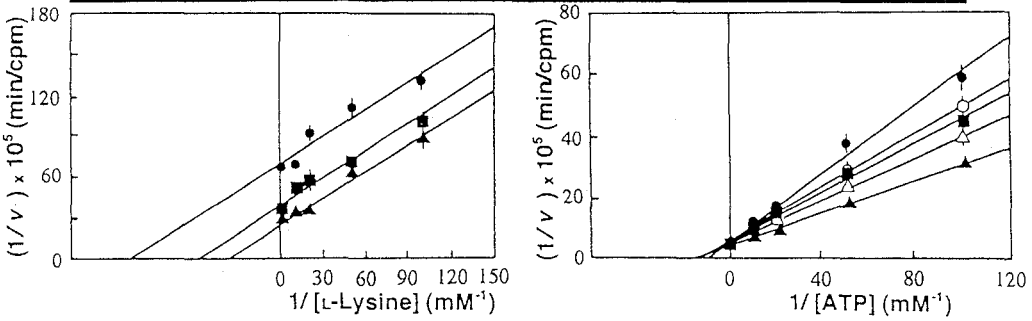

Appendix 2

Fluorometric Titration for the Two Substrate Reaction

We assume the following equations the *B.s.* LysRS reaction based on Equation 3, 4, and 5, and on the above disscussed asumptions. In these equations, L stands for either L-lysine or L-lysine analogues, A_T for ATP, and A_M for AMP.

$$K_1 = [E][L]/[EL] \quad \text{.....(9)}$$

$$K_2 = [EL][A_T]/[ELA_T] \quad \text{.....(10)}$$

$$K_3 = [ELA_T]/[ELA_M][PPi] \quad \text{.....(11)}$$

$$[E]_0 = [E] + [EL] + [ELA_T] + [ELA_M] \quad \text{.....(12)}$$

[A]

Under the conditions of $[L]_0 >> [E]_0$ and $[L]_0 >> K_i$, [E] could be nrgligialy small, and Equation 12 will be

$$[E]_0 = [EL] + [ELA_T] + [ELA_M]$$

$$\Delta F(\%) = \left(\frac{F_t - F_0}{F_{E,0}}\right) \times 100$$

where $F_t = f_{EL}[EL] + f_{ELAT}[ELA_T] + f_{ELAM}[ELA_M]$

$$F_0 = f_{EL}[EL] \quad ; \quad F_{E,0} = f_E[E]_0$$

and f_x's are the proportional constants for the fluorescence emission of the respective enzyme species in regard to their concentration. Accordingly,

$$\Delta F(\%) = 100 \times \left(\frac{f_{EL}[EL] + f_{ELAT}[ELA_T] + f_{ELAM}[ELA_M] - f_{EL}[EL]_0}{f_E[E]_0} \right)$$

$$= 100 \times \left\{ \frac{f_{EL}([EL] - [EL]_0)}{f_E[E]_0} + \frac{f_{ELAT}[ELA_T]}{f_E[E]_0} + \frac{f_{ELAM}[ELA_M]}{f_E[E]_0} \right\}$$

$$= 100 \times \left\{ \frac{f_{EL}(-[ELA_T])}{f_E[E]_0} - \frac{f_{EL}[ELA_M]}{f_E[E]_0} + \frac{f_{ELAT}[ELA_T]}{f_E[E]_0} + \frac{f_{ELAM}[ELA_M]}{f_E[E]_0} \right\}$$

$$= 100 \times \left\{ \frac{[ELA_T]}{[E]_0} \left(\frac{f_{ELAT}}{f_E} - \frac{f_{EL}}{f_E} \right) + \frac{[ELA_M]}{[E]_0} \left(\frac{f_{ELAM}}{f_E} - \frac{f_{EL}}{f_E} \right) \right\}$$

$$= 100 \times \left\{ \frac{[EL][ATP]}{K_2[E]_0} \left(\frac{f_{ELAT}}{f_E} - \frac{f_{EL}}{f_E} \right) + \frac{[EL][ATP]}{K_2 K_3[E]_0[PPi]} \left(\frac{f_{ELAM}}{f_E} - \frac{f_{EL}}{f_E} \right) \right\}$$

$$= 100 \times \frac{[EL][ATP]}{K_2[E]_0} \left\{ \left(\frac{f_{ELAT}}{f_E} - \frac{f_{EL}}{f_E} \right) + \frac{1}{K_3[PPi]} \left(\frac{f_{ELAM}}{f_E} - \frac{f_{EL}}{f_E} \right) \right\}$$

$$\frac{[EL]}{[E]_0} = \frac{[EL]}{[EL] + [ELA_T] + [ELA_M]}$$

$$= \frac{[EL]}{[EL] + \frac{[EL][ATP]}{K_2} + \frac{[EL][ATP]}{K_2 K_3[PPi]}}$$

$$= \frac{K_2 K_3[PPi]}{K_2 K_3[PPi] + [ATP](K_3[PPi] + 1)}$$

Since ΔF_{max} for those substartes of the ATP-PPi exchange reaction, L-lysine, SAEC, and threo-4-hydroxy-L-lysine, and ΔF_{max} for those inhibitors in which α-carboxyl group is modified, cadaverine, L-Lyshxt, L-Lysamd, are essentially similar (Table I), we can reasonably assume that the fluorescence change observed by the adding of ATP takes place mainly at the step E•L•A_T complex formation (Equation 7) rather than E•L•A_M formation (Equation 8). Those inhibitors are supposed not to react with ATP to form an aminoacyladenylate. Accordingly,

$$f_{ELAT} = f_{ELAM}$$

$$\left(\frac{f_{ELAT} - f_{EL}}{f_E}\right) \times 100 = \left(\frac{f_{ELAM} - f_{EL}}{f_E}\right) \times 100 \equiv \Delta F_{A,\,max}$$

From (A-2), (A-3), and (A-4)

$$\Delta F(\%) = \frac{K_2 K_3[PPi][ATP]}{K_2 K_3[PPi] + [ATP](K_3[PPi]+1)K_2}\left(1 + \frac{1}{K_3[PPi]}\right)\Delta F_{A,\,max}$$

$$= \frac{\Delta F_{A,\,max}[ATP](K_3[PPi]+1)}{K_2 K_3[PPi] + [ATP](K_3[PPi]+1)}$$

$$= \frac{\Delta F_{A,\,max}[ATP]_0}{\left(\frac{K_2 K_3[PPi]}{K_3[PPi]+1}\right) + [ATP]_0}$$

$$[ATP]_0 \gg [E]_0 \quad \therefore [ATP] \approx [ATP]_0$$

$$K_{d,\,app,\,A} = \frac{K_2 K_3[PPi]}{K_3[PPi]+1}$$

[B]

When L is added to *B.s.* LysRS in the presence of excess amount of ATP, molecular species EA_T does not exsist due to the order of substrate binding, and the molecular species EL would not be exsist either because as soon as EL was formed ATP should be bound to EL when $[ATP]_0 >> K_2$. Thus,

$$[E]_0 = [E] + [ELA_T] + [ELA_M]$$

$$\Delta F(\%) = \left(\frac{F_t - F_0}{F_{E,0}}\right) \times 100$$

$$= 100\left(\frac{f_E[E] + f_{ELAT}[ELA_T] + f_{ELAM}[ELA_M] - f_E[E]_0}{f_E[E]_0}\right)$$

$$= 100\left(\frac{f_E([E] - [E]_0)}{f_E[E]_0} + \frac{f_{ELAT}[ELA_T] + f_{ELAM}[ELA_M]}{f_E[E]_0}\right)$$

$$= 100\left(\frac{f_E(-[ELA_T] - [ELA_M])}{f_E[E]_0} + \frac{f_{ELAT}[ELA_T] + f_{ELAM}[ELA_M]}{f_E[E]_0}\right)$$

$$= 100\left\{\frac{(f_{ELAT} - f_E)[ELA_T]}{f_E[E]_0} + \frac{(f_{ELAM} - f_E)[ELA_M]}{f_E[E]_0}\right\}$$

Since we can assume as previously mentioned that $f_{ELA_T} = f_{ELA_M}$, then

$$\frac{(f_{ELAT} - f_E)}{f_E} \times 100 = \frac{(f_{ELAM} - f_E)}{f_E} \times 100 = \Delta F_{LA,\,max}$$

$$\Delta F(\%) = \Delta F_{LA,max}\left(\frac{[ELA_T]}{[E]_0} + \frac{[ELA_M]}{[E]_0}\right)$$

$$= \Delta F_{LA,max}\left(\frac{[ELA_T] + [ELA_M]}{[E] + [ELA_T] + [ELA_M]}\right)$$

$$= \Delta F_{LA,max}\left(\frac{\frac{[EL][ATP]}{K_2} + \frac{[EL][ATP]}{K_2K_3[PPi]}}{\frac{K_1[EL]}{[L]} + \frac{[EL][ATP]}{K_2} + \frac{[EL][ATP]}{K_2K_3[PPi]}}\right)$$

$$= \Delta F_{LA,max}\left\{\frac{\frac{[ATP]}{K_2}\left(1 + \frac{1}{K_3[PPi]}\right)}{\frac{K_1}{[L]} + \frac{[ATP]}{K_2}\left(1 + \frac{1}{K_3[PPi]}\right)}\right\}$$

$$= \frac{\Delta F_{LA,max}[L]}{\left\{\frac{K_1K_2K_3[PPi]}{(K_3[PPi]+1)[ATP]}\right\} + [L]}$$

Since $[ATP]_0 >> [E]_0$, $[ATP] \approx [ATP]_0$

(When $[L] >> [E]_0$, $[L] = [L]_0$)

$$K_{d,app,L} = \frac{K_1K_2K_3[PPi]}{(K_3[PPi]+1)[ATP]_0}$$

$$K_{d,app,L} / K_d = \frac{K_2K_3[PPi]}{(K_3[PPi]+1)[ATP]_0}$$

[C]

When L is added to the mixture of *B.s.* LysRS and ATP under the conditions that $[ATP]_0 >> [E]_0$ but $[ATP]_0 >> K_2$ does not hold, the molecular species of EL has to be taken into consideration: therefore,

$$[E]_0 = [E] + [EL] + [ELA_T] + [ELA_M]$$

$$\Delta F(\%) = \left(\frac{F_t - F_0}{F_0}\right) \times 100$$

$$= 100 \times \left(\frac{f_E[E] + f_{EL}[EL] + f_{ELAT}[ELA_T] + f_{ELAM}[ELA_M] - f_E[E]_0}{f_E[E]_0}\right)$$

$$= 100 \times \left(\frac{(f_{EL} - f_E)[EL] + (f_{ELAT} - f_E)[ELA_T] + (f_{ELAM} - f_E)[ELA_M]}{f_E[E]_0}\right)$$

As described in the previous section, we can assume that $f_{ELA_T} = f_{ELA_M} \equiv f_{ELA}$; accordingly,

$$\Delta F(\%) = 100 \times \left\{\frac{(f_{EL} - f_E)[EL] + (f_{ELA} - f_E)([ELA_T] + [ELA_M])}{f_E[E]_0}\right\}$$

$$= 100 \times \frac{(f_{EL} - f_E)}{f_E}\left\{\frac{[EL] + \frac{(f_{ELA} - f_E)}{(f_{EL} - f_E)}([ELA_T] + [ELA_M])}{[E]_0}\right\}$$

$$100 \times \frac{(f_{EL} - f_E)}{f_E} = \Delta F_{max,L}$$

$$\frac{(f_{ELA} - f_E)}{(f_{EL} - f_E)} = \frac{\Delta F_{max,LA}}{\Delta F_{max,L}} = \Delta F'$$

$$\Delta F(\%) = \Delta F_{max,L}\left\{\frac{[EL] + \Delta F'([ELA_T] + [ELA_M])}{[E]_0}\right\}$$

$$K_1 = \frac{[E][L]}{[EL]}$$

$$K_2 = \frac{[EL][ATP]}{[ELA_T]}$$

$$K_3 = \frac{[ELA_T]}{[ELA_M][PPi]} = \frac{[EL][ATP]}{K_2[ELA_M][PPi]}$$

$$\Delta F(\%) = \Delta F_{max,L}\left\{\frac{[EL] + \Delta F'([ELA_T] + [ELA_M])}{[E]_0}\right\}$$

$$= \Delta F_{max,L}\frac{[EL]}{[E]_0}\left\{1 + \Delta F'\left(\frac{[ATP]}{K_2} + \frac{[ATP]}{K_2K_3[PPi]}\right)\right\}$$

$$= \Delta F_{max,L}\frac{[EL]}{[E]_0}\left\{\frac{K_2K_3[PPi] + \Delta F'[ATP](1 + K_3[PPi])}{K_2K_3[PPi]}\right\}$$

$$\frac{[EL]}{[E]_0} = \frac{[EL]}{[E] + [EL] + [ELA_T] + [ELA_M]}$$

$$= \frac{1}{\frac{K_1}{[L]} + 1 + \frac{[ATP]}{K_2} + \frac{[ATP]}{}}$$

$$= \frac{K_2K_3[L][PPi]}{K_1K_2K_3[PPi] + K_2K_3[L][PPi] + K_3[L][PPi][ATP] + [L][ATP]}$$

$$\Delta F(\%) = \Delta F_{max,L}\left[\frac{\{K_2K_3[PPi] + \Delta F'[ATP](1 + K_3[PPi])\}[L]}{K_1K_2K_3[PPi] + \{K_2K_3[PPi] + [ATP](K_3[PPi] + 1)\}[L]}\right]$$

$$\Delta F_{max,L} \bullet \Delta F = \Delta F_{max,LA}$$

$$\Delta F(\%) = \frac{\left\{\frac{\Delta F_{max,L}K_2K_3[PPi] + \Delta F_{max,LA}[ATP](1 + K_3[PPi])}{K_2K_3[PPi] + [ATP](K_3[PPi] + 1)}\right\}[L]}{\left(\frac{K_1K_2K_3[PPi]}{K_2K_3[PPi] + [ATP](K_3[PPi] + 1)}\right) + [L]}$$

Since $[ATP]_0 >> [E]_0$, $[ATP] = [ATP]_0$

$$\Delta F(\%) = \frac{\Delta F_{max,K} \bullet [L]}{K_{d,app,LA} + [L]}$$

$$K_{d,app,LA} = \frac{K_1 K_2 K_3 [PPi]}{K_2 K_3 [PPi] + [ATP]_0 (K_3 [PPi] + 1)}$$

$$\Delta F_{max,K} = \frac{\Delta F_{max,L} K_2 K_3 [PPi] + \Delta F_{max,LA} [ATP]_0 (1 + K_3 [PPi])}{K_2 K_3 [PPi] + [ATP]_0 (K_3 [PPi] + 1)}$$

$$= \frac{\Delta F_{max,L}}{1 + \left(\frac{1 + K_3 [PPi]}{K_2 K_3 [PPi]}\right)[ATP]_0} + \frac{\Delta F_{max,LA}}{1 + \frac{K_2 K_3 [PPi]}{(1 + K_3 [PPi])[ATP]_0}}$$

$$= \frac{\Delta F_{max,L}}{1 + \frac{K_1}{K_{d,app,L}}} + \frac{\Delta F_{max,LA}}{1 + \frac{K_{d,app,L}}{K_1}}$$

$$= \frac{\Delta F_{max,L} \bullet K_{d,app,L} + \Delta F_{max,LA} \bullet K_1}{K_1 + K_{d,app,L}}$$

Appendix 3
Kinetic Analysis of the Stopped-Flow Reaction Binding of ATP to the Enzyme•L-Lysine Complex

$$\mathrm{E\cdot AA + ATP} \underset{k_{-1}}{\overset{k_{+1}}{\Leftrightarrow}} \mathrm{E\cdot AA \sim AMP + PPi}$$

$$\mathrm{A + B} \Leftrightarrow \mathrm{C + D}$$

$$\mathrm{cA} = \underline{\mathrm{cA}} - \Delta\mathrm{c}$$
$$\mathrm{cB} = \underline{\mathrm{cB}} - \Delta\mathrm{c}$$
$$\mathrm{cC} = \underline{\mathrm{cC}} - \Delta\mathrm{c}$$
$$\mathrm{cD} = \underline{\mathrm{cD}} + \Delta\mathrm{c}$$

$$\underline{\mathrm{cA}} = \underline{\mathrm{cB}} = \underline{\mathrm{cC}} = \underline{\mathrm{cD}}$$

$$-d\mathrm{cA}/d\mathrm{t} = -d\mathrm{cB}/d\mathrm{t} = d\mathrm{cC}/d\mathrm{t} = d\mathrm{cD}/d\mathrm{t}$$
$$= \mathrm{k}_{+1}\mathrm{cAcB} - \mathrm{k}_{-1}\mathrm{cCcD}$$

$$d\Delta\mathrm{c}/d\mathrm{t} = k_{+1}(\underline{\mathrm{cA}} - \Delta\mathrm{c})(\underline{\mathrm{cB}} - \Delta\mathrm{c}) - k_{-1}(\underline{\mathrm{cC}} + \Delta\mathrm{c})(\underline{\mathrm{cD}} + \Delta\mathrm{c})$$
$$= k_{+1}\{\underline{\mathrm{cAcB}} - (\underline{\mathrm{cA}} + \underline{\mathrm{cB}})\Delta\mathrm{c} + \Delta\mathrm{c}^2\}$$
$$- k_{-1}\{\underline{\mathrm{cCcD}} + (\underline{\mathrm{cC}} + \underline{\mathrm{cD}})\Delta\mathrm{c} + \Delta\mathrm{c}^2\}$$
$$= (k_{+1}\underline{\mathrm{cAcB}} - k_{-1}\underline{\mathrm{cCcD}}) - \{k_{+1}(\underline{\mathrm{cA}} + \underline{\mathrm{cB}})$$
$$+ k_{-1}(\underline{\mathrm{cC}} + \underline{\mathrm{cD}})\}\Delta\mathrm{c} + (\mathrm{k}_{+1} - \mathrm{k}_{-1})\Delta\mathrm{c}^2$$

$(k_{+1}\underline{\mathrm{cAcB}} = k_{-1}\underline{\mathrm{cCcD}})$

$$= 0 - \{k_{+1}(\underline{\mathrm{cA}} + \underline{\mathrm{cB}}) + k_{-1}(\underline{\mathrm{cC}} + \underline{\mathrm{cD}})\}\Delta\mathrm{c} + (k_{+1} - k_{-1})\Delta\mathrm{c}^2$$
$$= -\{k_{+1}(\underline{\mathrm{cA}} + \underline{\mathrm{cB}}) + k_{-1}(\underline{\mathrm{cC}} + \underline{\mathrm{cD}})\}\Delta\mathrm{c} + (k_{+1} - k_{-1})\Delta\mathrm{c}^2$$

$(\underline{\mathrm{cB}} >> \Delta\mathrm{c})$

$$= -\{k_{+1}(\underline{\mathrm{cA}} + \underline{\mathrm{cB}}) + k_{-1}(\underline{\mathrm{cC}} + \underline{\mathrm{cD}})\}\Delta\mathrm{c}$$

$$-d\Delta\mathrm{c}/d\mathrm{t} = \{k_{+1}(\underline{\mathrm{cA}} + \underline{\mathrm{cB}}) + k_{-1}(\underline{\mathrm{cC}} + \underline{\mathrm{cD}})\}\Delta\mathrm{c}$$
$$= \Delta\mathrm{c}/\mathrm{t}$$

$$1/t = k_{+1}(\underline{cA} + \underline{cB}) + k_{-1}(\underline{cC} + \underline{cD})$$

$(\underline{cB} >> \underline{cA}, \quad \underline{cD} >> \underline{cC})$

$$= k_{+1}\underline{cB} + k_{-1}\underline{cD}$$

$(\underline{cB} = cB_0, \quad \underline{cD} = cD_0)$

$$= k_{+1}cB_0 + k_{-1}cD_0$$

$(1/t = Y, \quad cB_0 = X)$

$$1/t = k_{+1}cB_0 + k_{-1}cD_0$$

$$Y = k_{+1}X + k_{-1}cD_0$$

$$\text{slope} = k_{+1}$$

$$\text{intercept} = k_{-1}cD_0$$

$(cD_0 = \text{constant})$

$$= k_{-1}.\text{constant}$$

$$\mathrm{E\cdot AA^{*}+ATP} \underset{k_{-1}}{\overset{k_{+1}}{\Leftrightarrow}} \mathrm{E\cdot AA\cdot ATP} \underset{k_{-2}}{\overset{k_{+2}}{\Leftrightarrow}} \mathrm{E\cdot AA-AMP+PPi}$$

$$\mathrm{A+B \Leftrightarrow Y \Leftrightarrow C+D}$$

$$\mathrm{cA} = \underline{\mathrm{cA}} - \Delta\mathrm{cA}$$
$$\mathrm{cB} = \underline{\mathrm{cB}} - \Delta\mathrm{cB}$$
$$\mathrm{cY} = \underline{\mathrm{cY}} - \Delta\mathrm{cY}$$
$$\mathrm{cC} = \underline{\mathrm{cC}} - \Delta\mathrm{cC}$$
$$\mathrm{cD} = \underline{\mathrm{cD}} - \Delta\mathrm{cD}$$

$$\Delta\mathrm{cA} = \Delta\mathrm{cB} = \underline{\mathrm{cA}} - \mathrm{cA} = \underline{\mathrm{cB}} - \mathrm{cB}$$
$$\Delta\mathrm{cY} = \underline{\mathrm{cY}} - \mathrm{cY}$$
$$\Delta\mathrm{cC} = \Delta\mathrm{cD} = \underline{\mathrm{cC}} - \mathrm{cC} = \underline{\mathrm{cD}} - \mathrm{cD}$$
$$-d\mathrm{cA}/d\mathrm{t} = -d\mathrm{cB}/d\mathrm{t} = k_{+1}\mathrm{cAcB} - k_{-1}\mathrm{cY}$$
$$-\Delta\mathrm{cA}/d\mathrm{t} = -\Delta\mathrm{cB}/d\mathrm{t} = k_{+1}\left(\underline{\mathrm{cA}} - \Delta\mathrm{cA}\right)\left(\underline{\mathrm{cB}} - \Delta\mathrm{cB}\right) - k_{-1}\left(\underline{\mathrm{cY}} - \Delta\mathrm{cY}\right)$$
$$= k_{+1}\left(\underline{\mathrm{cAcB}} - \underline{\mathrm{cA}}\Delta\mathrm{cB} - \Delta\mathrm{cA}\,\underline{\mathrm{cB}} + \Delta\mathrm{cA}\Delta\mathrm{cB}\right) - k_{-1}\left(\underline{\mathrm{cY}} - \Delta\mathrm{cY}\right)$$
$$\left(\Delta\mathrm{cA} = \Delta\mathrm{cB}\right) \quad = k_{+1}\left\{\underline{\mathrm{cAcB}} - \Delta\mathrm{cA}\left(\underline{\mathrm{cA}} + \underline{\mathrm{cB}}\right) + \Delta\mathrm{cA}^{2}\right\} - k_{-1}\left(\underline{\mathrm{cY}} - \Delta\mathrm{cY}\right)$$
$$\left(\underline{\mathrm{cB}} >> \Delta\mathrm{cA}\right) \quad = k_{+1}\left\{\underline{\mathrm{cAcB}} - \Delta\mathrm{cA}\left(\underline{\mathrm{cA}} + \underline{\mathrm{cB}}\right)\right\} - k_{-1}\left(\underline{\mathrm{cY}} - \Delta\mathrm{cY}\right)$$
$$\left(k_{+1}\underline{\mathrm{cAcB}} = k_{-1}\underline{\mathrm{cY}}\right) \quad = -k_{+1}\left(\underline{\mathrm{cA}} + \underline{\mathrm{cB}}\right)\Delta\mathrm{cA} + k_{-1}\Delta\mathrm{cY}$$

$$dcY/dt = k_{+1}cAcB + k_{-2}cCcD(k_{-1} + k_{+2})cY$$

$$\Delta cY/dt = k_{+1}(\underline{cA} - \Delta cA)(\underline{cB} - \Delta cB) + k_{-2}(\underline{cC} - \Delta cC)(\underline{cD} - \Delta cD)$$
$$-(k_{-1} + k_{+2})(\underline{cY} - \Delta cY)$$
$$= k_{+1}(\underline{cAcB} - \underline{cA}\Delta cB - \underline{cB}\Delta cA + \Delta cA\Delta cB)$$
$$+ k_{-2}(\underline{cCcD} - \underline{cC}\Delta cD - \underline{cD}\Delta cC + \Delta cC\Delta cD)$$
$$-(k_{-1} + k_{+2})(\underline{cY} - \Delta cY)$$

$(\Delta cA = \Delta cB)$

$(\Delta cC = \Delta cD)$

$$= k_{+1}\{\underline{cAcB} - (\underline{cA} + \underline{cB})\Delta cA + \Delta cA^2\}$$
$$+ k_{-2}\{\underline{cCcD} - (\underline{cC} + \underline{cD})\Delta cD + \Delta cD^2\}$$
$$-(k_{-1} + k_{+2})(\underline{cY} - \Delta cY)$$

$(\underline{cB} >> \Delta cA)$

$(\underline{cD} >> \Delta cD)$

$$= k_{+1}\{\underline{cAcB} - (\underline{cA} + \underline{cB})\Delta cA\}$$
$$+ k_{-2}\{\underline{cCcD} - (\underline{cC} + \underline{cD})\Delta cD\} - (k_{-1} + k_{+2})(\underline{cY} - \Delta cY)$$

$(k_{+1}\underline{cAcB} = k_{-1}\underline{cY})$

$(k_{+2}\underline{cY} = k_{-2}\underline{cCcD})$

$$= -k_{+1}(\underline{cA} + \underline{cB})\Delta cA - k_{-2}(\underline{cC} + \underline{cD})\Delta cD + (k_{-1} + k_{+2})\Delta cY$$

$$dcC/dt = dcD/dt = k_{+2}cY - k_{-2}cCcD$$

$$\Delta cC/dt = \Delta cD/dt = k_{+2}\left(\underline{cY} - \Delta cY\right) - k_{-2}\left(\underline{cC} - \Delta cC\right)\left(\underline{cD} - \Delta cD\right)$$

$$= k_{+2}\left(\underline{cY} - \Delta cY\right)$$

$$- k_{-2}\left\{\underline{cCcD} - \underline{cC}\Delta cD - \underline{cD}\Delta cC + \Delta cC\Delta cD\right\}$$

$$\left(\Delta cA = \Delta cB\right)$$

$$\left(\Delta cC = \Delta cD\right) \qquad = k_{+2}\left(\underline{cY} - \Delta cY\right) - k_{-2}\left\{\underline{cCcD} - \left(\underline{cC} + \underline{cD}\right)\Delta cD + \Delta cD^2\right\}$$

$$\left(\underline{cD} >> \Delta cD\right) \qquad = k_{+2}\left(\underline{cY} - \Delta cY\right) - k_{-2}\left\{\underline{cCcD} - \left(\underline{cC} + \underline{cD}\right)\Delta cD\right\}$$

$$\left(k_{+2}\underline{cY} = k_{-2}\underline{cCcD}\right) = -k_{+2}\Delta cY + k_{-2}\left(\underline{cC} + \underline{cD}\right)\Delta cD$$

$$-\Delta cA/dt = -\Delta cB/dt = -k_{+1}\left(\underline{cA} + \underline{cB}\right)\Delta cA + k_{-1}\Delta cY$$

$$\Delta cY/dt = -k_{+1}\left(\underline{cA} + \underline{cB}\right)\Delta cA - k_{-2}\left(\underline{cC} + \underline{cD}\right)\Delta cD + \left(k_{-1} + k_{+2}\right)\Delta cY$$

$$\Delta cC/dt = \Delta cD/dt = -k_{+2}\Delta cY + k_{-2}\left(\underline{cC} + \underline{cD}\right)\Delta cD$$

$$\left(\Delta cA + \Delta cY + \Delta cD = 0\right)$$

$$-\Delta cA/dt = -\Delta cB/dt = -k_{+1}\left(\underline{cA} + \underline{cB}\right)\Delta cA - k_{-1}\left(\Delta cA + \Delta cD\right)$$

$$= \left\{-k_{-1} - k_{+1}\left(\underline{cA} + \underline{cB}\right)\right\}\Delta cA - k_{-1}\Delta cD$$

$$\Delta cC/dt = \Delta cD/dt = k_{+2}\left(\Delta cA + \Delta cD\right) + k_{-2}\left(\underline{cC} + \underline{cD}\right)\Delta cD$$

$$= k_{+2}\Delta cA + \left\{k_{+2} + k_{-2}\left(\underline{cC} + \underline{cD}\right)\right\}\Delta cD$$

$$-\Delta cA / dt = \{-k_{-1} - k_{+1}(\underline{cA} + \underline{cB})\}\Delta cA - k_{-1}\Delta cD$$

$$-dx1 / dt = a11x1 + a22x2$$

$$\Delta cD / dt = k_{+2}\Delta cA + \{k_{+2} + k_{-2}(\underline{cC} + \underline{cD})\}\Delta cD$$

$$-\Delta cD / dt = -k_{+2}\Delta cA - \{k_{+2} + k_{-2}(\underline{cC} + \underline{cD})\}\Delta cD$$

$$-dx2 / dt = a21x1 + a22x2$$

$$Dx1 = dx1 / dt, Dx2 = dx2 / dt$$

$$-dx1 / dt = a11x1 + a12x2$$

$$-Dx1 = a11x1 + a12x2$$

$$0 = (D + a11)x1 + a12x2$$

$$-dx2 / dt = a21x1 + a22x2$$

$$-Dx2 = a21x1 + a22x2$$

$$0 = a21x1 + (D + a22)x2$$

$$[0 = a21(D + a11)x1 + a12a21x2]$$
$$-[0 = a21(D + a11)x1 + (D + a11)(D + a22)x2]$$

$$0 = a12a21x2 - (D + a11)(D + a22)x2$$

$$0 = a12a21x2 - D^2x2 - (a11 + a22)Dx2 - a11a22x2$$

$$D^2x2 + (a11 + a22)Dx2 + (a11a22 - a12a21)x2 = 0$$

$$\lambda^2 + (a11 + a22)\lambda + (a11a22 - a12a21) = 0$$

$$\lambda(\lambda1, \lambda2) = (1/2)[-(a11 + a22) \pm \sqrt{(a11 + a22)^2 - 4(a11a22 - a12a21)}]$$

$$x2 = C_{21}e^{\lambda 1t} + C_{22}e^{\lambda 2t}$$

$$[0 = (D + a11)(D + a22)x1 + a12(D + a22)x2]$$
$$-[0 = a12a21x1 + a12(D + a22)x2]$$

$$0 = D^2x1 + (a11 + a22)Dx1 + a11a22x1 - a12a21x1$$

$$0 = D^2x1 + (a11 + a22)Dx1 + (a11a22 - a12a21)x1$$

$$\lambda^2 + (a11 + a22)\lambda + (a11a22 - a12a21) = 0$$

$$\lambda(\lambda1, \lambda2) = (1/2)[-(a11 + a22) \pm \sqrt{(a11 + a22)^2 - 4(a11a22 - a12a21)}]$$

$$x1 = C_{11}e^{\lambda 1t} + C_{12}e^{\lambda 2t}$$

$$\lambda = 1/(\tau)$$

$$1/(\tau) = (1/2)[-(a11 + a22) \pm \sqrt{(a11 + a22)^2 - 4(a11a22 - a12a21)}]$$

$$\lambda 1 + \lambda 2 = (1/\tau 1) + (1/\tau 2)$$

$$= -(a11 + a22)$$

$$= -\{-k_{-1} - k_{+1}(\underline{cA} + \underline{cB})\} - [-\{k_{+2} + k_{-2}(\underline{cC} + \underline{cD})\}]$$

$$= k_{-1} + k_{+1}(\underline{cA} + \underline{cB}) + k_{+2} + k_{-2}(\underline{cC} + \underline{cD})$$

$$\lambda 1 \bullet \lambda 2 = (1/\tau 1)(1/\tau 2)$$

$$= k_{-1}k_{-2}(\underline{cC} + \underline{cD}) + k_{+2}k_{+1}(\underline{cA} + \underline{cB}) + k_{-2}k_{+1}(\underline{cA} + \underline{cB})(\underline{cC} + \underline{cD})$$

$$\tau 2 >> \tau 1$$

if $k_{-1} + k_{+1}(\underline{cA} + \underline{cB}) >> k_{+2} + k_{-2}(\underline{cC} + \underline{cD})$

$$\lambda 1 = 1/\tau 1 = k_{-1} + k_{+1}(\underline{cA} + \underline{cB})$$

$$\lambda 2 = 1/\tau 2 = \{(1/\tau 1)(1/\tau 2)\}/(1/\tau 1)$$

$$= \{k_{-1}k_{-2}(\underline{cC} + \underline{cD}) + k_{+2}k_{+1}(\underline{cA} + \underline{cB}) + k_{-2}k_{+1}(\underline{cA} + \underline{cB})(\underline{cC} + \underline{cD})\}$$
$$/\{k_{-1} + k_{+1}(\underline{cA} + \underline{cB})\}$$

$$= \{K_{-1}k_{-2}(\underline{cC} + \underline{cD}) + k_{+2}(\underline{cA} + \underline{cB}) + k_{-2}(\underline{cA} + \underline{cB})(\underline{cC} + \underline{cD})\}$$
$$/\{K_{-1} + (\underline{cA} + \underline{cB})\}$$

$$= \{k_{+2}(\underline{cA} + \underline{cB}) + K_{-1}k_{-2}(\underline{cC} + \underline{cD}) + k_{-2}(\underline{cA} + \underline{cB})(\underline{cC} + \underline{cD})\}$$
$$/\{K_{-1} + (\underline{cA} + \underline{cB})\}$$

$$= [k_{+2}(\underline{cA} + \underline{cB}) + k_{-2}(\underline{cC} + \underline{cD})\{K_{-1} + (\underline{cA} + \underline{cB}\}]$$
$$/\{K_{-1} + (\underline{cA} + \underline{cB})\}$$

$$= [\{k_{+2}(\underline{cA} + \underline{cB})\}/\{K_{-1} + (\underline{cA} + \underline{cB})\}] + k_{-2}(\underline{cC} + \underline{cD})$$

$(\underline{cB} >> \underline{cA},\ \underline{cD} >> \underline{cC})$

$$\lambda 1 = 1/\tau 1 = k_{-1} + k_{+1}\underline{cB}$$

$$\lambda 2 = 1/\tau 2 = [\{k_{+2}(\underline{cA} + \underline{cB})\}/\{K_{-1} + (\underline{cA} + \underline{cB})\}] + k_{-2}(\underline{cC} + \underline{cD})$$

$$= \{k_{+2}\underline{cB}/(K_{-1} + \underline{cB})\} + k_{-2}\underline{cD}$$

$(\underline{cB} = cB_0,\ \underline{cD} = cD_0)$

$$\lambda 1 = 1/\tau 1 = k_{-1} + k_{+1}cB_0$$

$$\lambda 2 = 1/\tau 2 = \{k_{+2}cB_0/(K_{-1} + cB_0)\} + k_{-2}cD_0$$

if $k_{+2} + k_{-2}(\underline{cC} + \underline{cD}) >> k_{-1} + k_{+1}(\underline{cA} + \underline{cB})$

$\lambda 1 = 1/\tau 1 = k_{+2} + k_{-2}(\underline{cC} + \underline{cD})$

$\lambda 2 = 1/\tau 2 = \{(1/\tau 1)(1/\tau 2)\}/(1/\tau 1)$

$= \{k_{-1}k_{-2}(\underline{cC} + \underline{cD}) + k_{+2}k_{+1}(\underline{cA} + \underline{cB}) + k_{-2}k_{+1}(\underline{cA} + \underline{cB})(\underline{cC} + \underline{cD})\}$
$/\{k_{+2} + k_{-2}(\underline{cC} + \underline{cD})\}$

$= \{k_{-1}(\underline{cC} + \underline{cD}) + K_{+2}k_{+1}(\underline{cA} + \underline{cB}) + k_{+1}(\underline{cA} + \underline{cB})(\underline{cC} + \underline{cD})\}$
$/\{K_{+2} + (\underline{cC} + \underline{cD})\}$

$= [k_{-1}(\underline{cC} + \underline{cD}) + k_{+1}(\underline{cA} + \underline{cB})\{K_{+2} + (\underline{cC} + \underline{cD})\}]$
$/\{K_{+2} + (\underline{cC} + \underline{cD})\}$

$= [\{k_{-1}(\underline{cC} + \underline{cD})\}/\{K_{+2} + (\underline{cC} + \underline{cD})\}] + k_{+1}(\underline{cA} + \underline{cB})$

$(\underline{cB} >> \underline{cA}, \underline{cD} >> \underline{cC})$

$\lambda 1 = 1/\tau 1 = k_{+2} + k_{-2}\underline{cD}$

$\lambda 2 = 1/\tau 2 = \{k_{-1}\underline{cD}/(K_{+2} + \underline{cD})\} + k_{+1}\underline{cB}$

$(\underline{cB} = cB_O, \underline{cD} = cD_O)$

$\lambda 1 = 1/\tau 1 = k_{+2} + k_{-2}cD_O$

$\lambda 2 = 1/\tau 2 = \{k_{-1}cD_O/(K_{+2} + cD_O)\} + k_{+1}cB_O$

if $k_{-1} + k_{+1}(\underline{cA} + \underline{cB}) >> k_{+2} + k_{-2}(\underline{cC} + \underline{cD})$

$\lambda 2 = 1/\tau 2 = \{k_{+2}cB_O/(K_{-1} + cB_O)\} + k_{-2}cD_O$

if $k_{+2} + k_{-2}(\underline{cC} + \underline{cD}) >> k_{-1} + k_{+1}(\underline{cA} + \underline{cB})$

$\lambda 2 = 1/\tau 2 = \{k_{-1}cD_O/(K_{+2} + cD_O)\} + k_{+1}cB_O$

Appendix 4
Salt-Induced Conformational Change of tRNA

[A]

Under the condition of **Fig. 6**,

$[AMP]_0, [PPi]_0, [Lys]_0, [ATP]_0 >> [tRNA]_0$ (2)

Then,

$K_{eq \cdot x} = [Lys\text{-}tRNA_A][AMP]_0[PPi]_0/[Lys]_0[ATP]_0[tRNA_A]$ (3)

$K_{eq \cdot tRNA \cdot x} = ([Lys\text{-}tRNA_A]+[tRNA_A])/[tRNA_I]$ (4)

From Equation (2)~(4), we can get Equation (5).

$$K_{eq \cdot x} = [Lys\text{-}tRNA_A][AMP]_0[PPi]_0 \,/\, [Lys]_0[ATP]_0[\{[tRNA]_0/(1+(1/K_{eq \cdot tRNA \cdot x})\}-[Lys\text{-}tRNA_A]] \quad (5)$$

If we shall assume $K_{eq \cdot tRNA \cdot x} = \infty$ at 0 (M) sodium chloride, Equation (5) gives

$$K_{eq \cdot 0} = [Lys\text{-}tRNA_A][AMP]_0[PPi]_0 \,/\, [Lys]_0[ATP]_0([tRNA]_0-[Lys\text{-}tRNA_A])$$

$$K_{eq \cdot 0}[Lys]_0/[AMP]_0[PPi]_0 = [Lys\text{-}tRNA_A]/[ATP]_0([tRNA]_0-[Lys\text{-}tRNA_A])$$

$$1/[ATP]_0 = K_{eq \cdot 0}[Lys]_0([tRNA]_0-[Lys\text{-}tRNA_A])/[AMP]_0[PPi]_0[Lys\text{-}tRNA_A]$$

$$= (K_{eq \cdot 0}[Lys]_0/[AMP]_0[PPi]_0)([tRNA]_0/[Lys\text{-}tRNA_A]-1)$$

$$= A[tRNA]_0/[Lys\text{-}tRNA_A]-A \quad (6)$$

Here,

$$A = K_{eq \cdot 0}[Lys]_0/[AMP]_0[PPi]_0$$

[B]

At x (M) sodium chloride in **Fig. 6**, we define $K_{eq\bullet A/0\bullet x}$ as follows.

$$K_{eq\bullet A/0\bullet x} = ([\text{Lys-tRNA}_A]+[\text{tRNA}_A])/[\text{tRNA}]_0 \quad (8)$$

$$=([\text{Lys-tRNA}_A]+[\text{tRNA}_A])$$

$$/([\text{Lys-tRNA}_A]+[\text{tRNA}_A]+[\text{tRNA}_I])$$

$$1/K_{eq\bullet A/0\bullet x}=1+1/K_{eq\bullet tRNA\bullet x} \quad (9)$$

When Equation (9) is substituted in Equation (5),

$$K_{eq\bullet x} =[\text{Lys-tRNA}_A][\text{AMP}]_0[\text{PPi}]_0$$

$$/[\text{Lys}]_0[\text{ATP}]_0(K_{eq\bullet A/0\bullet x}[\text{tRNA}]_0-[\text{Lys-tRNA}_A]) \quad (10)$$

Equation (10) is changed as follows.

$$K_{eq\bullet x}[\text{Lys}]_0[\text{ATP}]_0(K_{eq\bullet A/0\bullet x}[\text{tRNA}]_0-[\text{Lys-tRNA}_A])$$

$$=[\text{Lys-tRNA}_A][\text{AMP}]_0[\text{PPi}]_0$$

$$K_{eq\bullet x}[\text{Lys}]_0[\text{ATP}]_0[\text{tRNA}]_0K_{eq\bullet A/0\bullet x}$$

$$=[\text{Lys-tRNA}_A]([\text{AMP}]_0[\text{PPi}]_0+K_{eq\bullet x}[\text{Lys}]_0[\text{ATP}]_0)$$

$$[\text{tRNA}]_0K_{eq\bullet A/0\bullet x}(1/[\text{Lys-tRNA}_A])$$

$$=([\text{AMP}]_0[\text{PPi}]_0+K_{eq\bullet x}[\text{Lys}]_0[\text{ATP}]_0)/[\text{Lys}]_0[\text{ATP}]_0K_{eq\bullet x}$$

$$=([\text{AMP}]_0[\text{PPi}]_0/[\text{Lys}]_0[\text{ATP}]_0)(1/K_{eq\bullet x})+1$$

$$[\text{tRNA}]_0K_{eq\bullet A/0\bullet x}(1/[\text{Lys-tRNA}_A])([\text{Lys}]_0/[\text{AMP}]_0[\text{PPi}]_0)K_{eq\bullet x}$$

$$=1/[\text{ATP}]_0+[\text{Lys}]_0K_{eq\bullet x}/[\text{AMP}]_0[\text{PPi}]_0$$

$$1/[\text{ATP}]_0=$$

$$[\text{tRNA}]_0K_{eq\bullet A/0\bullet x}(1/[\text{Lys-tRNA}_A])([\text{Lys}]_0K_{eq\bullet x}/[\text{AMP}]_0[\text{PPi}]_0)$$

$$-[\text{Lys}]_0K_{eq\bullet x}/[\text{AMP}]_0[\text{PPi}]_0$$

$$=[\text{tRNA}]_0K_{eq\bullet A/0\bullet x}([\text{Lys}]_0K_{eq\bullet x}/[\text{AMP}]_0[\text{PPi}]_0)(1/[\text{Lys-tRNA}_A])$$

$$-[\text{Lys}]_0K_{eq\bullet x}/[\text{AMP}]_0[\text{PPi}]_0$$

$$1/[\text{ATP}]_0=B[\text{tRNA}]_0K_{eq\bullet A/0\bullet x}(1/[\text{Lys-tRNA}_A])-B \quad (11)$$

Here,

$$B=[\text{Lys}]_0K_{eq\bullet x}/[\text{AMP}]_0[\text{PPi}]_0 \quad (12)$$

Appendix 5

Lysine analogues

α -COOH modified

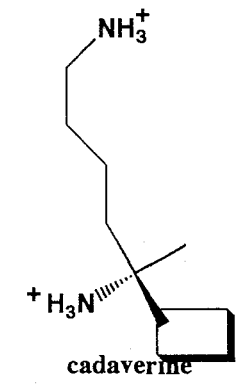

cadaverine

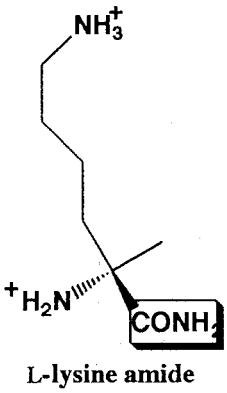

L-lysine amide

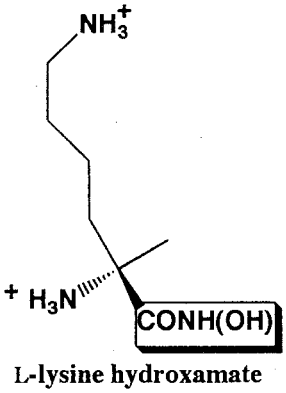

L-lysine hydroxamate

α -NH_2 modified

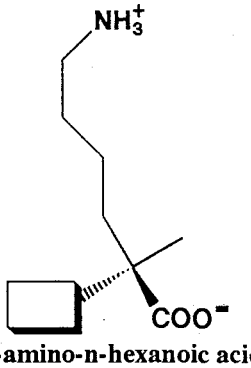

6-amino-n-hexanoic acid

ε -NH_2 modified

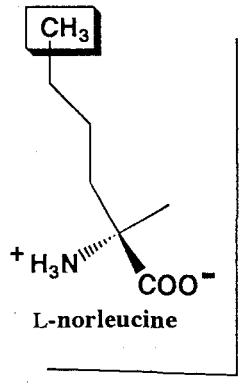

L-norleucine

Side-chain modified

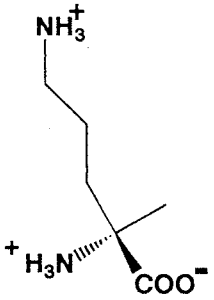

L-ornithine

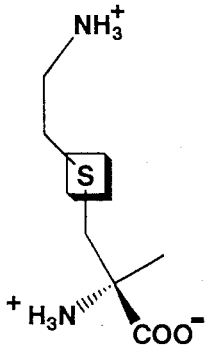

S-(2-aminoethyl)-L-cysteine

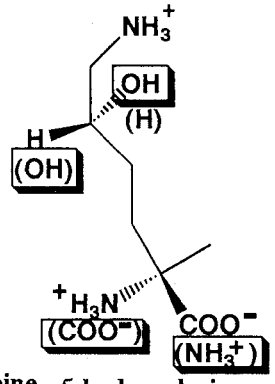

5-hydroxylysine

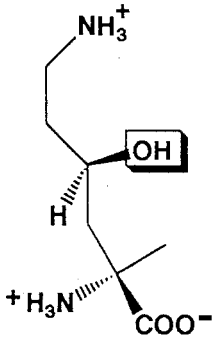

threo-4-hydroxy-L-lysine

Acknowledgments

I wish here to express my sincere gratitude to Dr. Ben'ichiro Tonomura, Professor of Kyoto University, for his abundant guidance during the course of this study. He guided a stubborn student with extraordinary patience. Only his inspiring advice and cautious criticism enabled me to carry on this work and kept me from going astray.

I am deeply grateful to Dr. Kuniyo Inouye, Associate Professor of Kyoto University, for his incessant enthusiastic encouragement. I am very grateful to Dr. Keitaro Hiromi, Emeritus Professor of Kyoto University for his warm encouragement. I would like to thank to Dr. Hiroshi Nakatani of Kyoto University for his useful advice.

I am greatly indebted to Professor Kenji Soda and Associate Professor Nobuyoshi Esaki, Kyoto University, Professor Yukiko Sasaki, Nagoya University, and the members of the department of Food Science and Technology, Kyoto University, for useful advice and allowing use of their facilities.

I thank Messrs. Takanori Muto, Naofumi Shimizu, Tokuo Sukata, Hiroshi Ito, Satoshi Hashimoto, and Takuya Yokota, and Ms. Sonomi Kaino and Eriko Akita, for their help. I express my appreciation in particular to Dr. Keiko Masuda-Momma, Dr. Hiroshi Yamashita, Dr. Seiji Masuda, Dr. Yukio Nagano, for their help and friendship.

Last, but not least, I would like to express my hearty gratitude to my parents and my sisters, without whose affection and assistance I have not continued this study.

List of publications

1.

Teisuke Takita, Yuji Ohkubo, Hideaki Shima, Takanori Muto, Naofumi Shimizu, Tokuo Sukata, Hiroshi Ito, Yukiko Saito, Kuniyo Inouye, Keitaro Hiromi, and Ben'ichiro Tonomura
Lysyl-tRNA Synthetase from *Bacillus stearothermophilus*. Purification, and Fluorometric and Kinetic Analysis of the Binding of Substrates, L-Lysine and ATP
J. Biochem. (1996) in press

2.

Teisuke Takita, Satoshi Hashimoto, Yuji Ohkubo, Takanori Muto, Naofumi Shimizu, Tokuo Sukata, Kuniyo Inouye, Keitaro Hiromi, and Ben'ichiro Tonomura
Lysyl-tRNA Synthetase from *Bacillus stearothermophilus*. Formation and Isolation of the Enzyme•Lysyladenylate Complex and its Analogue
in preparation

3.

Teisuke Takita, Satosi Hashimoto, Eriko Akita, Kuniyo Inouye, and Ben'ichiro Tonomura
Lysyl-tRNA Synthetase from *Bacillus stearothermophilus*. Stopped-Flow Analysis of Enzyme•lysyladenylate Formation
in preparation

4.

Teisuke Takita, Takanori Muto, Eriko Akita, Naofumi Shimizu, Tokuo Sukata, Satosi Hashimoto, Noriko Okada, Kuniyo Inouye, Keitaro Hiromi, and Ben'ichiro Tonomura

A Continuous Fluorophotometric Assay and Examination of the Proof-reading Mechanism of the Aminoacylation Reaction

in preparation

5.

Teisuke Takita, Eriko Akita, Kuniyo Inouye, and Ben'ichiro Tonomura

The Effect of Sodium Chloride on the Aminoacylation Reaction of Lysyl-tRNA Synthetase from *Bacillus stearothermophilus.*

in preparation

6.

Teisuke Takita, Naofumi Shimizu, Tokuo Sukata, Satoshi Hashimoto, Eriko Akita, Nobuyoshi Esaki, Kenji Soda, Kuniyo Inouye, and Ben'ichiro Tonomura

Molecular Cloning, Nicleotide Sequence, and Expression of the Lysyl-tRNA Synthetase Gene of *Bacillus stearothermophilus*

in preparation